Diversity and Biodiversity of Hadal Amphipoda

Johanna Nadia Jean Weston
Doctor of Philosophy
School of Natural and Environmental Sciences
May 2021

Abstract

The ocean's deepest ecosystem, the hadal zone (> 6000 m), is comprised of 47 subduction trenches, non-subduction troughs, and trench faults. These geomorphologically-complex features have been considered to function as ecological and evolutionary independent units, because of extreme environmental conditions, long-term geographical isolation, and evolutionary selection pressures. The order Amphipoda has emerged as a model taxon for understanding the evolution of life and ecology in the hadal zone. Much progress has been made identifying the diversity and understanding the ecology within individual features. This work, however, has solely focused on deep, subduction trenches around the Pacific Rim, leaving shallower features and non-Pacific features underrepresented.

This thesis aims to improve our understanding of the drivers of diversity and population and community structure among scavenging amphipods across the hadal zone. This body of work is executed through three lines of study, utilizing a specimen collection from 16 hadal features. The first line applied an integrative taxonomic approach to expand the known diversity of scavenging amphipods in the Indian and Pacific Oceans. This work has resulted in the description of *Eurythenes plasticus*, the world's first new species described to be impacted by microplastics, *Eurythenes atacamensis,* a unique hadal dominate lineage in the Peru-Chile Trench, *Stephonyx sigmacrus*, the deepest known species of this genus, and *Civifractura serendipia*, a new cryptic genus and species within the Alicellidae family. The second line assessed how the community shifts across the abyssal-hadal transition zone in a non-subduction hadal feature, the Wallaby-Zenith Fracture Zone, Indian Ocean. The third line investigated the global distribution and phylogeography of *Bathycallisoma schellenbergi* between twelve hadal features in four oceans. Together, this thesis expands our knowledge of hadal communities to features beyond subduction trenches and contributes to the disentanglement of the environmental, tectonic, and other drivers of contemporary diversity across the hadal zone.

Declaration of Authenticity

I hereby declare that this was composed by myself and the research has not been accepted in any previous application for a degree. All quotations have been distinguished by quotations marks, and all sources of information have been specifically acknowledged.

The work presented has been carried out by me, with the following exceptions:

Chapter 2: Amphipod samples were collected by Alan Jamieson, the map was created by Thomas Linley, the microplastic analysis was conducted by Priscilla Carrillo-Barragan.

Chapter 3: Amphipod samples were collected by Alan Jamieson, the map was created by Thomas Linley, the morphometric lab work and microscope imaging work was conducted by Jennifer Wainwright, and the *Atacamex* specimens processing integrative taxonomic analysis was conducted by Liliana Espinosa Leal and Carolina Gonzalez.

Chapter 4: Amphipod samples were collected by Alan Jamieson, the map was created by Heather Stewart, and the morphological phylogenetic analysis was conducted by Rachael Peart.

Chapter 5: Amphipod samples were collected by Alan Jamieson, the map and geological analysis was conducted by Heather Stewart, and the genetic work was conducted at the University of Aberdeen with Heather Ritchie and Stuart Piertney.

Chapter 6: Amphipods samples were collected by Alan Jamieson.

Chapters 2[1], 4[2], and 5[3] have been published as full research articles and are presented as unmodified versions of the published manuscripts. Chapter 3 is in press at *Marine Biodiversity* and is presented as the accepted manuscript following two rounds of peer review.

My original contributions to each chapter are as follows:

Chapter 1: Topic modeling, data analysis, and writing.

Chapter 2: Genetic lab work, illustrations, data analysis, writing, and submission.

---

[1] Weston, J.N.J., Carrillo-Barragan, P., Linley, T.D., Reid, W.D.K. and Jamieson, A.J., 2020. New species of *Eurythenes* from hadal depths of the Mariana Trench, Pacific Ocean (Crustacea: Amphipoda). Zootaxa, 4748(1), pp.163-181. doi:10.11646/zootaxa.4748.1.9

[2] Weston, J.N.J., Peart, R.A. and Jamieson, A.J., 2020. Amphipods from the Wallaby-Zenith Fracture Zone, Indian Ocean: new genus and two new species identified by integrative taxonomy. Systematics and Biodiversity, 18(1), pp.57-78. doi:10.1080/14772000.2020.1729891

[3] Weston, J.N.J., Peart, R.A., Stewart, H.A., Ritchie, H., Piertney, S.B., Linley, T.D. and Jamieson, A.J., 2021. Scavenging amphipods from the Wallaby-Zenith Fracture Zone: Extending the hadal paradigm beyond subduction trenches. Marine Biology, 168, pp.1-14. doi:10.1007/s00227-020-03798-4

Chapter 3: Sample processing, genetic lab work, illustrations[4], data analysis, writing, and submission.

Chapter 4: Sample processing, genetic lab work, illustrations, data analysis, writing, and submission.

Chapter 5: Taxonomic identification, sample processing, lab work, data analysis, writing, and submission.

Chapter 6: Sample collection[5], sample processing, genetic lab work, data analysis, and writing.

Chapter 7: Writing.

Johanna Weston
Newcastle University
04/05/2021

[4] Jennifer Wainwright and Eva Stewart did several illustrations as part of their undergraduate dissertations.
[5] Amphipod samples were collected across 13 different cruises. I took part in four expeditions as part of the Five Deeps Expedition (FDE): FDE-MAR, FDE-PRT, FDE-SOL, and FDE-TON.

Acknowledgments

I am very grateful to my supervisors, Alan Jamieson and Gary Caldwell, for their guidance, support, and encouragement throughout my PhD. I am especially grateful that Alan took a chance on me and then provided me with a wealth of unexpected experiences, ranging from getting a Guinness World Record for *Eurythenes plasticus* to spending long nights on the back deck of the DSSV *Pressure Drop*. It has truly been a privilege to be bestowed the title *Mongolian Battle Hamster*. Thank you to Gary for being a speedy running buddy and pushing me on those times.

Thanks to Thom Linley for teaching me the beauty and art of taxonomy, and for being an overall supportive friend. Thanks to Will Reid for your support and for allowing me to mentor Eva Stewart and Jenny Wainwright and show them the majesty of amphipods. Much thanks to Rachael Peart for answering the call for amphipod mouthpart help with an amazing dissection video of *Alicella gigantea*. I am incredibly lucky to have you as my amphipodoligist mother. Thank you to Heather Stewart for your GIS skills and for being a science inspiration. So many thanks to Stuart Piertney and Heather Ritchie for teaching me the ways of amphipod DNA barcoding. Special thanks, Heather, for being my amphipod beastie mentor, and more importantly my good friend. Thank you to Kirsten Wolff for being a ray of sunshine and support. Special thanks to the NEG group, Darren Evans, James Kitson, Kirsten Miller, Dimitris Petropoulos, Fred Windsor, Justin Byrne, and Claire Branston, for letting me a pseudo-member and helping me troubleshoot PCRs. I will always be grateful to my therapist for helping me finish “calmly and confidently”.

Thank you to all my friends, and in particular, my science friends who have provided important support through this journey. Rachael and Tim Schwartz-Narbonne, thanks for being our expat moving buddies and making us get on the allotment list. Sanem and Matthieu Cartigny, thank you for being our expat family and sharing meals throughout Lockdown. Dave and Lindsey Early, thank you for taking in all our jams, jellies, and ketchup. Cassie Bongiovanni, thank you for the joy of the drink umbrella — Texas Forever. Anke and Marcus Neumann, thanks for the delicious meals which made us step up our dinner game. Thank you to Evelyn and Eric Jensen for moving to the UK to help support me in the end and baking me the best PhD celebration. To the Alberta Boys, Kurt Konhauser and Dan Alessi, thanks for keeping part of the geoscience team and feedback

when I needed it most. Alison Haupt, thank you for coming to the UK for a population genetics course and making me travel to Wales to hang out together. You have been my science inspiration for years.

I am eternally grateful to my family. Thanks, Mom and Dad for all the encouragement and adventures throughout the years. Dad, it has been fun to share the *Eurythenes plasticus* discovery with you. Thanks to Alex, Caroline, and Christopher for your support and for letting me teach your kids about the deep ocean. Thank you to Grandma and Gigi for your support and the inspiration to explore and be fierce. Thanks to L'rae, Larry, Ryan, and Madeline for the winter retreats and "constructive critiques". Infinitely grateful to the allotment for giving me the space to dig in, sow seeds, grow up, and, most importantly, be nurtured.

All remaining thanks go to my life-long collaborator, Shannon — this body of work would not have been possible without your love, support, patience, laughter, and, of course, feedback.

Table of Contents

Chapter 1: The state of hadal science: How this thesis will use scavenging amphipods to advance the field

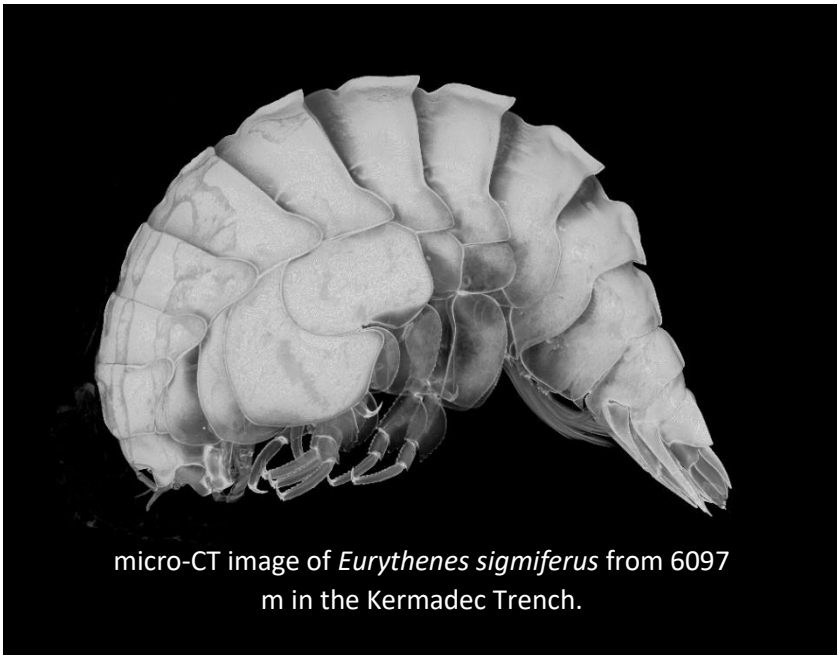

micro-CT image of *Eurythenes sigmiferus* from 6097 m in the Kermadec Trench.

1. Overview of the Hadal Zone and Hadal Science

The Earth is a blue planet–with the fives oceans covering over 70% of the Earth's surface. Nearly 90% of that surface lies beneath the littoral margins of the continents, with a mean depth of 3897 (Weatherall et al., 2015) and encompassing a three-dimensional space of 1.3 billion cubic meters of water (Charette & Smith, 2010). The vertical dimension of the ocean has led to the partition of the deep sea into three zones. These zones are generally based on observed faunal transitions, distinctions in ecologic processes, geologic features, and, in part, convenient means of nomenclature (Jamieson et al., 2010). The bathyal zone extends down the continental slope from 1000–3000 m. The abyssal zone, from 3000–6000 m, covers 54% of the Earth's surface with a vast network of abyssal plains (Smith et al., 2008). The deepest of the zones is the hadal zone, spanning from 6000 m to full ocean depth of nearly 11,000 m (Wolff, 1960).

Named as an homage to *Hades*, the Greek god of the underworld and his home (Bruun, 1956), the hadal zone accounts for the deepest 45% of the ocean (Jamieson et al., 2010). The hadal zone is comprised of 47 known geological features that form geographically disjunct and often isolated ecosystems (Figure 1; Stewart & Jamieson, 2018). Globally, the hadal footprint accounts for less than 2% of the total seafloor area (800,000 km^2). The seafloor extends from the abyssal plains to these depths in three main geomorphic features, namely subduction trenches, transform faults, and troughs. Twenty-seven hadal habitats are deep trenches and account for 93.7% of the total hadal area (Stewart & Jamieson, 2018). These striking features on the seafloor are formed at tectonic convergence zones where an older, dense oceanic plate (overriding) is forced towards the mantle and under the lighter plate (underriding; Stern, 2002). The subduction dynamics result in trenches typically being long and narrow with characteristic V-shaped cross-sections, with slopes ranging between 5^o and 15^o and up to 45^o (Angel, 1982). Twenty-three hadal trenches are in the Pacific Ocean, and the three trenches exceed 10,000 m (i.e., Mariana, Philippine, and Tonga trenches). Many of the Pacific Ocean trenches are found on the perimeter, at the convergence zone of the Pacific plate with its neighboring plates. The remaining four trenches are found in the Indian (Java), Atlantic (Puerto Rico), and Southern Oceans (South Orkney and South Sandwich; Stewart & Jamieson 2019). Seven hadal features are found as transform faults or fracture zones,

which are long, narrow zones of irregular topography formed perpendicular to the movement of tectonic plates (Intergovernmental Oceanographic Commission, 2001). Typically offset from the spreading ridge axis, the transform faults and fracture zones are found in the Atlantic, Pacific, and Indian Oceans. The remaining thirteen features are troughs or non-seismic basins within the abyssal plain interiors, characteristically long depressions, and flat across the bottom (Intergovernmental Oceanographic Commission, 2001). Seven of the known hadal troughs are in the Atlantic Ocean, with the remaining in the Pacific and Indian Oceans (Stewart & Jamieson, 2018).

In contrast to the connected continuum of the bathyal and abyssal zones, the hadal zone is geographically disjunct and characterized by feature-specific environmental conditions and geomorphologic attributions (Figure 2; Jamieson et al., 2010). Some aspects are shared and can be considered generically hadal. This includes the linear increase of hydrostatic pressure by 10 atms every 100 metres (~600–1100 atm), absence of light, and near-freezing temperatures (mean range 1.0–2.5^{o}C; Jamieson et al., 2010). They are also defined by low food availability, which includes the chance carrion falls, <2 % of the surface-derived particulate organic matter (POM), and localized chemosynthetic bacterial communities (Jamieson, 2011).

Yet, no two hadal features are the same, specifically varying in geomorphology, geography, total area, and maximum depth. The inter-hadal ecosystem is shaped by a unique suite of abiotic or extrinsic factors. The location of the feature and its proximity to land can influence sediment, nutrient, and primary productivity fluxes. In particular, the biogeographic province and overlying surface primary productivity (oligotrophic to eutrophic) shapes the amount of POM reaching the hadal zone (Ichino et al., 2015). Further, the global and local hydrography patterns control the oxygen supply, temperature, and salinity of the ecosystem (Kawabe & Fujio, 2010). As the majority of hadal ecosystems are situated at convergence zones, the intensity and frequency of seismic activity influence the amount of sediment transport across the trench and the level of disturbance organisms need to be adapted for and contend with (Oguri et al., 2013). The topography variability of the features creates habitat heterogeneity and further affects the transport and deposition of sediment and POM (Stewart & Jamieson, 2018). Additionally, the geologic age of the feature is likely to influence the species present and

level of endemism, as well as degrees of isolation from other hadal ecosystems (Belyaev, 1989).

The 1948 Swedish *Albatross* expedition proved that, despite the extreme conditions, life existed in the hadal zone with the first successful hadal trawl at the Puerto Rico Trench (Jamieson et al., 2020). Since then, the hadal faunal community has been found to be distinct from shallower zones and diverse with high levels of endemism (Belyaev, 1989). Representatives of most major taxa and functional groups are present at hadal depth, even though species richness decreases with depth (Lacey et al., 2016). The hadal community is comprised of fishes, cephalopods, crustaceans, echinoderms, polychaetes, molluscs, foraminifera, bacterium, cnidarians, bryozoans, with some taxa present to full ocean depth (Wolff, 1960, 1970; Belyaev, 1989; Jamieson & Vecchione, 2020). However, due to the technological limitations to sampling at these depths, understanding of most of these taxa is largely derived from very few samples and predominantly collected by the RV *Vitjaz* and RV *Galathea* expeditions. Similar to the extrinsic factors that shape the inter-hadal ecosystem, the hadal community is influenced and structured by a feature-specific set of intrinsic factors. These intrinsic features include the adaptions and life history of individual species to the abiotic conditions, predation, competition for resources, local hydrodynamics, and geomorphology that can influence both the quality and quantity and finding of food, habitat heterogeneity, and chemosynthesis (Jamieson et al., 2010).

As a result of the extreme depths and technological barriers, hadal research efforts have occurred along a disjunct timeline and developed slower relative to shallower deep-sea and coastal ecosystems (Danovaro et al., 2014; Jamieson, 2018). Around the turn of the 20th century, early pioneers began sampling at greater and greater depths, with the first physical sampling by the HMS *Challenger* with the recovery of sediment from the Japan Trench (Thomson & Murray, 1895). Following the burst of curiosity concerning the extent to which animal life could be found and the true depths of the oceans, there was a lull in progress. The 1950s saw the first two major research expeditions to survey and sample the hadal zone — the Danish RV *Galathea* and the former Soviet Union RV *Vityaz* expeditions. These pioneering expeditions sampled multiple trenches using fixed-mouth beam trawls and sediment grabs (Belyaev, 1989). From the biological perspective, these

expeditions laid the taxonomic and systematic foundation of species description and distribution across many taxa (Dalh, 1959; Wolff, 1960; Belyaev, 1989). Further, the findings from these expeditions drove the distinction of the hadal zone from a mere extension of the abyssal zone (Bruun, 1956).

The number of hadal-rated technologies has increased over the past fifteen years, such as sensors and cameras (Glud et al., 2013; Brandt et al., 2016), autonomous lander vehicles (Figure 3a; Jamieson et al., 2009; Peoples et al., 2019), epibenthic sledges (Brandt et al., 2013), and submersible vehicles (Kyo et al., 1995; Bowen et al., 2009; Jamieson et al., 2019). This technological advancement has coincided with a rise in the number of multi-depth and multi-trench sampling programs, such as the HADal Environment and Educational Program (HADEEP; Jamieson et al., 2010), HAdal Ecosystems Study (HADES; Mills et al., 2016), the Kurile-Kamchatka Biodiversity Studies (KuramBio; Brandt & Malyutina, 2015), and the Five Deeps Expedition (Jamieson et al., 2019; Stewart et al., 2019). The increase in sampling capabilities to full ocean depths and expansion of sampling programs has translated to an exponential increase in the number of peer-reviewed published papers. Search engine results with the term ‘hadal’ retrieved 191 papers between 1959 to 2017, with 2017 having a maximum of 12 papers and an exponential trend (Jamieson, 2018). Based on the exponential growth, it has been postulated that hadal science has passed the exploration era and is currently transitioning from an observational to an experimental era (Jamieson, 2018).

With the perceived growth of hadal science, there is an opportunity to quantitively assess the hadal body of literature to identify research strengths and opportunities in future directions. One synthesis method is text analysis or topic modeling - a statistical approach to assess the text in a corpus of abstracts and then identify topics that represent the key ideas based on the co-occurrence patterns of words (Westgate et al., 2015; Mair et al., 2018). Topic modeling is based on unsupervised classification, fit with a Latent Dirichlet Allocation model (LDA; Silge & Robinson, 2017). The LDA model handles each topic as a mixture of words and each document as a mixture of topics (Murakami et al., 2017; Silge & Robinson, 2017). The model outputs can be analyzed to investigate trends and gaps using ecological modeling statistical techniques, such as cluster and network analyses (Figure 4; Westgate et al., 2015). The topic modeling has been applied to

identify trends and gaps in a range of fields, such as conservation science and planning (Westgate et al., 2015; Mair et al., 2018), species distribution modeling use (Tulloch et al., 2016), arid ecology (Greenville et al., 2017), fisheries science (Syed et al., 2017), and animal pollination (Millard et al., 2020).

Here, topic modeling is used to assess the current state of research of the last marine frontier and provide context for this thesis. A body of literature (414 abstracts from 1991 to 2020) was examined for topic growth, co-occurrence, and relatively generality and specificity to uncover publishing trends in hadal science. Further, a gap analysis was used to identify existing research links and potential future research directions.

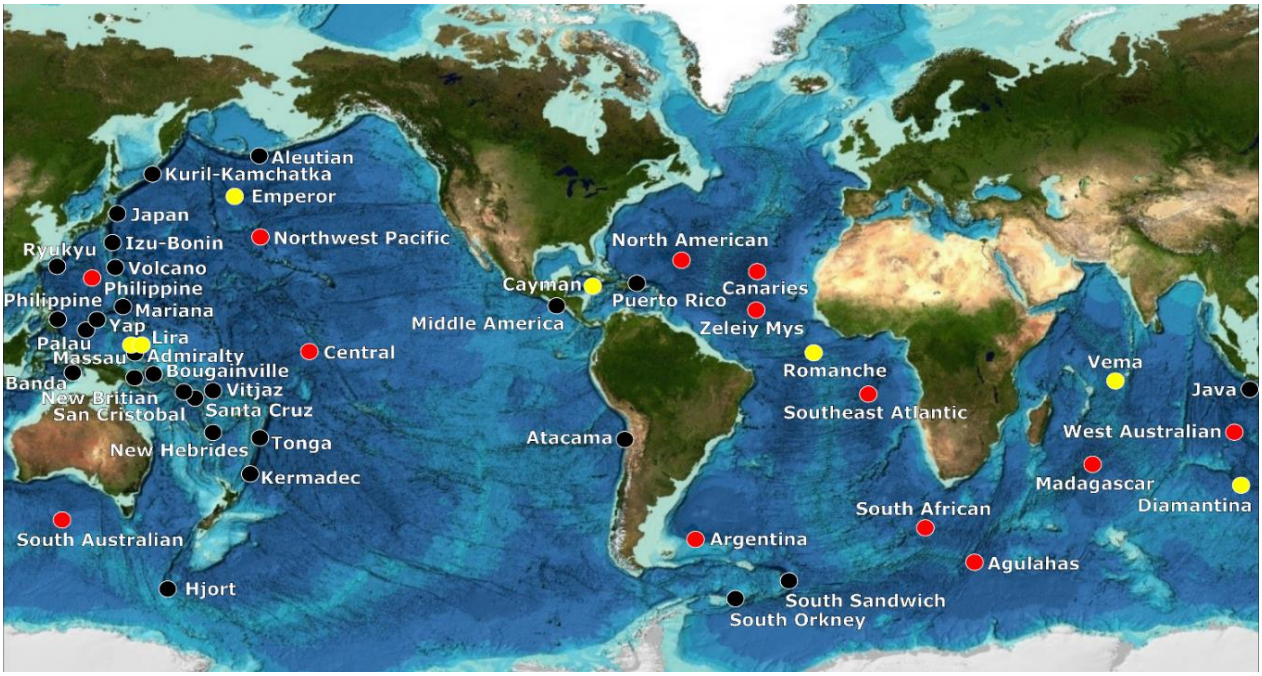

Figure 1. Worldwide distribution of the 47 known hadal features between 6000 m to full ocean depths defined in Stewart and Jamieson 2018. Subduction trenches (27; black). Troughs (13; red). Transform faults (7; white). Imagery reproduced from the GEBCO_2014 Grid, version 20150318, www.gebco.net.

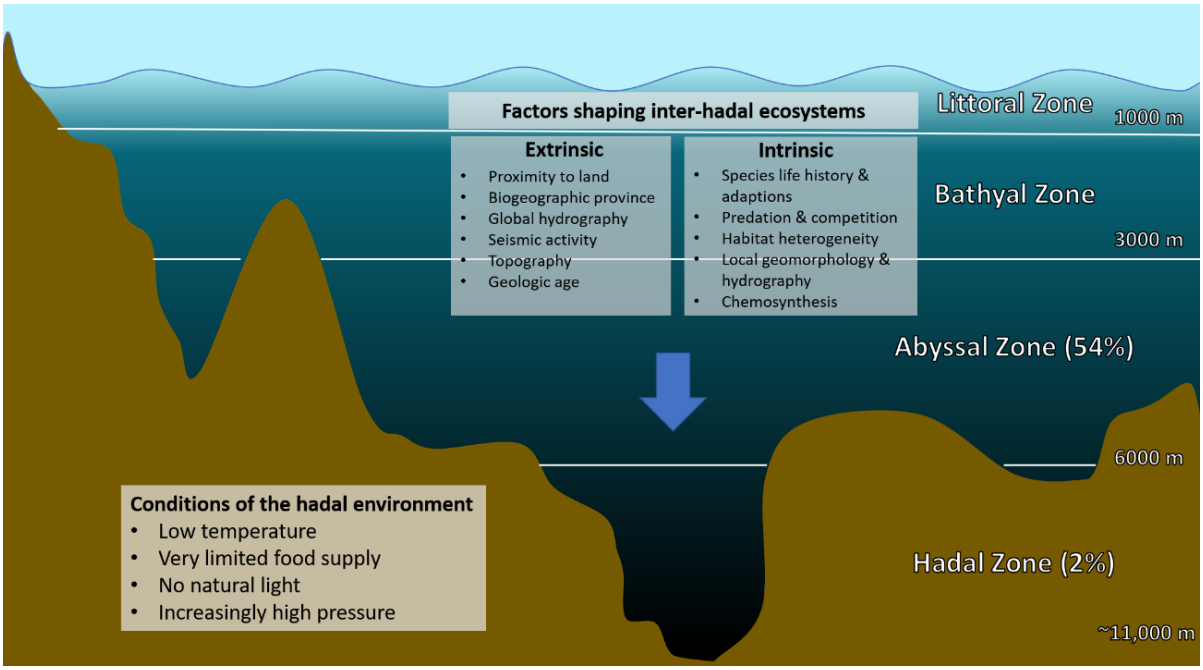

Figure 2. Profile of the four marine biozones with the extrinsic and intrinsic factors that shape the inter-hadal ecosystem. Adapted from Jamieson et al. (2010).

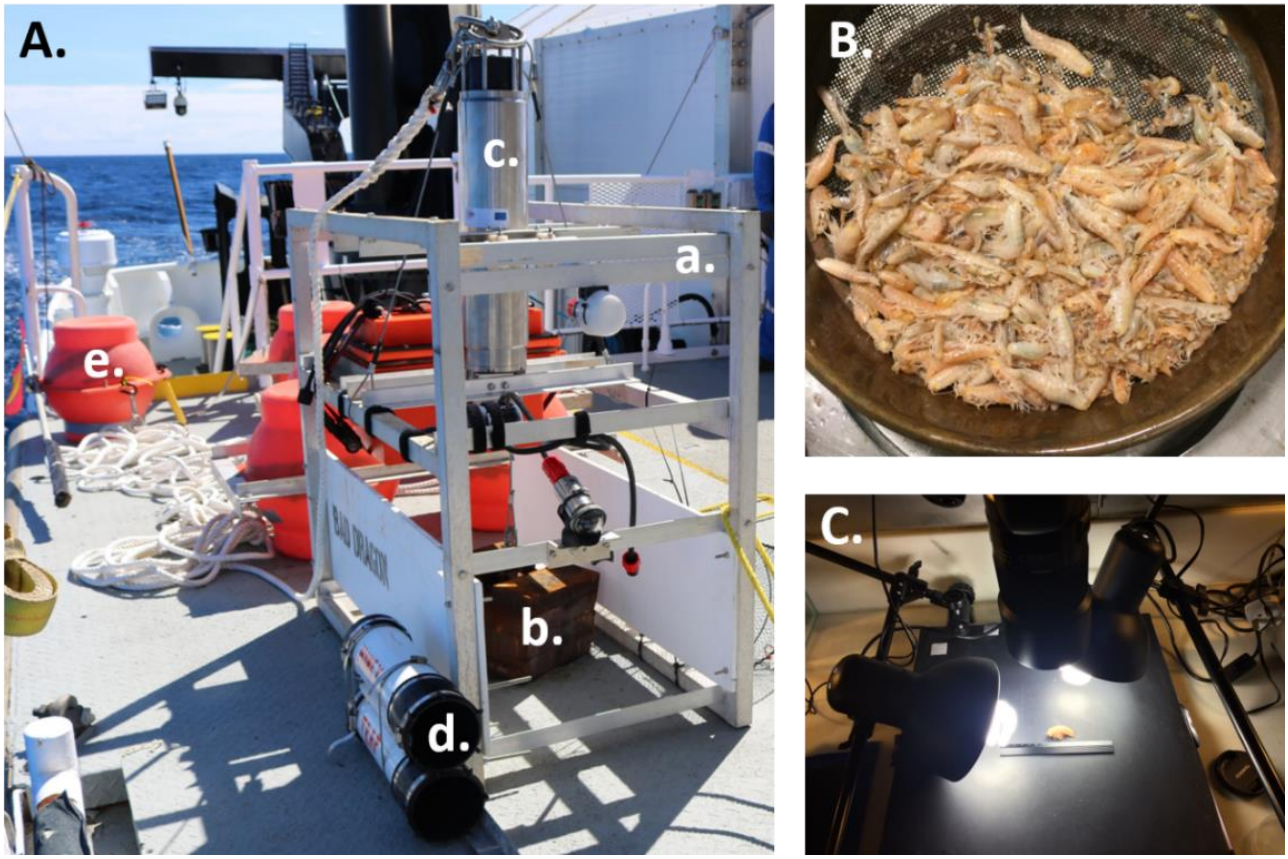

Figure 3. (A) Hadal lander vehicle: a. lander frame, b. ballast weight, c. hadal depth-rated acoustic release and pressure sensor, d. baited, funnel invertebrate traps, and e. surfacing floatation. (B) Newly recovered amphipods from 8370 m in the Puerto Rico Trench. (C) On-board photography of recently recovered amphipod specimens to capture natural pigments colours that are lost with preservation.

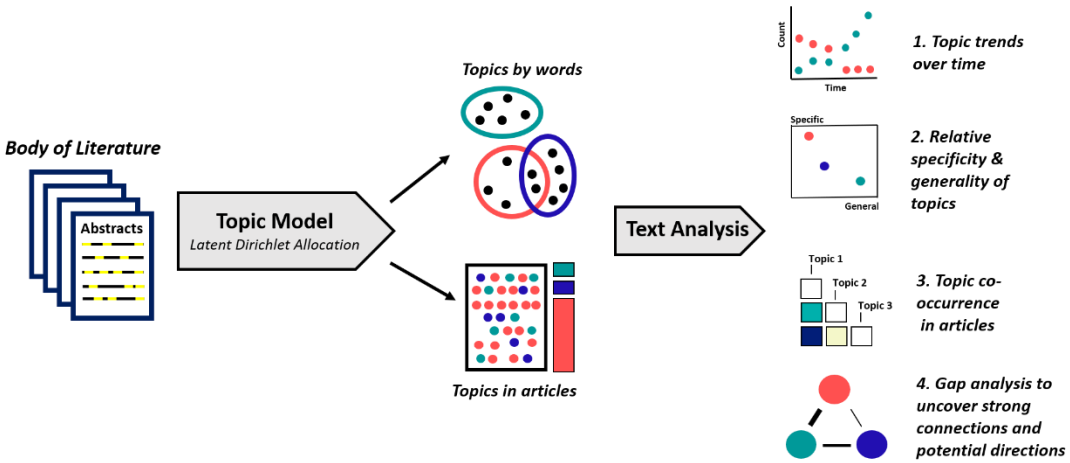

Figure 4. Conceptual framework of topic modeling with text analysis outputs aimed at uncovering trends, relationships, and gaps to identify current and potential future research directions.

2. Topic Modeling Methods

2.1. Literature search and abstract cleaning

A literature search was conducted on the Web of Science (ISI Web of Knowledge) Core Collection database for articles published between 1970 and 2020 on April 6, 2020. A total of 458 abstracts or reviews were retrieved using the search terms ‘hadal’, ‘full ocean depth’, ‘deep ocean trench’, or ‘Challenger Deep’. These search terms were selected to focus on research exclusive to the hadal zone. While a term as specific as ‘Challenger Deep’ is less desirable, this term caught several papers not captured by the other terms. Other place-specific terms, such as ‘Mariana Trench’ and ‘Japan Trench’, were determined to provide too broad of results with research at shallower depths. The search term was ‘subduction trench’ was also considered, but this term retrieved many non-marine studies.

Citations and abstracts were downloaded and imported into the program R v. 3.6.3 using the package *bibliometrix* v 2.3.2 (Aria & Cuccurullo, 2017). Forty-four articles lacked abstracts and were removed from the analysis. The remaining 414 abstracts were transformed into a corpus or ‘body of literature’ and processed using the text mining package *tm* v. 0.7 (Feinerer et al., 2008). The search terms were removed, as they were common to all abstracts. Numbers 1 to 11 written as words and numerals were also removed. The *tm* package’s pre-defined list of 174 common English words was also discarded. Further, the words ‘marine’, ‘ocean’, deep-sea’, ‘sea’, ‘also’, ‘can’, ‘may’, ‘like’, ‘well’, ‘will’, ‘along’, ‘the’, and publisher’s copywrite terms were removed. Hyphens and slashes were changed to spaces, and punctuation was stripped. Finally, the remaining terms were stemmed back to their root, and words that appeared in four or fewer abstracts were discarded. The final corpus had a vocabulary of 1467 words, and this was converted into a document term matrix.

2.2. Topic Modeling and Text Analysis

The LDA model is unsupervised and requires the user to pre-specify the number of topics. The optimal number of topics was estimated using the *ldatuning* package v 1.0 (Nikita, 2019) for two to 20, 25, 40, 50. 80. 100, 150, and 200 topics with the metrics Griffiths 2004, Cao Juan 2009, Arun 2010, and Deveaud 2014. The *ldatuning* results indicated 50–100 to be the optimal number of topics. Twenty-five topics were selected for

the LDA model input as a balance of capturing the corpus complexity and interpretability (Westgate et al., 2015). An LDA model with Gibbs sampling was fit with the *topicmodels* package v 0.2 (Hornik & Grün, 2011). The final model was calculated using 5000 iterations and discarding the first 1000 runs.

The LDA model defines a topic by the set of co-occurring words. Each article is assigned to the topic with the highest weight. The 20 highest weighted words in each topic were inspected to name the topic and aid in the presentation of findings (Table 1). The LDA model outputs included two matrixes: 1) the beta matrix of the words per topic probabilities, and 2) the gamma matrix of the topic per abstract probabilities (Grün & Hornik, 2011). The LDA model outputs were analyzed to assess for trends over time, topic generality and specificity, topic co-occurrence within abstracts, and a gap analysis focused on Topic 24 following protocols in Westgate et al. (2015) and Mair et al. (2018) (Figure 4).

Some topics are shared among many abstracts in the corpus and represent broad concepts. While other topics may be present in only a specific subset of abstracts in the corpus. The distribution of topic weights per article (gamma matrix) was used to assess the relative generality versus specificity of each topic. The mean weight was calculated for when each topic was selected and when it was not selected in each abstract (Westgate et al., 2015; Mair et al., 2018). The resulting values were plotted against each other using the *ggplot2* package (Wickham, 2016).

The co-occurrence of topics within an article was investigated across the corpus. The gamma matrix was log10-transformed, and then Euclidean distances were calculated. The distances were normalized from zero to one, where zero indicated the pair never co-occurred and one denotes the pair always co-occurred in the same abstract (Mair et al., 2018). The resulting matrix was visualized with the *corrplot* package v 0.84 (Wei & Simko, 2017).

A gap analysis was conducted between Topic 24 and other topics to draw out potential research gaps. The Euclidean distances of the log10-transformed beta and gamma matrices were calculated. Each matrix was normalized from zero to one, then summed together. In the resulting matrix, zero indicated a strong connection, and one

indicated a weak connection or high gap between topics (Westgate et al., 2015). The gap analysis was visualized as a network diagram with the *circleplot* package v 0.4.1.

Table 1. The 25 topics identified by the LDA model listed by the top 5 five words, topic name, and Theme.

No.	Top 5 words (stemmed)					Topic Name	Theme
1	develop	submers	year	first	technolog	Submersible vehicles	Engineering & Technology
2	system	cabl	vehicl	kaiko	use	Remotely operated vehicles	Engineering & Technology
3	global	ecosystem	earth	knowledg	process	Ecosystem ecology	Marine biology & ecology
4	studi	type	observ	differ	fig	Presence & observations	Contextual
5	vehicl	oper	design	system	underwat	Autonomous vehicles	Engineering & Technology
6	divers	abund	increas	region	indic	Biodiversity	Marine biology & ecology
7	gene	relat	sequenc	adapt	genom	'Omics	Marine biology & ecology
8	model	result	method	base	effect	Geophysical modeling	Ocean & Earth Sciences
9	mariana	plate	subduct	zone	arc	Plate tectonics	Ocean & Earth Sciences
10	observ	new	mariana	fish	includ	Fish	Marine biology & ecology
11	pressur	high	low	activ	temperatur	Pressure adaptions	Marine biology & ecology
12	degre	current	increas	estim	flow	Water properties & currents	Ocean & Earth Sciences
13	group	molecular	morpholog	within	famili	Systematics	Marine biology & ecology
14	organ	sediment	carbon	matter	benthic	Sediment organic geochemistry	Ocean & Earth Sciences
15	speci	new	describ	collect	genus	Taxonomy	Marine biology & ecology
16	communiti	microbi	domin	mariana	associ	Microbiology	Marine biology & ecology
17	abyss	speci	kuril	pacif	distribut	Kuril-Kamchatka Trench	Marine biology & ecology
18	environ	high	result	ecolog	live	Chemosynthesis	Marine biology & ecology
19	sampl	sediment	collect	obtain	element	Sediment sampling	Ocean & Earth Sciences
20	zone	differ	atlant	western	pattern	Geographic comparisons	Contextual
21	water	similar	found	rang	shallow	Vertical comparisons	Contextual
22	use	data	provid	show	structur	Interpretation of results	Contextual
23	test	organ	larg	suggest	extrem	Comparative	Contextual
24	amphipod	kermadec	compar	pacif	structur	Amphipods	Marine biology & ecology
25	measur	deploy	time	profil	bottom	Sampling equipment	Engineering & Technology

3. Topic Modeling Results

The 25 topics fit into four broad themes (Figure 5; Table 1). 'Engineering & Technology' had the fewest number of topics. Three of the four topics focused on the development and operation of *Submarine*, *Remotely operated*, and *Autonomous vehicles* that can withstand and perform in the extreme environment hadal zone. The fourth topic centered on the logistics and details of sampling equipment. 'Ocean & Earth Science' consisted of five topics. One topic pertained to large-scale plate tectonics, two topics addressed sediments from sampling to analysis, and the two other topics were modeling of process and water mass properties and circulation. 'Marine Biology & Ecology' was the largest theme, consisting of eleven topics and 52% of the abstracts. This theme could be separated into three sub-themes. One sub-theme encompassed ranged from biological fields of research, which ranged from the focus of individual species and classifications of systematics to large-scale macroecology. Within this theme, '*Omics* has the greatest number of articles (n = 31) out of any topic. A second sub-theme was specific taxa or community of organisms. This included *Fish*, *Microbiology*, *Amphipods,* and *Chemosynthesis*. *Amphipods* (Topic 24) consisted of 16 abstracts. The third sub-theme was a specific hadal trench, namely the *Kuril-Kamchatka Trench*. 'Contextual' is the fourth theme and consists of the fewest number of abstracts (n = 31). In contrast to the other three themes, the words associated with the five 'Contextual' topics provide external context, such as geographical comparisons and interpretation of results, rather than represent a particular aspect of hadal science.

The earliest abstract included in the analysis was published in 1991. Since 1991, there was an exponential increase in publications, with 2019 having the highest number of publications over the entire year (n = 72; Figure 5). To focus on growth, the average sum of papers per topic over the past five years (2015-2020) was 9.5 papers. Ten topics were above that average, specifically *Submersible vehicles* (n = 12), *Biodiversity* (n = 10), '*Omics* (n = 17), *Geophysical modeling* (n = 12), *Systematics* (n = 13), *Sediment organic geochemistry* (n = 17), *Taxonomy* (n = 17), *Microbiology* (n = 16), *Kuril-Kamchatka Trench* (n = 23), and *Amphipods* (n = 12).

Topic generality analysis allowed distinctions between topics that abstracts were the primary focus (specific) and topics that had a mean low weight between abstracts

(general; Figure 6). The ‘Earth & Ocean Science’ and ‘Engineering & Technology’ topics tended to be more specific, while ‘Marine Biology & Ecology’ and ‘Contextual’ topics tended to be more general. The two most specific topics were *Plate tectonics* and *Remotely operated vehicles*. Of ‘Marine Biology & Ecology’ and ‘Contextual’ topics, *Microbiology* and *Comparative* were the most specific, respectively. *Vertical comparisons*, *Interpretation of results*, and *Taxonomy* were the three most general topics. *Sediment sampling* and *Sampling equipment* were the most general of the ‘Earth & Ocean Science’ and ‘Engineering & Technology’ topics. *Amphipods* were intermediately placed along the specific-general spectrum.

For the co-occurrence of topics analysis, the ‘Contextual’ theme was excluded as these topics frequently co-occurred with nearly all the topics. By excluding those five topics, the analysis was focused on the 20 topics that dealt with specific aspects of hadal science (Figure 7). Of the three themes, ‘Engineering & Technology’ topics frequently co-occurred together, most strongly was *Submersible vehicles* and *Remotely operated vehicles*. Other pairs of frequently co-occurring topics within themes included *Geophysical modeling* and *Water properties & currents*, *Taxonomy* and *Kuril-Kamchatka trench*, *Amphipods* and *Fish*, and *Taxonomy* and *Systematics*. Several topics had high co-occurrence between themes, namely *Water properties & currents* and *Sampling equipment*, *Biodiversity* and *Submersible vehicles*, and *Chemosynthesis* and *Sediment sampling*. As opposed to co-occurrence, some topics seldom appeared in the same article together. *Plate tectonics* rarely co-occurred with most topics. Surprisingly, *Microbiology,* ‘*Omics, Pressure adaptions*, and *Biodiversity* rarely co-occurred with *Taxonomy* and *Kuril-Kamchatka Trench*. The topics of *Fish*, *Sediment sampling*, and *Chemosynthesis* appeared to have at least a moderate level of co-occurrence with all the topics. *Amphipods* had at least moderate levels of co-occurrence with topics in the ‘Marine Biology & Ecology’ and ‘Earth & Ocean Sciences’ themes. *Amphipods* rarely co-occurred with topics in the ‘Engineering & Technology’ theme and *Plate tectonics*.

The gap analysis showed similarity or strong connectivity links between *Amphipods* and *Fish* and *Vertical comparisons,* and moderate connections with *Sediment sampling, Geographic comparisons,* and *Pressure adaptions* (Figure 8). In contrast, there was dissimilarity between ‘Engineering & Technology’ and ‘Earth & Ocean Science’

topics, except for *Sediment sampling.* The largest gaps were with *Autonomous vehicles*, *Plate tectonics*, and *Sampling equipment*. Of 'Marine Biology & Ecology' topics, *Amphipods* were generally well connected. However, gaps were present between *Biodiversity*, *Microbiology*, and '*Omics*.

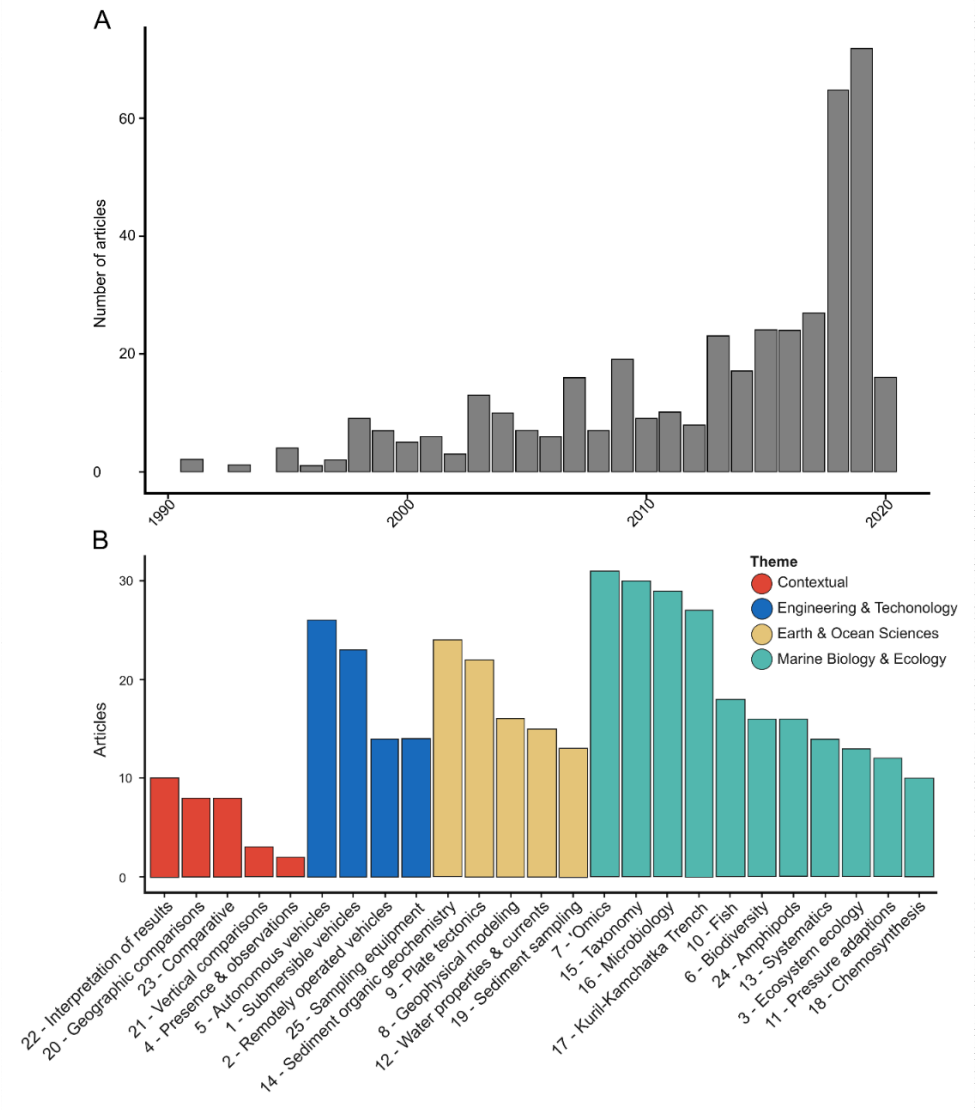

Figure 5. (A) Exponential increase in the number of papers with abstracts on hadal science since 1991. (B) Topic frequency within the corpus. Each article was assigned to the topic with the highest weight. The 25 topics were grouped into four broader Themes.

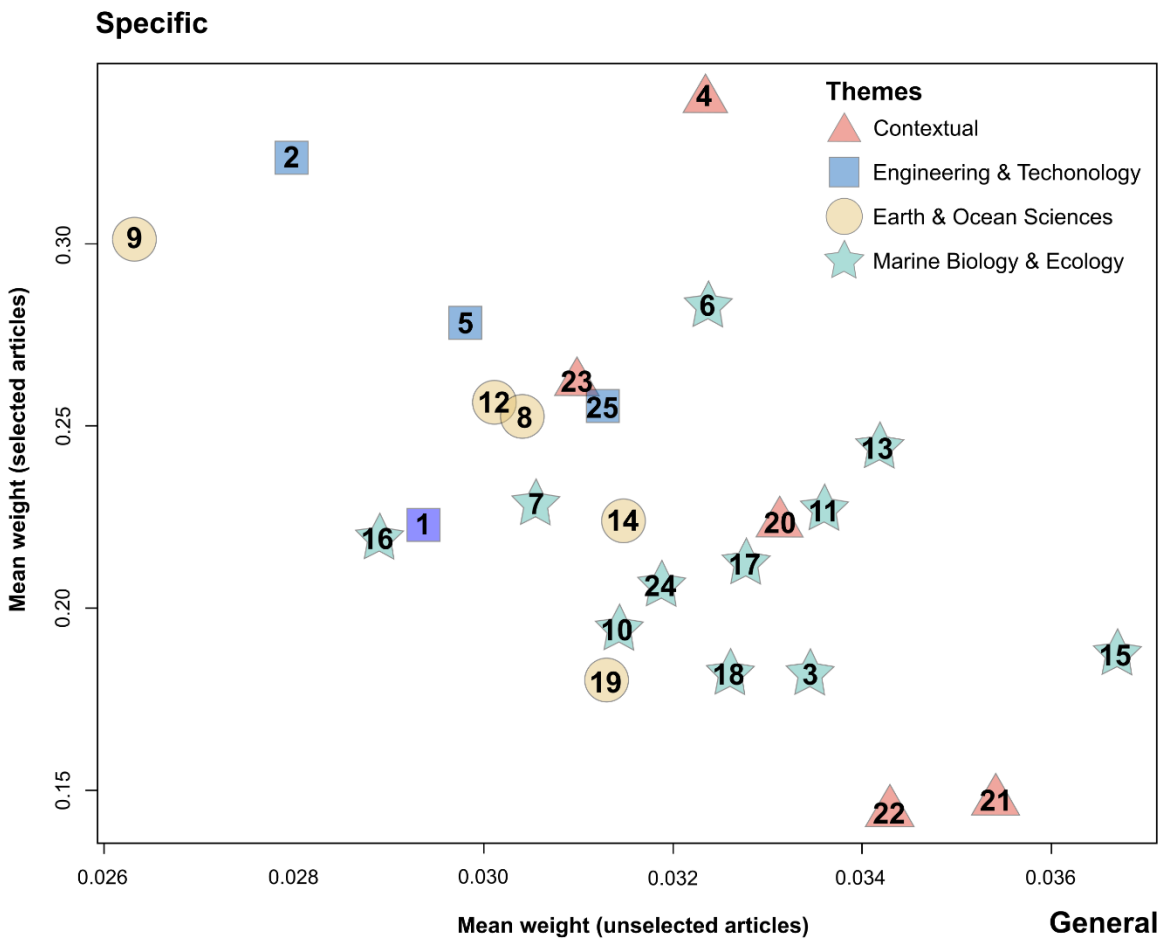

Figure 6. Topic generality analysis. The closer a topic is to the top left corner, the more specific that topic (the articles are more solely weighted to that topic). The closer a topic is to the bottom right corner, the more general the topic (the articles are weighted to other topics).

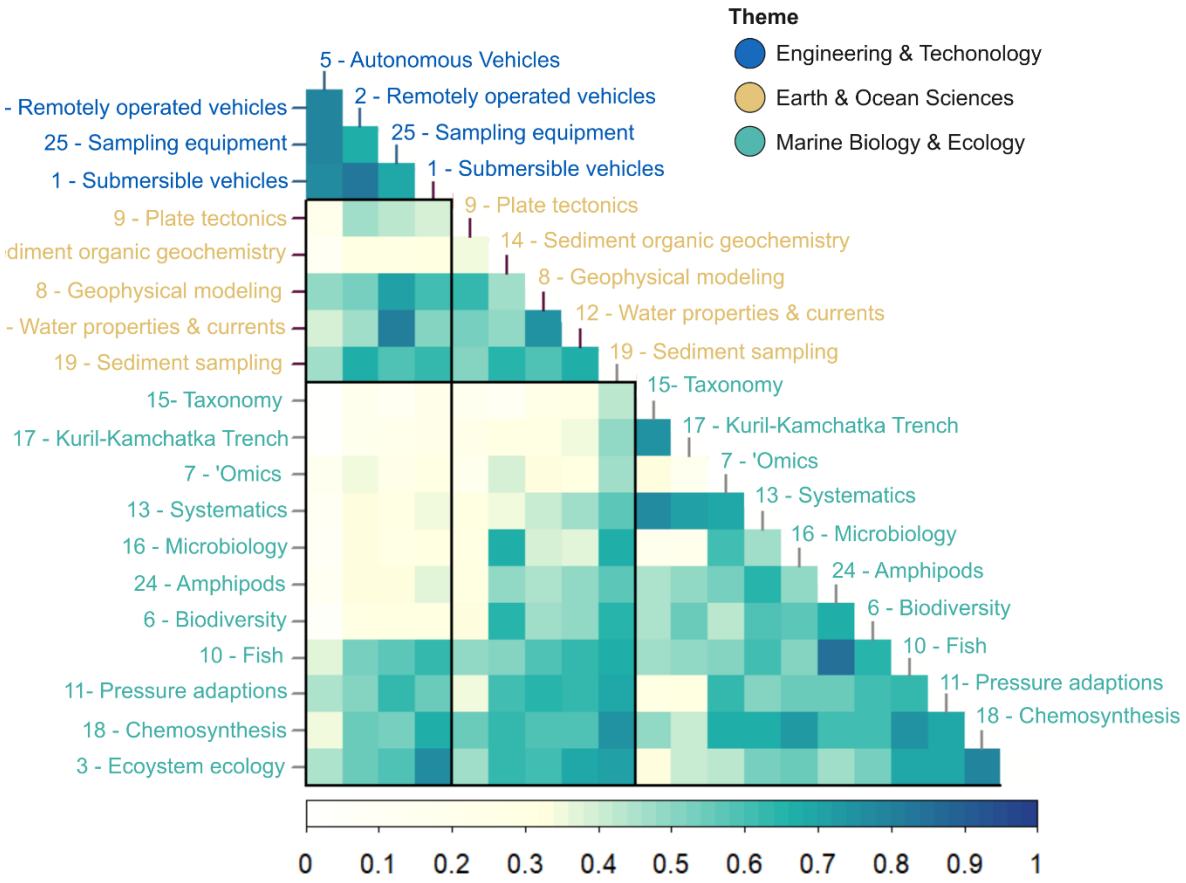

Figure 7. Correlation matrix of topic co-occurrence within abstracts. Zero (white) indicates that the two topics never co-occurred in an article, while one (dark blue) denotes that the pair of topics always co-occur in an article. Black outlined boxes indicate between-theme comparisons.

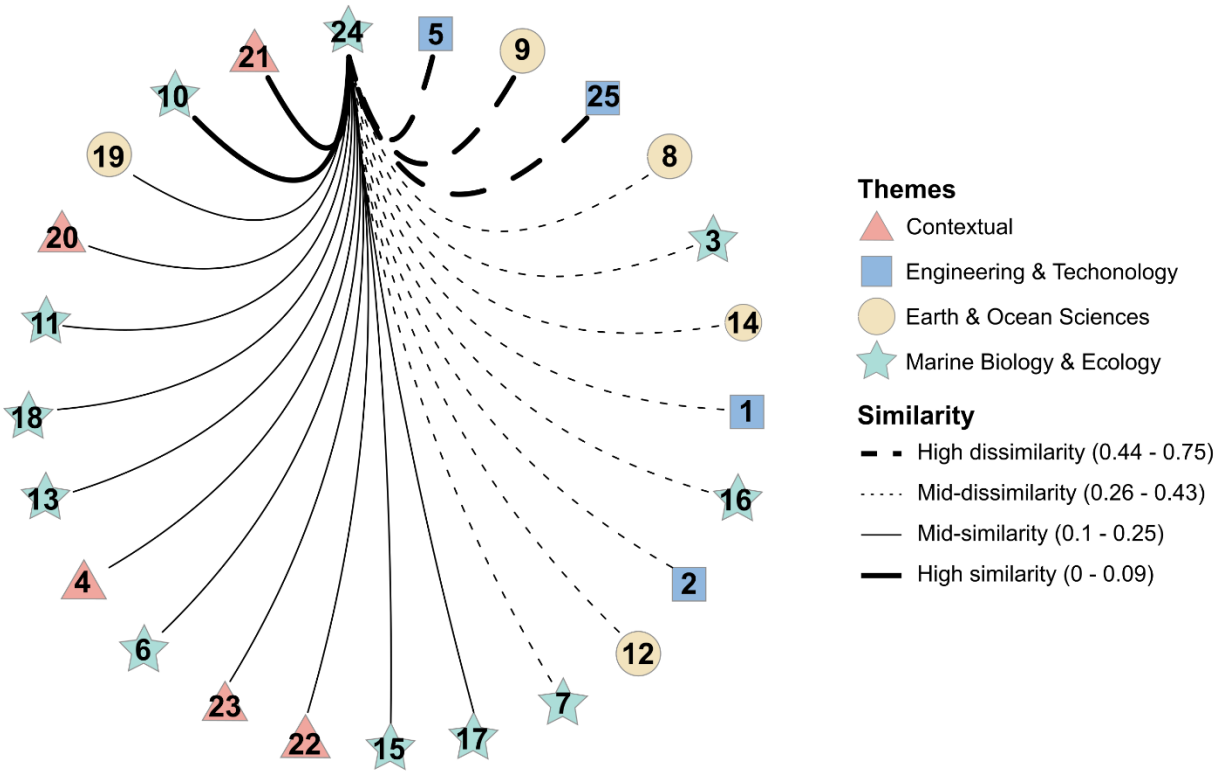

Figure 8. Gap analysis between *Amphipods* (Topic 24) and the 24 other topics based on the words per topic and topic per abstract probabilities. A thick solid line represents a high similarity between *Amphipods* and the other topics. A thick dotted line between *Amphipods* and the other topics represents high dissimilarity and highlights a potential research gap.

4. Discussion – State of Hadal Science

The topic modeling results highlight the exponential growth of hadal science over the past 29 years. In line with the birth of the field, the core of hadal research is focused on reaching the hadal zone ('Technology & Engineering'), measuring the environment ('Earth & Ocean Science'), documenting life ('Marine Biology & Ecology'), and making geographic and bathymetric comparisons ('Contextual'). With advances in capabilities of *in situ* sampling and molecular and modeling techniques, strong progress has been made to understand hadal ecosystems and the processes at play, especially at Challenger Deep. However, many hadal features are yet to be explored and observations to be made for many taxa along the hadal depth gradient. Amphipoda, well-connected across the corpus, represents a model taxon to address questions about ultra-deep-sea ecology and advance our understanding of the deepest marine habitat.

The growth of hadal research can be largely attributed to advances in the diversity and capability of technology and equipment to take physical samples (sediment, water, and biological), make measurements, and collect still images and videos (Jamieson, 2020). The theme 'Technology & Engineering' encompasses this diversity of sampling capabilities with submersible, remotely operated, and autonomous vehicles. The high co-occurrence within abstracts indicates that there are similar challenges faced when developing these technologies. A portion of the topic highlights the high cost and risk of loss of equipment. As an example, the loss of the ROV *Kaike* (Momma et al., 2004) and HROV *Nerus* (Cressay, 2014) underscores that reaching the hadal zone will always be a challenge, especially in comparison to shallower marine environments. The topic *Submersible vehicles* had grown over the past five years. This growth reflects the preferential use of free-fall 'lander' vehicles (Jamieson et al., 2010; Jamieson, 2016) and the focused effort to develop the capability to repeatably send human-piloted submersible vehicles to the hadal zone. Remarkably before 2019, only two human-piloted submersible vehicles had been to the deepest point on Earth, Challenger Deep (i.e., the bathyscaphe *Trieste* and submarine *Deepsea Challenger*; Jamieson 2015). This lack of human-piloted submersibles has shifted with the development of the DSV *Limiting Factor*. The circumglobal Five Deeps Expedition 2018-2019 (Jamieson et al., 2019; Stewart et al.,

2019) with the DSV *Limiting Factor* is anticipated to bring substantial expansion to the hadal science literature.

Improved capabilities to reach hadal depths correlated with the focus in the corpus to study the geophysical and hydrologic factors that shape the hadal environment ('Earth & Ocean Science') and characterize the biodiversity and drivers of life ('Marine Biology & Ecology'). This close association between science and engineering technology is readily visualized with high topic co-occurrence with *Geophysical Modeling*, *Water properties & current*, *Sediment sampling*, *Chemosynthesis,* and *Fish*. The 'Earth & Ocean Science' appeared to be a bipolar theme, with large-scale plate tectonic processes to specific-site specific sediment organic geochemical processes. Between the five 'Earth & Ocean Science' topics, *Sediment organic geochemistry* research is on the rise due to the increasing number of biogeochemical experiments in the deepest parts of Mariana, Tonga, Izu-Bonin, and Kermadec trenches. This research has revealed the importance of hadal ecosystems for deep-sea carbon and nitrogen cycling and diagenesis (Glud et al., 2013; Leduc et al., 2016; Wenzhöfer et al., 2016). This topic and theme are anticipated to see continued growth to understand how POM and other material is currently transported and processed in the hadal zone (Xu et al., 2018) and the implication of shifts in carbon inputs, temperature, and oxygen with climate change (Brito-Morales et al., 2020).

A strength of hadal science lies within 'Marine Biology & Ecology', as evident by the 11 topics. The expansion of this theme can be largely attributed to the investigation of the microbial communities in hadal sediments, expanding efforts to assess biodiversity and describe new species, and utilizing advanced 'Omic technologies (e.g., genomics, metabarcoding, proteomics) to address ecological and evolutionary questions. The biodiversity research trends at hadal depth are consistent with those in the shallower zones. A research science-mapping approach identified microbial and molecular analyses, biodiversity assessments, and zoology to be the biodiversity trends across the deep-sea (Costa et al., 2020). Among the diversity of life in the hadal zone, there is a focus on benthic biodiversity, with microbes, specifically piezophiles, scavenging amphipods, and snailfish, as the dominant megafauna of the hadal food web (Linley et al., 2016). Further, several of the topics focused on specimen identification, location,

description, and diversification. This highlights that knowing the individual species found in a deep-sea ecosystem is foundational to an understanding of biodiversity, connectivity, community ecology, and ecosystem function and services. This work is also ongoing at shallower depths, particularly at regions targeted for deep-sea mining and ecosystem-based management (e.g., Clarion-Clipperton Zone; Glover et al., 2018).

Amphipods, primarily from the Lysianassoidea and Allicelloidea superfamilies, emerged as one of the best sampled hadal fauna, as these mobile, invertebrates are readily recovered by different sampling techniques (trawling and baited landers; Figure 9; Jamieson 2016). They are conspicuous members of the benthic community, as voracious scavengers, and ubiquitous to full ocean depth (Dahl 1959; Ritchie et al., 2015; Lacey et al., 2016). With their moderate placement with the generality analysis and captured in sufficient numbers for statistically robust analysis, they have been used as a gateway for understanding hadal ecology. Research with amphipods has uncovered the presence of an ecotone between the abyssal and hadal zones (Fujii et al., 2013; Eustace et al., 2016; Lacey et al., 2016), vertical ontogenetic stratification (Blankenship et al., 2006; Lacey et al., 2018); trophic plasticity (Kaufmann, 1994; Blankenship & Levin, 2007; Kobayashi et al., 2012); predator-prey interactions (Linley et al., 2016), evolutionary history and cryptic speciation (Ritchie et al., 2015; Eustace et al., 2016), physiological, genome, and protein adaptions to hydrostatic pressure (Downing et al., 2018; Ritchie et al., 2017; 2018), connectivity between hadal habitats (Ritchie et al., 2019), and anthropogenic impacts (Jamieson et al., 2017; 2019; Weston et al., 2020).

While topic modeling illustrates an expansion of hadal research, these efforts have largely focused on one location. The underlying location bias resulted from the search terms ‘full ocean depth’, ‘deep ocean trench’, and ‘Challenger Deep’. These search terms increased the number of articles that were not captured by the term ‘hadal’ at the expense of largely focusing the corpus on the Mariana Trench and more specifically the Earth’s deepest point, Challenger Deep. This bias has been coined as the ‘Challenger Deep’ effect (Jamieson, 2018). Further, Jamieson (2018) warned that focusing on the outlier location would hinder progress at understanding the complexity across the hadal zone. The place terms within topics (i.e., Japan, Izu, Kermadec, and Peru) and an entire topic dedicated to the Kuril-Kamchatka Trench do illustrate that hadal science does exist

outside of the Mariana Trench. However, large knowledge gaps are present. This gap is readily seen with the uncertainty with the deepest location in each ocean and poorly resolved bathymetric maps (Stewart & Jamieson, 2019). Further, vast swathes of the hadal zone remain unexplored and unstudied (Jamieson, 2018), especially with non-subduction features and hadal features outside the Pacific Ocean (Stewart & Jamieson, 2019).

Jamieson (2018) suggested that hadal science is transitioning from an observational to an experimental era. However, the topic frequency and co-occurrence analysis imply that hadal science is still largely situated between explorational and observational eras, with topics of *Systematics*, *Biodiversity*, *Taxonomy*, *Presence & absence*, and *Kuril-Kamchatka Trench*. Yet, advances in sampling capabilities coupled with molecular and modeling techniques have allowed for more experimental questions, as highlighted with the rise of *'Omics* paired with *Systematics*, *Chemosynthesis,* and *Microbiology.*

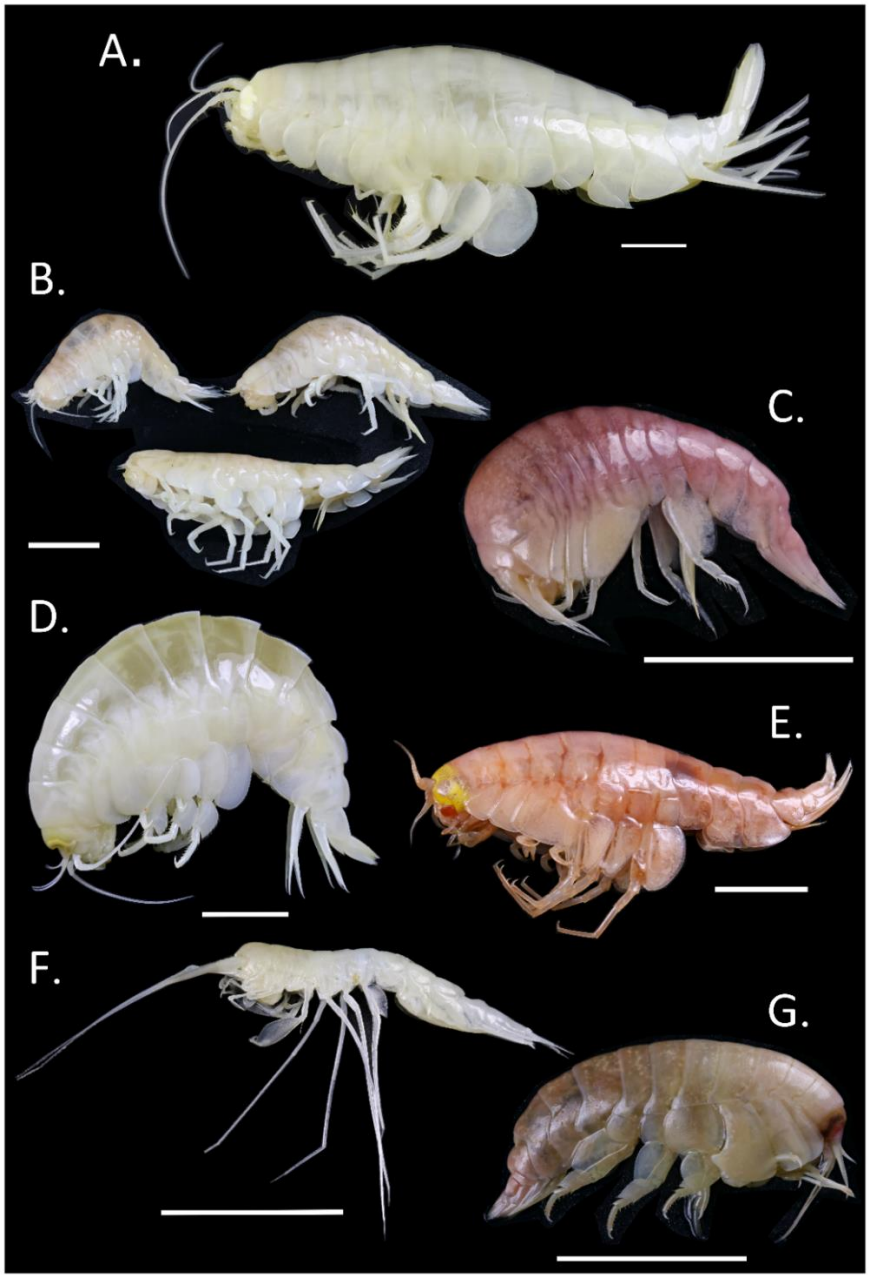

Figure 9. Hadal amphipods. (A) *Alicella gigantea* Chevreux, 1899 from 7094 m in the Mariana Trench. (B) *Bathycallisoma schellenbergi* (Birstein & Vinogradov, 1958) from 8370 m in the Puerto Rico Trench. (C) Stegocephalidae gen. sp. from 8380 m in the Puerto Rico Trench. (D) *Eurythenes magellanicus* (H. Milne Edwards, 1848) from 8094 m in the Mariana Trench. (E) *Hirondellea gigas* (Birstein & Vinogradov, 1955) from 10,936 m in Mariana Trench. (F) *Hyperiopsis laticarpa* Birstein & M. Vinogradov, 1955 from 10,936 m in the Mariana Trench. (G) *Stephonyx* sp. nov. from 8380 m in the Puerto Rico Trench. Scale bar 1 cm.

5. Thesis Aims and Objectives

As highlighted through topic modeling, hadal science is moving towards an experimental era but still has many locations to explore and observations to make. Scavenging amphipods represent a model taxon to expand our understanding of how the hadal environment drives diversity, shapes the structure of populations and communities, and influences connectivity of populations between the geographically disjunct features. Rooted by the existing body of literature on the ecology and genomics of amphipods, this thesis will use scavenging amphipods to move the state of hadal science forward by exploring the community of a non-subduction hadal feature, describing new species, and testing for traces of global connectivity between hadal features.

This thesis has three key aims and themes:

- First, to apply an integrative taxonomic approach to expand the known and described diversity of deep-sea scavenging amphipods and gain insights into biogeography.
- Second, to assess the patterns of amphipod community structure in a hadal non-subduction feature.
- Third, to investigate the level of genetic connectivity between hadal populations and test the traditional hypothesis that hadal ecosystems are evolutionarily and demographically independent units.

These aims will be addressed through the following five specific studies.

Chapter 2 describes the ninth species within the genus *Eurythenes,* namely *Eurythenes plasticus* sp. nov. While *Eurythenes* are iconic and quintessential members of the deep-sea benthic community, several phylogenetic studies have revealed elevated diversity with the genus, which has been masked by cryptic speciation (Havermans et al., 2013, d'Udekem & Havermans, 2015, Ritchie et al., 2015). This chapter will test the hypothesis that specimens recovered from upper hadal depths (6010–6949 m) of the Mariana Trench represent a distinct and undescribed lineage within *Eurythenes*. Additionally, hadal scavenging amphipods in Mariana, Kermadec, and Peru-Chile trenches have been found to inadvertently ingest microplastics, indicating that that depth is not a barrier to anthropogenic impacts (Jamieson et al., 2019). This study will continue

to track the presence of microplastics in the hadal zone and examine whether a species being unknown to science shields it from human pollutants.

Chapter 3 describes the tenth species of *Eurythenes*, namely *Eurythenes atacamensis* sp. nov. from the Peru-Chile Trench, western South Pacific Ocean. The Peru-Chile Trench is unique among hadal subduction features with a eutrophic environment and a largely endemic faunal community. Previous studies have determined this species to be a distinct species within *Eurythenes*, considered it endemic to hadal depths of the Peru-Chile Trench, and found patterns of ontogenetic vertical stratification. This chapter applies an integrative taxonomic approach to specimens recovered from the 2018 RV *Sonne* SO261 and *Atacamex* Expeditions to the Atacama Trench (4974–8081 m). Additionally, morphometric relationships and bathymetric trends in size and sex are assessed to better understand how ecological strategies are employed by amphipods to survive in the subduction trench environment.

Chapter 4 describes two new species of scavenging amphipods, *Stephonyx sigmacrus* sp. nov. and *Civifractura serendipia* gen. et. sp. nov., recovered from abyssal depths (4932 m) of the Wallaby-Zenith Fracture Zone (WZFZ), Indian Ocean. The abyssal and hadal zone of the Indian Ocean are some of the least explored depths in a field already defined by under-sampling. This chapter will focus on the identification of new specimens from the WZFZ to accurately resolved their taxonomic placement and illuminate their evolutionary relationships. As traditional morphological identification approaches underestimate diversity because of phenotypic plasticity, convergent evolution, and limited species (Ritchie et al., 2015), the study will apply a combined morphological with a molecular phylogenetic analysis of two mitochondrial (16S rDNA and COI) and two nuclear (Histone 3 and 28S rRNA) regions to specimens in the family Alicellidae. This approach is applied to test whether a specimen that morphological appears to fit within the existing genus, *Tectovalopsis*, or is best placed in a new genus.

Chapter 5 examines three aspects of the scavenging amphipod community across the abyssal-hadal transition zone in the WZFZ. This study represents the first biological account of a non-subduction hadal feature, which is just deep enough (~6600 m) to be considered hadal. This study tests the hypothesis that definition hadal is a function of the geomorphology not purely depth and thus the community at WZFZ is an extension of the

abyssal community. To do this, this chapter assesses the amphipod community structure across the abyssal-hadal transition zone, demographic patterns of the dominant hadal species, and the phylogeographic relationships between the WZFZ's *B. schellenbergi* population and four Pacific Ocean trench populations.

Chapter 6 is a global study to assess cryptic speciation and explore phylogeographic patterns in the hadal zone. This study tests the concept that hadal ecosystems are hotspots of endemism and genetically isolated units, resulting from extreme environmental conditions, long-term geographical isolation, and evolutionary selection pressures. The model species for testing hadal endemism is *Bathycallisoma schellenbergi* (Birstein & Vinogradov, 1958), considered to be a quintessential hadal amphipod with a cosmopolitan distribution (Figure 9b). This study will investigate sequence variation at two partial regions of the mitochondria (16S and COI) between populations from 12 hadal features across the Pacific, Atlantic, Indian, and Southern oceans.

This thesis is made possible by utilizing two core resources. The first key resource is an extensive library of specimens collected over ten years via baited trap landers. The unbridled access to this world-class library allowed for the investigations to not be limited by sample location, depth, and diversity. Additionally, as much of the historical collection has been previously identified and curated by taxonomists from NIWA (Kilgallen, 2015; Eustace et al., 2015; Lacey et al., 2016), this provided comparative material on-hand for the processing and identification of the newly collected specimens. Specimens were collected between 2008 and 2018 over 12 cruises that sampled six hadal trenches, one non-subduction hadal features, and two abyssal features: Japan Trench (RV *Hakuho-Maru* 2008-KH0803), Izu-Bonin Trench (RV *Tansei-Maru* 2009-KT0903), Kermadec Trench (RV *Kaharoa* 2009-KAH0910; 2011-KAH1109; 2012-KAH1202; 2013-KAH1301), Mariana Trench (RV *Falkor* 2014-FK141109; TV *Shinyo-Maru* 2015-SY1615), New Hebrides Trench (RV *Kaharoa* 2013-KAH1310), South Fiji Basin (RV *Kaharoa* 2013-KAH1310), Peru-Chile Trench (RV *Sonne* 2010-SO209; 2018-SO261), Wallaby-Zenith Fracture Zone (RV *Sonne* 2017-SO258), Afanasy Nikitin Seamount (RV *Sonne* 2017-SO258). Further, during the time frame of my thesis, amphipods were collected as part of the Five Deeps Expedition (FDE) on board the DSSV *Pressure Drop* from an additional

seven hadal features: Puerto Rico Trench (2018–FDE-PRT), South Sandwich Trench (2019–FDE-SST), Java Trench (2019–FDE-JAV), Diamantina Fracture Zone (2019-FDE-DIA), Mariana Trench (2019-FDE-MAR), San Cristobal Trench (2019-FDE-SOL), Santa Cruz Trench (2019-FDE-SOL), and Tonga Trench (2019-FDE-TON). While most of these cruises occurred before this thesis, I participated in the collection of specimens from Puerto Rico, San Cristobal, Santa Cruz, Marian, and Tonga trenches. In addition to baiting the traps, recovering the samples, and doing an initial sort, count, and identification of specimens, focused time was spent taking high-quality photographs of specimens (Figure 9; Figure 3c). This is a valuable identification resource, as many of the species are documented only in taxonomic illustrations or at best with low-quality photographs and some species of amphipod have a body natural colour (e.g., *Eurythenes* spp. can vary from white to dark red) and eye colour that can be lost with ethanol preservation.

Samples from Mariana Trench (FK141109) were used in **Chapter 2**. **Chapter 4** describes specimens from Wallaby-Zenith Fracture Zone and relies on the analysis of comparative material from Mariana Trench (FK141109), New Hebrides Trench, Peru-Chile Trench (SO209), and Afanasy Nikitin Seamount. **Chapter 5** is focused on samples from Wallaby-Zenith Fracture Zone and Afanasy Nikitin Seamount, and identification of specimens is supported by access to the entire library. **Chapter 6** includes specimens of *B. schellenbergi* from all available populations, including those newly collected in the Five Deeps Expedition to give a comprehensive global dataset.

Specimens were collected by the same sampling technique–baited invertebrate traps on an autonomous lander vehicle (Figure 3a). Across the diverse number of cruises, the specific lander vehicle varied, but the technical principle and sampling technique remained consistent. An autonomous lander vehicle has two main components: the delivery system and the scientific payload (Jamieson et al., 2010). The delivery system comprises of an expendable ballast weight to sink the lander, a device (timed or acoustic release) to jettison the ballast weight, and subsurface buoyancy to float the lander back to the surface. The scientific payload includes at a minimum a pressure sensor to measure depth and sampling devices (e.g., cameras and traps). The invertebrate traps are a cylindrical trap mounted to the base of the lander, with a funnel entrance on at least

one side. The traps are baited with mackerel or similarly oily fish to generate an odor plume to attract amphipods to the bait (Scombridae; Jamieson et al., 2011). The lander remains on the seafloor bottom for a minimum of 7 hours. When the lander arrives on the surface, the amphipods are removed from the trap and preserved in 70% ethanol, which allows for both morphological taxonomic identification and genetic analysis.

The second core resource is an established and working protocol for DNA barcoding of deep-sea amphipod and a growing library of comparative sequences available on GenBank. The morphological identification of abyssal and hadal amphipods is challenged by phenotypic plasticity, cryptic speciation, limited specimens, and gaps in historical description or descriptions still untranslated from their original language. DNA barcoding is a complementary, genetic method of identifying organisms based on short, standardized fragments of genomic DNA through a multiple-step process: DNA extraction, PCR amplification sequencing, and comparison against a library (Herbert et al., 2003; Figure 10). Thus, the ability for identification is only as good as the library of comparative sequences and confidence in those identifications. While DNA barcoding is applied across many taxa such as plants and insects, abyssal and hadal amphipods pose challenges to extracting sufficient quality and quantity of DNA for successful PCRs and subsequent sequencing. This is largely attributed to minimal white, muscle tissue, DNA sheering from depressurization, and DNA sheering while at the surface. Ritchie et al. (2015) established a suite of protocols for DNA extraction, PCR amplification of the partial regions of the mitochondrial 16S rRNA and COI gene, and Sanger sequencing that form the methodological foundation for each Chapter. In addition to the protocols, the sequence data for the 25 putative species are publicly available on GenBank. Those set of DNA barcodes and others generated in Havermans et al. (2013), Corrigan et al. (2014), Havermans (2016), Narahara-Nakano et al. (2017), and Ritchie et al. (2017) provide comparative sequences for the new DNA barcoding data generated in this thesis.

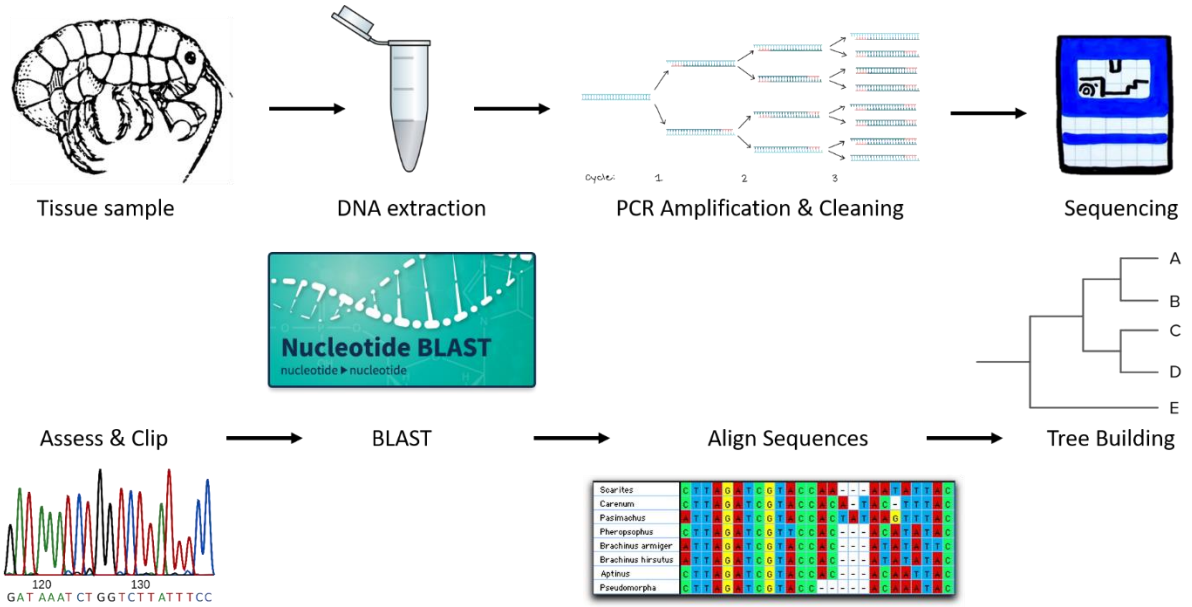

Figure 10. Conceptual schematic of the eight main steps in the DNA barcoding workflow.

Chapter 2: New species of *Eurythenes* from hadal depths of the Mariana Trench, Pacific Ocean (Crustacea: Amphipoda)

Published as: Weston, J.N.J., Carrillo-Barragan, P., Linley, T.D., Reid, W.D.K. and Jamieson, A.J., 2020. New species of *Eurythenes* from hadal depths of the Mariana Trench, Pacific Ocean (Crustacea: Amphipoda). *Zootaxa*, *4748*(1), pp.163-181. doi:10.11646/zootaxa.4748.1.9

Abstract

Eurythenes S. I. Smith in Scudder, 1882 are one of the largest scavenging deep-sea amphipods (max. 154 mm) and are found in every ocean across an extensive bathymetric range from the shallow polar waters to hadal depths. Recent systematic studies of the genus have illuminated a cryptic species complex and highlighted the benefits of using a combination of morphological and molecular identification approaches. In this study, we present the ninth species, *Eurythenes plasticus* sp. nov., which was recovered using baited traps between the depths 6010 and 6949 m in the Mariana Trench (Northwest Pacific Ocean) in 2014. This new *Eurythenes* species was found to have distinct morphological characteristics and be a well-supported clade based on sequence variation at two mitochondrial regions (16S rDNA and COI). While this species is new to science and lives in the remote hadal zone, it is not exempt from the impacts of anthropogenic pollution. Indeed, one individual was found to have a microplastic fibre, 83.74% similar to polyethylene terephthalate (PET), in its hindgut. As this species has a bathymetric range spanning from abyssal to hadal depths in the Central Pacific Ocean basin, it offers further insights into the biogeography of *Eurythenes*.

Keywords

Deep-sea, integrated taxonomy, cryptic species, molecular phylogeny, microplastic fibre, pollution

1. Introduction

While the deep sea is one of the largest ecosystems on Earth, it has traditionally been perceived as a homogenous environment, with few barriers to gene flow (Madsen, 1961; Charette & Smith, 2010). This led to the assumption that many deep-sea species are cosmopolitan, with several appearing to have large geographical and bathymetrical ranges (>3000 m; King & Priede, 2008; Brandt et al., 2012; Jamieson et al., 2013). The deep sea, however, has a high degree of topographic complexity including mid-oceanic ridges, submarine canyons, seamounts, and subduction trenches, which could act as barriers. These barriers potentially restrain gene flow and promote allopatric speciation (Palumbi, 1994). This cosmopolitan species concept has now been challenged on several occasions by genetic techniques, whereby widespread deep-sea species are in fact comprised of species complexes with several cryptic or pseudocryptic species (Garlitska et al., 2012; Cornils & Held, 2014).

The lysianassoid amphipod, *Eurythenes gryllus* (Lichtenstein in Mandt, 1822), is a quintessential and abundant member of the deep-sea benthic community. *Eurythenes gryllus* has long been considered cosmopolitan with an extensive bathymetric range (184 to 8000 m), which spans the bathyal, abyssal, and hadal zones (Hessler et al., 1978; Ingram & Hessler, 1987; Thurston et al., 2002). However, genetic diversity studies have indicated that *E. gryllus* is not a single species but a species complex (France & Kocher, 1992; Havermans et al., 2013), with nuclear and mitochondrial DNA sequence data indicating the *gryllus*-complex to be composed of at least nine to twelve distinct clades (Havermans et al., 2013; Eustace et al., 2016; Havermans, 2016). Our initial understanding of *E. gryllus* as a single cosmopolitan deep-sea species is reconceptualised when viewed as a species-complex. This provides a much more nuanced picture of their distribution, amphitropical at bathyal depths, and reveals a patchwork of distribution patterns with the complex's radiation. For example, *Eurythenes maldoror* d'Udekem d'Acoz & Havermans, 2015 (i.e., clade Eg3) is from abyssal depths in all oceans but the Arctic, while *Eurythenes* sp. 'hadal' is limited to hadal depths within the Peru-Chile Trench (Eustace et al., 2016).

Havermans et al. (2013) initiated a reverse taxonomic approach to determine the genetic diversity within the *Eurythenes* genus, whereby a potentially new species is first

genetically identified and then the morphological characters are determined (Markmann & Tautz, 2005). This resulted in *Eurythenes* S. I. Smith in Scudder, 1882 expanding from four to eight described species since the establishment of the monogeneric family (Stoddart & Lowry, 2004). Specifically, *Eurythenes aequailatus* Narhara-Nakano, Nakano & Tomikawa, 2017, *Eurythenes andhakarae* d'Udekem d'Acoz & Havermans, 2015, *E. maldoror*, and *Eurythenes sigmiferus* d'Udekem d'Acoz & Havermans, 2015 were described based on combined molecular and morphological methods. In addition to these described species within the *gryllus*-complex, two species from abyssal and hadal depths of the Peru-Chile Trench are awaiting formal description (Eustace et al., 2016) and at least six distinct genetic clades lack morphological examination (e.g., clades Eg7-9; Havermans et al., 2013; Havermans, 2016). The suite of morphological characters that separate species within the *gryllus*-complex remain unclear and are challenging to observe (d'Udekem d'Acoz & Havermans, 2015), which highlights the importance of integrating together molecular and morphological identification approaches.

The evolutionary success of *Eurythenes,* with the exception of the pelagic *Eurythenes obesus* (Chevreux, 1905), has largely been attributed to their scavenging plasticity, from detritivory, intercepting large carcasses, and ingesting mud (Barnard, 1962; Ingram & Hessler, 1983; Blankenship & Levin, 2007; Havermans & Smetacket, 2018). However, deep-sea amphipods, including *Eurythenes*, may be particularly susceptible to ingesting microplastics given they are voracious and non-selective scavengers (Hargrave, 1985; Blankenship & Levin, 2007). Indeed, microplastics fibres have already been found in the hindguts of hadal-dwelling amphipods, including the *Eurythenes* sp. 'hadal' from the Peru-Chile Trench at 7050 m (Jamieson et al., 2019). Furthermore, every individual of the hadal scavenging amphipod, *Hirondellea gigas* (Birstein & Vinogradov, 1955), examined from the deepest point in the Mariana Trench contained at least one man-made fibre in its hindgut (Jamieson et al., 2019). Microplastics are transferred to hadal environment via multiple mechanisms, including direct deposit in carrion, marine snow, and trench sediment consolidation (Taylor et al., 2016; Peng et al., 2018; Jamieson et al., 2019). With the increase in plastic debris entering the deep sea (Schlining et al., 2013; Chiba et al., 2018), including to full ocean depth (Peng et al., 2018; Peng et al., 2020), the probability of consuming such pollutants increases. It is highly

likely that individuals of other scavenger species residing in the Mariana Trench are similarly susceptible to ingesting microplastics fibres.

In this study, we examined the morphological characteristics and sequence variation at the mitochondrial 16S ribosomal DNA (16S) and cytochrome oxidase I (COI) regions of *Eurythenes* specimens collected from hadal depths in the Mariana Trench, Pacific Ocean and considered their taxonomic placement within the *gryllus*-complex. We describe the ninth species within the genus, *Eurythenes plasticus* sp. nov. We also examined the hindgut for the presence of microplastic fibres to continue to track the reach of this ubiquitous pollutant at hadal depths.

2. Material and Methods

2.1 Specimen collection

Specimens were collected in November 2014 as part of the HADES–M (HADal Ecosystems Studies) expedition cruise FK141109 on the RV *Falkor* to Sirena Deep, Mariana Trench, Pacific Ocean. The amphipods were recovered using the full-ocean depth *Hadal-lander* (Jamieson, 2015; Linley et al., 2016). The *Hadal-lander* was equipped with PVC funnel traps baited with whole mackerel bait (Scombridae) and a temperature and pressure sensor (SBE-39, SeaBird Electronics, USA). Pressure was converted to depth (m) following Saunders (1981). Collection sites are shown in Figure 11 and site details are provided in Table 2. Amphipods were preserved with 70% ethanol upon recovery.

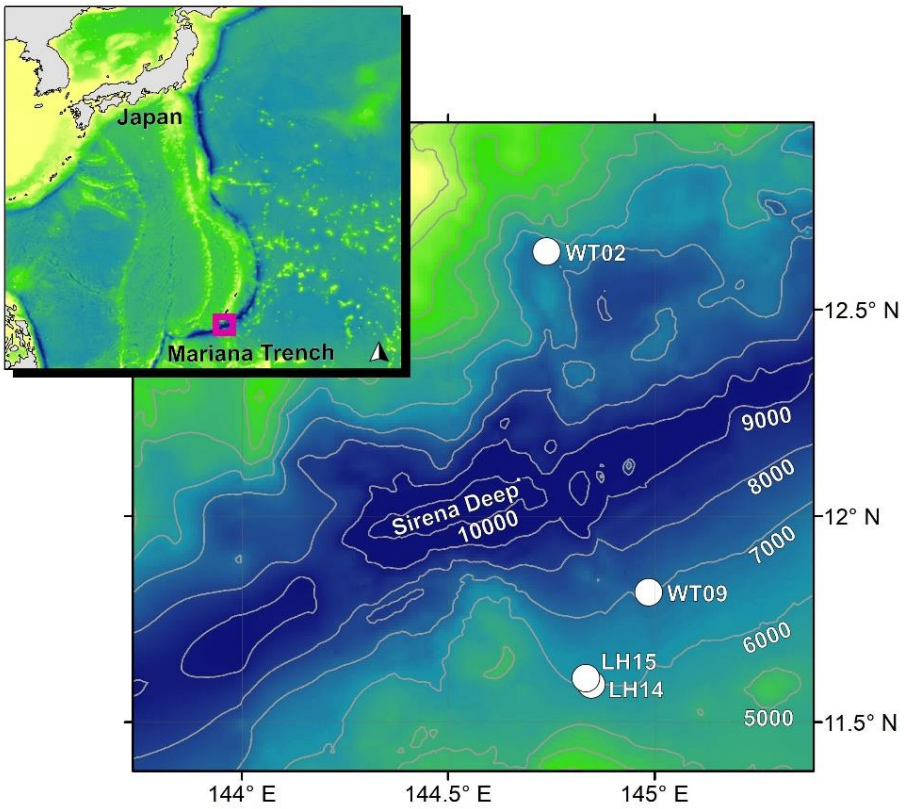

Figure 11. Map of sampling stations within across the Sirena Deep, Mariana Trench, Pacific Ocean (white circles). Maps were produced with GEBCO bathymetry data (GEBCO 2015). Isobaths are added for every 1000 m and labelled between 5000 to 10,000 m.

Table 2. Collection information for specimens collected on the 2014 cruise FK141109 of the RV *Falkor*. Included is the number of individuals by gender collected at each depth.

Station	Date	Latitude	Longitude	Depth (m)	Female	Male	Juvenile
LH14	26/11/2014	11.5911'N	144.84730'E	6010	–	1	–
LH15	27/11/2014	11.6071'N	144.8331'E	6142	1	–	–
WT02	14/11/2014	12.64065'N	144.73796'E	6865	1	–	7
WT09	24/11/2014	11.8147'N	144.98580'E	6949	–	–	1

2.2 Morphological Assessment and Digital Illustration

Whole specimens were photographed with a Canon EOS 750D DSLR camera, Tamron SP 90mm f/2.8 VC USD Macro 1:1 VC Lens with polarising filter, and Falcon Eyes CS-730 copy stand and processed with Helicon Focus and Helicon Remote software (HeliconSoft). Body length was measured from the rostrum to the tip of telson. Appendages were dissected using a Wild Heerbrugg M8 stereomicroscope and imaged with a Leica DMi8 inverted microscope and DFC295 camera. Lengths of appendages and articles were measured following Horton & Thurston (2014) to provide consistency regardless of the degree of flexion. Images were converted into digital illustrations using Inkscape v0.92.2 (Coleman, 2003; 2009). Type and non-type specimens are deposited at the Smithsonian Institution National Museum of Natural History, Washington, D.C., USA (USNM).

2.3 Phylogenetics

Total genomic DNA was extracted from either the head or a pair of pleopods depending on the size of the specimen using the Bioline ISOLATE II Genomic DNA Kit. Two partial regions of the mitochondrial DNA were amplified. The 16S (260 bp) was amplified with AMPH1 (France & Kocher, 1996) and 'Drosophila-type' 16SBr (Palumbi et al., 2002) primers and COI (624 bp) was amplified with LCO1490 and HCO12198 (Folmer et al., 1994) primers. PCR protocols were as described in Ritchie et al. (2015). PCR products were purified enzymatically using New England Biolabs Exonuclease 1 and Antarctic Phosphatase and sequenced with an ABI 3730XL sequencer (Eurofins Genomics, Germany).

Electropherograms were viewed and primers and any ambiguous sequences were trimmed in MEGA 7 (Kumar et al., 2016). Sequences were initially blasted using default parameters on NCBI BLASTn. COI sequences were translated into amino acid

sequences to confirm that no stop codons were present. Nucleotide alignments with comparative sequences were made using MAFFT v7 (Table 3; Katoh et al., 2019). The optimal evolutionary models for each alignment were identified by modeltest in the *phangorn* 2.4.0 package (Schliep et al., 2017). The optimal Akaike Information Criterion and Bayesian Information Criterion indicated the HKY + I + G model for both alignments (Hasegawa et al., 1985). Phylogenetic relationships were inferred via the maximum-likelihood approach using PhyML v3.1 (Guidon et al., 2010) and the Bayesian approach using BEAST v1.8.4 (Drummond et al., 2012). Maximum-likelihood analyses were conducted with a neighbour-joining starting tree and using nearest neighbour interchange branch swapping using the model of sequence evolution and parameters estimated by PhyML. The stability of nodes was assessed from bootstrap support based upon 10,000 iterations. Bayesian analyses were performed for two independent runs of 40,000,000 generations sampling every 10,000 generations using the respective evolutionary models and an uncorrelated relaxed clock (Drummond et al., 2006). Outputs were assessed in Tracer v1.7 to ensure convergence (ESS < 200) (Rambaut et al., 2018) and combined in LogCombiner v1.8.4. The first 4,000,000 states were discarded. The maximum clade credibility tree was generated through TreeAnnotator v1.8.4, viewed in FigTree v1.4.3, and annotated using Inkscape v0.92.2. Two independent methods were used to infer species delimitation on each dataset, specifically a Bayesian Poisson Tree Processes (bPTP) model (Zhang et al., 2013) and sequence divergence using the Kimura 2-parameter (K2P) distance model (Kimura, 1980).

Table 3. Species, sequence accession numbers and references for phylogenetic analysis of *Eurythenes plasticus* sp. nov.

Species	16S	COI	Reference
Alicella gigantea	KP456083	KP713893	Ritchie et al., 2015
Eurythenes aequilatus	LC229090	LC229094	Narahara-Nakano et al., 2017
Eurythenes aequilatus	LC229091	LC229095	Narahara-Nakano et al., 2017
Eurythenes andhakarae	JX887065	JX887114	Havermans et al., 2013
Eurythenes andhakarae	JX887066	JX887119	Havermans et al., 2013
Eurythenes gryllus	JX887060	JX887132	Havermans et al., 2013
Eurythenes gryllus	JX887063	JX887136	Havermans et al., 2013
Eurythenes magellanicus	LC192879	LC192881	Narahara-Nakano et al., 2017
Eurythenes magellanicus	JX887071	JX887144	Havermans et al., 2013
Eurythenes magellanicus	JX887074	JX887145	Havermans et al., 2013
Eurythenes magellanicus	–	KX078274	Havermans, 2016
Eurythenes maldoror	JX887069	JX887151	Havermans et al., 2013
Eurythenes maldoror	JX887068	JX887152	Havermans et al., 2013
Eurythenes maldoror	JX887067	JX887121	Havermans et al., 2013
Eurythenes maldoror	KX034310	KX365240	Ritchie et al., 2017
Eurythenes obseus	KP456144	KP713954	Ritchie et al., 2015
Eurythenes plasticus sp. nov.	MT021437	MT038070	This study
Eurythenes plasticus sp. nov.	MT021438	MT038071	This study
Eurythenes plasticus sp. nov.	MT021439	MT038072	This study
Eurythenes sigmiferus	JX887070	–	Havermans et al., 2013
Eurythenes sigmiferus	AY943568	–	Escobar-Briones et al., 2010
Eurythenes thurstoni	U40449	–	France & Kocher, 1996
Eurythenes cf. *thurstoni*	–	KX078272	Havermans 2016
Eurythenes sp. Eg7	U40445	–	France & Kocher, 1996
Eurythenes sp. Eg8	U40439	–	France & Kocher, 1996
Eurythenes sp. Eg8	U40440	–	France & Kocher, 1996
Eurythenes sp. Eg9	U40446	–	France & Kocher, 1996
Eurythenes sp. Eg9	U40448	–	France & Kocher, 1996
Eurythenes sp. 'PCT abyssal'	KP456140	KP713957	Ritchie et al., 2015
Eurythenes sp. 'PCT abyssal'	KP456141	KP713958	Ritchie et al., 2015
Eurythenes sp. 'PCT hadal'	KP456138	KP713955	Ritchie et al., 2015
Eurythenes sp. 'PCT hadal'	KP456139	KP713956	Ritchie et al., 2015
Eurythenes sp. 1 (WDL–d1)	–	KX078273	Havermans, 2016
Eurythenes sp. 2 (MOZ–1)	–	KX078271	Havermans, 2016

2.4 Sample Digestion and Analysis for Microplastic Ingestion

Preventive measures were taken to reduce and monitor for potential sources of contamination due to the ubiquity of microplastic fibres in the environment (Wesch et al., 2017). Samples were prepared and analysed in a clean laboratory with restricted access, where only one researcher, wearing a 100% clean lab coat at all times, was present conducting the experiment. Before any work session, benches were wiped with 70% ethanol on a 100% cotton cloth and allowed to dry fully. Only non-plastic equipment (glass and metal) were used to process the samples. Glass Petri dishes, graduated piston pipettes and test tubes were thoroughly washed with pre-filtered deionised water (DI),

rinsed with acetone, covered with aluminium foil, and allowed to dry at 70 °C in a drying oven. The digestion and filtration steps were conducted under a laminar flow cabinet (Purair, LS series, Air Science, USA LLC). The equipment and samples were covered wherever possible to minimize environmental exposure. Additionally, procedural blanks were run in parallel with samples to monitor environmental contamination. Meaning, a glass petri dish with a damped Whatman glass fibre filter was left open next to the microscope during the specimens' dissection (Murphy et al., 2016), while two empty glass tubes were processed as described below. The resulting three blanks filters were examined under a stereo microscope (Leica M205C, Leica Microsystems GmbH, Germany) to correct for potential air-borne and/or procedural plastic contamination.

Four *E. plasticus* sp. nov. specimens were selected for microplastic analysis: three juveniles (15.1, 15.6, and 23.1 mm body length) from 6865 m and one juvenile (15.6 mm body length) from 6949 m. Each specimen was individually rinsed with pre-filtered DI water and inspected under a stereo microscope (Leica M205C, Leica Microsystems GmbH, Germany), to ensure each specimen was free from external contamination. The hindgut was removed as described in Jamieson et al. (2019) and individually placed in 10 mL glass tubes. Aluminium foil was used to cover the tubes. After recording its wet mass, the hindgut was submerged in 10% m/v potassium hydroxide (KOH), using a volume at least three times greater than that occupied by the biological material (Foekema et al., 2013). The samples plus two procedural blanks (borosilicate tubes with 2 and 7 mL 10% KOH solution) were incubated for over a 36-hour period at 40 °C. After digestion, samples were left to cool inside a desiccator, following vacuum filtration through 0.6 µm glass fibre filters (Advantec Grade GA55, Advantec MSF Inc., Japan). Filters were individually placed onto a glass Petri dish until further microscopic inspection.

Once dried, glass fibre filters were examined under a stereo microscope. The physical appearance (e.g., colour, shape, size) of the putative particles (e.g., fibre, fragment) per filter was recorded. Said particles were then transferred onto gold platted slides (Thermo Fisher Scientific Inc., UK) for Fourier-transform infrared spectroscopy (FTIR) analysis. A Nicolet iN10 FTIR micro spectroscope (Thermo Fisher Scientific Inc., UK) was employed to obtain the particle's infrared transmittance spectra, using the liquid nitrogen cooled Mercury Cadmium Telluride detector. Results were then visualised and

matched against a series of inbuilt reference spectra libraries using the instrument's software (OMNIC Picta v1.7) to determine the chemical identity of the analysed particles.

3 Results

3.1 Phylogenetics and Species Delimitation Analysis

Three specimens of *Eurythenes plasticus* sp. nov. were successfully characterised across the two partial gene amplicons. The sequences have been annotated and deposited into GenBank (Table 3; 16S MT021437–39 and COI MT038070–72).

The phylogenetic relationship of *E*. *plasticus* sp. nov. within *Eurythenes* was investigated in separate16S and COI datasets. These comparative datasets were constructed from sequences that are associated with either: type material, specimens identified high degree of confidence, or specimens from a known clade or undescribed lineage (Table 3; France & Kocher, 1996; Escobar-Briones et al., 2010; Havermans et al., 2013; Ritchie et al., 2015; Eustace et al., 2016; Havermans, 2016; Narahara-Nakano et al., 2017; Ritchie et al., 2017). For the 16S dataset, 26 individuals consisting of the eight species of *Eurythenes* and five genetic clades fit these criteria. For the COI dataset, 25 individuals consisting of seven species of *Eurythenes* and four genetic clades fit these criteria. *Alicella gigantea* Chevreux, 1899 was selected as the outgroup for both datasets. The 16S and COI datasets contained 191 and 394 positions of which 33 and 115 bases were parsimony-informative, respectively.

The Bayesian-based topology based on variation across 16S and COI is shown in Figure 12. In general, the two topologies shared similar patterns and the differences were largely due to lacking both sets of sequences for a specimen. The COI topology showed *E*. *plasticus* sp. nov. to form a reciprocally monophyletic group. The 16S topology varied slightly with the inclusion of *Eurythenes* sp. (U40445; France & Kocher 1996) to the *E. plasticus* sp. nov. phylogroup. This *Eurythenes* sp. represents a singleton and recently distinguished as part of the species-level clade Eg7 (Havermans et al., 2013). In both topologies, *Eurythenes plasticus* sp. nov. was placed within a larger clade with *E. magellanicus, E. aequilatus, and Eurythenes* sp. 'PCT abyssal'. *Eurythenes plasticus* sp. nov. was consistently sister to *E. magellanicus*, with high support in the COI topology (0.99 posterior probability; Figure 12B).

Species delimitation analysis with bPTP for the COI datasets estimated the three specimens of *E*. *plasticus* sp. nov. to be the same species and distinct from all other *Eurythenes* taxon (mean: 14.33; acceptance rate: 0.0846; estimated number of species: 12–17). The bPTP analysis of the 16S dataset did not delineated *E. plasticus* sp. nov. from *E. magellanicus, E. andkakarae, E. sigmiferus, E. aequilatus, E. obseus, Eurythenes* sp. 'PCT abyssal', and *Eurythenes* spp. Eg7–9 (mean: 5.29; acceptance rate: 0.20456; estimated number of species: 3–13).

With alternative delimitation method, the average K2P estimates of divergence between *E*. *plasticus* sp. nov. and *E. magellanicus* were 0.034 ± 0.007 for 16S and 0.074 ± 0.008 for COI. The levels of interclade divergence between *E. plasticus* sp. nov. and *E. magellanicus* were comparable to the levels of divergence that have been previously used to detect cryptic speciation within the *gryllus*-complex (Havermans et al., 2013; Eustace et al., 2016; Narahara-Nakano et al., 2017). Furthermore, the '4x' criterion was satisfied, whereby the interclade divergences were at least four times the maximum interclade divergences (Birky et al., 2005).

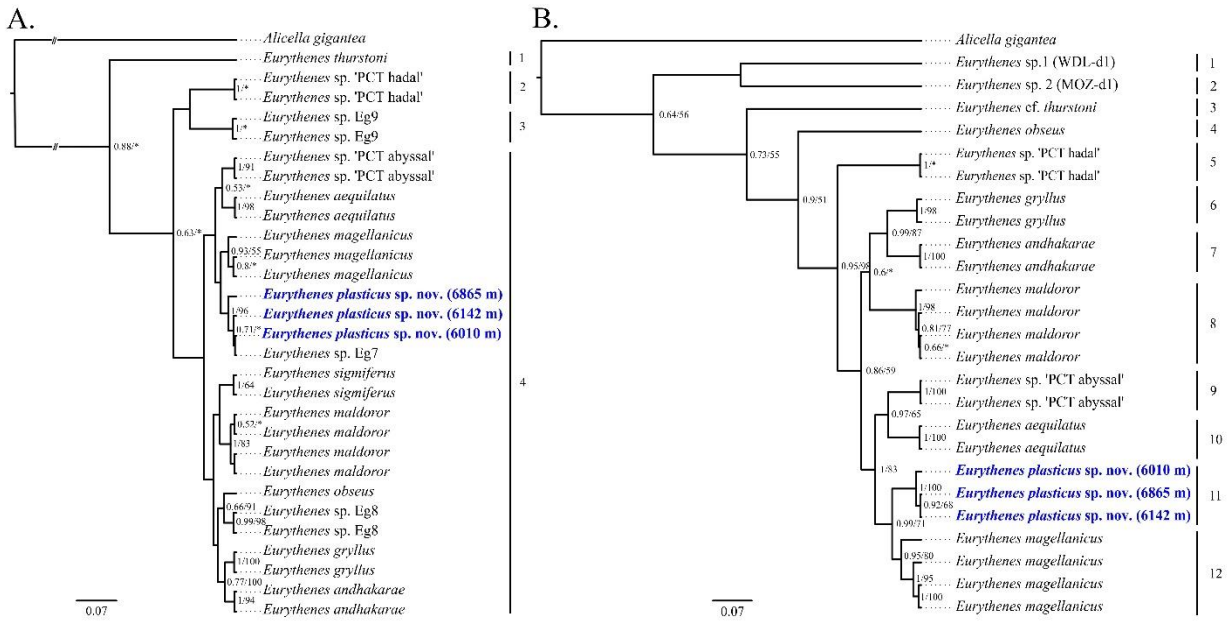

Figure 12. Bayesian trees showing the relationship of *E*. *plasticus* sp. nov. (bold blue) within the *Eurythenes* genus based on: A. 16S rDNA sequence data, and B. COI sequence data. References for comparative sequences are in using Table 3. Bayesian posterior probabilities and maximum likelihood bootstrap support are on branch nodes. Values less than 0.50 or 50 are not stated or depicted by asterisk. Species groups determined by bPTP analysis are shown on right side of each phylogeny.

3.2 Microplastics

Three particles were observed between the four specimens. One particle was a 649.648 µm long, dark fibre extracted from the juvenile from 6949 m (Figure 13). FTIR analysis determined this fibre to be 83.74% similar to polyethylene terephthalate (PET). FTIR analysis resolved the second and third particles to be of biological nature, likely undigested material. Additionally, one cotton fibre (74.08% similar to cellulose) was found in the filter used as a blank during the specimen dissection. No particles were present in the procedural blanks.

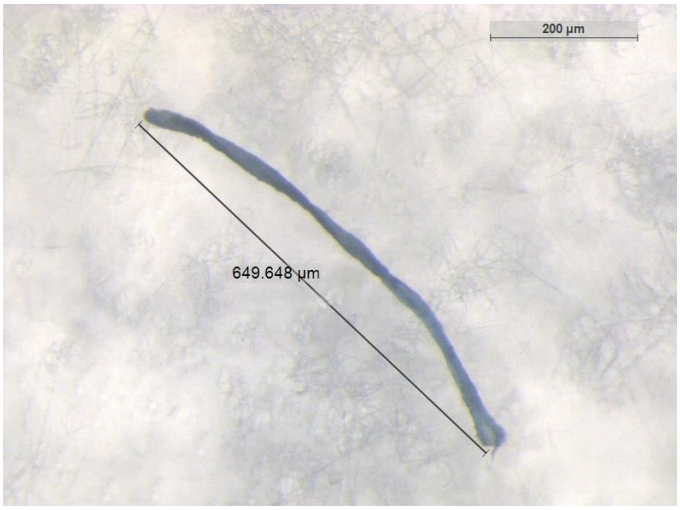

Figure 13. Microfibre found within the hindgut of a *E. plasticus* sp. nov. individual from 6949 m in the Mariana Trench.

4 Systematics

Order Amphipoda Latreille, 1816

Superfamily Lysianassoidea Dana, 1849

Family Eurytheneidae Stoddart & Lowry, 2004

Genus *Eurythenes* S. I. Smith in Scudder, 1882

***Eurythenes plasticus* sp. nov. Weston** (Figure 14, Figure 15, Figure 16, Figure 17, Figure 18)

Material Examined.

HOLOTYPE: Mature female, USNM 1615729, body length 48.1 mm.

PARATYPES: Mature male, USNM 1615732, GenBank (16S MT021437), (COI MT038070), body length 47.6 mm, Mariana Trench, Pacific Ocean (11.5911N, 144.84730E), cruise FK141109, station LH14, depth 6010 m. Immature female, USNM 1615733 GenBank (16S MT021438), (COI MT038071), body length 38.6 mm, Mariana Trench, Pacific Ocean (11.6071N, 144.8331E), cruise FK141109, station LH15, depth 6142 m. Juvenile, USNM 1615730, body length 15.6 mm, same collection location as type locality.

PARAGENETYPE: Juvenile, GenBank (16S MT021439), (COI MT038072), body length 15.1 mm, same collection location as type locality.

NON-TYPE SPECIMENS: Three juveniles, body lengths 12.5, 13.5 & 15.7 mm, same collection location as type locality.

Type Locality. Mariana Trench, Pacific Ocean (12.64065N, 144.73796E), cruise FK141109, station WT02, depth 6865 m.

Etymology. The species names, *plasticus*, stems from the Latin for plastic. This name speaks to the ubiquity of plastic pollution present in our oceans.

Diagnosis. Lateral cephalic lobe strongly produced, slightly triangular. Article 2 of mandibular palp narrow. Maxilliped inner plate with three to four apical protruding nodular setae. Gnathopod 1 subchelate, basis narrow (2.9x as long as wide), palm not protruding and weakly convex. Gnathopod 2 subchelate, coxa broad ventrally and weakly curved, palm convex. Pereopods 3 to 7 dactyli short. Pereopod 5 coxa bilobate and posterior lobe larger than anterior lobe. Epimeron 3 posteroventral corner subquadrate without small posteroventral tooth. Uropod 1 and 2 rami margins with spine-like setae. Dorsal carination with increasing degree on epimeron 1-3 and urosomite 1.

Description, based on holotype, female, USNM 1615729**.**

BODY (Figure 14, Figure **15**, Figure **16**): surface smooth, without setae; urosomite 3 with an anterodorsal depression. *Oostegites* present on gnathopod 2 to pereopod 5, elongate but lacking setae. *Coxa gills* present on gnathopod 2 to pereopod 7. *Colour pattern* at time of recovery unknown.

HEAD (Figure 15): rostrum absent; ventral corner of eye rounded and obliquely pointing backwards (Figure 15C). *Antenna 1* short, 0.1x as long as body length; accessory flagellum 12-articulate; primary flagellum 28-articulate; callynophore well-developed; calceoli absent (Figure 15A). *Antenna 2* medium length, 0.3x as long as body, 1.8x as long as antenna 1; flagellum 59-articulate; calceoli absent (Figure 15B).

MOUTHPART BUNDLE (Figure 15): *Mandible* left lacinia mobilis a long slender distally cuspidate robust seta; setal row left with 13 short, slender, robust setae; molar large, setose, vestigial distal triturating patch; palp article length ratio 1: 3.2: 2.6, article 2 posteriorly not expanded and distally not tapering, 3.4x as long as wide; article 3 blade-like (Figure 15I). *Maxilla 1* inner plate with nine apical and sub-apical plumose setae; outer plate with an 8/3 setal crown arrangement; palp longer than outer plate, 2-articulate, seven sub-apical and apical setae with one being a flag seta (Figure 15H). *Maxilla 2* inner and outer plates broad, inner plate 0.6x shorter than outer plate (Figure 15G). *Maxilliped* inner plate large, sub-rectangular, four apical protruding nodular setae; outer plate

subovate, with 12 apical setose setae; palp large and well-developed; dactylus well-developed, unguis present, six small apical setae (Figure 15D, F).

PEREON (Figure 16, Figure **17**): *Gnathopod 1* coxa very weakly anteriorly concave, anteroventral margin with setae; palm crenulate, 0.4x as long as width of propodus, defined by one robust seta at base of palm and another robust seta at end of palm that is 2.6x longer; dactylus curved posteriorly, one long anterodistal seta, unguis present (Figure 16A, B). *Gnathopod 2* subchelate, coxa obovate, broad ventrally and weakly curved; propodus elongate, not expanded distally, 6.1x as long as wide; propodus 2.7x as long as wide, moderately expanded distally; palm crenulate, distal end defined by three robust setae; dactylus not reaching palmar corner, curved posteriorly, unguis present, one long anterodistal seta (Figure 16A, B). *Pereopod 3* coxa sub-rectangular, 2.0x as long as wide, setae on surface of coxa and along ventral and posterior margins; basis weakly expanded posteriorly, 2.7x as long as wide; merus expanded anteriorly, tuft of setae on anteroventral corner; propodus 4.8x as long as wide; dactylus short, 0.4x as long as propodus, unguis present (Figure 16C). *Pereopod 4* coxa broad, 1.2x as long as wide, 1.1x length of coxa 3, junction between anterior and ventral border bluntly angular (sub-rectangular), ventral border straight, posteroventral border straight and weakly oblique; leg almost identical with pereopod 3 (Figure 16D). *Pereopod 5* coxa bilobate, posterior lobe 1.3x longer and 1.6x wider than anterior lobe, ventral border of posterior lobe sub-triangular; basis expanded posteriorly, posterior margin smooth; merus broadly expanded posteriorly, 1.5x as long as wide, curved posterior margin; propodus slender, 6.2x as long as wide, seven groups of robust setae on the anterior margin; dactylus short, 0.4x as long as propodus, unguis present (Figure 17A). *Pereopod 6* coxa subquadrate, posterior margin weakly bilobate or weakly concave; basis expanded posteriorly, posterior margin distinctly crenate; merus broadly expanded posteriorly, 1.7x as long as wide, convex posterior margin; propodus slender, 5.9x as long as wide, eight groups of robust setae on the anterior margin; dactylus slender, short, 0.3x as long as propodus, unguis present (Figure 17B). *Pereopod 7* coxa sub-rectangular; basis with posterior border crenulate and strongly expanded, distal lobe moderately protruding; merus broadly expanded posteriorly, 1.6x as long as wide, convex posterior margin; propodus with

normal stoutness, 5.6x as long as wide, eight groups of robust setae on the anterior margin; dactylus slender, short, 0.3x as long as propodus, unguis present (Figure 17C).

PLEON AND UROSOME (Figure 17, Figure **18**): *Epimeron 1* anteroventral corner rounded with long slender setae; posteroventral corner produced into a small tooth. *Epimeron 2* anteroventral margin lined with short fine setae; posteroventral corner produced into a strong tooth. *Epimeron 3* ventral margin lined with long fine setae, weakly curved (Figure 17D). *Urosomite 1* with anterodorsal notch (Figure 17D). *Uropod 1* peduncle with one apicomedial setae; inner ramus subequal in length to outer ramus; outer ramus 0.85x as long as peduncle; outer ramus with 18 lateral and eight medial spine-like setae; inner ramus with 20 lateral and 11 medial spine-like setae (Figure 18A). *Uropod 2* peduncle with one apicomedial setae; inner ramus subequal in length (0.9x) to outer ramus; outer ramus subequal in length to peduncle outer ramus with 20 lateral and three medial spine-like setae; inner ramus with seven lateral and 16 medial spine-like setae (Figure 18B). *Uropod 3* inner ramus subequal in length to article 1 of outer ramus; article 2 of outer rami short, 0.05x length of article 1; setae of distolateral angle of peduncle of normal length and stoutness; medial margins of both rami with plumose setae (Figure 18C). *Telson* 70% cleft, pair of apical setae on each lobe parallel with beginning of cleft, distal margin with a single apical seta on right lobe, distal end of left lob missing (Figure 18D).

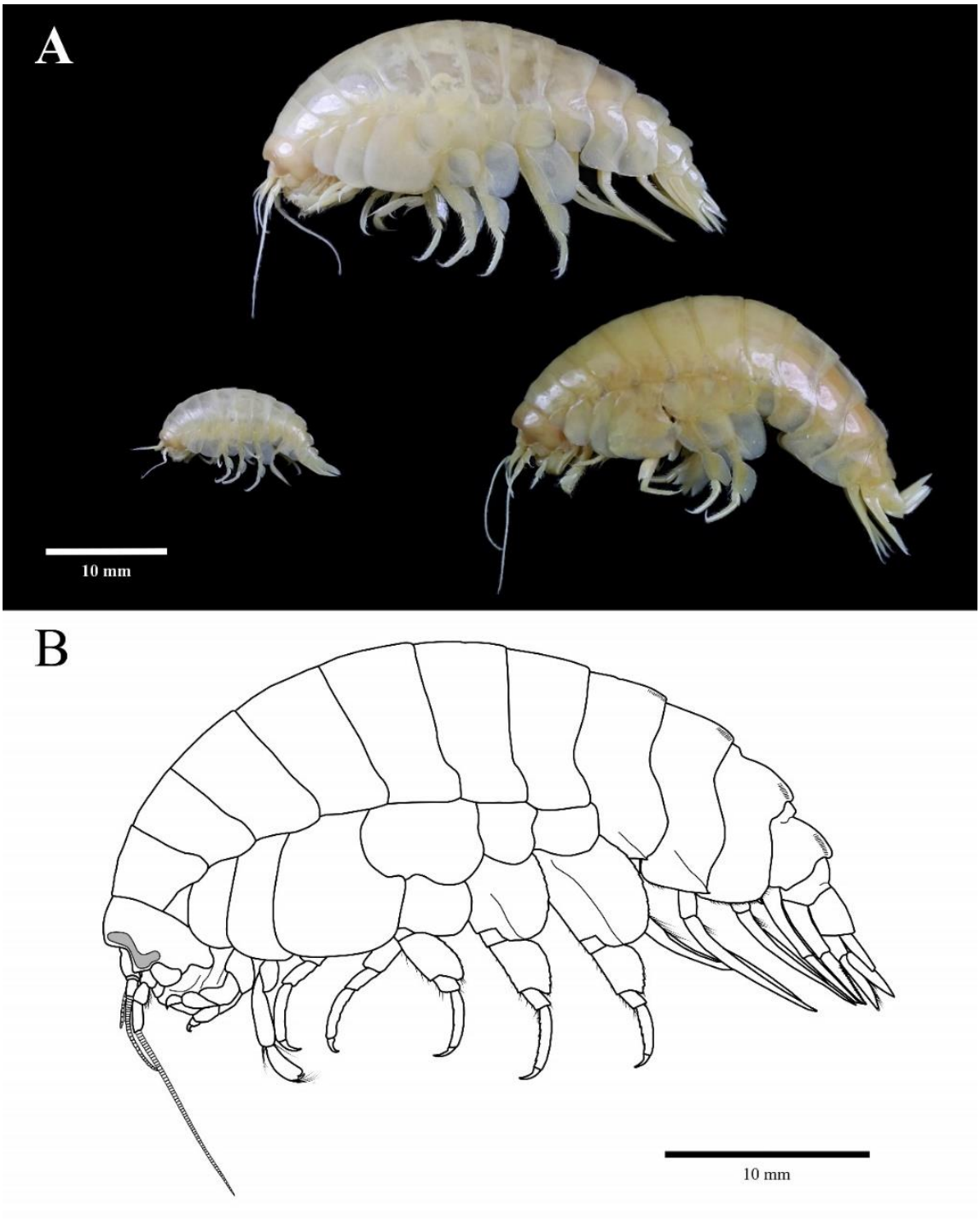

Figure 14. A, Photographs of specimens of *E*. *plasticus* sp. nov.: female holotype from 6865 m (A top; USNM 1615729), juvenile paratype from 6865 m (bottom left; USNM 1615730), male paratype from 6010 m (bottom right; USNM 1615732). B, *Eurythenes plasticus* sp. nov., mature female, holotype, USNM 1615729.

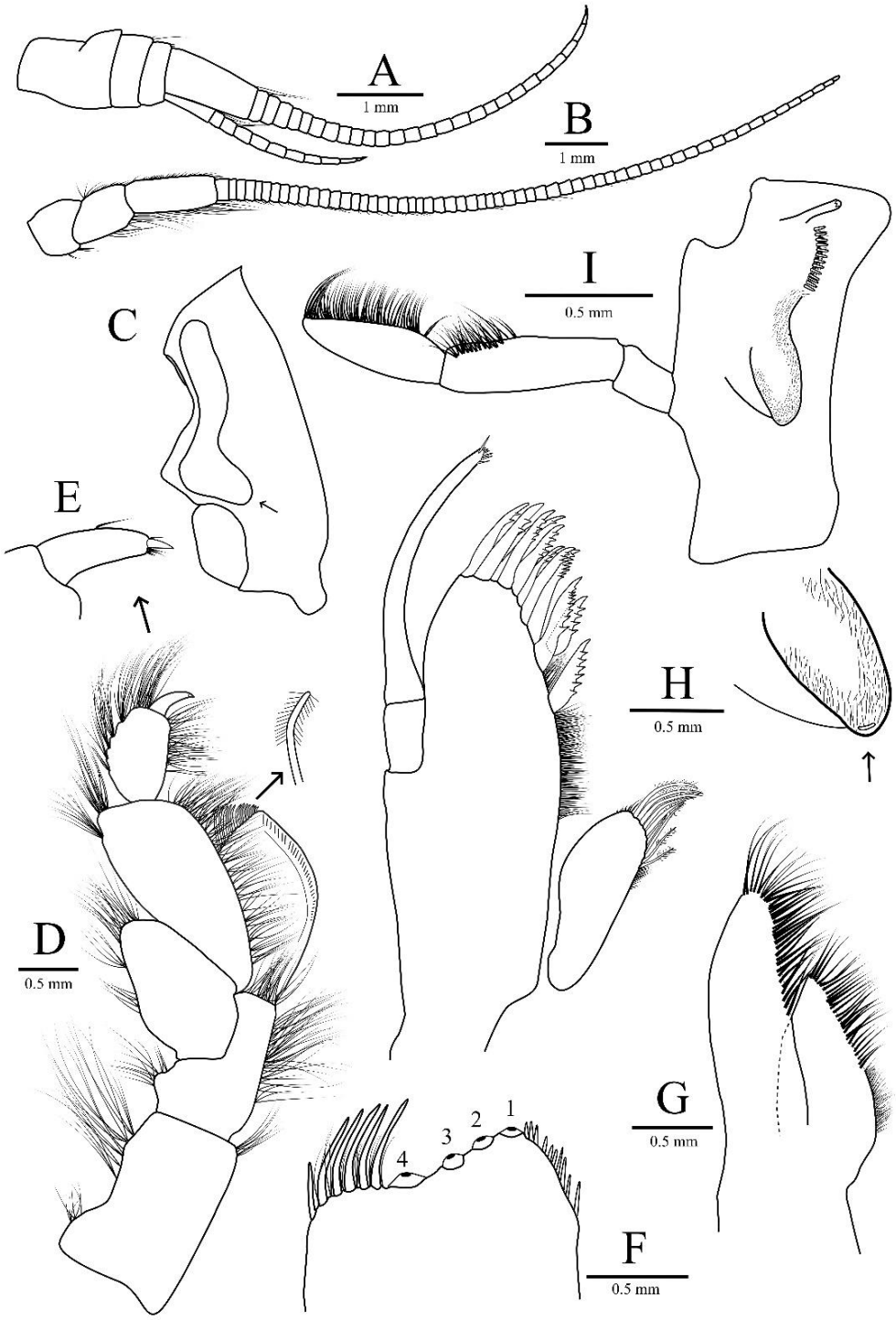

Figure 15. *Eurythenes plasticus* sp. nov. holotype (USNM 1615729). A, left antenna 1; B, left antenna 2; C, head; D, left maxilliped with inner plate removed; E, maxilliped dactylus; F, left maxilliped inner plate (medio-facial spines not shown); G, left maxilla 2; H, left maxilla 1 (palp not flattened); I, left mandible.

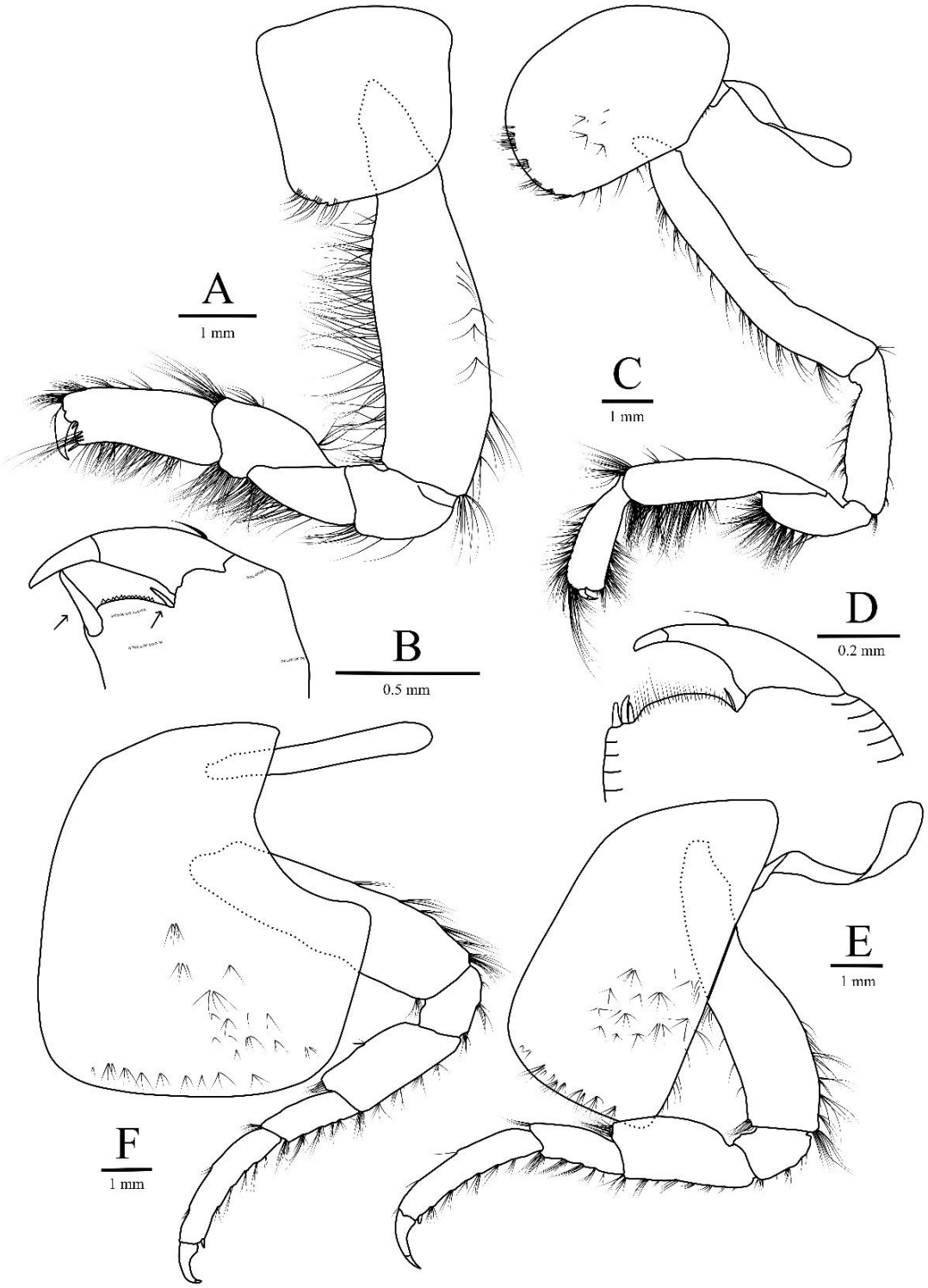

Figure 16. *Eurythenes plasticus* sp. nov. holotype (USNM 1615729). A, left gnathopod 1; B, chela of left gnathopod 1; C, left gnathopod 2; D, chela of left gnathopod 2; E, left pereopod 3; F, left pereopod 4.

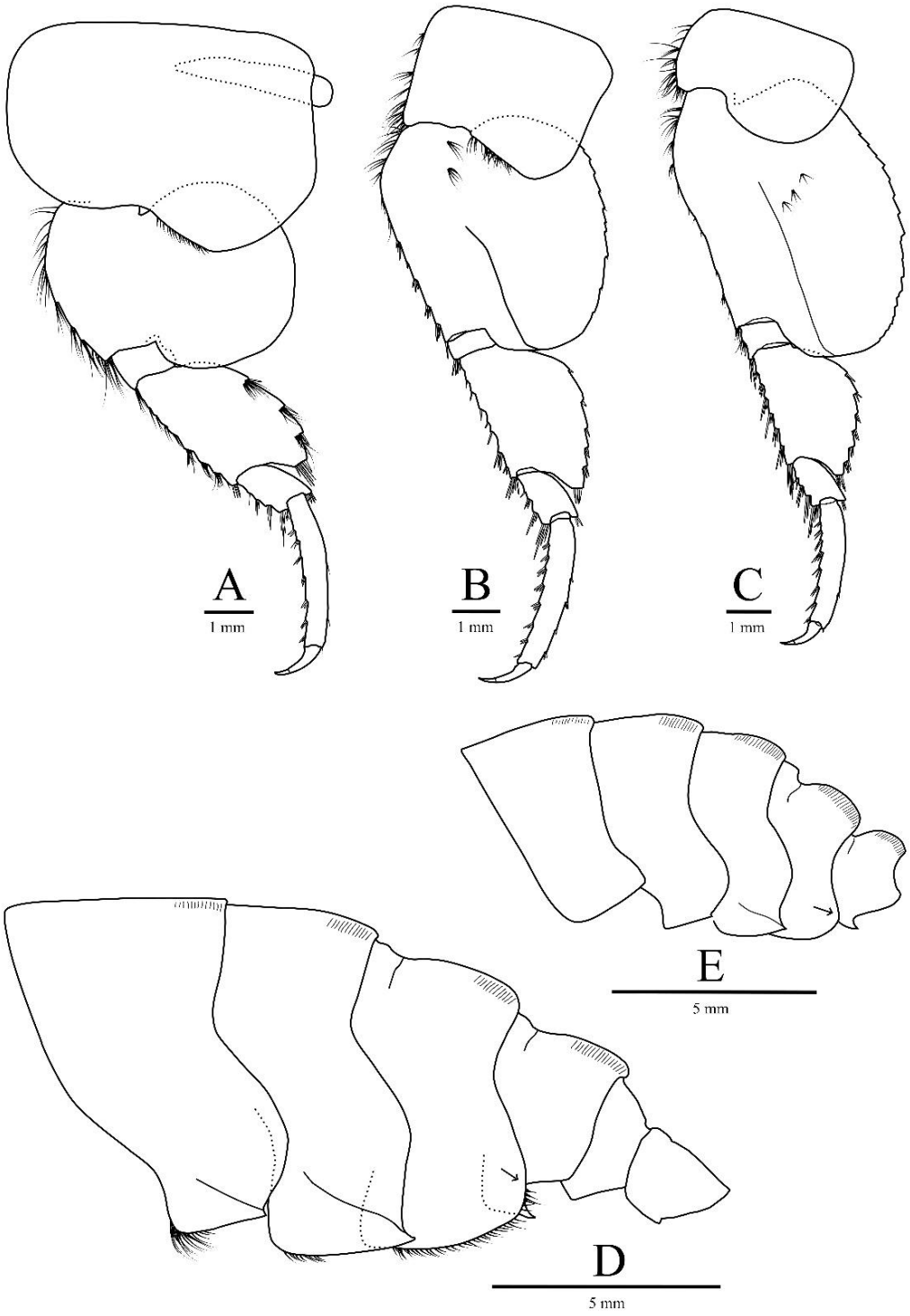

Figure 17. *Eurythenes plasticus* sp. nov. holotype (USNM 1615729). A, left pereopod 5; B, left pereopod 6; C, left pereopod 7; D, epimeron. *Eurythenes plasticus* sp. nov. paratype (USNM 1615730). E, epimeron.

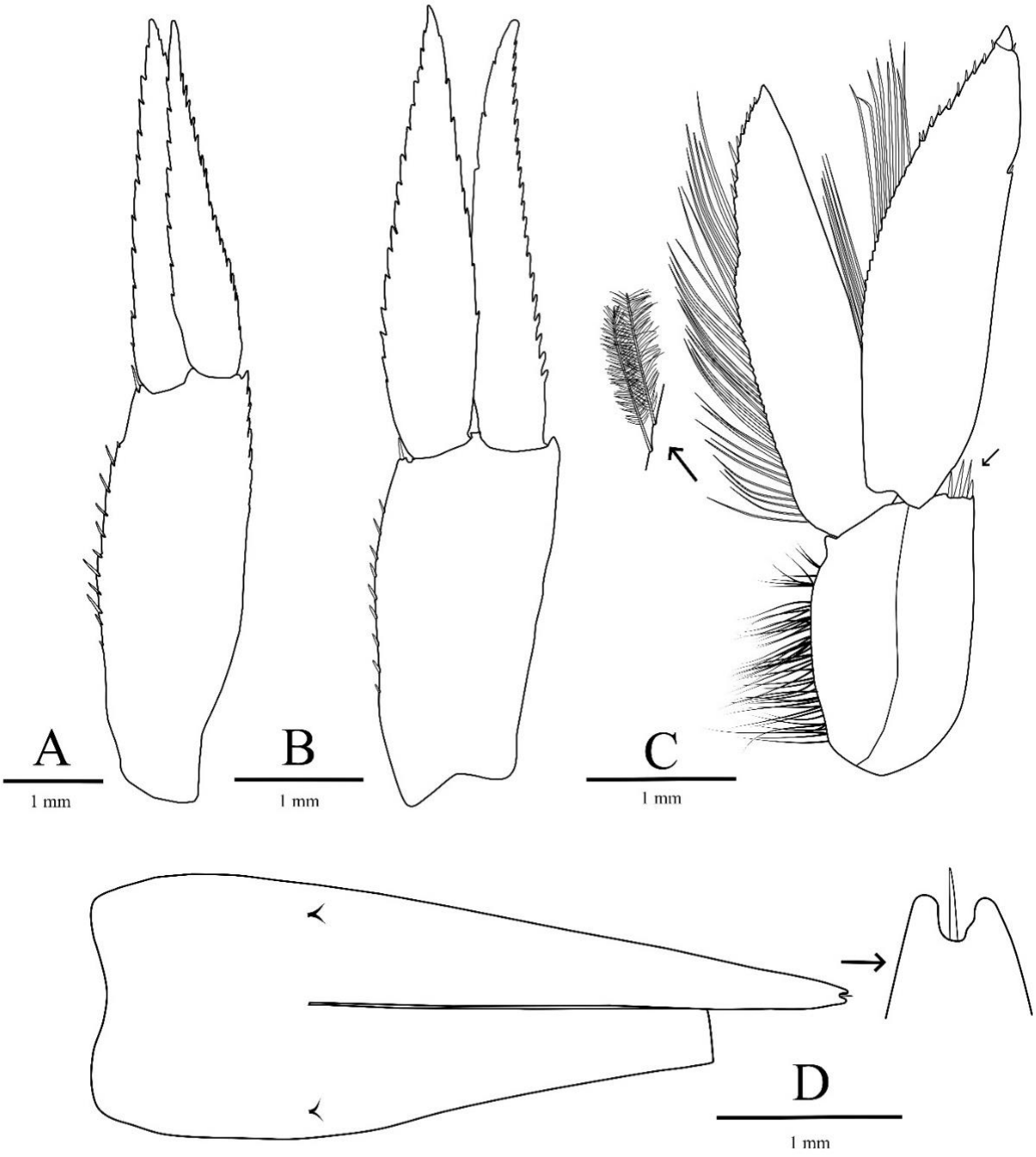

Figure 18. *Eurythenes plasticus* sp. nov. holotype (USNM 1615729). A, left uropod 1; B, left uropod 2; C, left uropod 3, D, telson with right distal margin insert.

Variations. As with other species of *Eurythenes*, there appears to be very little sexual dimorphism. In part, this could be limited to having a single male specimen. The mature male paratype (USNM 1615732) has calceoli present on both antenna 1 and antenna 2.

Both antennae are shorter than the holotype with antenna 1 accessory flagellum being 10-articulate, antenna 1 25-articulate, and antenna 2 54-articulate. Additionally, the maxilliped inner plate of the male paratype has three apical protruding nodular setae, specifically lacking the third setae present on the holotype (Figure 15F). There were differences present in the juvenile paratype (USNMS 1615730) that included typical cohort differences among *Eurythenes*, such as fewer setae on pereopods and uropods and reduced articulation on antennae (antenna 1 accessory flagellum 7-articulate, antenna 1 15-articulate, and antenna 2 38-articulate). In addition, the juvenile paratype had more pronounced and raised dorsal carination than on the adults (Figure 17E). This difference was present among all the juvenile specimens observed.

Differential Diagnosis. As highlighted in d'Udekem d'Acoz & Havermans (2015), the morphological characteristics that separate and define the species within the *gryllus*-complex are hard to observe and should be used with caution. *Eurythenes plasticus* sp. nov. is a member of the *gryllus*-complex morphologically and genetically. Nevertheless, there is a combination of characters that are unique to *E*. *plasticus* sp. nov. and allow it to be distinguished from the morphologically similar species *E. andhakarae*, *E. magellanicus*, and *E. aequilatus.* The most distinctive characteristics are the robust, spine-like setae on rami of uropod 1 and 2 (Figure 18A, B) and the lobes of coxa 5 (Figure 17A), here being unequal, which is novel within *Eurythenes*. *Eurythenes plasticus* sp. nov. can be differentiated from *E. andhakarae* with article 2 of the mandible palp being narrow (instead of expanded), four protruding nodular spines on the inner plate of the maxilliped (versus three non-protruding), and straight ventral border of coxa 4 (opposed to curved). *Eurythenes plasticus* sp. nov. can be separated from *E. magellanicus* with a long gnathopod 1 palm (instead of short), a straight ventral border of coxa 4 (opposed to curved), a subquadrate posteroventral corner in epimeron 3 (instead of bearing a small tooth), and the rami of uropod 1 and 2 being subequal (opposed to uropod 1 outer ramus being shorter than inner ramus and uropod 1 outer ramus being longer than inner ramus). *Eurythenes plasticus* sp. nov. can also be distinguished from *E. aequilatus* by its eyes with a variable width (opposed to constant width), the outer plate of maxilla 1 with 8/3 crown arrangement (instead of 9/3 arrangement), and a long gnathopod 1 palp (instead of short).

Habitat, Distribution, and Biology. *Eurythenes plasticus* sp. nov. was collected from the upper hadal depths of the Mariana Trench, between 6010 and 6949 m. Similar to sister species within the genus, *E. plasticus* sp. nov. is a benthic scavenger, as individuals of multiple cohorts entered the baited traps. *Eurythenes plasticus* sp. nov. is a member of a wider scavenging amphipod community comprised of *A. gigantea*, *Bathycallisoma schellenbergi* (Birstein & Vinogradov, 1958), *Hirondellea dubia* Dahl, 1959, *H. gigas*, *Paralicella caperesca* Shulenberger & Barnard, 1976, *Paralicella tenuipe*s Chevreux, 1908, and *Valettietta anacantha* (Birstein & Vinogradov, 1963), which were concurrently recovered in the traps (data unpublished).

5 Discussion

The salient finding of this study is the paired molecular and morphological identification approaches provided congruent evidence that *E. plasticus* sp. nov. represents an undescribed species within *Eurythenes*. Further, as a scavenger at upper hadal depths (6010–6949 m) in the Mariana Trench, *E. plasticus* sp. nov. is not exempt from ingesting microplastics that are bioavailable within the hadal zone.

In comparison to described *Eurythenes* species, *E*. *plasticus* sp. nov. was placed as part of the *gryllus*-complex and most closely related to the abyssal *E. magellanicus* (Figure 12). The bPTP analysis of COI and both K2P analyses delineated *E*. *plasticus* sp. nov. to be a distinctive lineage, and these methods aligned with previous studies that detected cryptic speciation within the *gryllus*-complex (Havermans et al., 2013; Eustace et al., 2016; Narahara-Nakano et al., 2017). The 16S phylogeny specifically showed *E*. *plasticus* sp. nov. to be nearly identical to Eg7 (Figure 12A; France & Kocher, 1996; Havermans et al., 2013). This *Eurythenes* sp. was a singleton recovered from abyssal depths at the Horizon Guyot seamount, Pacific Ocean, and it was collected along with another *Eurythenes* sp. from the divergent Eg9 clade (Havermans et al., 2013). Confidence in the identification of Eg7 would be further strengthened with additional genetic or morphological data.

The morphological variation seen in *E. plasticus* sp. nov., such as an uneven coxa 5 lobe and lack of a tooth on the posteroventral corner of epimeron 3, supported the phylogenetic results as an undescribed lineage. Consistent with previous studies, these morphological characteristics should be used with caution, as some are difficult to discern

objectively. Additional specimens, like from the Eg7 clade, may reveal phenotypic plasticity in the characteristics observed in this morphological study (d'Udekem d'Acoz & Havermans, 2015). Continued application of a combined molecular and morphological approaches in future studies is likely to reveal further species diversity within the *gryllus*-complex.

The discovery of *E. plasticus* sp. nov. continues to align with the pattern *Eurythenes* that the geographic and bathymetric species distributions are complex (Havermans, 2016). With the Eg7 singleton, the geographic range of *E. plasticus* sp. nov. thus far appears to be restricted to the Central Pacific Ocean. Across that ocean basin, *E. plasticus* sp. nov. has a broad bathymetric range, ~3000 m. While it is common among *Eurythenes* to be found only in a single ocean basin and have a wide vertical distribution (Eustace et al., 2016; Havermans, 2016), it is less common to span across the abyssal and hadal zones. Although, this is not unique, as it has been documented in other amphipods, such as *A. gigantea* (Jamieson et al., 2013). A species needs to be able to cope at the cellular, reproductive, and physiological levels in both the stable abyssal (Smith et al., 2008) and the dynamic hadal environments (Jamieson, 2015; Downing et al., 2018). Yet, it was curious that during the present study, *E*. *plasticus* sp. nov. was only collected from upper hadal depths, despite amphipods being captured at shallower and deeper depths (43 additional deployments 4506 to 10545 m; data unpublished). This highlights that the distribution of *E. plasticus* sp. nov. is a patchwork. Further work and sampling will be required to understand the conditions that support the presence of this species.

The finding of a microplastic fibre in the hindgut of a juvenile was not unexpected. Deep-sea scavenging amphipods, as an adaption to their food limited environment, indiscriminately consume carrion (Blankenship & Levin, 2007) and are known to inadvertently ingest microfibres present in the carrion and sediment (Jamieson et al., 2019). The detection of a microplastic adds to the number of hadal scavenging amphipods, including adult specimens of *H. gigas* from the Mariana Trench and *Eurythenes* sp. 'hadal' the Peru-Chile Trench (Jamieson et al., 2019), which have been found to have consumed plastic microfibers. Microplastic consumption by a juvenile indicates that scavenging amphipods are potentially ingesting microplastics throughout

their life, which could pose acute and chronic health effects. While the ecotoxicological impacts of microplastic exposure have yet to be investigated on deep-sea amphipods, early work on other Malacostraca indicates that the ingestion of polypropylene fibres by the sand crab, *Emerita analoga*, increases adult mortality and decreases in retention of egg clutches (Horn et al., 2019).

This study adds to the growing body of literature on marine organisms ingesting plastic and microfibres (Besseling et al., 2015; Lusher et al., 2015; Bellas et al., 2016; Alomar & Deudero, 2017). The microplastic found in the hindgut of *E. plasticus* sp. nov. was most similar to PET, which is one of the top five most prevalent synthetic plastic polymers produced and discarded globally (Geyer et al., 2017). Without substantial global changes to the life cycle of plastic, from reducing the rate of plastic production to improving waste management (Forrest et al., 2019), plastics and microfibres will continue to be transported to the deep sea and be ubiquitous in the hadal food chain for the foreseeable future.

6 Acknowledgments

We extend thanks to Eva Stewart and Jenny Wainwright (Newcastle University) for their dissertation work that laid the foundation for this description. We are grateful to Drs Shannon Flynn (Newcastle University) and Renate Matzke-Karasz (Ludwig-Maximilians-Universitat Muchen) for their constructive comments on manuscript drafts. We thank the collections staff at the Smithsonian Institution National Museum of Natural History for their efficiency and generosity in curating the type material. We sincerely thank the HADES-M Chief Scientist Dr Jeffrey Drazen (University of Hawai'i at Manoa) and the Captain and crew of the RV *Falkor* (FK141109) for their work to collect the specimens. We thank the National Oceanic and Atmospheric Administration (NOAA), National Marine Fisheries Service (NMFS) Pacific Islands Fisheries Science Center, the Pacific Islands Regional Office, the Marine National Monuments Program, and Eric Breuer (NOAA/NMFS) for their collaboration with HADES-M. Thank you to the reviewer for their constructive comments that improved the manuscript.

7 Funding

HADES-M and the expedition cruise FK141109 on the RV *Falkor* was supported by the National Science Foundation Grant OCE #1130712, the Schmidt Ocean Institute, and

the Marine Alliance for Science and Technology for Scotland. The molecular analysis was funded by Newcastle University, UK through internal support. The microplastics analysis and laboratory was funded by the European Maritime and Fisheries Fund (EMFF), under grant number ENG2954. The description was supported by the World Wildlife Fund (WWF).

Chapter 3: *Eurythenes atacamensis* sp. nov. (Crustacea: Amphipoda) exhibits ontogenetic vertical stratification across abyssal and hadal depths in the Atacama Trench, eastern South Pacific Ocean

In Press As: Weston, J.N.J., Espinosa-Leal, L., Wainwright, J.A., Stewart, E.C.D., Gonzalez, C.E., Linley, T.D., Reid, W.D.K., Hidalgo, P., Oliva, M.E., Ulloa, O., Wenzhöfer, F., Glud, R.N., Escribano, R. and Jamieson, A.J. (in Press) *Eurythenes atacamensis* sp. nov. (Crustacea: Amphipoda) exhibits ontogenetic vertical stratification across abyssal and hadal depths in the Atacama Trench, eastern South Pacific Ocean. *Marine Biodiversity*. doi:10.1007/s12526-021-01182-z

Abstract

Eurythenes S.I. Smith in Scudder, 1882 (Crustacea: Amphipoda) are prevalent scavengers of the benthopelagic community from bathyal to hadal depths. While a well-studied genus, molecular systematic studies have uncovered cryptic speciation and multiple undescribed lineages. Here, we apply an integrative taxonomic approach and describe the tenth species, *Eurythenes atacamensis* sp. nov., based on specimens from the 2018 *Atacamex* and RV Sonne SO261 Expeditions to the southern sector of the Peru-Chile Trench, the Atacama Trench (24–21°S). *Eurythenes atacamensis* sp. nov. is a large species, max. observed length 83.2 mm, possesses diagnostic features, including a short gnathopod 1 palm and a chelate gnathopod 2 palm, and a distinct genetic lineage based on a 16S rRNA and COI phylogeny. This species is a dominant bait-attending fauna with an extensive bathymetric range, spanning from 4974 to 8081 m. The RV Sonne SO261 specimens were recovered along a 10-station transect from abyssal to hadal depths and further examined for demographic and bathymetric-related patterns. Ontogenetic vertical stratification was evident across the trench axis, with only juveniles present at abyssal depths (4974–6025 m). Total length-depth analysis revealed that the size of females was unrelated to depth, whereas juveniles followed a sigmoidal relationship with a step-up in size at depths >7200 m. Thus, these bathymetric trends suggest that juveniles and females employ differing ecological strategies in subduction trench environments. This study highlights that even dominant and ecologically important species are still being discovered within the abyssal and hadal environments. Continued systematic expeditions will lead to an improved understanding of the eco-evolutionary drivers of speciation in the world's largest ecosystem.

Keywords

Peru-Chile Trench, new species, cryptic species, deep-sea, integrated taxonomy, *Eurythenes* key

1. Introduction

The deep ocean is the Earth's largest ecosystem, extending from the edge of the continental shelf (200 m) to the bottom of the subduction trenches (~11,000 m; Thiel, 2003, Stewart & Jamieson, 2019), covering approximately 1.4 x 10^9 km^3 (Charette & Smith, 2010). Despite the extreme environmental conditions of high pressure, low temperature, and limited food availability (Grassle & Maciolek, 1992; Smith et al., 2008; Jamieson et al., 2009), the deep ocean harbors a wide range of adapted species (Belyaev 1989, Ebbe et al., 2010). The amphipod genus *Eurythenes* S.I. Smith in Scudder, 1882 are prevalent members of the deep ocean, benthopelagic community (Stoddart & Lowry, 2004; Havermans, 2016). This genus inhabits every ocean across an extensive bathymetric range–observed in polar waters (Ainley et al., 1986; Bowman & Manning, 1972), on the abyssal plains (Barnard, 1961; Brandt et al., 2012; Havermans, 2016), and at hadal depths (Thurston et al., 2002; Fujii et al., 2013; Eustace et al., 2016; Weston et al., 2020a; Weston et al., 2021). They have been the focus of ecological and physiological studies, including metabolism (Premke & Graeve, 2009), feeding strategies (Hargrave, 1985; Premke et al., 2006; Blankenship & Levin, 2007), population demographics (Ingram & Hessler, 1987; Christiansen et al., 1990; Thurston et al., 2002; Blankenship et al., 2006), and biomonitoring (Reid et al., 2018). However, most studies have presumed to be studying *Eurythenes gryllus* (Lichtenstein in Mandt, 1822). Questions to the identification of *E. gryllus* were first raised by France and Kocher (1996). Cryptic speciation with the *gryllus*-complex has since been confirmed by integrative taxonomic studies (Havermans et al., 2013; Havermans, 2016; Eustace et al., 2016). Since 2015, *Eurythenes* has expanded from three to nine described species (d'Udekem d'Acoz & Havermans, 2015; Narahara-Nakano et al., 2018; Weston et al., 2020a). Furthermore, at least five distinct genetic lineages are awaiting formal description (France & Kocher, 1996; Havermans et al., 2013; Eustace et al., 2016; Horton et al., 2020) and more are likely to be discovered via expansion of sampling programs (Havermans, 2016).

One undescribed lineage is from hadal depths in the Peru-Chile Trench, eastern South Pacific Ocean (Thurston et al., 2002; Ritchie et al., 2015; Eustace et al., 2016). This species was first recorded from 7196 m by *in situ* still images during the Scripps Institution of Oceanography Expedition SOUTHTOW (Hessler et al., 1978). The first

specimens were recovered via baited traps from 7230 m during SIO BI72–20 (Ingram & Hessler, 1987), and subsequently from 7800 m in September 1997 during the Atacama Trench International Expedition (ATIE; Thurston et al., 2002). In these three studies, specimens were identified as *E. gryllus*. However, distinct morphological differences from the *E. gryllus* description were observed with the gnathopods, coxa 4, and epimeron 3 (Thurston et al., 2002). These differences were proposed to indicate the population was undergoing incipient speciation. Based on specimens from the 2010 RV *Sonne* SO209 expedition, a combined morphological and molecular identification approach resolved that this population is a distinct lineage, *Eurythenes* sp. 'PCT hadal' (Ritchie et al., 2015; Eustace et al., 2016). This undescribed species is considered to be restricted to hadal depths (6173–8074 m) of the Peru-Chile Trench (Eustace et al., 2016), which is partitioned by the ~4000 m deep Nazca Ridge to northern (Milne-Edwards Trench) and southern (Atacama Trench) sectors (Hampel et al., 2004). The pattern of ontogenetic vertical stratification across the depth gradient was found, whereby juveniles were prevalent at shallower depths and females dominated the deepest depths (Eustace et al., 2016). However, the SO209 specimens were recovered from only three sampling locations widely spaced along the north-south axis of the trench.

This present study is based on specimens collected using baited landers across abyssal to hadal depths of the Atacama Trench during the 2018 RV *Sonne* SO261 Expedition and at the deepest point as part of the 2018 *Atacamex* Expedition. We applied an integrative taxonomic approach to describe the tenth species of *Eurythenes*, namely *Eurythenes atacamensis* sp. nov., and provided an updated key for the genus. Further, we investigated morphometric and bathymetric trends related to size and ontogeny across a latitudinally-focused sampling transect.

2. Materials and Methods

2.1 Specimen collection and processing

Specimens were collected during two expeditions in 2018 to the ultra-deep waters of the Atacama Trench off northern Chile (24–21°S). The *Atacamex* Expedition was during January-February 2018 onboard the RV *Cabo de Hornos*, and the RV *Sonne* SO261 Expedition was conducted during March 2018 as part of the HADES-ERC project (Wenzhöfer, 2019). Both expeditions deployed baited free-fall landers. The *Atacamex*

Expedition used a custom-design Nano Lander from Global Ocean Design (San Diego, CA) named “Audacia” — equipped with a baited mesh catching trap, a conductivity-temperature-depth-oxygen (CTD-O) profiler, a small video camera, and two 30-L Niskin bottles. The “Audacia” was recovered after 24 h by means of an acoustic releaser. The RV Sonne SO261 Expedition deployed two landers, Camera Lander 1 and Lander 2, between depths of 2548–8052 m. The Camera Lander 1 & 2 were equipped with a RBRduet3 TD pressure sensor (RBR, Canada) and a bespoke funnel trap. The trap was an acrylic tube (20 cm diameter and 100 cm long) with a funnel (5 cm diameter) at one end and a 1 mm steel mesh at the other end. When the ballast weight was released, the funnel was plugged to minimize the loss of samples during surfacing and recovery. The traps were baited with whole-bait mackerel (Scombridae; Jamieson et al., 2011). Pressure records were converted to depth (m) following Saunders (1981). The seven abyssal and hadal stations from the RV *Sonne* SO261 Expedition and a single station from the *Atacamex* Expedition are shown in Figure 19, and the details for the entire eleven deployments are provided in Table 4.

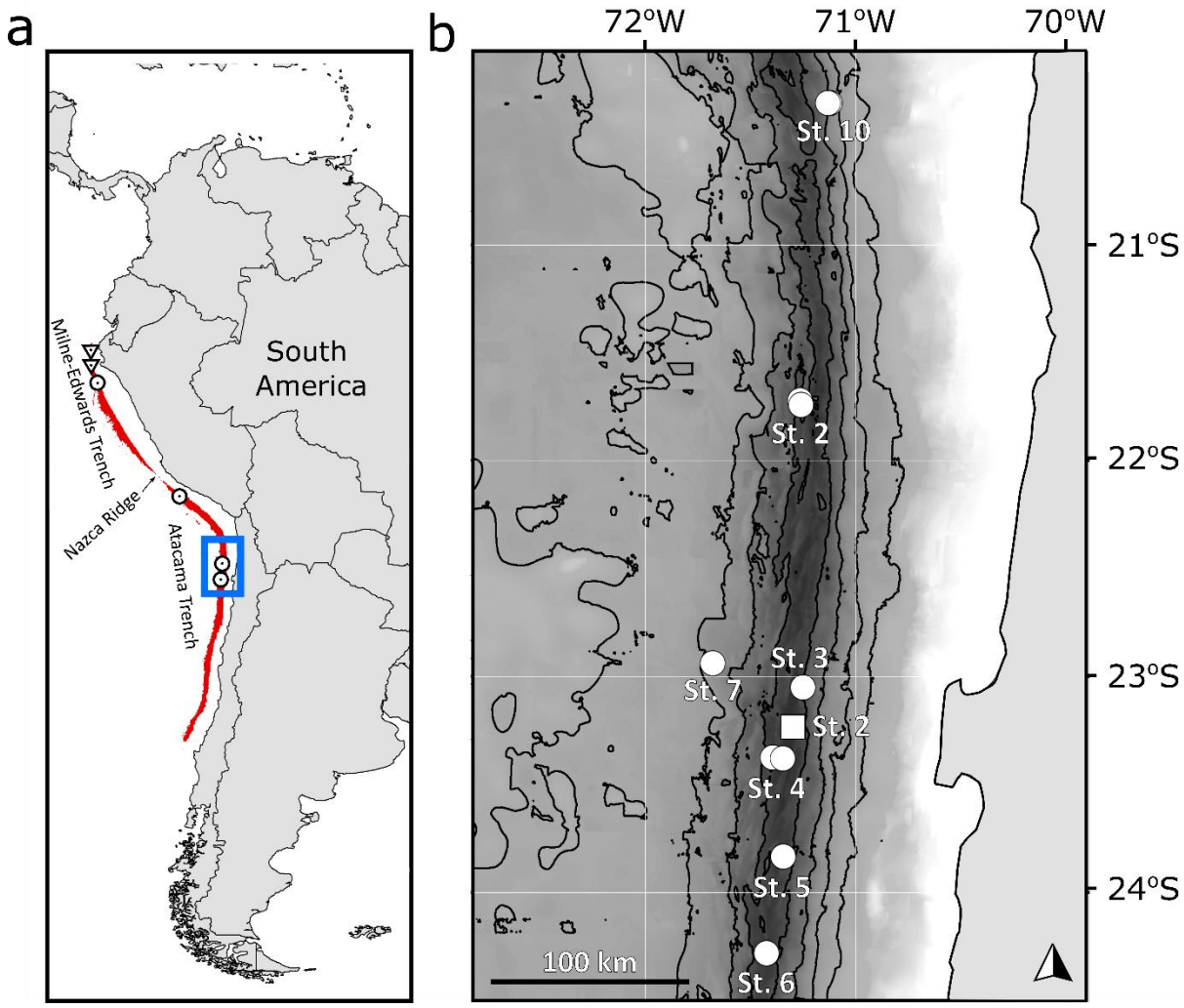

Figure 19. (a) Map of the Peru-Chile Trench defined by depths >4900 m (red). Historical collection records of this species (circle), and the historical abyssal sampling with the absence of *Eurythenes atacamensis* sp. nov. (triangle). The extent of map (b) is indicated by the blue box. (b) The eleven deployments where *E. atacamensis* sp. nov. was recovered during the *Atacamex* Expedition (square) and the RV *Sonne* SO216 Expedition (circle). Isobaths are shown every 1000 m between 3000–7000 m depth contours.

Table 4. Collection information for *Eurythenes acatamensis* sp. nov. during the *Atacamex* and RV *Sonne* SO261 Expeditions. Included is the number of individuals collected by sex for each depth.

Depth (m)	Latitude	Longitude	Expedition	Station	Date	Female	Male	Intersex	Juvenile
4974	22°56.282'S	71°40.686'W	SO261	7	20/03/2018	-	-	-	15
5920	20°20.608'S	71°07.821'W	SO261	10	27/03/2018	-	-	-	16
6025	20°20.610'S	71°07.824'W	SO261	10	27/03/2018	-	-	-	20
6520	21°43.200'S	71°15.813'W	SO261	2	24/03/2018	3	-	-	56
6714	21°44.497'S	71°15.465'W	SO261	2	24/03/2018	14	-	-	103
7139	23°02.998'S	71°15.044'W	SO261	3	18/03/2018	5	-	-	1
7204	23°22.384'S	71°23.577'W	SO261	4	14/03/2018	117	1	-	88
7493	23°49.981'S	71°20.635'W	SO261	5	12/03/2018	20	-	-	9
7834	24°16.504'S	71°25.388'W	SO261	6	08/03/2018	60	-	1	3
8052	23°22,774'S	71°20.683'W	SO261	4	14/03/2018	138	-	-	8
8081	23°24.48'S	71°19.91'W	*Atacamex*	2	30/01/2018	2	-	-	-
					Total	356	1	1	319

2.2 DNA Barcoding and Phylogenetics

The phylogenetic placement of *E. atacamensis* sp. nov. within the genus was assessed at two partial mitochondrial barcoding regions, 16S rRNA (16S; 260 bp) and cytochrome c oxidase subunit I (COI; 624 bp), for specimens collected on both expeditions. For the *Atacamex* Expedition, total genomic DNA was extracted from a single specimen using the Forensic DNA Kit (Omega) based on the manufacturer protocol, except for incubation in the lysis buffer and proteinase K overnight. For the RV Sonne SO216 specimens, the Bioline ISOLATE II Genomic DNA Kit was used to extract total genomic DNA from the pleopods of five *E. atacamensis* sp. nov. specimens collected between 4974–8052 m (**Error! Reference source not found.**). DNA was extracted from comparative specimens of *Eurythenes maldoror* d'Udekem d'Acoz & Havermans, 2015 and one of *Eurythenes magellanicus* (H. Milne Edwards, 1848), both recovered from 4974 m at Station 7 (Table 5). The primer sets used for amplification were AMPH1 (France & Kocher, 1996) and 'Drosophila-type' 16SBr (Palumbi et al., 2002) for 16S and LCO1490 and HCO12198 (Folmer et al., 1994) for COI. PCR protocols were followed as described in Ritchie et al., (2015). Sequences were cleaned enzymatically using New England Biolabs Exonuclease 1 and Antarctic Phosphatase.

The RV *Sonne* SO216 PCR products were sequenced with an ABI 3730XL sequencer (Eurofins Genomics, Germany), and the *Atacamex* Expedition PCR products were sequenced by the Sequencing Service of P. Universidad Católica de Chile.

Electropherograms were confirmed and trimmed by eye in MEGA 7 (Kumar et al., 2016). Nucleotide sequence quality and absence of contamination were verified on NCBI BLASTn. Each COI sequence was translated into their amino acid sequence to assess for stop codon presence.

The phylogenetic relationship of *E. atacamensis* sp. nov. within *Eurythenes* was investigated with publicly available data in two datasets, namely 16S and COI. The comparative sequences were selected to represent type material, high-confident identifications, or from defined undescribed lineages (Table 5; France and Kocher 1996; Escobar-Briones et al., 2010; Havermans et al., 2013; d'Udekem & Havermans, 2015; Ritchie et al., 2015; Havermans, 2016; Narahara-Nakano et al., 2018; Ritchie et al., 2017; Horton et al., 2020; Weston et al., 2020a). The sequences associated with *Eurythenes* cf. *thurstoni* (KX078272), *Eurythenes* n. sp. 1 (KX078273), and *Eurythenes* n. sp. 2 (KX078271) from Havermans (2016) were excluded from the COI alignment due to low percent identity (<70%) with other *Eurythenes* in NCBI BLASTn search. *Alicella gigantea* Chevreux, 1899 was selected as the outgroup for both genes in the phylogenetic analysis, as it is a large deep-sea scavenger in a separate superfamily with sufficient phylogenetic distance (Table 5; Lowry & De Broyer, 2008; Ritchie et al., 2015). Sequence alignments were constructed by MAFFT v7 using default parameters (Katoh et al., 2017). The final 16S alignment consisted of 41 individuals from nine *Eurythenes* species, four genetic, undescribed lineages, and the outgroup. The final alignment for COI consisted of 31 individuals from seven described species, three genetic, undescribed lineages, and the outgroup.

Phylogenetic relationships were inferred via a Bayesian Inference (BI) using the Bayesian Evolutionary Analysis by Sampling Trees (BEAST) software package v1.10.4 (Suchard et al., 2018) and a Maximum likelihood (ML) phylogenetic analysis with PhyML v3.1 (Guindon et al., 2010). The optimal evolutionary models were identified in MEGA 7 based on by the Bayesian Information Criterion (BIC) as the HKY + G model for 16S and the HKY + I + G model for COI (Hasegawa et al., 1985). On BEAST, two independent runs of 40,000,000 generations were conducted by sampling every 10,000 generations using an uncorrelated relaxed clock (Drummond et al., 2012). Model convergence was assessed in Tracer v1.7 (ESS > 200; Rambaut et al., 2018). The first ten percent of states

were discarded. The maximum clade credibility tree was generated using TreeAnnotator v1.8.4 (Drummond et al., 2012), viewed in FigTree v1.4.3, and annotated using Inkscape v0.92.2 (https://inkscape.org). The ML analysis was setup with a neighbour-joining starting tree and interchange branch swapping using the model of sequence evolution and parameters estimated by PhyML (Guidon et al., 2010; http://www.atgc-montpellier.fr/phyml/). The node stability was based on bootstrap support with 10,000 iterations.

Two analytical approaches were used for delimiting the *Eurythenes* species, namely the Generalized Mixed Yule Coalescent (GMYC) likelihood method and the Bayesian Poisson Tree Process (bPTP) model. For the GYMC analysis, the following parameters were selected: the GTR nucleotide substitution model for COI and HKY for 16S, a normalized exponential relaxed clock, and a Yule process of speciation for both genes. Three independent runs were performed to ensure convergence. Each run was conducted for 10^9 generations, and every 10,000 generations were sampled. The output files were visualized in Tracer v1.4 to determine the convergence of the chains (ESS >200; Rambaut et al., 2018). The maximum clade credibility (MCC) tree was determined by TreeAnnotator BEAST v2.6.2 (Bouckaert et al., 2019), after burning the first 25% of the trees. The number of delimited species was determined using each MCC gene tree through the 'gymc' function in the *splits* package in R (Ezard et al., 2017). Model results were evaluated from a likelihood ratio test that calculates significance from the chi-square test. The bPTP model was used to infer species boundaries through the PTP webserver (Zhang et al., 2013; http://species.h-its.org/ptp/). The BI-derived 16S and COI topologies were used as the input tree. The bPTP analysis was conducted for 100,000 generations of MCMC sampling, with a thinning value of 100 and burn-in of 25%.

Table 5. Species, GenBank sequence accession numbers, and references for phylogenetic analysis of *Eurythenes atacamensis* sp. nov. No amp. means either no PCR product or sequence.

Species	16S	COI	Reference
Alicella gigantea	KP456083	KP713893	Ritchie et al., 2015
Eurythenes aequilatus	LC229090	LC229094	Narahara-Nakano et al., 2018
Eurythenes aequilatus	LC229091	LC229095	Narahara-Nakano et al., 2018
Eurythenes andhakarae	JX887065	JX887114	Havermans et al., 2013
Eurythenes andhakarae	JX887066	JX887119	Havermans et al., 2013
Eurythenes atacamensis sp. nov.	MW042880	no amp	This study (4974 m)
Eurythenes atacamensis sp. nov.	MW042881	MW048993	This study (5920 m)
Eurythenes atacamensis sp. nov.	MW042882	MW048994	This study (7139 m)
Eurythenes atacamensis sp. nov.	MW042883	no amp	This study (7834 m)
Eurythenes atacamensis sp. nov.	MW042884	MW048996	This study (8052 m)
Eurythenes atacamensis sp. nov.	MW290039	MW288146	This study (8081 m)
Eurythenes gryllus	JX887060	JX887132	Havermans et al., 2013
Eurythenes gryllus	JX887063	JX887136	Havermans et al., 2013
Eurythenes magellanicus	LC192879	LC192881	Narahara-Nakano et al., 2018
Eurythenes magellanicus (‘Eg5’)	JX887071	JX887144	Havermans et al., 2013
Eurythenes magellanicus	JX887074	JX887145	Havermans et al., 2013
Eurythenes magellanicus	no data	KX078274	Havermans, 2016
Eurythenes magellanicus	MW042879	no amp	This study (4974 m)
Eurythenes maldoror	JX887069	JX887151	Havermans et al., 2013
Eurythenes maldoror	JX887068	JX887152	Havermans et al., 2013
Eurythenes maldoror	JX887067	JX887121	Havermans et al., 2013
Eurythenes maldoror	KX034310	KX365240	Ritchie et al., 2017
Eurythenes maldoror	MW042878	MW048992	This study (4974 m)
Eurythenes obseus	KP456144	KP713954	Ritchie et al., 2015
Eurythenes obseus	no data	Eob-C103	d’Udekem d’Acoz & Havermans, 2015
Eurythenes plasticus	MT021437	MT038070	Weston et al., 2020a
Eurythenes plasticus	MT021438	MT038071	Weston et al., 2020a
Eurythenes plasticus	MT021439	MT038072	Weston et al., 2020a
Eurythenes plasticus (‘Eg7’)	U40445	no data	France and Kocher 1996
Eurythenes sigmiferus	JX887070	no data	Havermans et al., 2013
Eurythenes sigmiferus	AY943568	no data	Escobar-Briones et al., 2010
Eurythenes thurstoni	U40449	no data	France & Kocher, 1996
Eurythenes sp. ‘Eg8’	U40439	no data	France & Kocher, 1996
Eurythenes sp. ‘Eg8’	U40440	no data	France & Kocher, 1996
Eurythenes sp. ‘Eg9’	U40446	no data	France & Kocher, 1996
Eurythenes sp. ‘Eg9’	U40448	no data	France & Kocher, 1996
Eurythenes sp. ‘PAP’	no data	MN832603	Horton et al., 2020
Eurythenes sp. ‘PAP’	no data	MN832604	Horton et al., 2020
Eurythenes sp. ‘PCT abyssal’	KP456140	KP713957	Ritchie et al., 2015
Eurythenes sp. ‘PCT abyssal’	KP456141	KP713958	Ritchie et al., 2015
Eurythenes sp. ‘PCT hadal’	KP456138	KP713955	Ritchie et al., 2015 (7050 m)
Eurythenes sp. ‘PCT hadal’	KP456139	KP713956	Ritchie et al., 2015 (7050 m)
Eurythenes sp. ‘PCT hadal’	KR527251	no data	Eustace et al., 2016
Eurythenes sp. ‘PCT hadal’	KR527252	no data	Eustace et al., 2016

2.3 Morphometric Relationship and Bathymetric Trends

Bathymetric trends were assessed in relation to sex for the RV *Sonne* SO261 specimens. Males were identified by the presence of penile papillae, and females were identified by the presence of oostegites. Intersex was classified by the presence of both oostegites and penile papillae. Juveniles were classified by the visual absence of oostegites and penile papillae (Ingram & Hessler, 1987; Eustace et al., 2016). Total body length (rostrum to the end of telson) and coxa 4 length (diagonal) were measured to the nearest 0.1 mm using digital callipers (Fisher Scientific; Duffy et al., 2016; Lacey et al., 2018). Individuals were weighed to the nearest 0.001 g, following 1 minute of drying.

The total length-weight relationship was calculated using all individuals from the RV *Sonne* SO261 between 6714–8052 m. The relationship was based on the following non-linear formula: $W = a \times TL^b$, where w = weight, TL = total length, and *a* and *b* are regression-derived parameters. The total length-coxa 4 relationship was examined using an ordinary least squares linear regression, with nearly the same set of individuals as the total length-weight relationship, apart from the intersex individual. The model assumptions were checked for normality and heterogeneity of variance using histograms of the residuals and by examining qqplots and the fitted values versus residuals. The relationship between total length by depth for females was examined using Spearman correlation. The relationship between total length and depth was sigmoidal for juveniles. As such, a non-linear 4-part self-starting logistic regression was fit using the package *nlme* v3.1 (Pinheiro et al., 2020). The analysis was conducted in R version 3.6.3.

3. Results

3.1 Systematics

Order Amphipoda Latreille, 1816

Superfamily Lysianassoidea Dana, 1849

Family Eurytheneidae Stoddart and Lowry, 2004

Genus *Eurythenes* S. I. Smith in Scudder, 1882

***Eurythenes atacamensis* sp. nov. Weston & Espinosa-Leal** (Figure 20, Figure 21, Figure 22, Figure 23, Figure 24)

ZooBank: http://zoobank.org/51f715e8-ad60-403c-b39a-06f3a3223935

Eurythenes gryllus—Ingram and Hessler, 1987: 1889.—Thurston et al., 2002: 205–210, figs. 1–7, table 1.—Jamieson et al., 2019: 1–9, fig. 1, table 1.

Eurythenes gryllus Peru-Chile(H)—Ritchie et al., 2015: 121–129, figs.2, 4, tables 1, 2.

Eurythenes sp. (Hadal Form)—Eustace et al., 2016: 91–97, fig. 1, fig. 2 (d)(e)(f), fig. 5, tables 2, 3.

Material Examined.

HOLOTYPE: *Female*, total body length 76.2 mm, Atacama Trench, eastern South Pacific Ocean (23°22.774'S, 71°20.683'W), expedition SO216, station 4, depth 8052 m, MNHNCL AMP-15816, genseq-1 16S (MW042884), COI (MW048996).

PARATYPES: *Female*, total body length 70 mm, Atacama Trench, Pacific Ocean (23°24.48'S, 71°19.91'W), *Atacamex* Expedition, station 2, depth 8081 m, MZUC/UCCC 46674. *Female*, total body length 72 mm, Atacama Trench, Pacific Ocean (23°24.48'S, 71°19.91'W), *Atacamex* Expedition, station 2, depth 8081 m, MZUC/UCCC 46675, genseq-2 16S (MW290039), COI (MW288146). *Male*, total body length 50.8 mm, Atacama Trench, Pacific Ocean (23°22.384'S, 71°23.577'W), expedition SO216, station 4, depth 7204 m, MNHNCL AMP-15817. *Female*, type locality, MNHNCL AMP-15822. *Intersex*, total body length 58.8 mm, Atacama Trench, Pacific Ocean (24°16.233'S, 71°25.386'S), expedition SO216, station 6, depth 7834 m, MNHNCL AMP-15820, genseq-2 16S (MW042883). *Juvenile*, total body length 16.1 mm, Atacama Trench, Pacific Ocean (21°44.497'S, 71°15.465'W), expedition SO216, station 2, depth 6738 m, MNHNCL AMP-15819. *Juvenile*, total body length 38.4 mm, Atacama Trench, Pacific Ocean (21°44.497'S, 71°15.465'W), expedition SO216, station 2, depth 6714 m,

MNHNCL AMP-15818. *Juvenile*, Atacama Trench, Pacific Ocean (22°56.282’S, 71°40.686’W), expedition SO216, station 7, depth 4974 m, MNHNCL AMP-15821.

PARAGENETYPE: *Juvenile*, Atacama Trench, Pacific Ocean (22°56.282’S, 71°40.686’W), expedition SO216, station 7, depth 4974 m, genseq-2 16S (MW042880). *Juvenile*, Atacama Trench, Pacific Ocean (20°20.608’S, 71°07.821’W), expedition SO216, station 10, depth 5920 m, genseq-2 16S (MW042881), COI (MW048993). *Female*, Atacama Trench, Pacific Ocean (23°02.998’S, 71°15.044’W), expedition SO216, station 3, depth 7139 m, genseq-2 16S (MW042882), COI (MW048994).

Type Locality. Atacama Trench, eastern South Pacific Ocean (23°22.774’S, 71°20.683’W), expedition SO216, station 4, depth 8052 m.

Etymology. The species name, *atacamensis*, references the type locality, Atacama Trench, of this conspicuously abundant scavenging amphipod.

Diagnosis. Lateral cephalic lobe rounded and weakly pronounced. Ventral corner of the eye points linearly downwards. Article 2 of mandibular palp expanded posteriorly but not distally tapering. Maxilliped inner plate with three apical, non-protruding nodular setae. Gnathopod 1 subchelate; palm weakly formed, short. Gnathopod 2 minutely chelate; coxa sub-rectangular and posterior margin slightly rounded; palm obtusely angled. Pereopods 3 to 7 dactylus short. Epimeron 3 ventral margin rounded with a small tooth on the posteroventral corner. Uropod 2 inner ramus longer than outer ramus. Lack of dorsal carination or ridging, specifically at pereonite 3.

Description, based on holotype, female, MNHNCL AMP-15816.

BODY (Figure 20): surface smooth, without setae; urosomite 3 with an anterodorsal depression. *Oostegites* present on gnathopod 2 to pereopod 5, setae absent. *Coxa gills* present on gnathopod 2 to pereopod 7. *Colour pattern* before ethanol preservation unknown as the holotype was selected post-expedition.

HEAD (Figure 21): rostrum absent; antennal sinus quadrate (Figure 21d). *Antenna 1* short, 0.13x as long as body length; accessory flagellum 14-articulate; primary flagellum 34-articulate; calceoli absent (Figure 21a). *Antenna 2* 2.4x the length of antenna 1, 0.25x as long as body; article 4–5 with brush setae; flagellum 68-articulate with some brush setae; calceoli absent (Figure 21b).

MOUTHPART BUNDLE (Figure 21): *Mandible* left lacinia mobilis a long slender robust seta with smooth distal margin; incisor smooth and convex; setal row with 11 short, slender, robust setae; molar large, setose, small triturating surface; palp article-length ratio 1: 1.8: 1.6, article 3 sickle-shaped (Figure 21c). *Maxilla 1* inner plate with nine apical plumose setae; outer plate with an 8/3-crown arrangement; palp longer than the outer plate, 2-articulate, four apical and one apicolateral robust setae, with one subapical long setae (Figure 21e–h). *Maxilla 2* both plates broad, inner plate 0.6 x shorter than the outer plate (Figure 21). *Maxilliped* inner plate sub-rectangular, three apical, non-protruding nodular setae; outer plate subovate; palp 4-articulate, left and right are asymmetric with right palp exceeding past the outer plate, dactylus well-developed, unguis present (Figure 21j–l).

PEREON (Figure 22, Figure 23): *Gnathopod 1* coxa sub-quadrate, weakly concave on anterior and ventral margins; basis, long, length 2.2x breadth; palm weakly formed and short (0.1x as long as the posterior margin of propodus), crenulate with one robust seta at base of the palm and another at the end of palm (Figure 22a–b). *Gnathopod 2* coxa with setae along the posteroventral corner; basis elongate, length 6.9 times width, setae along posterior and ventral margins; posterior margin of merus expanded; propodus sub-rectangular, length 4.5 times width; palm with 2 robust setae on the posterodistal corner; dactylus not reaching palmar corner (Figure 22c–d). *Pereopod 3* coxa sub-quadrate, 1.5x as long as wide, setae on the surface of coxa and along ventral margin; basis expanded posteriorly, 2.3x as long as wide; merus expanded anteriorly, tuft of setae on the anteroventral corner; carpus stout, 0.6x as long as propodus; propodus 3.9x as long as wide; dactylus slender, short 0.3x as long as propodus, unguis present (Figure 22e). *Pereopod 4* coxa broad, 0.9x as long as wide, 1.1x length of coxa 3, the junction between anterior and ventral border bluntly angular (sub-rectangular), ventral border straight, posteroventral border weakly oblique; leg almost identical to pereopod 3 (Figure 22f). *Pereopod 5* coxa sub-rectangular, rounded on both the anterior and posterior margins; basis expanded posteriorly, posterior margin weakly crenulated; merus broadly expanded posteriorly, 1.5x as long as wide, posteroventral margin producing a point; carpus stout, 0.4x as long as propodus; propodus long and slender, 5.5x as long as wide, 11 groups robust setae along anterior margin; dactylus short, 0.4x as long as propodus, unguis

present (Figure 23a). *Pereopod 6* coxa sub-rectangular, setae along the ventral margin, posterior margin straight; basis expanded posteriorly with posterior margin crenulated; merus expanded posteriorly, 1.5x as long as wide, convex posterior margin; propodus and dactylus nearly identical to pereopod 5 (Figure 23b). *Pereopod 7* coxa sub-rectangular; basis expanded posteriorly, posterior margin distinctly crenulated, distal lobe weakly protruding; merus broad and strongly expanded posteriorly, subequal length to width; propodus and dactylus nearly identical to pereopod 5 (Figure 23c).

PLEON AND UROSOME (Figure 23): *Epimeron 1* with setae along the anteroventral corner (Figure 23d). *Epimeron 2* with setae along the ventral margin, posteroventral corner produced into a strong tooth (Figure 23d). *Epimeron 3* ventral margin rounded with a small tooth on the posteroventral corner (Figure 23d). *Uropod 1* peduncle with 1 apicomedial seta, rami subequal, outer ramus 0.8x as long as peduncle (Figure 23e). *Uropod 2* peduncle with 2 apicomedial setae, outer ramus subequal in length to peduncle, inner ramus longer than outer ramus (1.2x; Figure 23f). *Uropod 3* setae of the distolateral angle of peduncle of normal length and stoutness; inner ramus subequal in length to article 1 of the outer ramus; outer rami article 2 0.8x the length of article 1, medial margins of both rami with plumose setae (Figure 23g). *Telson* 77% cleft, distal margin of each lobe with one robust and one slender setae (Figure 23h–i).

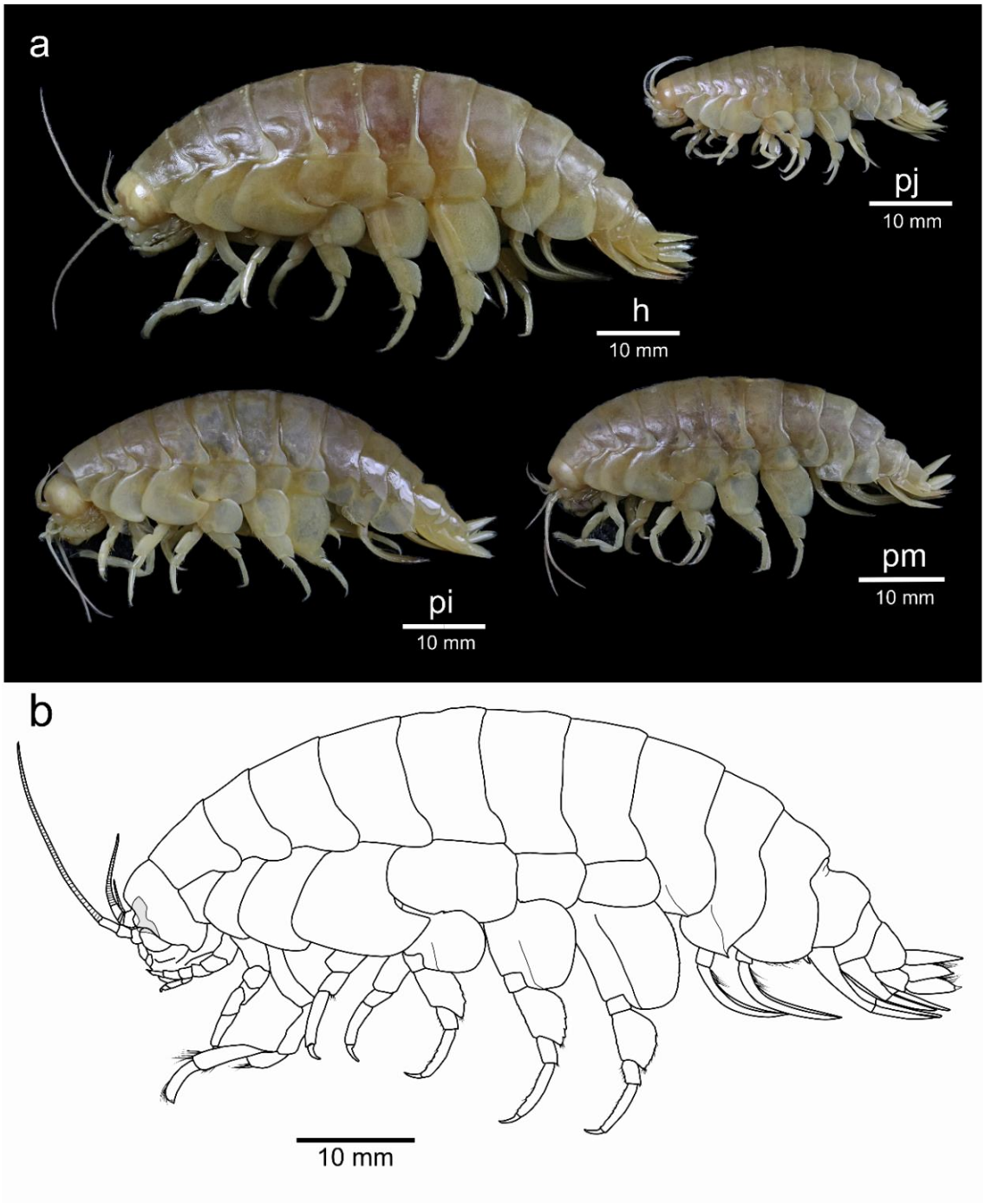

Figure 20. (a) *Eurythenes atacamensis* sp. nov.: female holotype from 8052 m (h; MNHNCL AMP-15816), juvenile paratype from 6714 m (pj; MNHNCL AMP-15818), intersex paratype from 7834m (pi; MNHNCL AMP-15820), male paratype from 7204 m (pm; MNHNCL AMP-15817). (b) *Eurythenes atacamensis* sp. nov., mature female, holotype, MNHNCL AMP-15816.

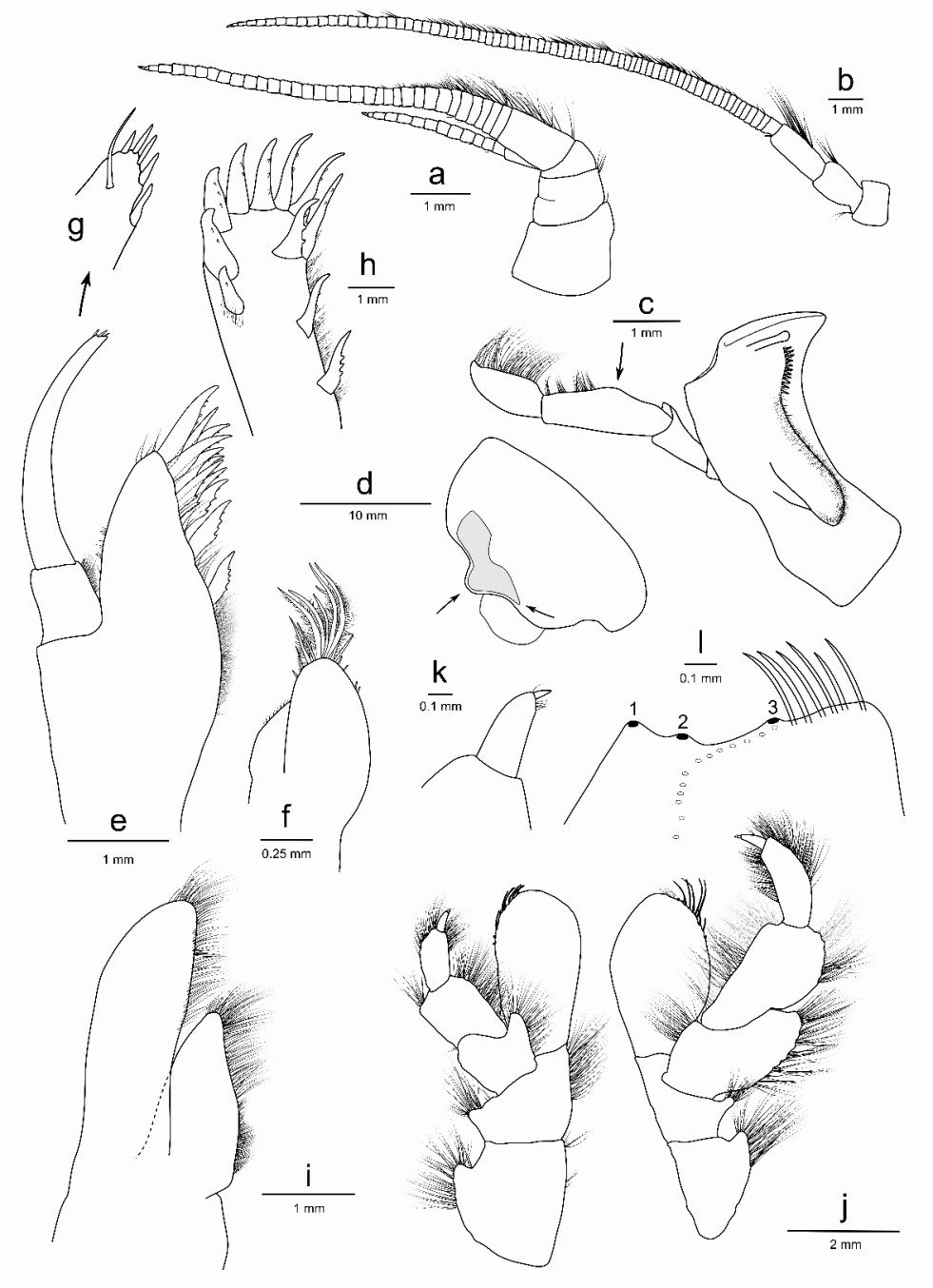

Figure 21. *Eurythenes atacamensis* sp. nov. holotype (MNHNCL AMP-15816). (a) left antenna 1; (b) left antenna 2; (c) left mandible; (d) head; (e) left maxilla 1 outer plate and palp not flattened;(f) left maxilla 1 inner plate; (g) left maxilla 1 palp insert; (h) left maxilla 1 outer plate face; (i) left maxilla 2; (j) left and right maxillipeds with inner plates removed; (k) left maxilliped dactylus insert; (l) left maxilliped inner plate (medio-facial spines not shown).

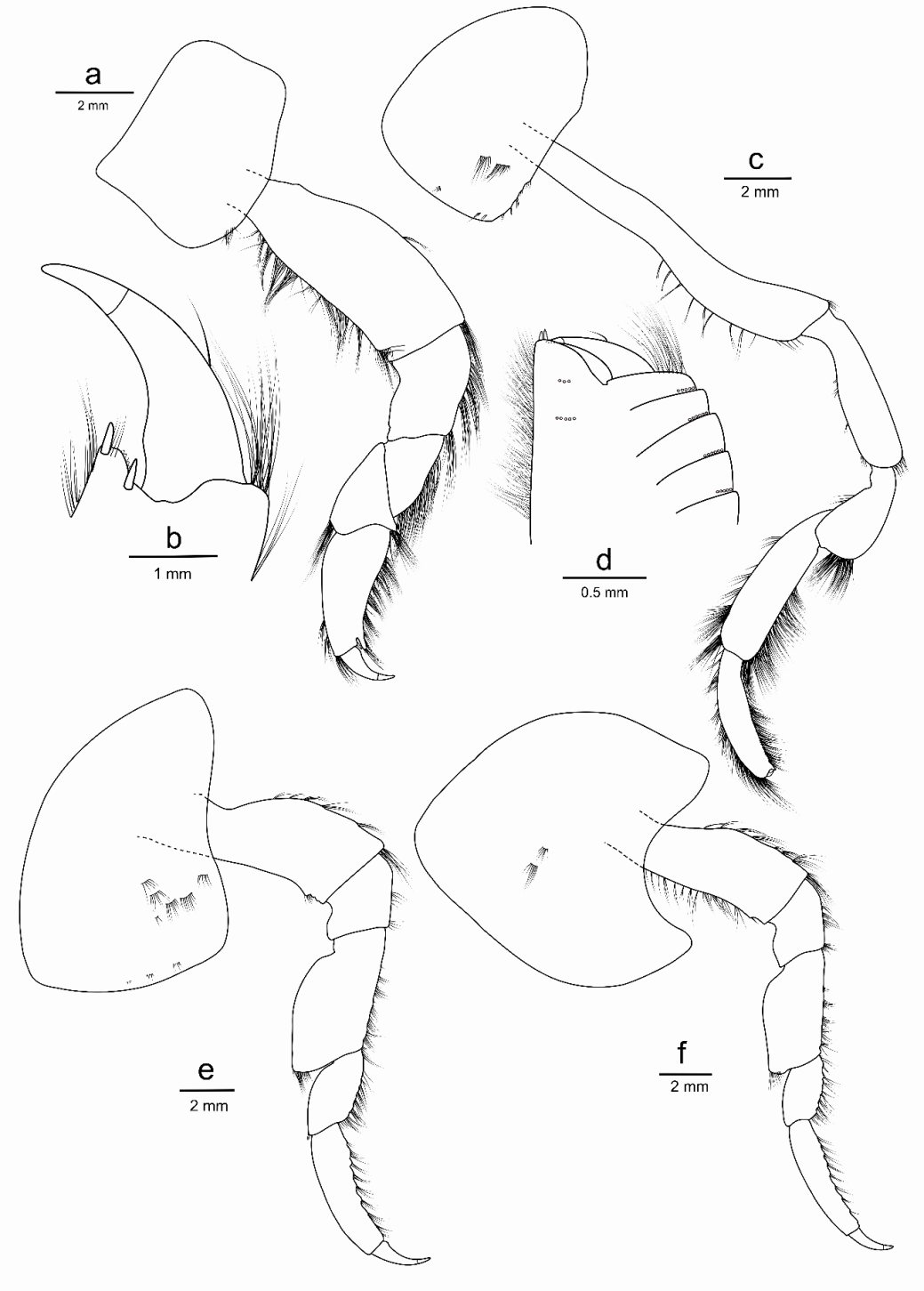

Figure 22. *Eurythenes atacamensis* sp. nov. holotype (MNHNCL AMP-15816). (a) left gnathopod 1; (b) chela of left gnathopod 1; (c) left gnathopod 2; (d) chela of left gnathopod 2; (e) left pereopod 3; (f) left pereopod 4.

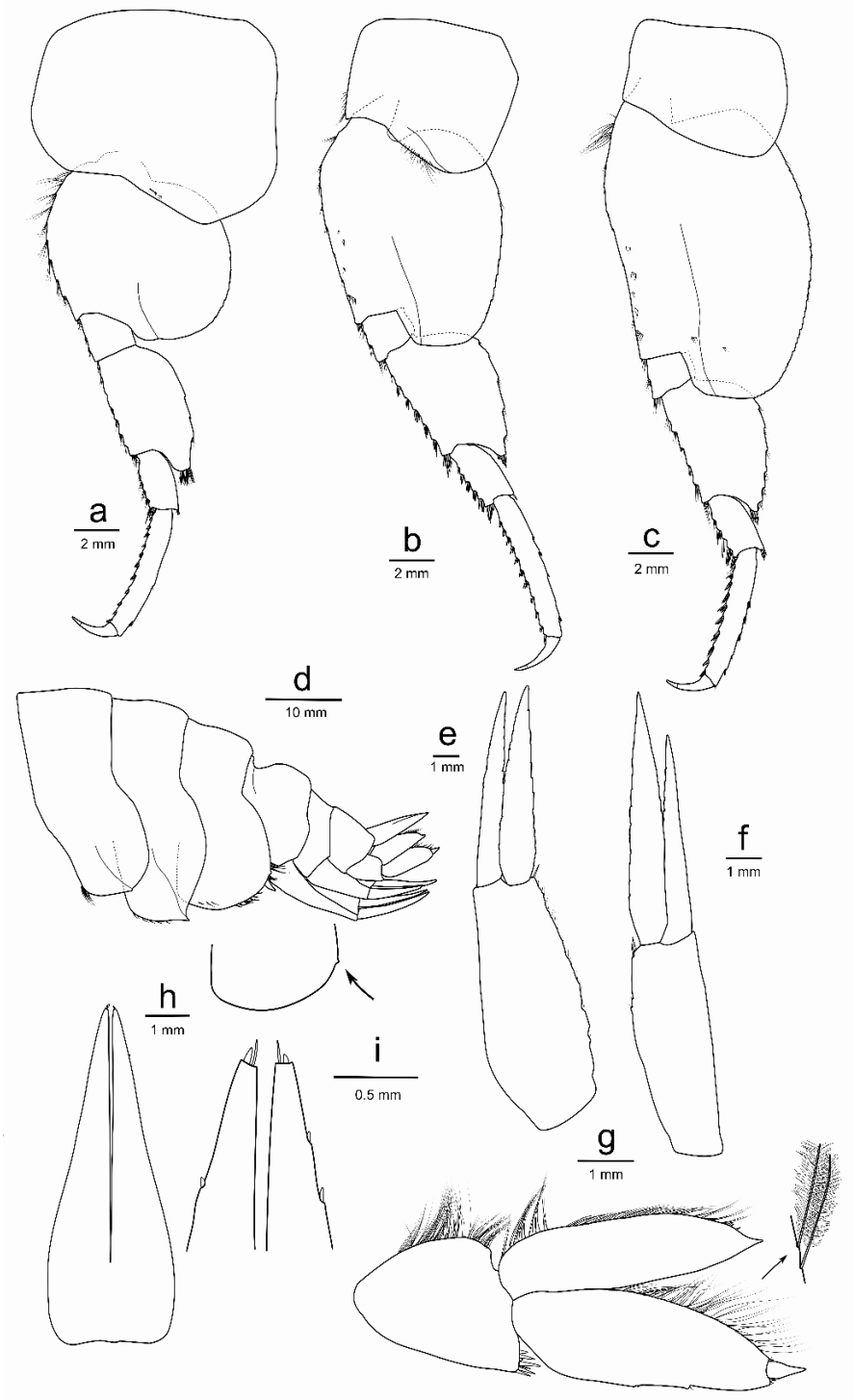

Figure 23. *Eurythenes atacamensis* sp. nov. holotype (MNHNCL AMP-15816). (a) left pereopod 5; (b) left pereopod 6; (c) left pereopod 7; (d) epimeron and epimeron 3 insert; (e) left uropod 1; (f). left uropod 2; (g) left uropod 3; (h) telson; I; telson distal margin insert.

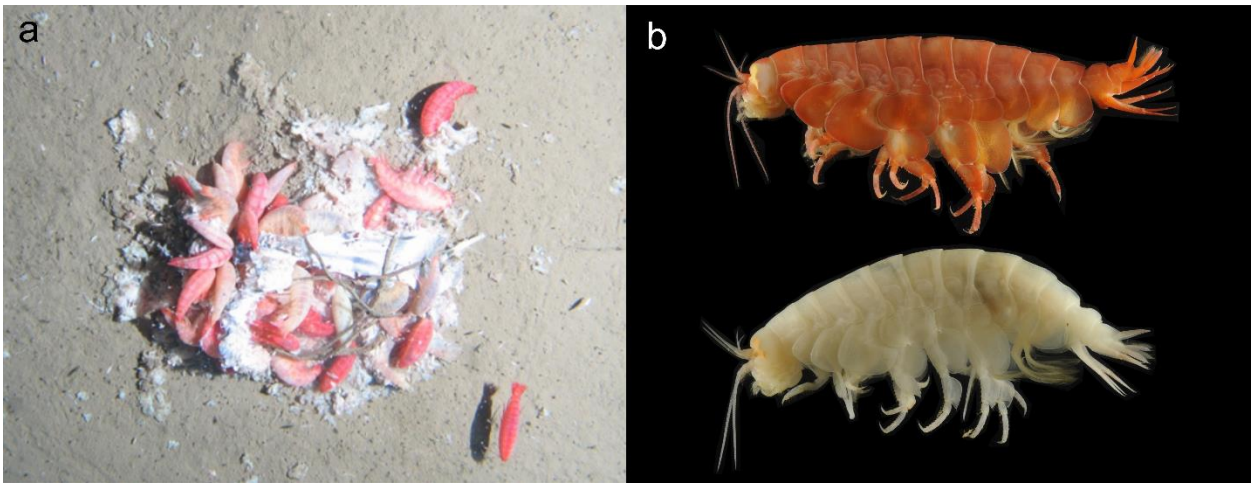

Figure 24. (a) *Eurythenes atacamensis* sp. nov. feeding on bait, and (b) two colour morphs prior to ethanol preservation. Still image and specimens are from 8074 m during the 2010 RV *Sonne* SO209 Expedition.

Variations. Prior to ethanol preservation, body colour of specimens ranged from white, pink, crimson, to dark red and the eye shape and colour were more defined (Figure 24). This wide variation in body pigmentation is likely attributed to the moult/intermoult cycle (Baldwin & Smith, 1987). Minor differences were observed between females and the male. The mature male paratype (MNHNCL AMP-15817) had calceoli present on both antennas 1 and 2. The primary flagellum of antenna 1 was 31-articulate with calceoli present between articles 8–20, and the accessory flagellum was 12-articulate. Antenna 2 was 65-articulate. The intersex paratype (MNHNCL AMP-15820) had protruding penile papillae that flexed towards each other but lacked calceoli on antenna 1 or 2. As with the holotype, the oostegites were present on pereopod 2–5, however, the flattened oostegites were not of full length relative to the total body length and lacked setae. Moderate differences were present between sexed and juvenile specimens, with fewer setae on pereopods and uropods and a reduction in articulation on antennae. Specifically, in the juvenile paratype (MNHNCL AMP-15818), the antenna 1 accessory flagellum was 10-articulate, antenna 1 was 26-articulate, and antenna 2 was 57-articulate. Further, the juvenile had more pronounced crenulation of the posterior margin of the basis on pereopods 5–7.

Feeding and Distribution. This species is a benthopelagic scavenger, which is well documented by its rapid aggregation and feeding at the baited camera landers (Figure 23a; Hessler et al., 1978). As with *E. plasticus*, individuals of *E. atacamensis* sp. nov. have been previously documented to ingest microplastics (Jamieson et al., 2019; Weston et al., 2020a). *Eurythenes atacamensis* sp. nov. has a wide bathymetric range (>3000 m) across abyssal to hadal depths (4974–8081 m), including the deepest point of the Atacama Trench. This species is considered to have a distribution localised to both sectors of the Peru-Chile Trench. *Eurythenes atacamensis* sp. nov. is a prominent member of a wider scavenging amphipod community (Fujii et al., 2013). This community is comprised of three species also endemic to the Peru-Chile Trench, *Hirondellea thurstoni* Kilgallen, 2015, *Hirondellea sonne* Kilgallen, 2015, and *Hirondellea wagneri* Kilgallen, 2015.

Differential Diagnosis. In a genus with cryptic speciation (Havermans et al., 2013), *Eurythenes atacamensis* sp. nov. has distinct diagnostic features. These features include a smooth dorsal body, the palm of gnathopod 1 being very short, and the palm of gnathopod 2 being minutely chelate with an obtusely angled palm. *Eurythenes atacamensis* sp. nov. is most similar morphologically to *E. thurstoni*, as they both have a minutely chelate gnathopod 2. Yet, *E. atacamensis* sp. nov. can be readily differentiated by the lack of an upturned ridge on the anterodorsal margin of head (present in *E. thurstoni*), uropod 2 inner ramus longer than outer ramus (opposed to subequal), and small tooth on the posteroventral corner of epimeron 3 (versus subquadrate). *Eurythenes thurstoni* is also smaller in total body size, most commonly not longer than 35 mm (Stoddart & Lowry, 2004). Additionally, the two species have a disjunct vertical distribution, where *E. thurstoni* lives at bathyal depths (Stoddart & Lowry, 2004; d'Udekem d'Acoz & Havermans, 2015).

Key to *Eurythenes* specimens larger than 25 mm

This key is expanded from d'Udekem d'Acoz & Havermans (2015), and the caution of use remains. Character differences can be tough to objectively discern, and certain characteristics can be phenotypically variable between cohorts. Visual identification paired with DNA barcoding is strongly recommended.

1. Dactylus of pereopods 3–7 short (less than 0.3 of propodus) 2
   Dactylus of pereopods 3–7 long (more than 0.6 of propodus) *Eurythenes obesus* (Chevreux, 1905)
2. The palm of gnathopod 2 minutely chelate or very protruding 3
   The palm of gnathopod 2 subchelate or weakly protruding 4
3. The anterodorsal margin of the head forming an upturned ridge; posterodistal lobe of the basis of pereopod 7 very long *Eurythenes thurstoni* Stoddart & Lowry, 2004
   The anterodorsal margin of the head not forming an upturned ridge; palm of gnathopod 1 very short; posterodistal lobe of the basis of pereopod 7 short or fairly short ***Eurythenes atacamensis* sp. nov.**
4. Pereopods 6–7 and epimerons 1–3 not dorsally keeled to slightly keeled; pereopods 6–7 and epimeron 1–2 dorsally not sigmoid (without anterior concavity), epimeron 3 with distinct anterior concavity 5
   Pereopods 6–7 and epimerons 1–3 dorsally strongly keeled and sigmoid (anteriorly slightly to distinctly concave) *Eurythenes sigmiferus* d'Udekem d'Acoz & Havermans, 2015
5. Eyes of variable width; the outer plate of maxilla 1 with 8/3 crown arrangement 6
   Eyes of constant width; the outer plate of maxilla 1 with 9/3 crown arrangement *Eurythenes aequilatus* Narahara-Nakano, Nakano & Tomikawa, 2017
6. Article 2 of mandibular palp moderately to strongly expanded posteriorly 7
   Article 2 of mandibular palp not to weakly expanded posteriorly 8
7. Maxilliped with 3 non-protruding nodular spines; pereopod 7 with basis posteriorly strongly expanded, with merus narrow *Eurythenes andhakarae* d'Udekem d'Acoz & Havermans, 2015

Maxilliped with 8–9 non-protruding nodular spines; pereopod 7 with basis posterior border weakly expanded, with merus stout *Eurythenes maldoror* d'Udekem d'Acoz & Havermans, 2015

8. Gnathopod 2 palm convex; uropod 1 and 2 rami subequal 9

Gnathopod 2 palm straight; the outer ramus of uropod 1 and 2 are shorter than paired inner ramus *Eurythenes magellanicus* (H. Milne Edwards, 1848)

9. Ventral corner of eye rounded and obliquely pointing backward; maxilliped with 3–4 protruding nodular spines; gnathopod 1 palm convex *Eurythenes plasticus* Weston, 2020

Ventral corner of eye sharp and pointing downward; maxilliped with 3–4 non-protruding nodular spines; gnathopod 1 palm straight *Eurythenes gryllus* (Lichtenstein in Mandt, 1822)

3.2 DNA Barcoding and Phylogenetics

Thirteen sequences have been annotated, deposited on GenBank, and assigned GenSeq nomenclature (**Error! Reference source not found.**; 16S: MW042878–84, MW290039 and COI: MW048992–96, MW288146; ncbi.nlm.nih.gov/genbank). Four *E. atacamensis* sp. nov. and one *E. maldoror* were successfully characterised across both 16S and COI (Table 2). Two *E. atacamensis* sp. nov. and one *E. magellanicus* were only characterised across 16S (Table 2). The depths of the *E. atacamensis* sp. nov. specimens spanned from 4974–8081 m.

The phylogenetic relationship of *E. atacamensis* sp. nov. within *Eurythenes* was studied separately for 16S and COI genes (Figure 25). The *E. atacamensis* sp. nov. specimens of this study were placed within the same undescribed clade as those presented in Ritchie et al. (2015) and Eustace et al. (2016), namely the *Eurythenes* sp. 'PCT hadal', with high support values (16S: BI =0.62, ML = 100; COI: BI = 0.94, ML = 75). This clade was repeatedly placed more basal in the phylogenies. In the 16S topology, only *E. thurstoni* was basal to *E. atacamensis* sp. nov. The *E. atacamensis* sp. nov. clade in the 16S topology had two subclades, however, this distinction was not present in the COI phylogeny. Within the *E. atacamensis* sp. nov. clade, there was a lack of apparent patterns based on depth or station proximity to the trench axis.

The species delimitation analysis showed agreement among the individual phylogenies to support multiple species being present within *Eurythenes*. For 16S, the bPTP analysis inferred six species (mean: 6.78; acceptance rate: 0.179; the estimated number of species: 5–16). However, no distinct entities were differentiated by the GYMC analysis ($p>0.436$), due to low support values (<0.7). There was bPTP support for *E. atacamensis* sp. nov. to be a discrete lineage (0.96; Figure 25a). The bPTP model estimated 11 species of *Eurythenes* within the COI topology (mean: 12.58; acceptance rate: 0.13; the estimated number of species: 10–16). In concordance, GMYC found 11 distinct entities to be associated with the highest likelihood score (confidence interval 11–18; $p < 0.005$). *Eurythenes atacamensis* sp. nov. was delineated into a distinct lineage by both analyses (bPTP: 0.99; GMYC: 0.9; Figure 25b).

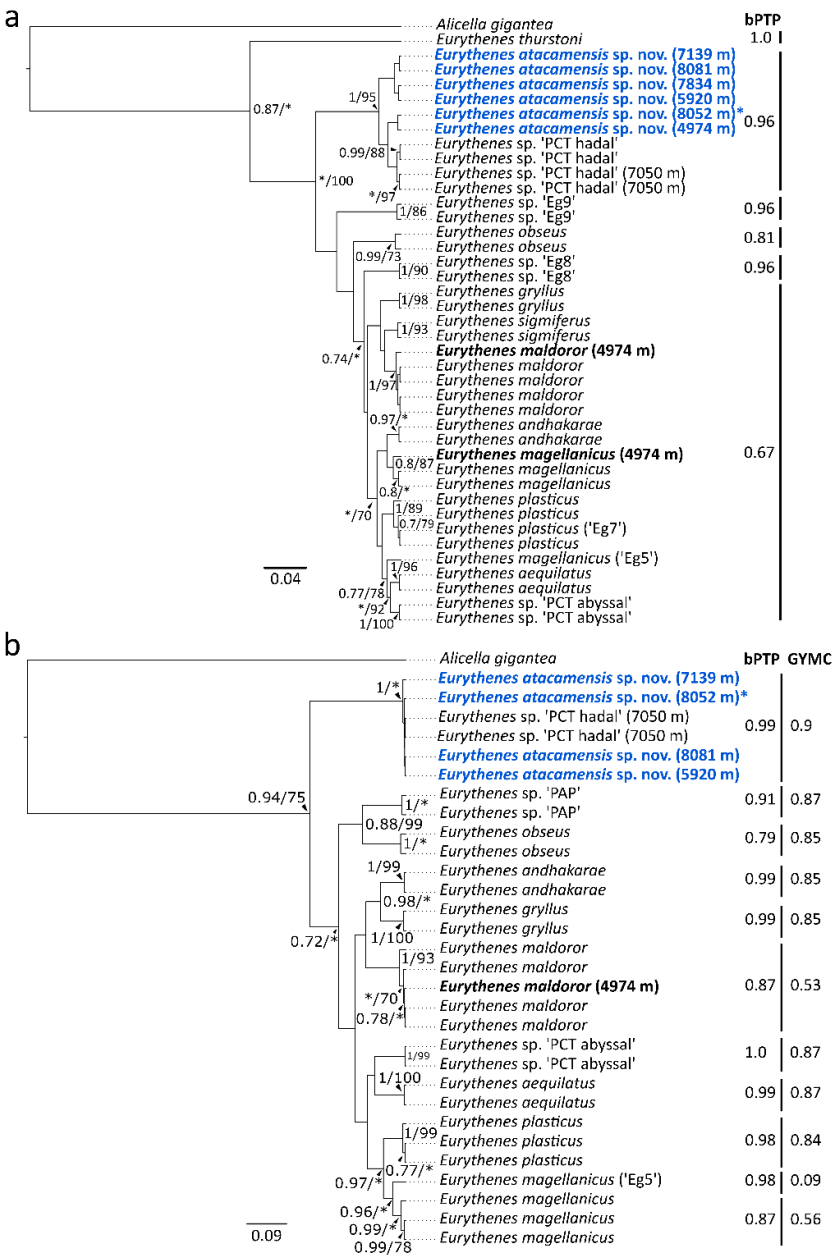

Figure 25. Bayesian phylogenies showing the relationship of *Eurythenes atacamensis* sp. nov. within *Eurythenes* based on: (a) 16S rRNA, and (b) COI. Specimens added by this study are in bold, with *E. atacamensis* sp. nov. in blue. An asterisk next to the name denotes holotype. References for comparative sequences are in Table 5. Branch nodes have Bayesian posterior probabilities and maximum likelihood bootstrap support values. Values less than 0.7 or 70 are not stated or depicted by an asterisk. Species delimitation inferences by the bPTP and/or GYMC analyses are shown on the right side of each phylogeny.

3.3 Morphometric relationships and bathymetric trends

A total of 677 specimens of *E. atacamensis* sp. nov. were recovered from the 11 stations (Table 4). None of the 319 females had setae on oostegites or were found to be ovigerous. A single male and a single intersex individual were recovered from 7204 m and 7834 m, respectively (Figure 26). The 356 juveniles were found across the entire depth range sampled (4974–8052 m) and dominated in relative abundance at 6714 m and shallower (88–100%; Figure 26). In contrast, females were found between 6520–8052 m and increased in relative abundance with depth from 5% to 95% (Figure 26).

Female *E. atacamensis* sp. nov. ranged in total length from 44.3–83.2 mm and weight from 1.09–9.10 g (Figure 27a, b). Juveniles ranged in total length from 12.1–49.9 mm and ranged in weight from 0.042–4.22 g (Figure 27a, b). The only male specimen measured 50.8 mm and weighed 2.18 g (Figure 27a, b), and the only intersex individual measured 58.8 mm in total length, but no weight was recorded (Figure 27b). The relationship between length and weight was:

$$W = 0.00004569 * TL^{2.753}$$

The parameters *a* (t = 6.01, p = 3.44e^{-09}) and *b* (t = 69.20, p < 2e^{-16}) were both significant (Figure 27a).

Coxa 4 varied in length between 6.1–12.9 mm for females and 1.9–10.3 mm for juveniles. The relationship between total length and coxa 4 (t = 132.281, p < 2e^{-16}, r^2 adjusted = 0.9694) followed a linear relationship (Figure 27b):

$$TL = 2.46262\ (\text{standard error}\ \pm 0.36585) + 6.19965\ (\text{standard error}\ \pm 0.04687) * coxa4$$

The relationship between total length and depth appeared to follow a sigmoidal relationship for juveniles (Figure 27c). Total length remains constant with depth (33.7 ± 19.6 mm) until ~6500 m before it begins to increase. Around 7200 m, the relationship between total length of juveniles begins to increase rapidly and then reaches an asymptote by ~7700 m (59.9 ± 8.2 mm). The inflection point of the sigmoidal relationship is at ~7300 m, and no juveniles were smaller than 35 mm beyond this depth. There was no relationship between total length and depth in females (Spearman correlation: rho = 0.05, p = 0.3235; Figure 27d).

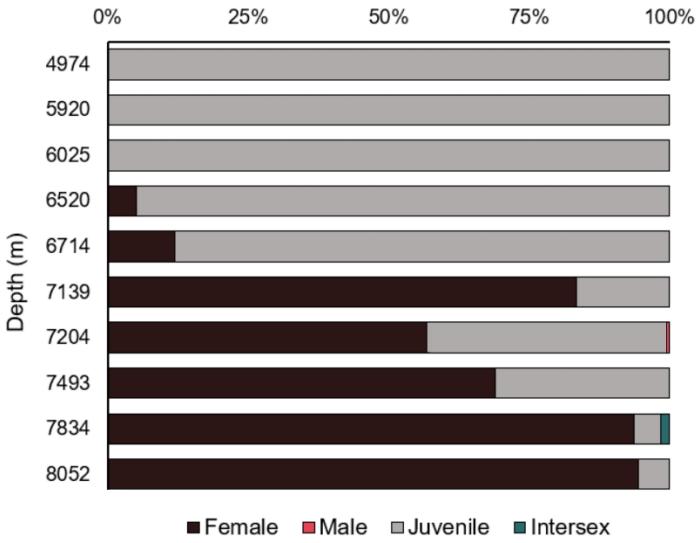

Figure 26. The relative proportion of females, males, juveniles, and intersex of *Eurythenes atacamensis* sp. nov. by depth at the Atacama Trench.

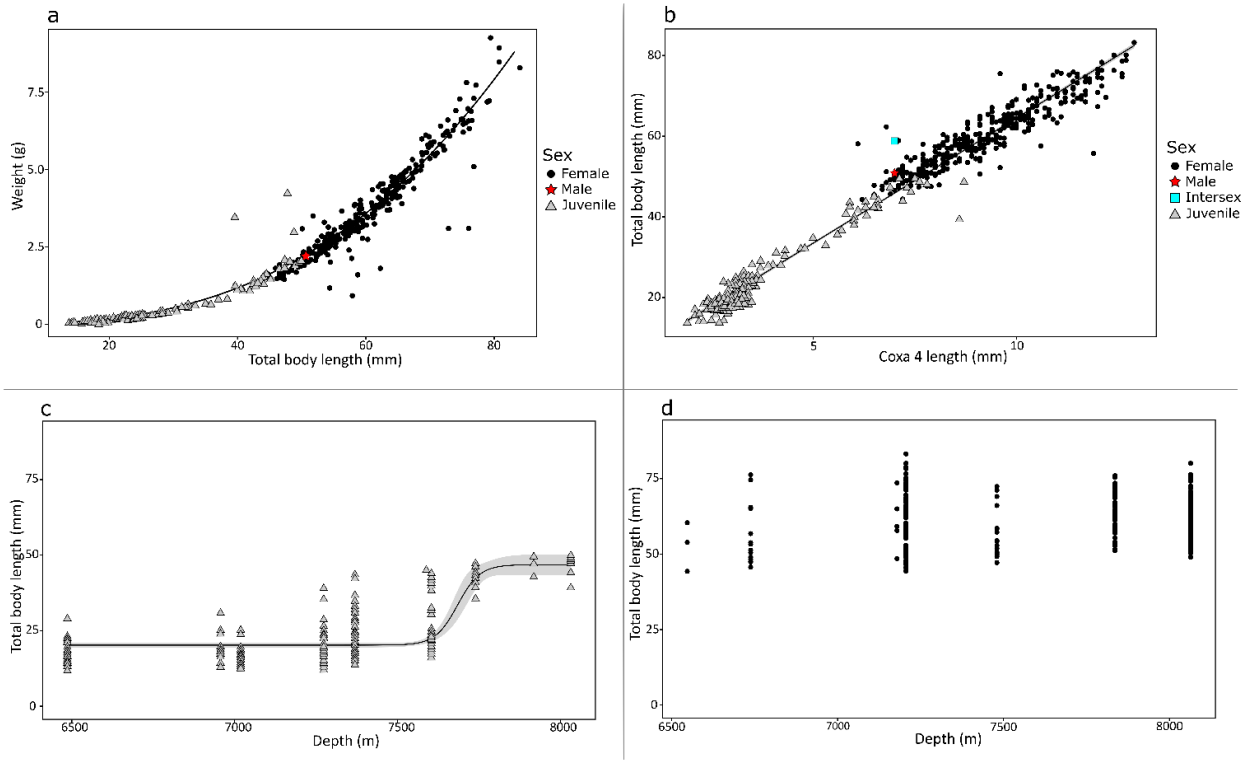

Figure 27. Morphometric relationship between (a) total length and weight, and (b) coxa 4 and total length. Bathymetric relationship of total length for (c) juvenile and (d) female *Eurythenes atacamensis* sp. nov. 95% confidence intervals of the model mean are grey areas in (b) and (c).

4. Discussion

This study described a scavenging amphipod endemic to the Peru-Chile Trench, *Eurythenes atacamensis* sp. nov., by applying an integrative taxonomic approach. Analysis of the *Atacamex* and RV *Sonne* SO261 Expeditions specimens expanded the bathymetric range of *E. atacamensis* sp. nov. from only hadal to include abyssal depths, confirmation of ontogenetic vertical stratification across the trench axis, and revealed differing size-to-depth trends between juveniles and females.

Eurythenes atacamensis sp. nov. represents a unique lineage within *Eurythenes*. The two mtDNA topologies supported that the *Eurythenes* sp. 'PCT hadal' recovered from SO209 expedition are *E. atacamensis* sp. nov. (Figure 27; Ritchie et al., 2015; Eustace et al., 2016). While comparative sequences from the SOUTHTOW, SIO BI72–20, and ATIE specimens were not available, the combination of the morphological characterisation, photographs, and sampling locations provide sufficient evidence to conclude they were *E. atacamensis* sp. nov. (Hessler et al., 1978; Ingram & Hessler, 1987; Thurston et al., 2002). Notably, this species is not part of the *gryllus*-complex and basally rooted within the presented phylogenies, more closely related to *E. thurstoni* and *Eurythenes* sp. 'Eg9' (France & Kocher, 1992; Havermans et al., 2013). Morphologically, *E. atacamensis* sp. nov. possesses distinguishable and non-cryptic characteristics (d'Udekem d'Acoz & Havermans, 2015), specifically the short palm of gnathopod 1 and chelate palm of gnathopod 2 (Figure 22). *Eurythenes thurstoni* is the only other known *Eurythenes* species with a chelate gnathopod 2 (Stoddart & Lowry, 2004). Evidence suggests that among gammaridean amphipods the gnathopods serve a range of functions, including feeding (Klages & Gutt, 1990), grooming (Holmquist, 1985), and reproduction (Borowsky, 1984). However, the current dearth of understanding regarding the functional significance of gnathopod morphological differences in *Eurythenes* amphipods precludes the assignment of any particular selection pressure as the driver of this divergence.

Based on historical expeditions, *E. atacamensis* sp. nov. was considered restricted to hadal depths, with a total range of 1901 m (Eustace et al., 2016). These two expeditions have expanded the known bathymetric range of *E. atacamensis* sp. nov. to 3099 m, showing it is not restricted solely to hadal depths. Rather, *E. atacamensis* sp. nov. spans

the abyssal-hadal transition zone and extends to the deepest point in the Peru-Chile Trench (Figure 26). Eurybathic distribution is common within *Eurythenes,* specifically *E. gryllus*, *E. magellanicus*, *E. maldoror*, and *E. sigmiferus* have ranges spanning over 2500 m (Escobar-Briones et al*.,* 2010; d'Udekem d'Acoz & Havermans, 2015; Lacey et al*.,* 2016). As with geographic distributions, the known bathymetric range of *Eurythenes* species is likely to continue widening with expanded global sampling efforts (Havermans, 2016).

The latitudinal distribution of *E. atacamensis* sp. nov. spans the entire Peru-Chile Trench, with the presence at the Milne-Edwards Trench (northern sector; Eustace et al*.,* 2016) and the Atacama Trench (southern sector; Figure 19a; Hessler et al*.,* 1978; Ingram & Hessler, 1987; Thurston et al*.,* 2002; Eustace et al*.,* 2016). While this could be the full extent of their distribution, it remains outstanding whether the distribution extends west to the neighboring abyssal plains. As this study found juveniles as shallow as 4974 m at the Atacama Trench, it is curious that no specimens were previously collected from abyssal depths (4602 and 5329 m) in the Milne-Edwards Trench (Eustace et al*.,* 2016). This could be a false absence. Another possibility is the abyssal absence in the Milne-Edwards Trench reflects distributional differences in response to the distinctive environmental and surface productivity conditions of each trench sector. For instance, the Milne-Edwards Trench is considered sediment-starved with highly productive year-round upwelling, while the Atacama Trench has high sediment loads with seasonal upwelling (Montecino & Lange, 2009; Geersen et al*.,* 2018; Geersen, 2019). Additionally, the Nazca Ridge partitioning the two sectors of the Peru-Chile Trench is ~4000 m deep (Figure 19a; Hampel et al*.,* 2004). It remains outstanding whether this is a barrier to *E. atacamensis* sp. nov. Future research investigating population connectivity across the Nazca Ridge and the role of environmental and surface productivity differences between the two sectors would enhance the interpretation of their population structure and distribution ecology.

Along with *E. atacamensis* sp. nov.*, E. magellanicus* and *E. maldoror* co-occurred at the shallowest station of the RV *Sonne* SO261 Expedition (4974 m). *Eurythenes magellanicus* is known from the Milne-Edwards Trench (Eustace et al*.,* 2016), and this study expands its range southward into the Atacama Trench. Further, this is the first

account of *E. maldoror* in the Peru-Chile Trench, expanding its distribution to the eastern South Pacific Ocean (Havermans 2016; Weston et al., 2021). Surprisingly, *Eurythenes* sp. 'PCT abyssal' was not recovered, as previously found at the Milne-Edwards Trench (Eustace et al., 2016). This may indicate that *Eurythenes* sp. 'PCT abyssal' is restricted to the Milne-Edwards Trench. Together, the presence of *E. magellanicus*, *E. maldoror, E. atacamensis* sp. nov. highlights the complexity of the patchwork geographic and bathymetric distributions within *Eurythenes*.

Ontogenetic vertical stratification was evident with the RV *Sonne* SO261 specimens, whereby juveniles dominated the upper depths (<6714 m) and females were dominant at the deeper depths (>7139 m; Figure 26). Ontogenetic vertical stratification by *E. atacamensis* sp. nov. is not novel to *Eurythenes* or the Peru-Chile Trench (Eustace et al., 2016). Similar instances have been documented in other abundant hadal scavenging amphipods, including *Bathycallisoma schellenbergi* (Birstein & Vinogradov, 1958) from the Kermadec and New Hebrides trenches (Lacey et al., 2018), *Hirondellea dubia* Dahl, 1959 from the Tonga and Kermadec trenches (Blankenship et al., 2006; Lacey et al., 2018; Wilson et al., 2018), and *Hirondellea gigas* (Birstein & Vinogradov, 1955) from the Izu-Bonin Trench (Eustace et al., 2013). This demographic trend was consistent with the SO209 expedition, indicating that the ontogenetic vertical stratification pattern is constrained by depth in the Peru-Chile Trench and not confounded by latitude. Lacey et al., (2018) proposed that ontogenetic vertical stratification is an ecological strategy to reduce competition for food resources and alleviate pressure-induced physiological and metabolic limitations. The bathymetric trends in the size of *E. atacamensis* sp. nov. support this hypothesis, and further reveal this strategy is applied differently by females and juveniles.

Based on this dataset and the body of literature on *Eurythenes* biology, it is plausible to visualise the following population dynamic for *E. atacamensis* sp. nov. in the Atacama Trench. Here, the early-stage juveniles are small (<30 mm; Figure 27c) and have not built-up wax esters and lipid reserves (Bühring & Christiansen, 2001). Thus, they may be constrained to locating food over a small area (Hargrave et al., 1994) at the shallower depths. The trade-offs to living at depths with lower metabolic pressures are food resources at a lower concentration (Danovaro et al., 2003; Ichino et al., 2015; Glud

et al., 2021) and predation risks (Havermans & Smetacek, 2018) from fauna such as cusk eels, snailfish, or penaeid decapods (Wenzhöfer, 2019). As the juveniles grow to a later stage (Figure 27c), their extra lipid reserves and larger body size perhaps allow them to descend to depths beyond predatory species (Wilson & Ahyong, 2015; Linley et al., 2016), and then they exploit the higher concentration of phytodetritus and organic carbon to continue developing towards maturity (Danovaro et al., 2003; Ichino et al., 2015; Lacey et al., 2018; Glud et al., 2021). The females have the lipid reserves, metabolic capacity, and strong swimming ability (Havermans, 2016) to expand their horizontal and vertical ranges (Figure 27d; Hargrave et al., 1994) across the trench axis.

While the bathymetric trend of juveniles and females across hadal depths can be rationalised, it remains less clear why small stage juveniles were found ~1,500 m shallower than the shallowest females (Figure 26). More questionably, how do the small stage juveniles arrive at abyssal depths? Ovigerous females are presumed to stop feeding to prevent expulsion of the brood (Bregazzi, 1972; Christiansen et al., 1990; Johnson et al., 2001; Lacey et al., 2018) and are thus systematically excluded from the baited traps. Several hypotheses, constrained by the lack of behaviour and bathymetric evidence of ovigerous females, may explain the presence of abyssal *E. atacamensis* sp. nov. juveniles. Previously work has postulated that the Atacama Trench population receives continuous recruitment from abyssal depths (Thurston et al., 2002). However, this is a less plausible scenario, given that adults have not been found shallower than 6103 m (Eustace et al., 2016), high abundance at hadal depths, and the nearby abyssal plains have not been sampled. Another potential explanation is that females release their hatchlings at shallow hadal depths. The newly hatched juveniles, with functional mouthparts and developed pleopods (Thurston & Bett, 1995), then migrate to even shallower, abyssal depths. While there are metabolic benefits to migrate shallower, this transit to shallower depths with low lipid reserves is challenging to reconcile. A more complex hypothesis is that ovigerous females migrate and release their brood between the abyssal and shallow hadal depths (~4900–6500 m) and then those females die shortly after. *Eurythenes* are assumed to be iteroparous (Ingram & Hessler, 1987) and have an extreme K-selected to A-selected life history due to nutrient limitations (Sainte-Marie, 1991). Yet, none of the recovered *E. atacamensis* sp. nov. females had fully setose

oostegites, which would suggest an interim resting stage between broods. This lack of fully mature females is consistent with Eustace et al., (2016) and Thurston et al., (2002). Thurston et al., (2002) suggested that the eutrophic environment of the Atacama Trench would release them from an extreme K-selected strategy. Thus, with the high level of resources in the Atacama Trench, *E. atacamensis* sp. nov. may fall more towards semelparity on the semelparous-iteroparous continuum (Varpe & Ejsmond, 2018). *Hirondellea thurstoni*, also a hadal endemic in the Atacama Trench, is considered to display a semelparous life history strategy (Perrone et al., 2002). Another feature that is challenging to reconcile is the lack of males. This skewed sex ratio was similarly found by Thurston et al. (2002) and Eustace et al. (2016), which indicates that males are either not attracted to the bait or not present. Unlike ovigerous females, no evidence suggests a lack of attraction to bait. While the lack of males is curious, the evidence is insufficient to speculate on their absence. Confirmation of any of these hypotheses on the abyssal presence of juveniles and more broadly the life history strategy of the *E. atacamensis* sp. nov. warrants further investigations. Future work would benefit from additional sampling to assess seasonal population dynamics and more detailed instar analysis.

Eurythenes atacamensis sp. nov. represents a key addition to *Eurythenes*, one of the most intensely studied genera of deep ocean Amphipoda. This species represents a unique lineage with its eurybathic distribution across the abyssal and hadal depths of the eutrophic Peru-Chile Trench. This study highlights the importance of systematic sampling expeditions to resolve the geographic and bathymetric range of a species more fully. Further research of *Eurythenes* should continue to apply an integrative taxonomic approach and work towards a fuller understanding of life history. Together, this will ultimately lead to increased understanding of the biogeographic ranges of these key deep-ocean fauna, and the eco-evolutionary drivers of speciation in the world's largest ecosystem.

5. Acknowledgments

We grateful to the captain, crew, and scientific personnel at the RV *Cabo de Hornos Atacamex* Expedition (25/01–02/02/2018) and the RV *Sonne* SO261 Expedition (02/03–02/04/2018) for their excellent support to obtain these specimens. We are grateful to Dr Kevin Hardy (Global Ocean Design LLC), Nadín Ramírez (Instituto Milenio de

Oceanografía), and Victor Villagrán (Instituto Milenio de Oceanografía) for the “Audacia” lander design and operation, and Oliver Alarcón (Universidad de Concepción) for help with mesh trap design and construction. We thank Heather Stewart (British Geological Survey) and Dr Mackenzie E. Gerringer (SUNY Geneseo) for their assistance in the launch and recovery of Camera Lander 1 & 2 and recovery and on-board specimen processing. We are appreciative to Camilla Sharkey and Dr Julian Partridge (Bristol University, UK) for taking freshly recovered photos of specimens on the 2010 RV *Sonne* SO209 expedition. We are appreciative to Dr Erica Goetze (University of Hawai`i at Manoa) and Sandra Ferrada-Fuentes (Universidad de Concepción) for their advice on the DNA amplification steps. We extend appreciation to Andrea Paz Martinez Salinas, Catalina Amanda Merino Yunnissi, and Jorge Pérez-Schultheiss at the Invertebrate Zoology Department of the Museo Nacional de Historia Natural of Chile for their support and flexibility with curating the material during the global COVID-19 pandemic.

6. Declarations

6.1 Funding

The 2018 RV *Sonne* SO261 Expedition was made possible by the HADES–ERC Advanced Grant “Benthic diagenesis and microbiology of hadal trenches” (Grant Agreement Number 669947) awarded to Prof Ronnie N Glud (University of Southern Denmark) and ship time provided by the German Federal Ministry of Education and Research. The ship time for the *Atacamex* Expedition was provided by the National Agency for Research and Development of Chile (ANID; grant AUB 150006/12806). Additional funding support was supplied by Danish National Research Foundation, HADAL, (Grant number DNRF145) and ANID through the Millennium Science Initiative Program (Grant ICN 12_019-IMO). Participation of Drs Alan J Jamieson and Thomas D Linley on the 2018 RV *Sonne* SO216 expedition was supported by Newcastle University's Research Infrastructure Fund (RiF), Exploration of Extreme Ocean Environments, awarded to Dr Alan J Jamieson. The integrated taxonomic analysis was internally funded by Newcastle University.

6.2 Author contributions

All authors contributed to the study conception and design. Dr Frank Wenzhöfer was the 2018 RV *Sonne* SO216 expedition leader, and Prof Ronnie N Glud was the

scientific leader. Dr Osvaldo Ulloa was the *Atacamex* Expedition leader. Sampling design and specimen collection was conducted by Dr Alan J Jamieson, Dr Thomas D Linley, Dr Rubén Escribano, Dr Osvaldo Ulloa, and Dr Marcelo Oliva. Taxonomic analysis, description, and demographics were conducted by Johanna NJ Weston, Dr Liliana Espinosa-Leal, Jennifer A Wainwright, Eva CD Stewart, Dr Pamela Hidalgo, and Dr. William DK Reid. Phylogenetic analysis was completed by Johanna NJ Weston, Dr Carolina E González, Jennifer A Wainwright, and Eva CD Stewart. All authors contributed to the interpretation of the results. The first draft of the manuscript was written by Johanna NJ Weston, Jennifer A Wainwright, and Eva CD Stewart, and subsequently integrated with material provided by Drs Liliana Espinosa-Leal and Carolina E González. All authors commented on previous versions of the manuscript. All authors read and approved the final manuscript.

6.3 Availability of data

All genetic sequences have been deposited into NCBI GenBank under accession numbers MW042878-MW042884, MW290039 for 16S sequences and MW048992-MW048996, MW288146 for COI sequences.

6.4 Conflicts of interest/Competing interests

The authors declare they have no competing or conflicts of interest.

6.5 Ethical approval

All applicable international, national, and/or institutional guidelines for the care and use of animals were followed. The invertebrates in this study were non-cephalopod.

Chapter 4: Amphipods from the Wallaby-Zenith Fracture Zone, Indian Ocean: New genus and two new species identified by integrative taxonomy

Published as: Weston, J.N.J., Peart, R.A. and Jamieson, A.J., 2020. Amphipods from the Wallaby-Zenith Fracture Zone, Indian Ocean: new genus and two new species identified by integrative taxonomy. *Systematics and Biodiversity*, *18*(1), pp.57-78. doi:10.1080/14772000.2020.1729891

Abstract

The Wallaby-Zenith Fracture Zone, in the Wharton Basin of the East Indian Ocean, is a geomorphologically complex structure with depths from abyssal to hadal (~6600 m) with limited published taxonomic data. To fill this knowledge gap, this study describes two new species of scavenging amphipods, *Stephonyx sigmacrus* sp. nov. (Uristidae) and *Civifractura serendipia* gen. et sp. nov. (Alicellidae), collected using baited traps from a depth of 4932 m. As identification of deep-sea amphipods is challenged by phenotypic plasticity and convergent evolution, we combined a morphological with a molecular phylogenetic analysis of two mitochondrial (16S rDNA and COI) and two nuclear (Histone 3 and 28S rRNA) regions, where possible (no genetic material was obtainable from *S. sigmacrus* sp. nov.). The genetic data uncovered cryptic taxonomy and elevated diversity within the non-monophyletic Alicellidae family and provided evidence for establishing a new genus. Additionally, we identified morphological variations from the *Tectovalopsis wegeneri* description, genetically resolved two previously identified specimens of *Diatectonia* sp. as *T. wegeneri*, and identified two new species of *Tectovalopsis* for future description. These investigations highlight the application of integrative taxonomic approaches and represent a potential model for resolving incongruent morphological and molecular phylogenies for deep-sea amphipods and other specimen-limited taxa.

Keywords

abyssal, Alicellidae, Amphipoda, Indian Ocean, integrative taxonomy, new genus, new species, *Stephonyx*

1. Introduction

The abyssal seafloor (3000–6000 m) covers 54% of the Earth's surface, where the expansive plains are punctuated with seamounts, mid-ocean ridges, and trenches. Abyssal environments are characterised by a lack of natural light, low temperatures, and high hydrostatic pressures (Smith et al., 2008). While food supply is limited at these depths, amphipods are important members of the seafloor faunal community as scavengers and prey for predators (Linley et al., 2017). Adapted to these environmental conditions (Dahl, 1979), scavenging amphipods are efficient at detecting and consuming a wide range of organic matter (Blankenship & Levin, 2007; Thurston, 1979). Thus, they play a central role in deep-ocean organic carbon cycling.

The abyssal zone is a major reservoir of undiscovered biodiversity (Smith et al., 2008). New species continue to be discovered through ongoing sampling and integrative taxonomy, and in particular, where species are delimited through simultaneous morphological and molecular scrutiny (Beermann et al., 2018; Padial et al., 2010; Pante et al., 2015). An exemplar approach has been applied to the giant Lysianassoid amphipod *Eurythenes gryllus* (Lichtenstein in Mandt, 1822), which was originally assumed to have a cosmopolitan distribution from bathyal to hadal depths (Eustace et al., 2016; France & Kocher 1996). However, phylogeographic and species delimitation analyses of mitochondrial markers resulted in the identification of twelve distinct lineages and description of three species from the *gryllus*-complex (d'Udekem d'Acoz & Havermans, 2015; Havermans et al., 2013). Combining these two methodologies has clarified phylogenetically divergent and morphologically-similar species and unmasked cryptic species, whose identification is partially obscured due to phenotypic plasticity, convergent evolution, or overlooked morphological differences (Corrigan et al., 2014; Englisch et al., 2003; Havermans et al., 2010; Ritchie et al., 2015).

The first species described in this study is from the genus *Stephonyx* (Uristidae). The 15 species of the genus are distributed from bathyal to abyssal depths across all non-polar oceans and in a range of habitats, including abyssal plains, cold seeps, and hydrothermal vents (Lowry & Kilgallen, 2014; Sumida et al., 2016; Winfield et al., 2017). Diagnostic characters of this genus include a reduced coxa 1, symmetrical incisors with a well-developed lacinia mobilis, a molar with a vestigial triturating surface, and uropod 3

with plumose setae on both rami (Diffenthal & Horton, 2007; Lowry & Kilgallen, 2014). The most distinctive character is a pincer-like chelate gnathopod 1, which indicates that *Stephonyx* may be specialist scavengers (Corrigan et al., 2014).

The second species is from the small family of Alicellidae Lowry & De Broyer, 2008. Established in 2008, Alicellidae only has six genera, four of which are monotypic (*Alicella* Chevreux, 1899, *Apotectonia* Barnard & Ingram, 1990, *Diatectonia* Barnard & Ingram, 1990, and *Transtectonia* Barnard & Ingram, 1990). All members are bathyal to hadal scavengers, living in a range of habitats from hydrothermal vents, abyssal plains, to hadal trenches (Barnard & Ingram 1990; Lacey et al., 2016). Of the Alicellids, *Alicella gigantea* Chevreux, 1899 is the most recognizable member, as the largest known amphipod. (Barnard & Ingram, 1986; Jamieson et al., 2013).

Alicella and *Paralicella* Chevreux, 1908 are anecdotally considered to be sister taxa and were brought together in the family Alicellidae by Lowry & De Broyer (2008). The other four genera are considered closely related, with only minor characters preventing assignment to other genera. These minor characters include the length of antennae, the number of setae on inner plate of maxillae 1-2, the size of left lacinia mobilis, presence of right lacinia mobilis, the length of coxa 1, the shape of gnathopod 1, and the presence of dorsal tooth on epimeron 3 (Barnard & Ingram 1990). When establishing the family, Lowry & De Broyer (2008) considered Alicellidae to be monophyletic based: on the presence of a lacinia mobilis on both mandibles; asymmetrical incisors, non to small triturating surface of molar, a non-mitten-shaped gnathopod 2; gnathopod 2 with elongate ischium, carpus, and propodus; lack of robust apical setae on uropods 1-2; and deeply cleft telson. Despite assumptions of monophyly, Ritchie et al. (2015), using three molecular markers, investigated phylogenetic relationships of 25 abyssal and hadal scavenging amphipods, including *A. gigantea*, *Tectovalopsis wegeneri* Barnard & Ingram, 1990, *Paralicella tenuipes* Chevreux, 1908, and *Paralicella caperesca* Shulenberger & Barnard, 1976. A monophyletic grouping of these three genera was hindered by the placement of specimens from *Cyclocaris* Stebbing, 1888, *Hirondellea* Chevreux 1889, and *Valettietta* Lincoln & Thurston, 1983, thus indicating the need for taxonomic delimitation refinement within the Alicellidae family. Further, these results suggested the need for additional molecular data from both type

material and additional specimens, especially from *Diatectonia*, *Apotectonia*, *Transtectonia*, and *Tectovalopsis*, to build a more robust phylogeny of the family Alicellidae.

Considering the current discord between morphology and genetics in the family Alicellidae, we applied an integrative taxonomic approach for two undescribed scavenging amphipods collected from abyssal depths at the Wallaby-Zenith Fracture Zone (WZFZ), Indian Ocean: *Stephonyx sigmacrus* sp. nov. and *Civifractura serendipia* gen. et sp. nov. The establishment of *Civifractura* is strongly supported by multi-locus molecular evidence and morphological methods. Keys are provided for the related genera of the species described.

2. Material and Methods

2.1 Specimen Collection

The WZFZ is situated in the East Indian Ocean approximately 500 km off the west coast of Australia, as part of the larger Wharton Basin and Perth Basin complex (Figure 28). During the RV *Sonne* Expedition SO258 Leg 1, the WZFZ was sampled with free-fall autonomous landers on June 10-12, 2017 (Jamieson, 2016). A combination of trap and video landers were deployed eleven times between depths of 4730–6546 m, and the landers remained on the seafloor for 7-10 hours. Five of the landers were equipped with a 2-litre funnel invertebrate trap baited with whole mackerel bait (Scombridae) and a temperature and pressure sensor (SBE-39, SeaBird Electronics, USA). Pressure was converted to depth (m) following Saunders (1981). Upon recovery, the amphipods were fixed directly with 70% ethanol.

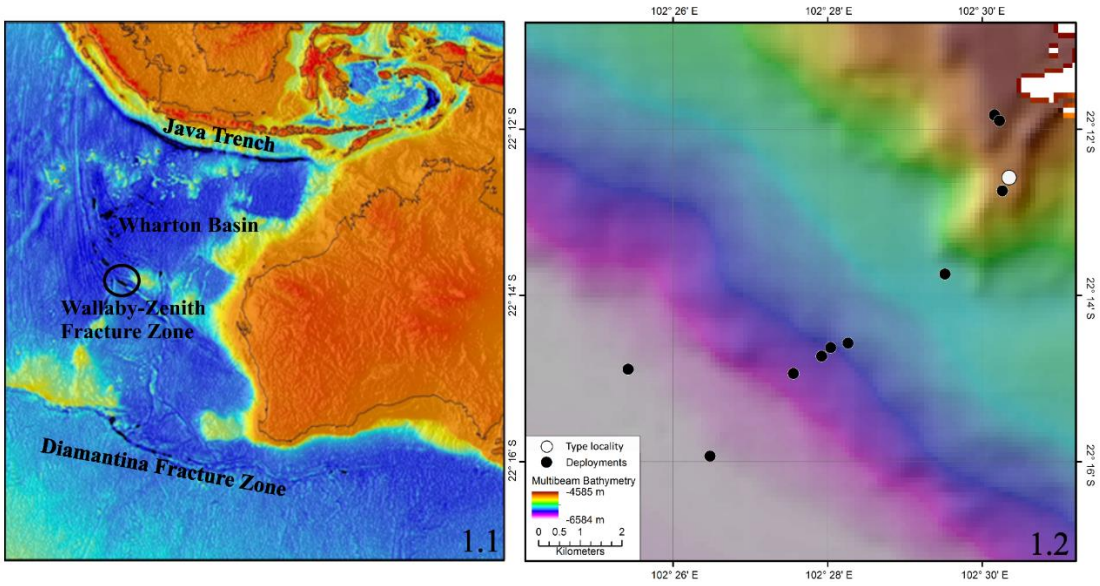

Figure 28. Map of the East Indian Ocean. The black circle is the WZFZ (1.1). Multibeam bathymetry map of the WZFZ with the 11 lander deployments to depths ranging from 4730 to 6546 m. The white circle is the type locality of *Stephonyx sigmacrus* sp. nov. and *Civifractura serendipia* gen. et sp. nov (1.2).

2.2 Morphological Assessment and Digital Illustration

Whole specimens were photographed with a Canon EOS 750D DSLR camera, Tamron SP 90mm f/2.8 VC USD Macro 1:1 VC Lens with polarising filter, and Falcon Eyes CS-730 copy stand and processed with Helicon Focus and Helicon Remote software. Complete specimens were measured and dissected using a Wild Heerbrugg M8 stereomicroscope. Body length was measured from the rostrum to the tip of telson. Dissected appendages were imaged with a Leica DMi8 inverted microscope and DFC295 camera. Images were converted into digital illustrations using Inkscape v0.92.2 (Coleman, 2003; 2009). Permanent slides were made using Aquatex™.

Type specimens are lodged in the National Institute of Water and Atmospheric Research (NIWA) Invertebrate Collection, Wellington, New Zealand and the Natural History Museum (NHM), London, United Kingdom. Abbreviations used in digital illustrations include: H - head, A–antenna, Md–mandible, Mx–maxilla, Mxp–maxilliped, G–gnathopod, P–pereopod, O–oostegite; Epm–epimeron, U–uropod, T–telson, z–zoom; Y - paratype. All parts are left side unless otherwise indicated.

2.3 Morphological Phylogenetic Analysis

Morphological phylogenetic analysis was carried out for two purposes. Firstly, to make a direct (as much as possible) comparison between the molecular sequences and the morphology of the type descriptions; and secondly, to place the new alicellid genus and species within the greater group of known related species. This analysis was carried out using PAUP*4.0a164 (Swofford 2003), parsimony methods, using a heuristic search, step-wise addition, add seq-random reps = 8000, and Tree Bisection/Reconnection. The stability was tested using bootstrap methods, branch and bound, and reps = 1000. This analysis used 73 morphological characters. Originally, 79 characters were scored, but characters 4, 6, 20, 39, 50, 57, and 67 were constant and disregarded in the analysis (Table A1). All characters are unordered, of equal weight, and scored using OpenDELTA software v1.02 (2088; Dallwitz et al., 1999).

The characters were scored for a total of 33 species and 36 specimens. Thirty species were scored from original descriptions in the three families: Cyclocaridae Lowry & Stoddart, 2011, Alicellidae, and Valettiopsidae Lowry & De Broyer, 2008. The analysis included all species within these three families apart from *Paralicella microps* Birstein & M. Vinogradov, 1958 and *Valettietta cavernicola* Stock & Iliffe, 1990. These two species were excluded from analysis due to the lack of detail within the description. Additionally, six specimens of three different genera were directly scored and furthered used in the molecular phylogenetic analysis. These six specimens were *A. gigantea* from WZFZ 4932 m (*A. gigantea* WZFZ4932), c.f. *Diatectonia* from New Hebrides Trench 3400 m (*Diatectonia* sp. NH3400a; Lacey et al., 2016), *T. wegeneri* from New Hebrides Trench 2500 m (*T. wegeneri* NH2500; Lacey et al., 2016), *T. wegeneri* from New Hebrides Trench 3400 m (*T. wegeneri* NH3400; Lacey et al., 2016), *Tectovalopsis* sp. from Peru-Chile Trench 4602 m (*Tectovalopsis* sp. PC4602; Fujii et al., 2013), and *Tectovalopsis* sp. from Mariana Trench 5641 m (*Tectovalopsis* sp. M5641; unpublished data). *Diatectonia* sp. from New Hebrides Trench 3400 m (*Diatectonia* sp. NH3400b; Lacey et al., 2016) was additionally scored but not included in the analysis as characters 3 and 7 were unable to be scored and the remaining scores were identical to *Diatectonia* sp. NH3400a. Two related taxa were selected as outgroups, *Hirondellea brevicaudata* Chevreux, 1910 and

Podoprion ruffoi Lowry & Stoddart, 1996. The subsequent matrix produced of the characters versus species is shown in Table A2.

2.4 DNA Extraction, PCR Amplification, and Phylogenetic Analysis

For *C. serendipia* gen. et sp. nov., total genomic DNA was isolated from two specimens with the Bioline ISOLATE II Genomic DNA Kit following the manufacturer's protocol. To increase the robustness of the phylogenetic analysis of *C. serendipia* gen. et sp. nov. reported here, additional material was sequenced from comparative specimens of *A. gigantea* WZFZ4932 & Afanasy Nikitin Seamount 4733 m (*A. gigantea* ANS4733), *T. wegeneri* NH3400 & NH4694, *Tectovalopsis* sp. PC4602 & M5601, *Diatectonia* sp. NH3400a & *Diatectonia* sp. NH3400b (see Table A3 for full details of comparative material). Regions of the mitochondrial 16S rDNA (16S), cytochrome c oxidase subunit I (COI), nuclear 28S rDNA (28S), and Histone 3 (His3) were amplified with published primer sets: AMPH1 (France & Kocher 1996) and 'Drosophila-type' 16SBr (Palumbi et al., 2002) for 16S, LCO1490 and HCO12198 (Folmer et al., 1994) for COI, HisH3f and HisH3e (Corrigan et al., 2014) for His3, and 28Sftw and 28Srtw (Corrigan et al., 2014) for 28S. PCR protocols were followed as described in Ritchie et al., (2015) for 16S and COI and Corrigan et al., (2014) for 28S and His3. Sequences were cleaned enzymatically using New England Biolabs Exonuclease 1 and Antarctic Phosphatase and sequenced with an ABI 3730XL sequencer (Eurofins Genomics, Germany).

For *S. sigmacrus* sp. nov., the following DNA extraction methods were used with 10 individuals: the Bioline ISOLATE II Genomic DNA Kit, a standard phenol-chloroform approach (Ritchie et al., 2015), the Qiagen DNeasy PowerSoil Kit, and a modified protocol of the Omega Bio-Tek E.Z.N.A® Tissue DNA Kit (Kitson et al., 2019). In addition to the above-mentioned 16S and COI primer sets, the following primers sets were attempted: 16Sar and 16Sbr (France & Kocher, 1996), CO1-LCO-AMP1 and CO1-HCO-AMP2 (Beermann et al., 2018), and mlCOIintF and jgHCO2198 (Lerary et al., 2013). The four DNA extraction methods failed to produce a sufficient template for a successful PCR. The reason for the failed DNA extractions was unclear, as other species of similar size and depth were successfully sequenced and with sister species having been previously sequenced (Corrigan et al., 2014).

Electropherograms were viewed in MEGA7 (Kumar et al., 2016), and primer and ambiguous sequences were clipped by eye. COI and His3 sequences were translated into the equivalent amino acid sequence to confirm that no stop codons were present. To construct phylogenetic trees, comparative species sequences were retrieved from GenBank for available species from the families Alicellidae, Valettiopsidae, and Cyclocaridae (Corrigan et al., 2014; Jamieson et al., 2013; Ritchie et al., 2015; 2017; Table A3). For each loci dataset, nucleotide alignments were made using MAFFT v7 (Katoh et al., 2017). The optimal evolutionary models for each locus alignments were identified by modeltest in the *phangorn* 2.4.0 package (Schliep et al., 2017): the Hasegawa, Kishino, and Yano model (HKY+G) for 16S, HKY+I+G for COI, HYK+I for His3, and HKY+I for 28S (Hasegawa et al., 1985; Yang 1994). The phylogenetic relationships between individuals were derived via a Bayesian approach in BEAST v1.8.4 (Drummond et al., 2012). Each analysis was run twice for 50,000,000 generations sampling every 10,000 generations using the respective evolutionary models and an uncorrelated relaxed clock (Drummond et al., 2006). Outputs were analysed in Tracer v1.7 to ensure convergence (Rambaut et al., 2018). In TreeAnnotator v1.8.4, the first 5,000,000 generations were discarded as burn-in and a maximum clade credibility tree was generated. The resulting trees were viewed and edited in FigTree v1.4.3. Species delimitation was done using a Bayesian Poisson Tree Processes (bPTP) model to infer species boundaries using speciation or branching events in terms of the number of substitutions (Zhang et al., 2013).

3. Results

3.1 Morphological Phylogenetic Analysis

The morphological phylogenetic analysis produced the three most parsimonious trees, which are summarized as a 50% majority-rule consensus tree (Figure 29) The consensus tree had a length of 360 steps, ci = 0.314, ri = 0.601. For the analysis, the >50% bootstrap values were placed below the nodes.

The resulting 50% majority-rule consensus tree shows the placement of the new genus in a large clade, allied with *Diatectonia typhodes* Barnard & Ingram, 1990, *Paralicella vaporalis* Barnard & Ingram, 1990, and *A. gigantea* basal to this larger group. The clade containing all the *Tectovalopsis* species, and the new genus is only defined by

the width of the uropod three rami changing from wide to narrow. However, the new genus is sister taxa to *Tectovalopsis fusilus* Barnard & Ingram, 1990*,* with these two species being allied to *Tectovalopsis diabolus* Barnard & Ingram, 1990 and *Tectovalopsis nebulosus* Barnard & Ingram, 1990*.* These four species form a sub-clade defined by mouthpart characters and the shape of the lateral cephalic lobe. *Tectovalopsis* sp. PC4602 and M5641 fall uniquely within the *Tectovalopsis* clade, with *Tectovalopsis* sp. PC4602 being the most basal in the clade.

Of the other clades, the strongest bootstrap support belongs to the Cyclocaridae species (97), with the *Valettietta* Lincoln & Thurston, 1983 species also showing support (52). Sister to *Valettietta*, *Paralicella* forms a clade, except for *P. vaporalis*, but the placement is not strongly supported.

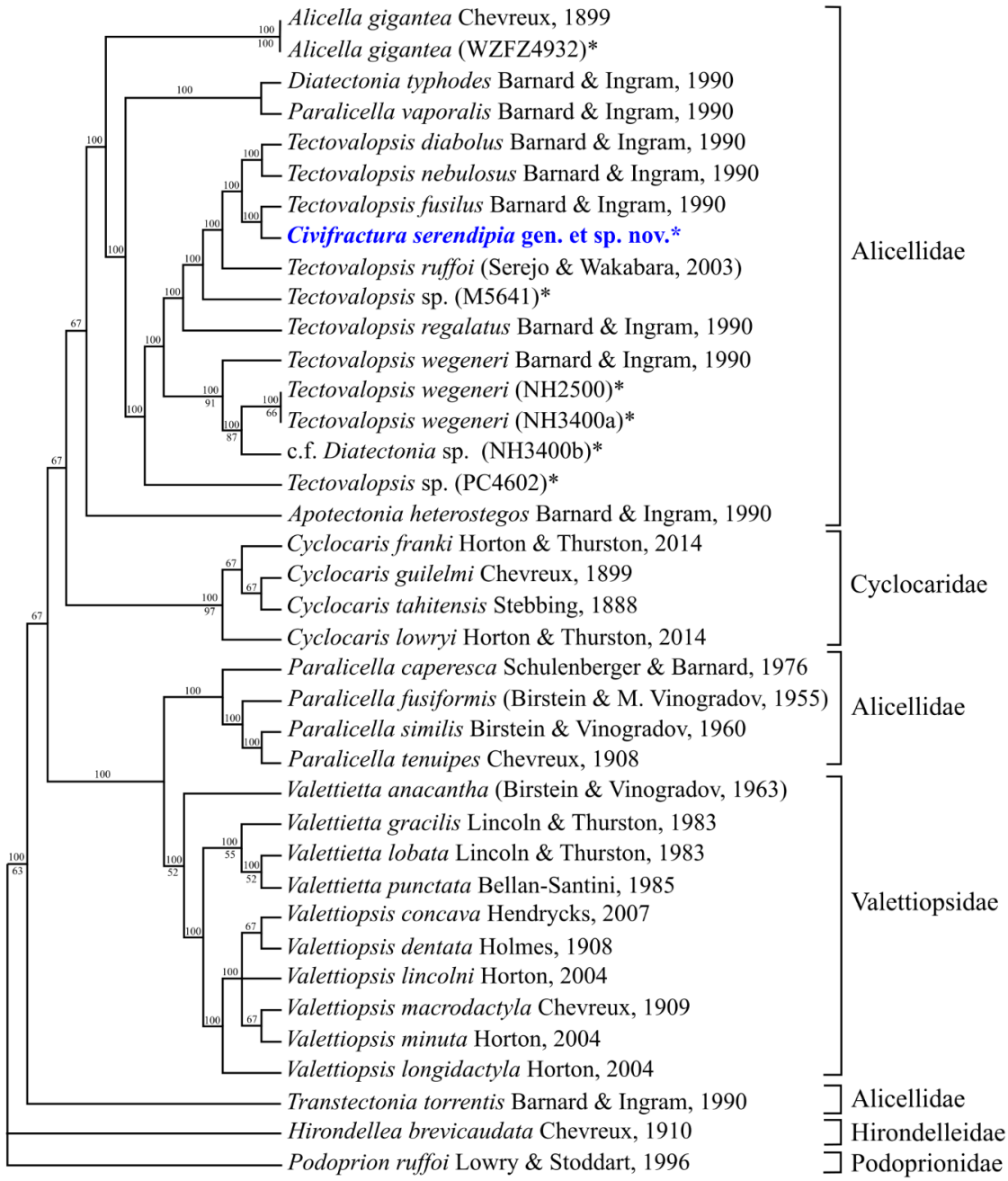

Figure 29. 50% majority-rule consensus tree summarized from 3 parsimony trees. The phylogeny was constructed through the scoring of 73 morphological characters across 33 species from the Cyclocaridae, Alicellidae, and Valettiopsidae families. Family is denoted on right. Bootstrap values greater than 50% are shown on branch nodes. Asterisks represent specimens with corresponding sequences.

3.2 Molecular Phylogenetic Analysis

Broadly within Alicellidae, ten individuals from seven putative species were successfully sequenced for a total of 36 gene amplicons: ten for 16S, ten for COI, eight for 28S, and eight for His3. As some individuals yielded poor quality of DNA, not all individuals were sequenced across all four loci. For *C. serendipia* gen. et sp. nov., 16S and CO1 were successfully sequenced and analysed for two individuals (isolate 1 and 2) and His3 and 28S for one individual (isolate 1). GenBank accession numbers, size of gene amplicons, and nucleotide frequencies are provided in Table A4. Subsequently, we present phylogenies for a wider concatenated dataset of 16S and COI for 13 putative species (mtDNA; Figure 30) and a focused concatenated dataset of 16S, COI, His3, and 28S for 10 putative species (mtDNA + nuclear; Figure 31). In the mtDNA phylogeny, the outgroup was *Lanceola* sp. In the mtDNA + nuclear phylogeny, *Cyclocaris* sp., *P. caperesca*, and *E. gryllus* were outgroups.

The mtDNA phylogeny shows both isolates of *C. serendipia* gen. et sp. nov. form their own clade. This clade is sister to *A. gigantea* and reciprocally monophyletic to a Tectovalopsis clade, consisting of *T. wegeneri*, *Tectovalopsis* sp. PC4602, *Tectovalopsis* sp. M5641, *Diatectonia* sp. NH3400a and NH3400b. Depending on the sequence type, the placement of *C. serendipia* gen. et sp. nov. varies. In the 16S phylogeny, *C. serendipia* gen. et sp. nov. is basal to *A. gigantea* and the *Tectovalopsis* clade (Figure A1). Whereas in the COI phylogeny, *Tectovalopsis* clade is basal and *C. serendipia* gen. et sp. nov. is a sister taxa to *A. gigantea* (Figure A2).

Further, species-delimitation analysis of the mtDNA phylogeny suggests that within this clade there are six species (Table A5), of which two are *C. serendipia* gen. et sp. nov. and *A. gigantea.* The newly sequenced specimens of *A. gigantea* WZFZ4932 and ANS4757 have nearly identical 16S and COI sequences to previously sequenced *A. gigantea* specimens collected from the Pacific Ocean (Jamieson et al., 2013; Ritchie et al., 2015). There is a lack of phylogeographic signal across latitude, longitude, or depth.

The other four potential species from the species-delimitation fall within a *Tectovalopsis* clade. Of those species, *Tectovalopsis* sp. PC4602 and M5641 have the possibility of being new to science. While full description investigation will need to be undertaken, a corresponding morphological assessment preliminarily agreed with the

species-delimitation. The fifth and sixth delimited species are both from the New Hebrides Trench and separated by depth. The fifth delimited species, *T. wegeneri* NH4694, could be a new species per bPTP analysis based on the mtDNA topology. However, this is not supported by a morphological assessment. The bPTP analysis groups together as the sixth species *T. wegeneri* NH2500 and NH3400 with *Diatectonia* sp. NH3400a and NH3400b.

Further within the mtDNA phylogeny, the *Paralicella* clade is polyphyletic to the *Alicella*, *Tectovalopsis*, and *Civifractura* clade and separated by *Cyclocaris* sp. The sequenced specimens identified as *P. tenuipes* and *P. caperesca* resolve into six potential species by the bPTP analysis, which is similar to the four delineated by Ritchie et al. (2015) (Figure 31). Within the *P. caperesca* clade from 6007 m at the Kermadec Trench, *V. anacantha* from the same depth in Kermadec Trench is present. This *V. anacantha* is far removed from the two other *Valettietta*, *V. gracilis* and *V. anacantha* from 5469 m at the Mariana Trench. In the individual gene topologies, there is instability with the positioning of three sets of *Valettietta* sequences. In the 16S phylogeny, both *V. anacantha* are sister to *Cyclocaris* sp., separating *Paralicella* from the rest of the Alicellidae, and *V. gracilis* is within the Paralicella clade (Figure A1). In the COI phylogeny, the position of three sets of *Valettietta* sequences is more similar to the mtDNA phylogeny (Figure A2).

The mtDNA + nuclear phylogeny shows a clade of *C. serendipia, A. gigantea,* and *Tectovalopsis/Diatectonia* spp (Figure 31). This clade is polyphyletic to *P. caperesca*, which was more closely placed to *E. gryllus*. This phylogeny was consistent with the mtDNA topology in placing *C. serendipia* directly basal to *A. gigantea* with a high posterior probability of support. Similar to the mtDNA phylogeny, there was a nested sub-clade of *Tectovalopsis/Diatectonia* spp. The bPTP analysis indicated three potential species: 1) *Tectovalopsis* sp. M5641, 2) *Tectovalopsis* sp. PC4602, and 3) *T. wegeneri* from 3400 and 4694 m with *Diatectonia* sp. NH3400a and NH3400b.

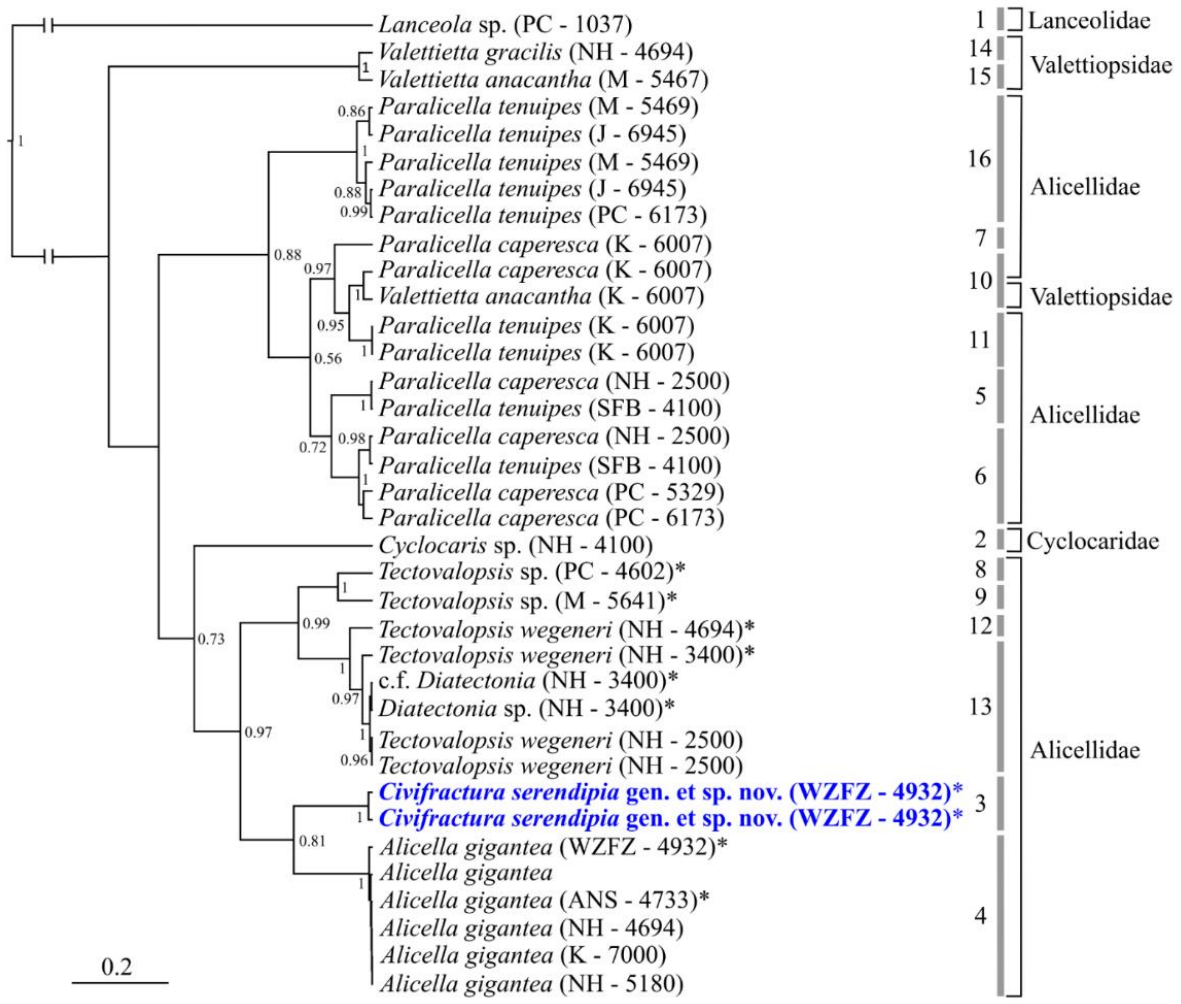

Figure 30. Bayesian tree showing the relationships between amphipod species based on a concatenated dataset of 16S and COI sequence data. Bayesian posterior probabilities greater than 0.5 are shown on branch nodes. Asterisks denote the sequences added by this study. Branches are labelled by species name and collection location and depth (m). bPTP delimitation and family is denoted on right. For the locations, PC is Peru-Chile Trench, M is Mariana Trench, NH is New Hebrides Trench, WZFZ is Wallaby-Zenith Fracture Zone, ANS is Afanasij Nikitin Seamount, J is Japan Trench, K is Kermadec Trench, and SFB is South Fiji Basin. For complete reference of sequences see Table A3.

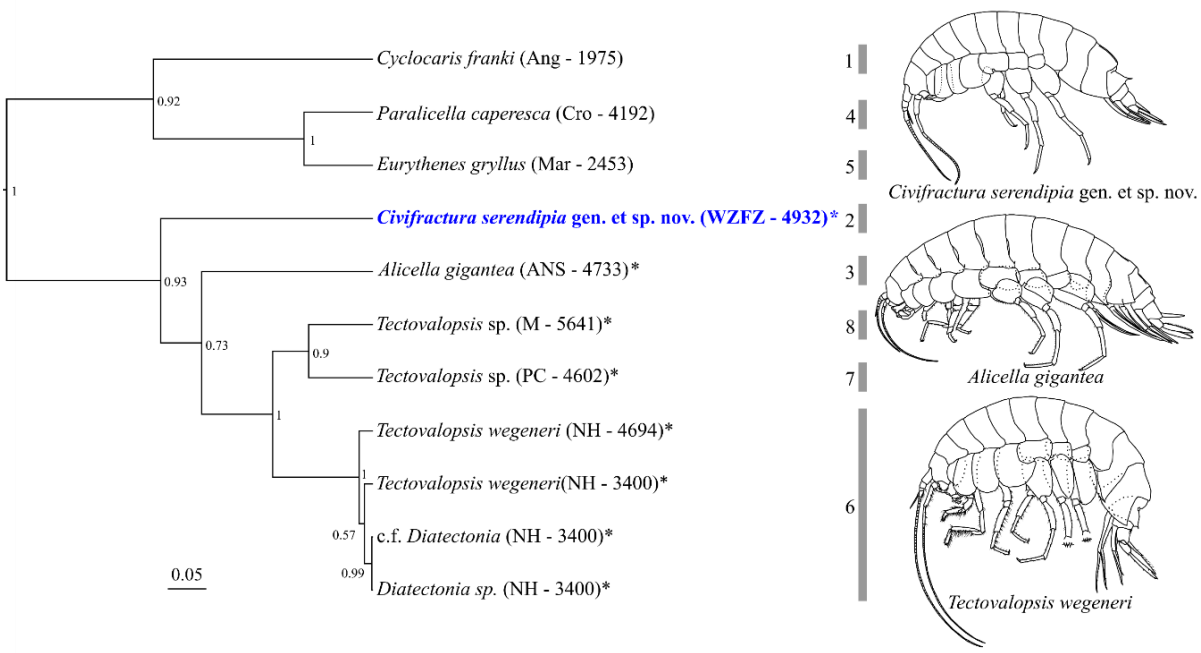

Figure 31. Bayesian tree showing the relationships between amphipod species based on a concatenated dataset of 16S, COI, Histone 3, and 28S sequence data. Bayesian posterior probabilities greater than 0.5 are shown on branch nodes. Asterisks denote the sequences added by this study. The branches are labelled by species name, collection location, and depth (m). bPTP delimitation is denoted on right. For the locations, Mar is Mid-Atlantic Ridge, Cro is Crozet Island, Ang is Angola, PC is Peru-Chile Trench, M is Mariana Trench, NH is New Hebrides Trench, and WZFZ is Wallaby-Zenith Fracture Zone, ANS is Afanasij Nikitin Seamount. For complete reference of sequences see Table A3. *T. wegeneri* and *A. gigantea* illustrations from Barnard & Ingram 1990 and Lowry & De Broyer 2008, respectively.

4. Systematics

Family Uristidae Hurley, 1963

Genus Stephonyx Lowry & Stoddart, 1989

***Stephonyx sigmacrus* sp. nov.** (Figure 32, Figure 33, Figure 34)

Type Material. Holotype: Immature female, 21.2 mm, NIWA 139160. Paratypes: Immature female, 20.8 mm, NIWA 139161; Immature male, 14.5 mm, NIWA 139162, immature male 12.6 mm, NHM UK 2019.1; and Juvenile, 8.6 mm, NIWA 139163, Juvenile 7.0 mm, NHM UK 2019.18; collection data same as the holotype.

Type Locality. Wallaby-Zenith Fracture Zone (Wharton Basin), Indian Ocean (22 12.579S, 102 30.347E), cruise SO258, station L7, depth 4932 m.

Additional Material Examined. Female, 18.6 mm, male, 15.1 mm, and juvenile, 11.1 mm. Material is lodged at Newcastle University.

Etymology. The species name, *sigmacrus*, is derived from the Greek letter *Sigma* (eighteenth letter of the Greek alphabet) and *crus* (a leg-like part). In combination and as an adjective, it describes the distinctive sigmoid profile of the posterior edge of basis of pereopod 5 and 6.

Diagnosis. Head anterior lateral cephalic lobe upturned with acute bifid tip. Coxae 1–4 ventral margin straight. Gnathopod 2 palm convex. Pereopod 5 and 6 basis sigmoid with posterodorsal margin expanded and posteroventral corner acute, serrate posterior margins, ventral margins straight. Epimeron 3 posteroventral corner with small tooth.

Description, based on holotype, female, 21.2 mm length, NIWA 139160.

BODY: wide, smooth, not dorsally carinate. *Urosomite 1* produced dorsally to form a slight, rounded carination.

HEAD: deeper than long; rostrum absent. Eyes not apparent but may be faded in ethanol. Lateral cephalic lobe well-developed. *Antenna 1* shorter than antenna 2 (0.6x) and 0.3x length of body; peduncular articles 1–3 length ratio of 1: 0.4: 0.2, with brushed long setae on peduncular article 3 and callynophore, accessory flagellum 9-articulate, primary flagellum 27-articulate. *Antenna 2* slender, half the length of the body; peduncular articles 4 and 5 sub-equal in length, with several brushed seta; flagellum 48-articulate; calceoli absent.

MOUTHPART BUNDLE: *Mandible* incisor smooth and symmetrical; lacinia mobilis a simple, robust peg; accessory spine row with five robust setae; molar finely setose, distally triturating; palp article length ratio 1: 4.9: 2.8; article 2 with setae along distal quarter of the medial surface, article 3 blade-like. *Maxilla 1* inner plate narrow with one stout subterminal seta and three smaller plumose setae; outer plate narrow with a 7/4 crown of large multi-denticulate setal-teeth; palp large, 2-articulate, terminal article with eight broad setae and one slender flag seta. *Maxilla 2* inner plate shorter than outer plate (0.8x), lateral margins of both plates have long simple, plumose setae. *Maxilliped* inner plate sub-rectangular, 0.4x the width of the outer plate, two short, robust setae near apical inner corner and one near outer corner, oblique setal row well-developed; outer plate large, subovate; palp well-developed; dactylus well-developed, unguis present, surface with small setae.

PEREON: *Gnathopod 1* coxa reduced, sub-quadrate; basis 3.5x longer than wide, posteroventral margin with six setae; ischium linear and parallel, elongate 5.3x longer, shorter than basis (0.5x); merus linear, 2x longer than wide; carpus linear and elongate, margins subparallel, 10x longer than wide; propodus linear, shorter than carpus (0.8x), 7.4x as long as wide; palm narrowly obtuse, straight and then weakly convex on the distal edge, dentate on the distal 1/3 margin, two setae on the anterior margin, three setae on the palm margin, five long setae on the palm, one subapical robust seta; dactylus 6x longer than wide, two subapical robust setae. *Gnathopod 2* subchelate; coxa larger than coxa 1, subequal in size to coxa 3; basis curved, 6x longer than wide; ischium 3x longer than wide; merus shorter than carpus (0.6x), 2x as long as wide; carpus elongate, 4x as long as wide, anterior margin straight, posterior margin convex; propodus sub-rectangular, shorter than carpus (0.5x), 0.5x wide as long, anterior and posterior margins with rows of slender crenate setae that are bifid and have a minute apical accessory seta, medial rows of single setae; palm convex, s-shaped, with many thin setae on the distal margin, posterodistal corner with six medial robust setae; dactylus curved posteriorly, not reaching the palmar corner, anterior margin with one seta, posterior margin reaches palm. *Pereopod 3* oostegite elongate without setae; coxa large, sub-rectangular, corners rounded, four pairs of setae on the ventral margin, 2.7x longer than wide; dactylus simple, short, curved posteriorly, posterior margin with cusps/serrations, single simple seta on

posterior margin, single plumose seta on anterior margin. *Pereopod 4* coxa with well-developed posteroventral lobe, posterodistal corner weakly convex, anterodistal corner weakly rounded; dactylus simple, short, posterior margin with cusps/serrations, single simple seta on posterior margin, single plumose seta on anterior margin. *Pereopod 5* oostegite elongate without setae; coxa bilobate, posterior lobe pronounced ventrally; dactylus simple, short, no cusps on anterior margin, single plumose seta on posterior margin. *Pereopod 6* coxa weakly bilobate, anterior margin straight, posterior corners rounded. *Pereopod 7* coxa 0.5x length of basis.

PLEON AND UROSOME*: Epimeron 1* posteroventral corner broadly rounded. *Epimeron 2* posteroventral corner produced to form a small tooth. *Epimeron 3* ventral margin with several setae, posteroventral corner produced to a small tooth. *Uropod 1* 1.25x the length of uropod 2, rami subequal in length, longer than peduncle (1.8 x). *Uropod 2* with single robust seta on outer margin of peduncle; inner ramus 2.2x longer than peduncle, inner ramus 1.3x longer than outer ramus. *Uropod 3* 1.5x long as wide; outer ramus 1.2x longer than inner rami, ramus lanceolate; inner ramus with plumose setae; outer ramus bi-articulate, article 2 with two distal setae. *Telson* deeply cleft (75 %), apical margin truncate, left apical margin with a stout seta and medial seta, right apical margin with medial seta (other setae to give symmetry potentially broken off).

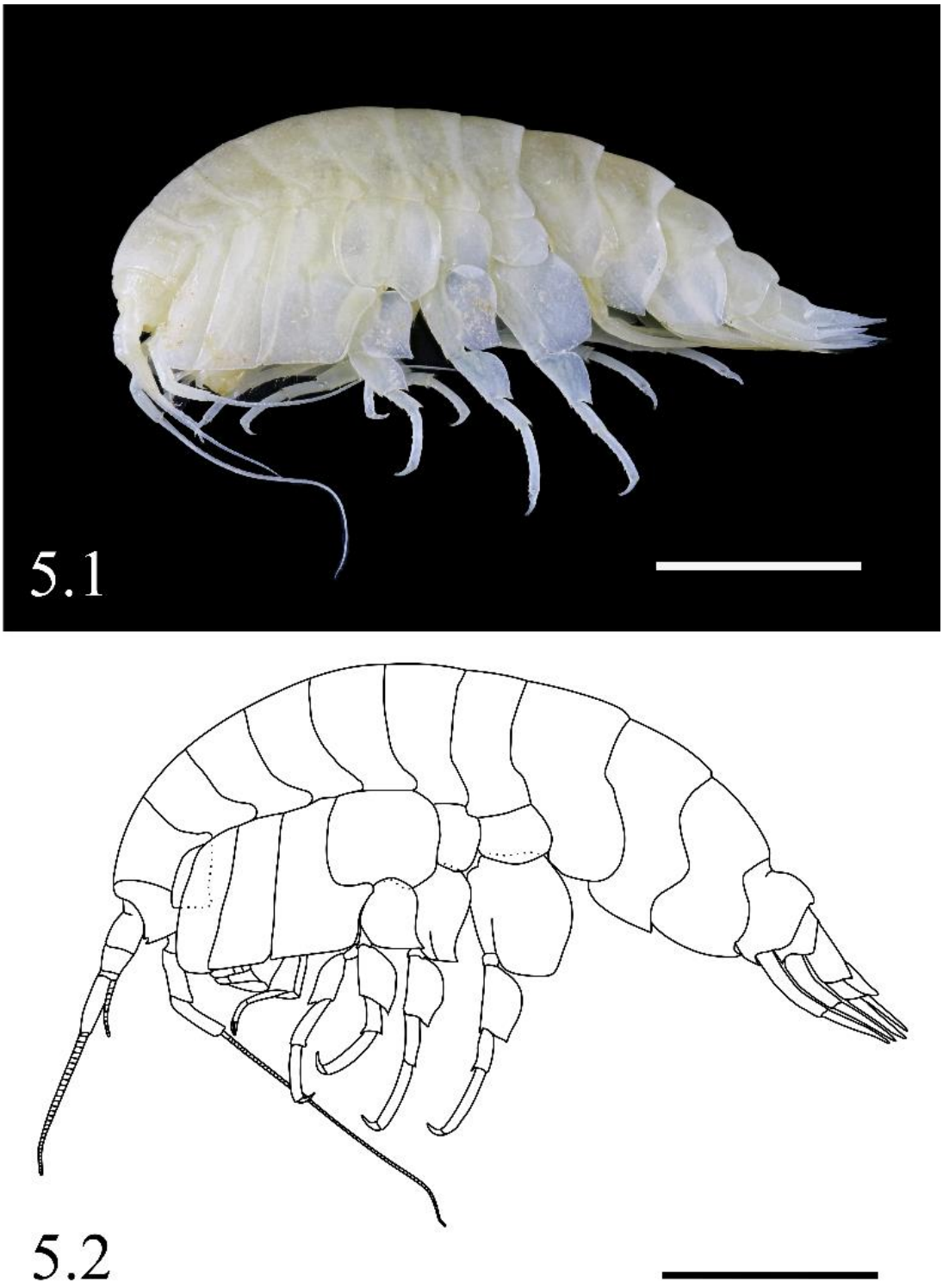

Figure 32. Photograph of *Stephonyx sigmacrus* sp. nov. holotype (5.1). *Stephonyx sigmacrus* sp. nov. holotype, scale bar 5 mm (5.2).

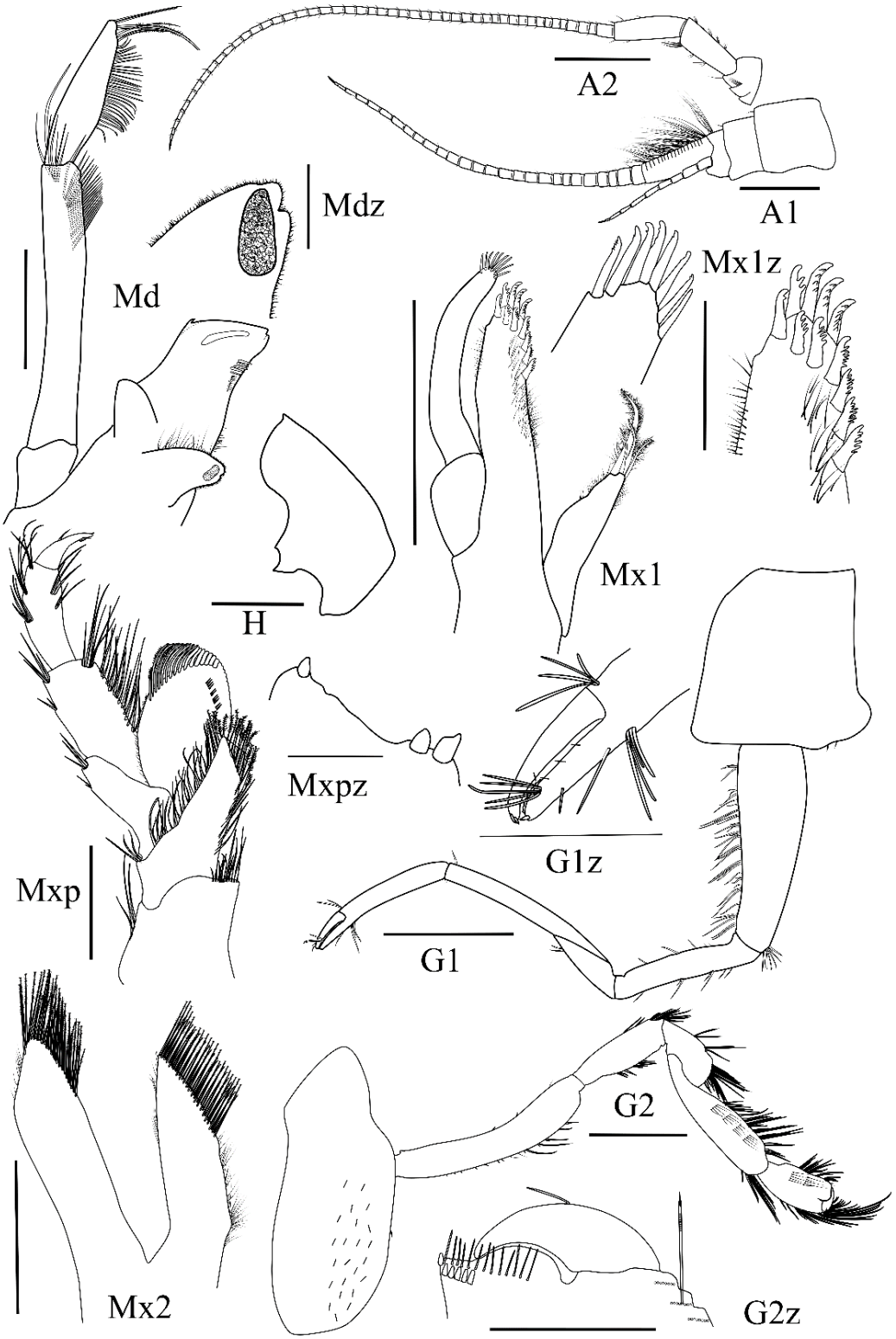

Figure 33. *Stephonyx sigmacrus* sp. nov. holotype. Scale bars: H, G1, & G2 1 mm; Md, Mx1, Mx2, Mxp, & G2z 0.5 mm; Mx1z 0.25 mm; Mxpz & Mdz 0.1 mm.

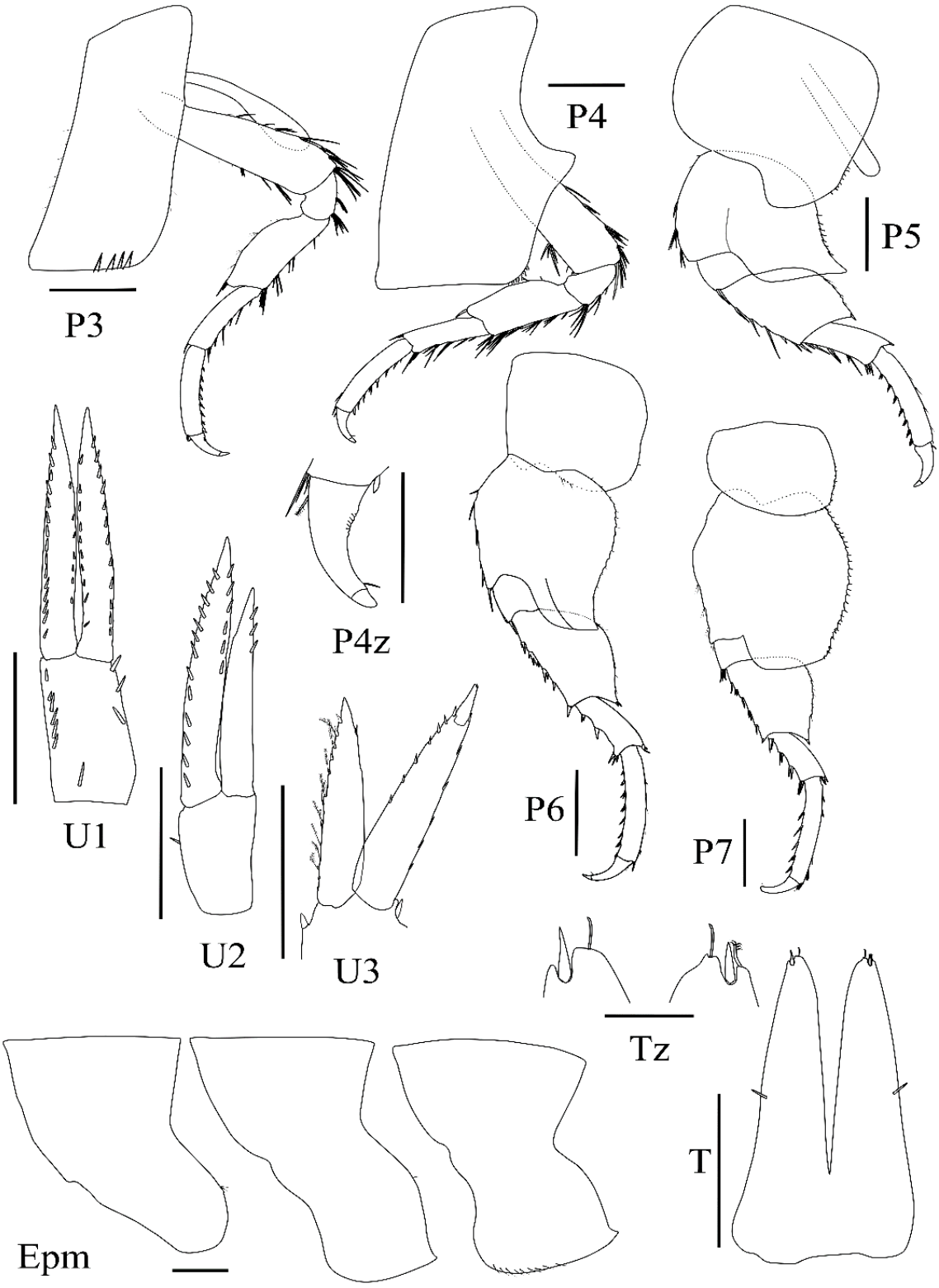

Figure 34. *Stephonyx sigmacrus* sp. nov. holotype. Scale bars: Tz 0.1 mm; P4z 0.5 mm; remainder 1 mm.

Variations. Males of *S. sigmacrus* resemble females except for a generally shorter body length. Paratype male (NIWA 139162), as holotype except: *Head* eyes faded from ethanol preservation but present in an inverted S-shape; *Antennae 1* accessory flagellum 8-articulate; flagellum 26-articulate; *Antennae 2* peduncular article 4 shorter than article 5 (0.8x), flagellum 47-articulate. Paratype juvenile (NIWA 139163), as holotype except: *Head* eyes faded but present in an inverted S-shape; *antennae 1* accessory flagellum 6-articulate; flagellum 18-articulate, lacking brushed long setae on peduncular article 3 and callynophore, callynophore shorter; *antennae 2* peduncular article 4 shorter than article 5 (0.8x), flagellum 30-articulate.

Habitat and Biology. Only known from type locality. The chelate gnathopod 1 indicates they should be considered as specialised scavengers (Corrigan et al., 2014). Females were the largest specimens with a total body length of 13.1 - 21.2 mm (n = 7). Juveniles ranged from 4.5 to 11.1 mm (n = 8), and males ranged from 12.9 and 15.1 mm (n = 4).

Remarks. With a convex palm on gnathopod 2, carpus of gnathopod 1 longer than the propodus, and carpus of gnathopod 2 about double the length of the propodus, *S. sigmacrus* sp. nov. is closely allied with *S. biscayensis, S. uncinatus, S. transversus,* and *S. mytilus.* Yet, *Stephonyx sigmacrus* sp. nov. is easily distinguishable by the sigmoid shape of the pereopod 5 and 6 basis and the acute bifid upturned point of the anterior cephalic lobe. These two features are not shared by any members of the genus. Other minor distinctive characters include long antennae, three setae on the inner plate of the maxilliped, carination on solely urosomite 1, epimeron 3 posteroventral corner with a small tooth, and apical margin of telson with robust setae.

While seven of the species, including *S. sigmacrus* sp. nov., are only known from a single locality, the genus *Stephonyx* has a global distribution except for the polar oceans (Winfield et al., 2017). In the Indo-Pacific, *S. arabiensis* has been found in the north Arabian Sea and near New South Wales, Queensland, and Tasmania and *S. biscayensis* has been found off Kenya and Madagascar (Lowry & Kilgallen, 2014; Winfield et al., 2017). With *S. arabiensis*, *S. sigmacrus* sp. nov. shares three setae on the inner plate of the maxilliped and tooth on the posteroventral corners of epimeron 2 and 3. However, *S. sigmacrus* sp. nov. can be easily distinguished by the convex palm of gnathopod 2 (concave/excavate on *S. arabiensis*).

Thus far, all species of *Stephonyx* are primarily bathyal zone scavengers with a combined depth range of 3 to 2635 m. *S. pirloti* was recorded to be found at 3 m, but this depth is highly doubtful and likely a sampling artefact (Winfield et al., 2017). Until now, *S. mytilus* was the deepest known species, distributed between 2447 - 2635 m. Sumida et al., (2016) did collect *Stephonyx* sp. from a whale fall at 4204 m, thus indicating their abyssal zone presence. However, the specimens were not identified to species level. *S. sigmacrus* sp. nov. extends the known range of *Stephonyx* into the abyssal zone with a new depth record (4932 m) and expands the Indo-Pacific distribution into the East Indian Ocean. A population of juvenile to adult instars indicates that *S. sigmacrus* sp. nov. is adapted to cope with the high pressure and limited food of abyssal depths. Cellular adaptions to pressure at these depths are likely similar to other abyssal scavenging amphipods with elevated concentrations of osmolytes, such as trimethylamine N-oxide and *scyllo*-insoitol (Downing et al., 2018). This indicates that with further sampling of abyssal and potentially hadal depths with baited traps could continue to expand the distribution and diversity of *Stephonyx* in the deep ocean.

Key to the species of *Stephonyx*

1. Lateral cephalic lobe broad, apically truncated/rounded … 2
   Lateral cephalic lobe narrow, apically acute/subacute/bifid … 9
2. Gnathopod 2 palm excavate … 3
   Gnathopod 2 palm straight … 5
   Gnathopod 2 palm convex … 8
3. Epimeron 3 posteroventral corner produced to form a distinct tooth; gnathopod 2 palm slightly excavate … 4
   Epimeron 3 posteroventral corner sub-quadrate with a distinct corner, but no tooth; gnathopod 2 palm deeply excavate … *S. perexcavatus* Narahara, Tomikawa & Torigoe, 2012
4. Gnathopod 1 propodus broad, longer than carpus … *S. normani* (Stebbing, 1888)
   Gnathopod 1 propodus narrow, subequal to/longer than carpus … *S. laqueus* (J. L. Barnard, 1967)
5. Uropod 2 rami equal in length … *S. incertus* Bellan-Santini, 1997
   Uropod 2 outer ramus shorter than inner ramus … 6

6. Lateral cephalic lobe truncated … *S. mytilus* (Barnard & Ingram, 1990)
   Lateral cephalic lobe rounded … 7
7. Epistome and upper lip fused (no notch); mandibular palp article 1 long (subequal to/longer than article 3 … *S. pirloti* (Sheard, 1938)
   Epistome and upper lip not fused (separated/notch); mandibular palp article 1 short (shorter than article 3) … *S. rafaeli* Lowry & Kilgallen, 2014
8. Epimeron 3 ventral margin lined with setae; uropod 1 outer ramus with 1 lateral seta/setae absent … *S. uncinatus* Senna & Serejo, 2007
   Epimeron 3 ventral without setae; uropod 1 outer ramus lined with many marginal robust setae … *S. transversus* Sorrentino, Souza-Filhou & Senna, 2018.
9. Urosomite 1 with carination … 10
   Urosomite 1 without carination … 12
10. Pereonites dorsally carinated; pereopods 5–6 basis posterior margin rounded; lateral cephalic lobe with single point … 11
    Pereonites dorsally smooth, not carinated; pereopods 5–6 basis posterior margin sinusoidal; lateral cephalic lobe bifid … *S. sigmacrus* sp. nov.
11. Urosomite 1 carination rounded, uropod 3 inner ramus reaching to end of outer ramus article 1 … *S. carinatus* Bellan-Santini, 1997
    Urosomite 1 carination angular; uropod 3 inner ramus reaching to the tip of outer ramus article 2 … *S. scutatus* (Griffiths, 1977)
12. Gnathopod 2 palm excavate … 13
    Gnathopod 2 palm not excavate … *S. biscayensis* (Chevreux, 1908)
13. Antenna 1 subequal in length to antenna 2 … *S. californiensis* Winfield, Hendrickx & Ortiz, 2017
    Antenna 1 shorter than antenna 2 … 14
14. Gnathopod 2 deeply excavate … *S. talismani* (Chevreux, 1919)
    Gnathopod 2 weakly excavate … *S. arabiensis* Diffenthal & Horton, 2007

Family Alicellidae Lowry & De Broyer, 2008

Genus Civifractura gen. nov.

Type species. *Civifractura serendipia* sp. nov.

Etymology. The genus name, *Civifractura*, stems from the Latin *civis* (citizen) combined with *fractura* (fracture or fault). This name references both the type locality, the WZFZ, and other potential habitats, such as trenches. Used as a noun in apposition. Gender, feminine.

Diagnosis. Mouthparts forming quadrate bundle. Epistome and upper lip separate, neither dominant in size, blunt. Incisor weakly toothed or smooth; left and right lacinia mobilis shorter than broad; left and right molar large, conical, setulose, with small apical trituration surface; palp attached strongly distal to molar. Inner plate of maxilla 1 with 15 setae; palp 2 -articulate, large. Inner plate of maxilla 2 slightly shorter than outer, with strong row of mediofacial setae (13). Inner and outer plates of maxilliped well-developed, inner not bevelled, with three spines grouped medially, apicolateral margin bulging, palp strongly exceeding outer plate, dactyl well-developed, ordinary, with tooth, with one apical nail and several accessory setae. Coxa 1 slightly shortened and partly covered by coxa 2, straight sided. Gnathopod 1 elongate, simple/weakly subchelate, palm extremely oblique, carpus longer than propodus, ischium slightly elongate; dactyl small. Coxa 2 not tapering. Gnathopod 2 propodus subequal to carpus, both very elongate and linear, propodus subchelate. Posteroventral lobe on coxa 4 strong to medium. Pereopods 5-7 elongate. Outer ramus of uropod 2 shortened. Inner ramus of uropod 2 without notch. Uropod 3 inner ramus shorter than outer ramus, peduncle ordinary, outer ramus 2-articulate. Telson elongate, deeply cleft.

Species composition. *C. serendipia* sp. nov.

Remarks. This genus is morphologically closest to *Tectovalopsis*, but can be separated primarily by the very weakly subchelate or even simple looking gnathopod 1 propodus (weakly to strongly subchelate in *Tectovalopsis*), the distinctly shortened inner ramus of the uropod 3 (rami of equal length in *Tectovalopsis,* except for *T. fusilus* where the inner ramus is shortened), and the only slightly shortened coxa 1 (strongly shortened in *Tectovalopsis*) and only one apical nail on the maxilliped palp dactylus (two present in

Tectovalopsis). Secondary characters to distinguish this genus from *Tectovalopsis* include a more strongly developed posteroventral lobe of coxa 4.

While more genetically similar, this genus is morphologically distinct from *Alicella*, primarily by the gnathopod 1 propodus being very weakly subchelate (simple in *Alicella*), the ovoid shape of basis of pereopods 5-7 (subrectangular in *Alicella*), apicolateral margin bulging of inner plate of maxilliped (depressed in *Alicella*), and the outer ramus of uropod 1 longer than the inner ramus (equal length in *Alicella*).

This genus also differs from a morphologically similar *Diatectonia* with the single dorsal tooth of urosomite 1 (multi-fib in *Diatectonia*), fewer setae on the oblique facial row on the inner plate of maxilla 2 (27 setae in *Diatectonia*), fewer setae on the inner plate of maxilla 1 (19 setae in *Diatectonia*), coxa 1 slightly shorter than coxa 2 (strongly shortened in *Diatectonia*), and gnathopod 1 weakly subchelate (strongly subchelate in *Diatectonia*). *Civifractura* gen. nov. differs from *Transtectonia* with smooth incisors (strongly toothed in *Transtectonia*), presence of a right lacinia mobilis (vestigial on *Transtectonia*), one less seta on the inner plate of maxilla 1 (16 setae in *Transtectonia*), and reduced coxa 1 (unreduced in *Transtectonia*). *Civifractura* gen. nov. differs from *Apotectonia* presence of a right lacinia mobilis (vestigial on *Apotectonia*), fewer setae on the inner plate of maxilla 1 (13 on *Apotectonia*), fewer setae on the inner plate of maxilla 2 (20 on *Apotectonia*), concave gnathopod 2 palm (straight on *Apotectonia*), strong epimeron 3 dorsal tooth strong (weak on *Apotectonia*), and inner ramus of uropod 3 shortened (equal length on *Apotectonia*).

As is the nature of deep-sea systematics, conservative morphology, most likely arising from convergent evolution, is prevalent. Thus, the genus is diagnosed with only a relatively small but distinct suite of morphological characters. It is, however, strongly supported by the genetic evidence provided (Figure 30, Figure 31). As plasticity and convergent evolution of phenotypes is revealed by genetics, there was no sufficient morphological evidence to reassign other species in the Alicellidae family to *Civifractura*.

***Civifractura serendipia* sp. nov.** (Figure 35,Figure 36, Figure 37)

Type material. Holotype: Mature male, 27.2 mm, NIWA 139164. Paratypes: Mature male, 28.8 mm, NIWA 139165, Immature male, 17.8 mm, NHM UK 2019.15; Mature female, 26.0 mm, NHM UK 2019.14, Immature female, 18.7 mm, NIWA 139166; and Juvenile,

13.5 mm, NIWA 139167, Juvenile 9.8 mm, NHM UK 2019.16. Paragenetypes: Male, 27.8 mm (isolate 1), NIWA 139168, GenBank MK503197 for 16s, MK503207 for COI, MK503224 for His3, and MK503216 for 28S, and Juvenile, 14.8 mm (isolate 2, entire specimen used for DNA extraction), GenBank MK503198 for 16s, and MK503208 for COI.

Type-locality. Wallaby-Zenith Facture Zone (Wharton Basin), Indian Ocean (22 12.579S, 102 30.347E), cruise SO258, station L7, depth 4932 m.

Additional Material Examined. Three males, 18.6 - 29.1 mm; two females, 17.5 & 28.4 mm; and one juvenile, 12.5 mm. Material is lodged at Newcastle University.

Diagnosis. Left incisor smooth with a single tooth on posterior corner. Left lacinia mobilis well-developed, comb-like in shape, jaggedly serrate, 3x wider than long, accessory spine row well-developed, 23-25 tufts of setae. Coxa 1–2 not of broadened form. Coxa 1 reduced, sub-rectangular, posterior margin weakly tapering. Coxa 2 weakly adz-shaped, rounded apically. Palm of gnathopod 1 strongly oblique and nearly parallel to anterior margin, with the appearance of gnathopod 1 being simple and not subchelate. Palm of gnathopod 2 weakly oblique and concave. Posteroventral corners of epimeron 2–3 produced to form a distinct tooth. Strong dorsal tooth on urosomite 1. Inner ramus of uropod 3 shorter than outer ramus.

Etymology. The species name, *serendipia*, stems from the English word, serendipity - an unexpected discovery/happening or good luck in finding valuable things. This name was selected to reference serendipity on several levels. First, our participation in the first sampling of a hadal fracture zone was serendipitous. Second, routine DNA barcoding revealed this to be a new species. Third, the name pays homage to the lead author's favourite beer, Serendipity from New Glarus Brewing Company. Used as a noun in apposition.

Description, based on holotype, male, 27.2 mm, NIWA 139164.

BODY: narrow and slender, dorsally smooth, slight dorsal ridge on pleon 3.

HEAD: deeper than long; rostrum absent. Eyes not observed. Lateral cephalic lobe well-developed, broadly rounded. *Antenna 1* subequal in length to antenna 2 and 0.3x long as body; peduncular articles 1–3 length ratio of 1: 0.4: 0.2; accessory flagellum 7-articulate. Callynophore well-developed with long brushed-setae. Flagellum 33-articulate. *Antenna*

2 slender, and 0.3x long as body; peduncular articles 3–5 length ratio of 1: 1.7: 2.5, peduncular article 4 with tufts of short setae; flagellum 45-articulate; calceoli present.

MOUTHPART BUNDLE: epistome and upper lip weakly articulate, separated by notch from lateral view, epistome slightly protruding and forms a point with a tuft of long setae at end. *Mandible* right incisor smooth with a single tooth, lacinia mobilis well-developed, comb-like in shape, jaggedly serrate, 2.5 wider than long, accessory spine row moderately developed, 5 tufts of setae; left and right molars medium-sized, subconcial, densely setulose, tapering to a weak triturating surface; palp article length ratio of 1: 6.3: 4.2, article 2 elongate with setae along distal half of the medial surface, setae scattered along whole length (not dense proximally), article 3 long, blade-like, 0.6x length of article 2, simple setae starting at a third up the anterior margin and several plumose setae at the distal end. *Maxilla 1* inner plate 2.5 x long as wide, 15 setae; outer plate narrow with 8/3 setal-tooth formula; palp large, bi-articulate, broadly paddle shaped, terminal article has five simple setae on lateral margin, distal margin has 18 robust setae and submarginal row of 15 slender setae with one being a flag seta. *Maxilla 2* inner plate is 0.8x as long as outer plate, lateral margins of outer plate has simple and plumose setae, inner plate has simple setae on the lateral margin and 13 mediofacial plumose setae. *Maxilliped* inner plate sub-rectangular, 0.7x the width of the outer plate, three short, robust setae near apical inner corner and five simple setae on the outer corner, oblique setal row well-developed but short with plumose setae; outer plate large, subovate, inner margin with a row of short and stout spines, longer spines apically, small medial facile stout setae present; palp well-developed, 4-articulate, articles 1-4 with long facial and distal setae; dactylus well-developed, with inner apical tooth, 1 main apical nail, and several accessory setae; palp well-developed, dactyl well-developed, ordinary, with tooth, with one apical nail and several accessory setae.

PEREON: *Gnathopod 1* coxa 0.8x the length of coxa 2, posterodistal margin weakly convex with three slender setae, facial setae; basis linear and weakly parallel with the posterior margin being slightly convex, 3.8x longer than wide; ischium sublinear, 1.5x longer than wide, shorter than basis (0.3x); merus short, 1.6x longer than wide; carpus linear and elongate, 2.8x longer than wide; propodus linear and tapering, 3x as long as wide, palm 0.3x the length of the propodus, palm has five setae and terminates with three

robust setae, dentate on 0.6 of the length of the palm; dactylus curved posteriorly, five subapical stout setae, one long anterodistal seta, unguis. *Gnathopod 2* subchelate; basis 5.2x longer than wide, margins parallel; ischium 3.5x longer than wide, anterior margin concave; merus 2.3x as long as wide, shorter than carpus (0.5x); carpus elongate, 4.5x as long as wide; propodus elongate and parallel, 4x as long as wide, posterior margin with dense rows of slender crenate setae; palm with thin setae on margin, dentate on nearly entire palm, 11 robust seta, dactylus reaches 1/3 across palm; dactylus 2.5x longer than wide, three subapical stout setae, one long anterodistal seta, unguis. *Pereopod 3* coxa subequal in size to coxa 2, sub-rectangular, corners rounded, not adz-shaped, small setae on posteroventral corner, four facial setae near ventral margin; basis elongate and curved, 4.3x times longer than wide; ischium shorter than basis (5.7x); merus parallel and lacking expansion; dactylus simple, short, curved posteriorly. *Pereopod 4* coxa large, posterodistal corner strongly convex, ventral margin weakly convex; ischium shorter than basis (0.2x); merus parallel and lacking expansion; carpus shorter than merus (0.7x); propodus longer than merus (1.2x); dactylus simple, short, curved posteriorly, single short seta on anterior margin. *Pereopod 5* coxa bilobate, anterior lobe more pronounced ventrally; basis expanded with posterior lobe rounded; ischium short; merus posterior margin weakly expanded and convex. *Pereopod 6* coxa small; basis expanded with posterior lobe rounded; ischium short; merus posterior margin weakly expanded and convex. *Pereopod 7* coxa small, 0.3x length of basis, adz-shaped; basis expanded, posterior lobe deeply rounded, reaching to merus; ischium short; merus posterior margin weakly expanded and convex.

PLEON*: Epimeron 1* two unpaired setae near the anteroventral margin, posteroventral corner produced to form a weak, rounded tooth. *Epimeron 2* with three unpaired setae widely spread ventrally, posteroventral corner produced to form a distinct tooth. *Epimeron 3* with nine, unpaired setae spread evenly along the anteroventral margin, posteroventral corner produced to form a distinct tooth.

UROSOME*:* Strong dorsal tooth on urosomite 1. Dorsal tooth lacking on urosomite 2. Middle keel on urosomite 3 absent. *Uropod 1* peduncle long, 3.8x as long as wide, apicolateral corner of peduncle with large robust seta, without simple setae; inner ramus subequal to outer ramus, 1.2x length of rami to peduncle. *Uropod 2* peduncle long, 2.5x

as long as wide; robust seta apicolateral corner of the peduncle which are not substantially larger than other peduncle setae; inner ramus longer than outer ramus (1.4x), inner ramus 1.6x longer than peduncle. *Uropod 3* peduncle short, 1.7x wide as long, robust setae on both apicolateral corners of the peduncle; inner ramus longer than peduncle (1.5x), outer ramus longer than inner ramus (1.2x); inner ramus with plumose setae on lateral and medial margins; outer ramus bi-articulate, plumose setae on medial margin, article 1 17x longer than article 2. *Telson* 2.0x length to width, deeply cleft (85%), apical margin strongly bifid, one robust seta at apical margin of each lobe.

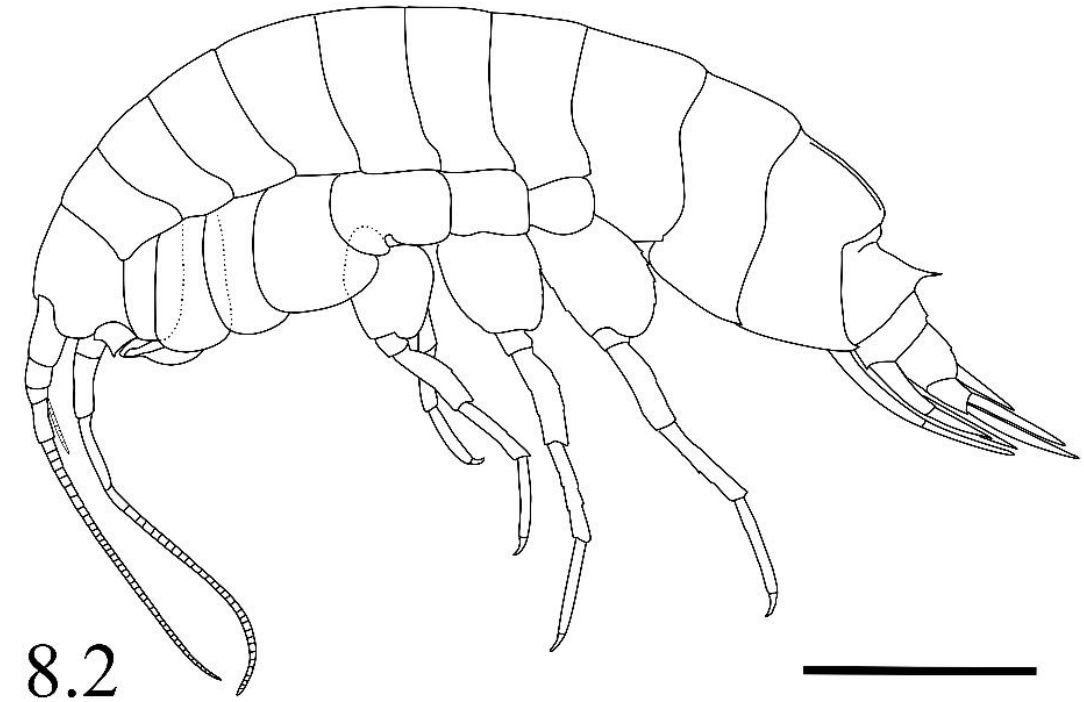

Figure 35. Photograph of *Civifractura serendipia* gen. et sp. nov. holotype (8.1). *Civifractura serendipia* gen. et sp. nov. holotype, scale bar 5 mm (8.2).

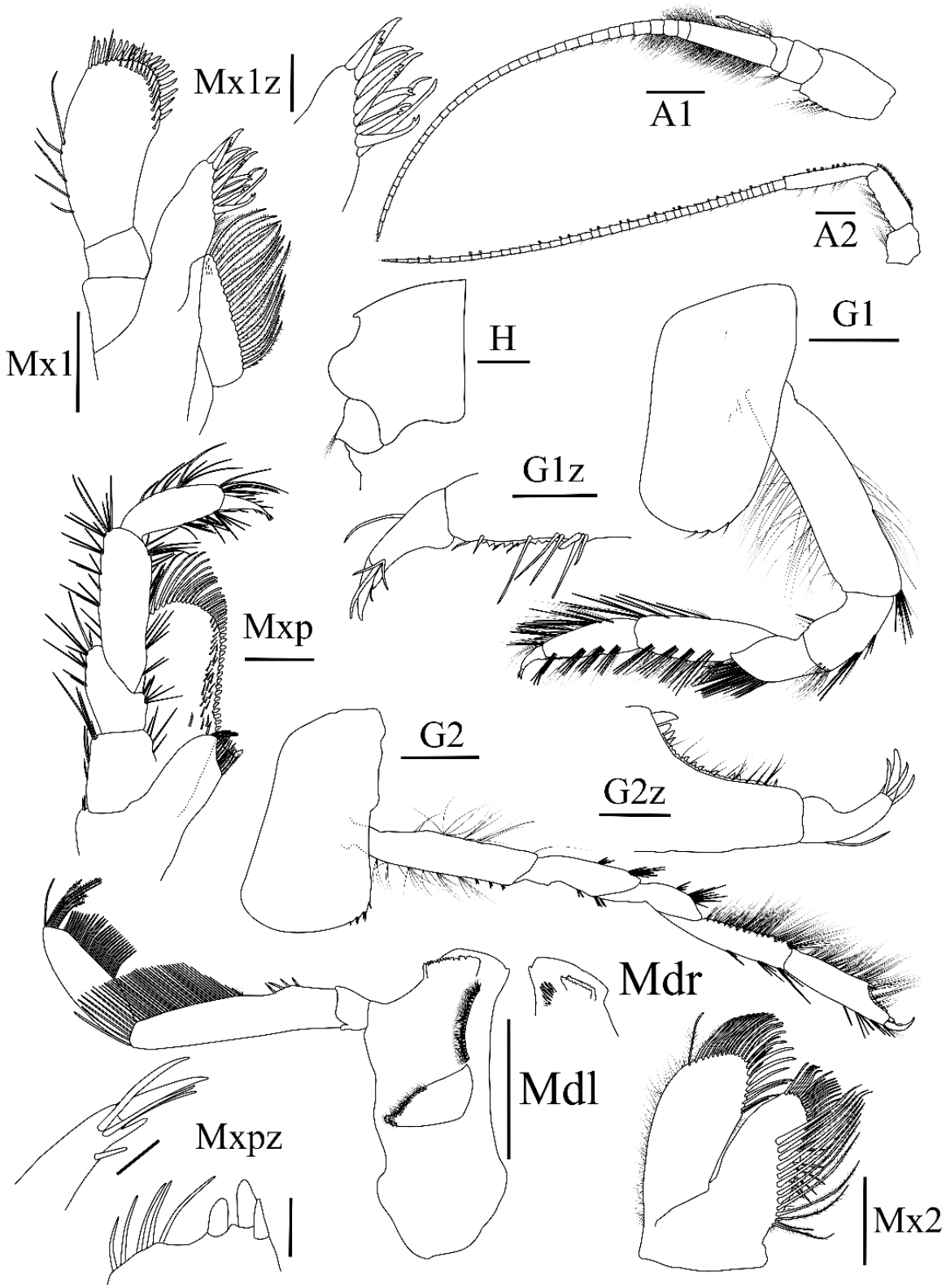

Figure 36. *Civifractura serendipia* gen. et sp. nov. holotype. Scale bars: Mxpz & Mx1z 0.1 mm; G1z & G2z 0.2 mm; Md, Mx1, Mx2, & Mxp 0.5 mm; H, A1, A2, G1, & G2 1 mm.

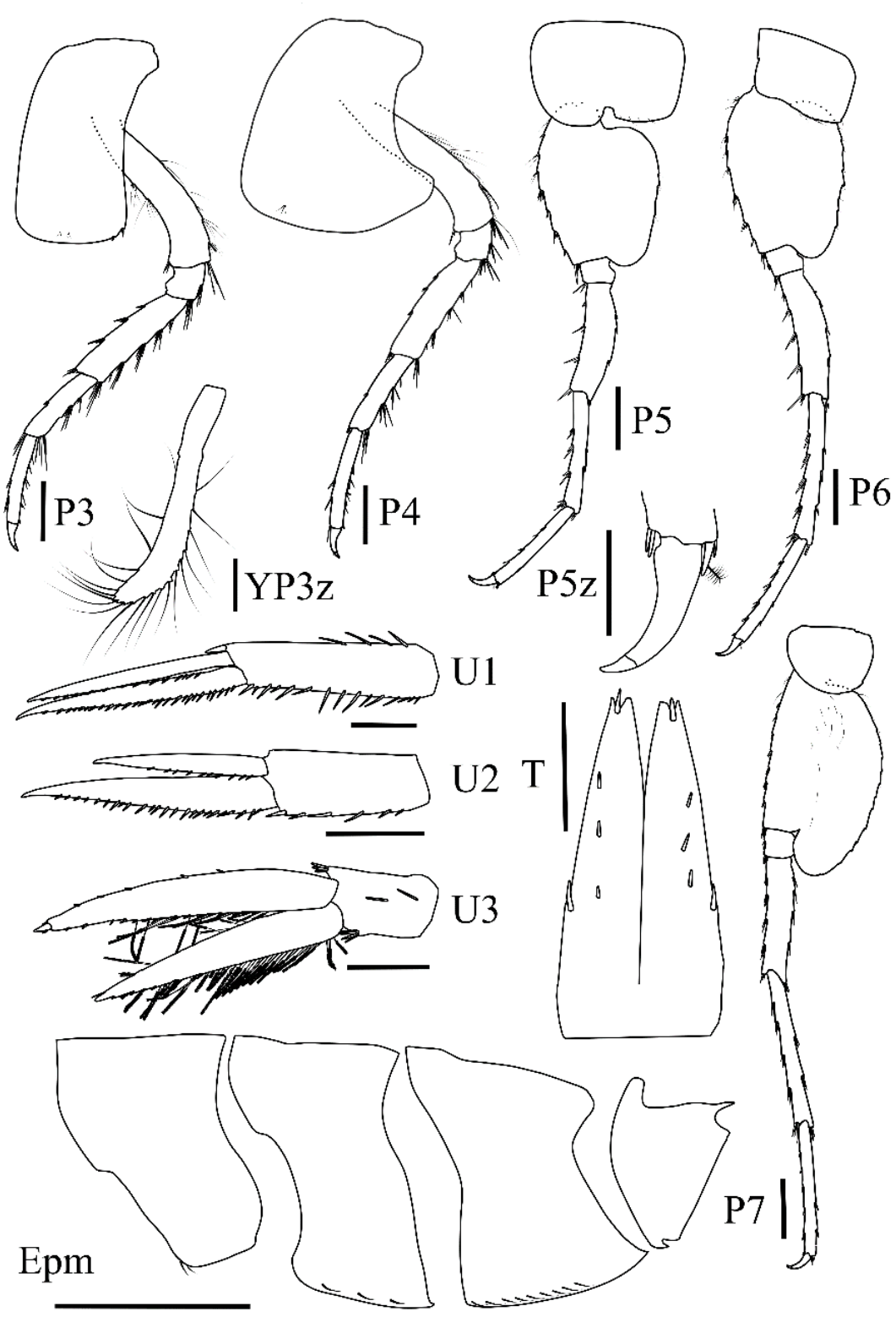

Figure 37. *Civifractura serendipia* gen. et sp. nov. holotype and paratype NHM UK 2019.14. Scale bars: P5z 0.5 mm; remainder 1 mm.

Variations. In general, females of *C. serendipia* resemble males except for smaller body sizes. Paratype immature female (NIWA 139166), as holotype except: *Body* pleon 3 is dorsally smooth. *Antennae 1* accessory flagellum 5-articulate; callynophore 0.5x length of holotype and lacking brushed setae; flagellum 29-articulate. *Antennae 2* peduncular article 4 sub-rectangular and lacking tufts of setae; flagellum 32-articulate; calceoli not present. Paratype mature female (NHM UK 2019.14), as holotype except: *Urosome* missing. *Pleon* 3 is dorsally smooth. *Oostegites* present on gnathopod 2 and pereopods 3-6, well-developed, curved at the distal end and possess elongated setae. *Gills* present on gnathopod 1 & 2 and pereopods 3-6. Paratype juvenile (NHM UK 2019.16), as holotype except: *Antennae 1* accessory flagellum 4-articulate; callynophore 0.25x length of holotype and lacking brushed setae; flagellum 19-articulate; *Antennae 2* peduncular article 4 sub-rectangular and lacking tufts of setae; flagellum 23-articulate; calceoli not present.

Habitat and Biology. Only known from the type locality. With the mandible similarities to allied species and collection via baited trap, they are presumed to be benthic scavengers. Males were the largest with a total body length of 18.6 - 29.1 mm (n = 6). Females ranged from 12.9 - 28.4 mm (n = 5), and juveniles ranged from 6.5 - 14.8 mm (n = 15).

Key to Alicellidae (adapted from Lowry & De Broyer, 2008)

1. Gnathopod 1 simple…2
   Gnathopod 1 subchelate (very weakly to strongly)…3
2. Urosomite 1 with rounded hump…*Alicella*
   Urosomite 1 with sharp carina…*Apotectonia*
3. Urosomite 1 with sharp carina…4
   Urosomite 1 with rounded hump…*Paralicella*
4. Urosomite 1 carina single…5
   Urosomite 1 carina double…*Diatectonia*
5. Gnathopod 1 coxa reduced, smaller than coxa 2…6
   Gnathopod 1 coxa large, subequal to coxa 2…*Transtectonia*
6. Gnathopod 2 palm straight…*Tectovalopsis*
   Gnathopod 2 palm concave…*Civifractura*

6. Discussion

The incongruities between the morphological and molecular phylogenetic analysis raised the issue of how the boundaries between species and genera of scavenging amphipods from abyssal depths are delineated. The scoring of 73 morphological traits across three families firmly nested *C. serendipia* gen. et sp. nov. within the Alicellidae family and in the genus *Tectovalopsis* (Figure 29). Morphology placed *Alicella* basal to *Tectovalopsis* and *Diatectonia*, thus *Tectovalopsis* was more morphologically similar to *Diatectonia* and *Alicella* than other genera within the family. Solely based on morphology, the new species would be the seventh species in *Tectovalopsis*, however, the mtDNA phylogeny placed the new species sister to *Alicella* and reciprocally monophyletic to *Tectovalopsis* (Figure 30). Based only on the mtDNA dataset, *C. serendipia* gen. et sp. nov. could be placed within *Alicella.* Yet, this placement would not marry with either the morphology or the mtDNA + nuclear DNA phylogeny, which placed the new species basal to *Alicella* and *Tectovalopsis*. With the multiple lines of evidence, we have selected a third option to establish a new genus within the Alicellidae family for *C. serendipia* gen. et sp. nov. This integrative taxonomy by congruence selection acknowledges that *C. serendipia* gen. et sp. nov. is a new species within a family where the evolutionarily important diagnostic traits are still being determined and the multi-locus phylogenies are well supported for a new genus.

The morphological analysis further indicated that the Alicellidae family is polyphyletic. This contrasts the monophyletic assumption used by Lowry & De Broyer (2008) to establish the Alicellidae family. The family was established based on characteristics of the lacinia mobilis, molar, and gnathopod 1 and 2. These are morphological traits associated with necrophagy, which are believed to have arisen independently multiple times within the colonization of the deep-sea by Lysianassoidea (Corrigan et al., 2014). These characters also change multiple times within the ‘Alicellidae’ and therefore do not support monophyly. Congruous with Ritchie et al. (2015), our multi-locus phylogenies support that Alicellidae is not monophyletic, as the additional Alicellidae sequences maintain the polyphyletic separation of *Paralicella* and cryptic speciation within the *P. tenuipes* & *caperesca*-complex. An integrative taxonomic approach should be applied to future work to revise the Alicellidae family and *Paralicella* genus and

reassess the *Valettietta* genus, with considerations given to clarifying morphological identifications and curation of existing GenBank identifications (Diechmann et al., 2017).

Our study is limited by the lack of comparative type material. To address this, we sequenced nine additional specimens identified belonging to the genera *Alicella*, *Tectovalopsis*, and *Diatectonia* that were thought to fall with this clade (i.e., *A. gigantea* WZFZ4932 & ANS4733, *T. wegeneri* NH3400 & NH4694, *Tectovalopsis* sp. PC4602 & M5601, and *Diatectonia* sp. NH3400a & NH3400b). Characteristics such as the distinctively large body size of juveniles and adults and the simple palm of gnathopod 1 allow for the robust identification of *A. gigantea* (Barnard & Ingram, 1986; Jamieson et al., 2011). The morphological scoring showed *A. gigantea* from WZFZ to be identical with the type description (Figure 29). Thus, the sequence placement of *A. gigantea* from five locations in the Pacific and Indian Oceans should be given high confidence. Three additional specimens of *Tectovalopsis* and two specimens of *Diatectonia* from Peru-Chile Trench and New Hebrides Trench were previously identified by taxonomists (included in Fujii et al., 2013; Lacey et al., 2016) and were re-examined for this study.

We identified four morphological variations in the *T. wegeneri* specimens from the New Hebrides Trench (*T. wegeneri* NH3400 & NH4694; Lacey et al., 2016), compared to the original description in Barnard & Ingram (1990): 1) presence of dorsal setae on urosomite 3, 2) 10 instead of 11 setae on the facial setal row of the inner plate of maxilla 2, 3) the right lacinia mobilis was a smooth, small peg instead of a small and serrate flake, and 4) the left incisor was barely crenulated instead of fully smooth on the dorsal side. Even with these differences, *T. wegeneri* NH3400 and NH4694 were still closely morphologically related to the type description (bootstrap 91). These variations were determined to be minor and likely represent geographic intraspecific variation as the holotype is from 2635 m at the East Pacific 13^{o}N Vents (Barnard & Ingram, 1990; France & Kocher, 1996). From this assessment, confidence was gained for the genetic placement of the *Tectovalopsis* clade (Figure3). Both the morphological and genetic species-delimitation analysis suggested that the two specimens *Diatectonia* sp. NH3400a and NH3400b (Lacey et al., 2016) are not separate species but both *T. wegeneri*. As a result, the GenBank entries for *Diatectonia* sp. NH3400a and NH3400b are listed as *T. wegeneri* to reflect correct identifications. This further highlights the challenges of visually

identifying these cryptic species (d'Udekem d'Acoz & Havermans, 2015; Havermans et al., 2010).

Morphological and molecular assessment of *Tectovalopsis* sp. M5641 and PC4602 supported those specimens to be new species *Tectovalopsis*, which will be described at a later date (Figure 29). These specimens do potentially introduce novel characteristics to the genus. Both have a reduced left lacinia mobilis, whereas, for all described *Tectovalopsis* species, the left lacinia mobilis is well-developed (Barnard & Ingram, 1990). This highlights that the diversity of species and phenotypes is much greater within this taxon than previously known. As more specimens are collected and both morphological and genetically analysed, a more detailed understanding of their distribution and evolutionary history will be uncovered. Similar findings are being uncovered in the other large, deep-sea amphipod genus, *Eurythenes* (d'Udekem d'Acoz & Havermans, 2015; Havermans, 2016).

While this paper has focused on deep-sea amphipods, the challenge of morphological versus molecular data with limited specimens applies to many other taxa, such as Antarctic polychaetes (Brasier et al., 2016), tardigrades (Sands et al., 2008), and deep-sea sponges (Lim et al., 2017). In new or poorly sampled ecosystems, like the deep sea, there is still a considerable amount of work to describe new species. These new species could be discovered by the sampling of new locations, uncovering cryptic species with genetic methods, or while rectifying taxonomic classifications to align with molecular phylogenies. Even though a species is the most fundamental concept in ecology, it is also one of the most problematic and debated concepts (Baum & Shaw, 1995), with multiple existing ways to defining such as the morphological species and phylogenetic species concepts (de Queiroz, 2005; Elredge & Cracraft, 1980). Now with multiple tools for discovery, such as DNA sequencing and computed tomography, there are continued qualitative challenges to reach agreement on defining and delimiting a species with multiple lines of evidence (Padial et al., 2010).

In the study, we utilized the conceptual workflow for integrative taxonomy laid out by Padial et al. (2010) to determine the taxonomic placement of new species from abyssal depths of the WZFZ. At first, the morphological and multi-locus datasets seemed to be at odds, with one providing support for the morphological species concept and the other for

the phylogenetic species concept. They are, however, functioning at two different resolutions. The morphological analysis provided a coarser resolution and placed this species in the focused range of existing taxa, an *Alicella* and *Tectovalopsis* clade. The multi-locus dataset provided a finer resolution of evolutionary placement and highlighted the need for a new genus (Padial et al., 2011; Ritchie et al., 2015). Future studies should aim to utilize an integrative taxonomic approach with multiple lines of evidence to identify and describe new species and revised existing classifications. Although, while an integrative taxonomic approach is desired, *S. sigmacrus* highlights the difficulties it can raise such as viable DNA extraction that can render this method infeasible. By using an integrative taxonomic approach, we will likely uncover greater diversity within the deep sea and further illuminate patterns of speciation, connectivity, and community structure.

6. Acknowledgments

We would like to thank Dr Thomas Linley (Newcastle University) for support with photography and illustrations, Prof Stuart Piertney (University of Aberdeen), Dr Heather Ritchie (University of Aberdeen), and Dr James Kitson (Newcastle University) for their support with genetic sequencing, Heather Stewart (British Geological Survey) for support with the map, and the Captain and crew on the 2017 RV *Sonne* Expedition SO258 Leg 1. We would also like to thank the collections staff at the NIWA Invertebrate Collection and the Natural History Museum for their efficiency and generosity in curating the type material. Thank you to the reviewer for their constructive comments that improved the manuscript. The genetic analysis was funded by Newcastle University.

Supplementary Materials

Appendix A, pages 218-226

Chapter 5: Scavenging amphipods from the Wallaby-Zenith Fracture Zone: Extending the hadal paradigm beyond subduction trenches

Published as: Weston, J.N.J., Peart, R.A., Stewart, H.A., Ritchie, H., Piertney, S.B., Linley, T.D. and Jamieson, A.J., 2021. Scavenging amphipods from the Wallaby-Zenith Fracture Zone: Extending the hadal paradigm beyond subduction trenches. *Marine Biology*, *168*, pp.1-14. doi:10.1007/s00227-020-03798-4

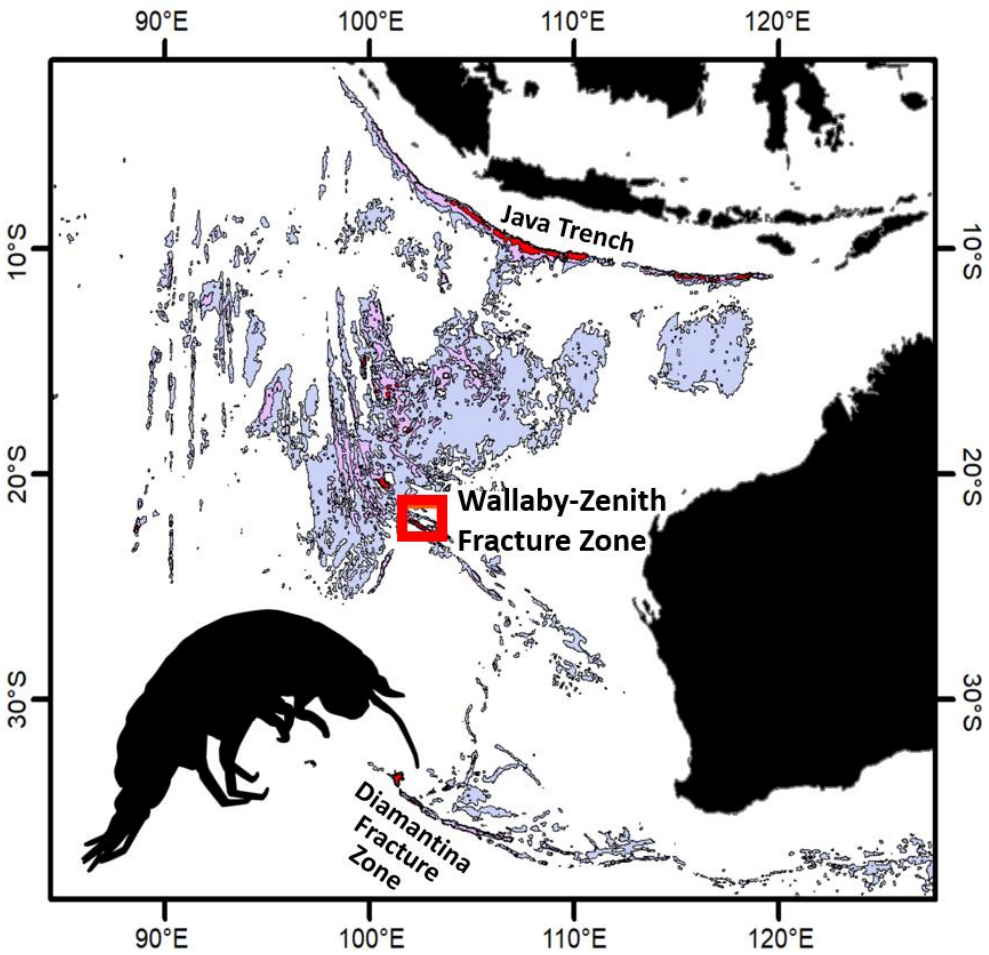

Abstract

Our understanding of the ecology of the hadal zone (> 6000 m depth) is based solely on subduction trenches, leaving other geomorphological features, such as fracture zones, troughs, and basins, understudied. To address this knowledge gap, the Wallaby-Zenith Fracture Zone, Indian Ocean (WZFZ; ~ 22°S, 102°E; maximum depth 6625 m measured during Expedition SO258) was studied using free-fall baited landers. We assessed the amphipod distribution and community assemblage of this non-subduction hadal feature and compared it to subduction hadal features. Eleven species were identified across the abyssal-hadal transition zone using a paired morphological and DNA barcoding approach. The community composition was found to change gradually from abyssal to hadal depths, which contrasts with the ecotone shift characteristic of subduction trenches. A large population of *Bathycallisoma schellenbergi* (Birstein & Vinogradov, 1958), a quintessential hadal amphipod, was present at the flatbottom of the WZFZ. Further, an mtDNA phylogeny resolved a degree of phylogeographic structure between the *B. schellenbergi* WZFZ population and four previously sampled Pacific Ocean subduction trench populations, indicating these features are not interconnected through ongoing gene flow. Combined, these data indicate that some amphipods have far broader distributions than previously understood, with some species present in both hadal subduction trenches and non-subduction fracture zones and basins interspersed across the abyssal plains. This initial exploration highlights that whilst non-subduction features are an overlooked minor fraction of the total hadal area, they are essential to our understanding of the ecological and evolutionary dynamics across the hadal zone.

1. Introduction

The hadal zone comprises 47 known, geographically disjunct, marine features that extend deeper than 6000 m below sea level. Of these, 27 are subduction trenches situated at tectonic plate subduction boundaries and account for 93.7% of the total hadal area (~750,000 km; Jamieson, 2015). The remaining features are troughs, fracture zones, trench faults, and other features that are not necessarily associated with plate convergence zones and can span across the abyssal plain interiors (~50,500 km; Jamieson, 2015). Whilst these features all experience high hydrostatic pressure, low temperature, and limited food availability, the geomorphological characteristics, such as total depth, total area, geographic isolation, seismicity, geologic age, and topographic complexity, vary widely between each habitat (Stewart & Jamieson, 2018).

These deep marine regions host faunal communities with a high degree of endemism, comprised of crustaceans, echinoderms, polychaetes, molluscs, foraminifera, cnidarians, and fishes (Wolff, 1960; 1970; Belyaev, 1989). Patterns of population and community structure, and species distribution are being uncovered with an increase in the number of hadal sampling expeditions since 2000 and the preferential use of baited landers to visualize the seafloor and study bait-attending fauna (Lacey et al., 2016; Jamieson, 2018). Much of our recent understanding has largely focused on scavenging amphipods (Fujji et al., 2013; Eustace et al., 2016; Lacey et al., 2016). Scavenging amphipods, primarily from the Lysianassoidea and Allicelloidea superfamilies, are abundant in the deep-sea benthic community and dominate at depths greater than 8000 m (Ritchie et al., 2015; Lacey et al., 2016). As scavenging amphipods can be readily and consistently recovered in large numbers via baited trap landers, they represent model taxa to study the ecological dynamics of the abyssal and hadal zones across the wide variation of geomorphic settings (Fujji et al., 2013; Duffy et al 2016; Lacey et al., 2016).

The faunal community at hadal subduction trenches is distinct from, and not merely an extension of, the abyssal faunal community (Wolff, 1970; Belyaev, 1989; Jamieson et al., 2011). At the Kermadec, New Hebrides, and Peru-Chile trenches, the scavenging amphipod communities have been documented to abruptly shift from an abyssal to hadal community (Jamieson et al., 2011, Fujji et al., 2013; Lacey et al., 2016), with similar shifts documented in sediment microbial (Hiraoka et al., 2020) and bait-attending fish (Linley et

al., 2017) communities. This shift has been interpreted to reflect the presence of an ecotone boundary between zones (Jamieson et al., 2011). While the hadal zone is bluntly defined to begin at 6000 m, the community shift occurs at some depth between 6000 and 7000 m depending on the feature (Jamieson et al., 2011, Fujii et al., 2013; Lacey et al., 2016). For instance, this shift has been documented to occur between 6097 - 6709 m in the Kermadec Trench (Lacey et al., 2016) and 6173–7050 m in the Peru-Chile Trench (Fujji et al., 2013). The among-trench variation coincides with the break-in slope between the abyssal plain and the subduction trench (Lacey et al., 2016). This further indicates that rapid changes in environmental factors and topography at the trench boundary, differing between the trenches, contribute to the distinct faunal change. Additionally, there are inter-trench assemblage differences (Eustace et al., 2013; Lacey et al., 2016; Jażdżewska & Mamos, 2019), which may be attributed to the amount of particulate organic carbon flux (Ichino et al., 2015) and species evolutionary history and physiological pressure tolerance (Downing et al., 2018).

The trench scavenging amphipod communities at hadal depths appear to be largely dominated by a few species. These species include *Hirondellea gigas* (Birstein & Vinogradov, 1955) in the northwest Pacific Ocean trenches (Hessler et al., 1978; France 1993; Eustace et al., 2013; Jażdżewska & Mamos, 2019), *Hirondellea dubia* Dahl, 1959 largely in the southwest Pacific Ocean trenches (Blankenship et al., 2006; Lacey et al., 2016), and *Eurythenes* sp. and *Hirondellea thurstoni* Kilgallen, 2015 in the Peru-Chile Trench (Eustace et al., 2016; Lacey et al., 2016). *Bathycallisoma schellenbergi* (Birstein & Vinogradov, 1958) is a cosmopolitan hadal species found in trenches across four oceans (Kilgallen & Lowry, 2015). Populations of these species have been observed to exhibit ontogenetic vertical stratification, whereby juveniles inhabit the shallower depths, and adults, primarily females, reside in the deeper depths (Blankenship et al., 2006; Eustace et al., 2013; 2016; Lacey et al., 2018). Further, this intra-specific partitioning has been found to scale to the topography of the trench (Lacey et al., 2018). This consistency of ontogenetic vertical stratification indicates that the population structure of scavenging amphipods in trenches is not solely driven by depth but also the physiological constraints involving hydrostatic pressure, predator avoidance, and food distribution driven by topography.

Hadal subduction trench ecosystems are often purported to be evolutionarily and demographically independent units. While this holds for certain species, like *Eurythenes* sp. from hadal depths of the Peru-Chile Trench (Eustace et al., 2016) and some hadal snailfish (Linley et al., 2016), a growing body of evidence challenges this traditional understanding, e.g., *H. dubia* (Ritchie et al., 2015) and *B. schellenbergi* (Kilgallen & Lowry, 2015). Indeed, population genetic analysis has shown that occasional gene flow does occur between five disparate, abyssal populations of *Paralicella* spp. across the Pacific Ocean (Ritchie et al., 2017). How this is mediated over such large geographical expanses remains unclear.

The study of hadal amphipod ecology has so far been limited to subduction trenches and whether the diversity and community composition patterns are reflective across the hadal zone remains unresolved. Specifically, are species diversity and community structure patterns at hadal depth simply a function of being 'hadal' (depth) or driven by geomorphic and seismic processes? Resolving this requires sampling across the abyssal-hadal transition zone of non-subduction features, specifically areas that have few topographical and seismic similarities to subduction trenches.

To begin to address this knowledge and sampling gap, we present the first biological investigation of a non-subduction hadal feature, the Wallaby-Zenith Fracture Zone (WZFZ) in the Indian Ocean and the abyssal base of the Afanasy Nikitin Seamount as a comparative Indian Ocean reference point. In this study, we describe the geomorphology of the WZFZ based on multibeam mapping and include characterisation of the seafloor habitat based on in-situ imaging. We examine three aspects of the amphipod community for both features, namely the community composition across the abyssal-hadal transition zone, demographics of the dominant hadal species *B. schellenbergi*, and the phylogeographic relationships between the WZFZ *B. schellenbergi* population and four previously sampled Pacific Ocean subduction trench populations.

2. Materials and methods

2.1 Study region

The WZFZ is part of the larger Wharton Basin and Perth Basin complex. The nearest hadal features are the Java Trench, 2100 km north, and the Diamantina Fracture Zone, 1300 km south (Figure 38A; Daniell et al., 2010). The WZFZ formed as a transform fault between 130–124 Ma with the opening of the Indian Ocean during the breakup of the Greater India and Australia (Veevers & Cotterill, 1978; White et al., 2013; Olierrok et al., 2015). Extending south of the Zenith Plateau, the WZFZ spans an area of 12,960 km^2. Two elongated depressions account for 32% of the total area, in addition to four other geomorphic features (i.e., terrace, non-incised slope, ridge, and scarp; Daniell et al., 2010). The WZFZ is positioned under the Indian Ocean South Subtropical Gyre biogeochemical province (Longhurst et al., 1995).

The Afanasy Nikitin Seamount is part of the Central Indian Basin and located at the southern end of the 85^{o}E Ridge (Figure 38A; Sclater & Fischer, 1974; Sborshchikov et al., 1995). Formed 80–73 Ma by the Conrad Rise hotspot, the main plateau rises to ~1200 m above the surrounding 4800 m ocean floor (Krishna et al., 2014). The Afanasy Nikitin Seamount is positioned under the Indian Ocean Monsoon Gyres biogeochemical province (Longhurst et al., 1995).

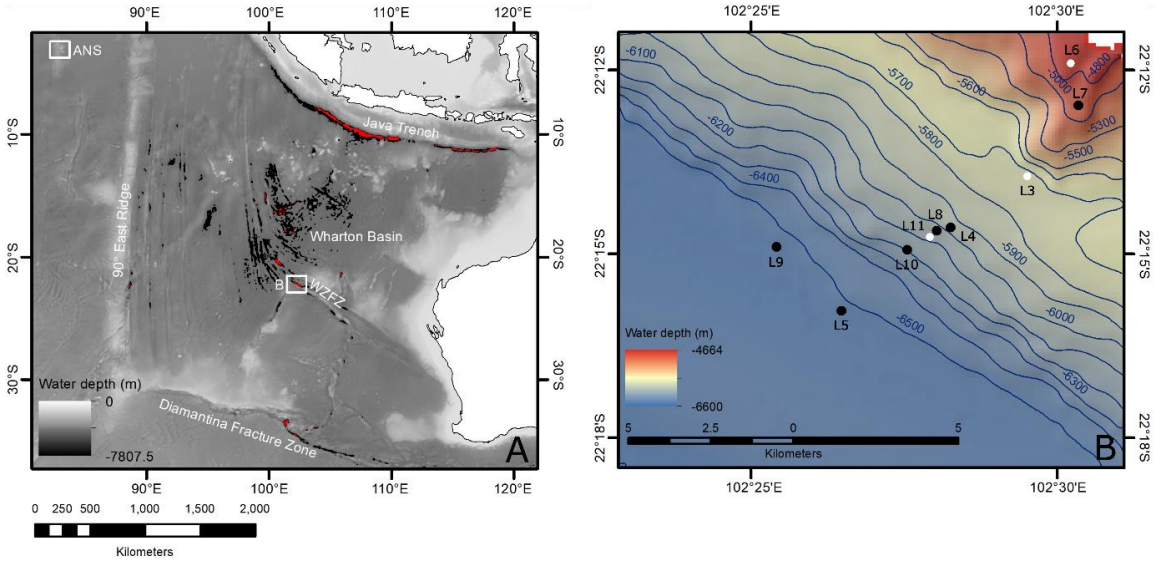

Figure 38. (A) Map of two study sites in the East Indian Ocean with major features labelled and areas with a depth of 6000–6500 m in black and >6500 m in red. (B) Subset of multibeam bathymetry data acquired over the Zenith Plateau and Wallaby-Zenith Fracture Zone (for location see (A)), lander deployments where amphipods were collected (black circles), lander deployments with only camera data acquired (white circles) are shown. Regional bathymetric data displayed in (A) sourced from the Global Multi-Resolution Topography Synthesis (Ryan et al., 2009). Multibeam bathymetric data displayed in (B) sourced from *RV Sonne* Expedition SO258 (Werner et al., 2017). ANS is Afanasy Nikitin Seamount, and WZFZ is Zenith Plateau &Wallaby-Zenith Fracture Zone. Multibeam bathymetric map for ANS can be found in Figure B2.

2.2 Physical mapping

The WZFZ and Afanasy Nikitin Seamount were studied as part of the RV *Sonne* expedition SO258 Leg 1 in June–July 2017 (Werner et al., 2017). Prior to the expedition, satellite altimetry estimated the WZFZ to have a maximum depth of 7883 m (Smith & Marks, 2014; Marghany et al., 2016). Although, recent studies have demonstrated that the error associated with satellite altimetry measurements is elevated at depths exceeding 3000 m (e.g., Weatherall et al., 2015; Mayer et al., 2018; Stewart & Jamieson, 2019). The RV *Sonne* is equipped with a Kongsberg EM122 full ocean depth multibeam echosounder, which was operated by onboard operators. Werner et al. (2017) include

details on system acquisition parameters and data processing of the multibeam bathymetry data.

2.3 Biological sampling and processing

Five autonomous landers (three imaging and two baited trap landers; Jamieson et al., 2009b) were launched and recovered nine times from the top of the Zenith Plateau, along the northern ridge, to the base of the WZFZ from June 10–12, 2017 (Figure 38B) and three times to the base of the Afanasy Nikitin Seamount on June 29, 2017 (Figure B2; Table 6). The sampled depth ranges spanned from 4747–6546 m at the WZFZ and 4724–4757 m at the Afanasy Nikitin Seamount. Landers remained at depth for 7 - 10 hours and were equipped with a temperature and pressure sensor (SBE-39, SeaBird Electronics, US). Pressure (dbar) was converted to depth (m) following Saunders (1981). Imaging landers were outfitted with bespoke HD video and still cameras to characterise the substrate. The cameras were located 2 m above the seafloor looking vertically down. Specimens were collected with the baited trap landers, which were equipped with 2-litre funnel traps baited with whole mackerel (Scombridae; Jamieson et al., 2011). Upon recovery and initial sorting, amphipods were preserved using 70% ethanol.

An integrated taxonomic approach was taken as deep-sea amphipod identification is challenged by phenotypic plasticity, and intra-specific and ontogenetic variation (Ritchie et al., 2015; Weston et al., 2020). Amphipods were morphologically identified to lowest rank possible, following Barnard & Ingram (1990) and Barnard & Karaman (1991), with updates after Lowry & De Broyer (2008), Lowry & Kilgallen (2014), d'Udekem & Havermans (2015), Kilgallen (2015), and Kilgallen & Lowry (2015).

A total of 25 amphipods were selected for DNA barcoding to support morphological identification. The individuals were chosen to represent at least one individual of each species or morphospecies and, where possible, coverage at multiple depths. Total genomic DNA was extracted using the Bioline ISOLATE II Genomic DNA Kit. Partial regions of the mitochondrial 16S rRNA gene (16S) and cytochrome c oxidase subunit I (COI) were amplified with published primer sets: AMPH1 (France & Kocher, 1996) and 'Drosophila-type' 16SBr (Palumbi et al., 2002) for 16S and LCO1490 and HCO12198 (Folmer et al., 1994) for COI. PCR protocols were followed as described in Ritchie et al. (2015). Sequences were cleaned enzymatically using New England Biolabs Exonuclease

1 and Antarctic Phosphatase and sequenced with an ABI 3730XL sequencer (Eurofins Genomics, Germany).

Electropherograms were examined in MEGA v7 (Kumar et al., 2016), primer and ambiguous sequences were clipped by eye, and COI sequences were translated into equivalent amino acid sequences to confirm an absence of stop codons. Each sequence was compared with species diagnostic barcodes on NCBI using BLASTn with default parameters. Individuals were identified to species-level with a 98-100% match and to genus-level with >90%. Final identifications were determined by accounting for both morphological and DNA barcoding identifications.

Table 6. Imaging and baited trap lander stations. Location abbreviations: Zenith Plateau (ZP), Wallaby-Zenith Fracture Zone (WZFZ), and Afanasy Nikitin Seamount (ANS).

Depth (m)	Latitude	Longitude	Station	Date	Location	Lander
4767	22 11.898S	102 30.221E	L6	11/6/2017	ZP	Imaging
4932	22 12.579S	102 30.347E	L7	11/6/2017	ZP	Trap
5724	22 13.741S	102 29.515E	L3	10/6/2017	WZFZ	Imaging
5990	22 14.574S	102 28.262E	L4	10/6/2017	WZFZ	Trap
6068	22 14.628S	102 28.037E	L8	11/6/2017	WZFZ	Trap
6084	22 14.730S	102 27.919E	L11	12/6/2017	WZFZ	Imaging
6162	22 14.939S	102 27.554E	L10	12/6/2017	WZFZ	Trap
6537	22 15.931S	102 26.477E	L5	10/6/2017	WZFZ	Imaging
6546	22 14.887S	102 25.415E	L9	11/6/2017	WZFZ	Trap
4724	3 08.932S	82 26.007E	L12	29/6/2017	ANS	Imaging
4733	3 09.236S	82 25.986E	L13	29/6/2017	ANS	Trap
4757	3 09.542S	82 25.993E	L14	29/6/2017	ANS	Trap

2.4 Amphipod community composition

The amphipod community was characterised using a cluster analysis and non-metric dimensional scaling (nMDS) ordination approach to identify structure and trends across the abyssal-hadal transition zone. Amphipod counts by depth were first divided by the deployment time (h) to standardize for sampling effort and then fourth root-transformed to account for the influence of highly abundant species. The transformed data were converted into a Bray-Curtis similarity matrix and a hierarchical cluster analysis (group-average linkage) was performed (Fujji et al., 2013; Lacey et al., 2016). A similarity profile analysis permutation test (SIMPROF; Clarke et al., 2008; significance level of $p < 0.05$) was conducted to identify the number of significant clusters or ‘communities’. A similarity percentage analysis (SIMPER) was applied to identify the species of greatest

similarity within a community and those species most responsible for the differences between the SIMPROF communities. Standardization by deployment time was conducted in Excel, and subsequent analysis was conducted in PRIMER v7 (Clarke & Gorley, 2015).

The WZFZ and Afanasy Nikitin Seamount data were assessed and compared with abundance data from 32 sites at bathyal to hadal depths (1488–9908 m) at the South Fiji Basin and the Kermadec, New Hebrides, and Peru-Chile trenches (Fujji et al., 2013; Lacey et al., 2016). The identification of *Eurythenes gryllus* (Lichtenstein in Mandt, 1822) presented in Fujji et al. (2013) was updated to reflect the three morphospecies of *Eurythenes* present in the Peru-Chile Trench (Eustace et al., 2016). The multivariate analysis was conducted at species-level and genus-level identifications. Assessment with genus-level identification was done to remove identification bias due to lack of intact specimens, cryptic speciation, and/or specimens requiring description.

2.5 Bathycallisoma schellenbergi demographics and phylogeography

The biometric data of the dominant hadal species, *B. schellenbergi*, were analysed to characterise the sex and stage structure of the population. Specimens were classified as a male with the presence of penile papillae, female with the presence of oostegites, juvenile with the lack of penile papillae and oostegites, and intersex with the presence of both penile papillae and oostegites (Eustace et al., 2013; Lacey et al., 2018). Total body length was measured from the tip of the rostrum to the end of the telson with straightened posture using digital calipers (Fisher Scientific with a resolution of 0.1 mm ± 0.2 mm; Lacey et al., 2018). The coxa 4 length was measured diagonally across the coxa and used as a proxy for total body length for damaged individuals. Deviations from an expected 1: 1 ratio for sex (female versus male) and maturity (adult versus juvenile) at 6537 m and 6546 m were evaluated using a one-tailed binomial test ($\alpha = 0.05$). The intersex individual was included in the maturity bias analysis but excluded from the sex bias analysis. The number of cohorts or stages based on coxa 4 length was assessed with the *mixdist* package v0.5-5 (Duffy et al., 2016; Macdonald, 2018). The analysis was conducted in R v3.4.2 with the *stats* package (R Core Team, 2007).

A concatenated 16S and COI dataset was constructed to investigate phylogeographic relationships between *B. schellenbergi* hadal populations from the WZFZ and four Pacific Ocean populations, specifically the Kermadec, Tonga, New

Hebrides, and Massau (also known as Mussau) trenches. The comparative sequences are comprised of seven individuals, which represent the only 16S and COI sequences publicly available on GenBank for *B. schellenbergi* (Table B3; Ritchie et al., 2015; Blankenship et al., unpublished data; Chan et al., unpublished data). The phylogeny was rooted *by H. dubia* and *H. gigas* (Table B3; Ritchie et al., 2015), as they are both hadal scavengers and the Hirondelleidae family is sufficiently distant from the Scopelocheiridae family (Ritchie et al., 2015).

Nucleotide sequences were aligned with MAFFT v7 (Katoh et al., 2017). The optimal evolutional model for each 16S and COI alignment was identified by modeltest in the phangorn v2.4.0 package (Schliep, 2011; Schliep et al., 2017) in R v3.4.2. The optimal Akaike Information Criterion and the Bayesian Information Criterion indicated the best-fit models as the Hasegawa, Kishino, and Yano model (HKY) for 16S and the HKY with gamma distribution for COI (Hasegawa et al., 1985). Phylogeographic relationships were constructed via a maximum-likelihood approach using PhyML v3.1 (Guindon et al., 2010) and a Bayesian approach using the Bayesian Evolutionary Analysis by Sampling Trees (BEAST) software package v1.8.4 (Drummond et al., 2012). Maximum-likelihood analyses were conducted with a neighbour-joining starting tree and nearest neighbour interchange branch swapping using the model of sequence evolution and parameters estimated by PhyML. The stability of nodes was assessed from bootstrap support based upon 10,000 iterations. Bayesian analyses were undertaken in two independent runs, which were performed for 40,000,000 generations sampling every 10,000 generations using the respective evolutionary models and an uncorrelated relaxed clock. Outputs were assessed with Tracer v1.7 to ensure convergence (effective sample size > 200; Rambaut et al., 2018) and combined in LogCombiner v1.8.4. The first 4,000,000 states were discarded. The maximum clade credibility tree was generated through TreeAnnotator v1.8.4, viewed in FigTree v1.4.3, and annotated using Inkscape v0.92.2. A Bayesian Poisson Tree Processes (bPTP) model was used to delineate species (Zhang et al., 2013).

3. Results

3.1 Habitat and environmental conditions

The WZFZ was flat-bottomed. The deepest point, at 6625 m, was located approximately 12 km south of Station L9 (6546 m; Figure B1). The surface area of the WZFZ deeper than 6000 m was 2798 km^2 and only 1059 km^2 for areas deeper than 6500 m.

At the WZFZ, the near-bottom temperatures varied from 1.14°C at 4767 m to 1.32°C at 6537 m. At the Zenith Plateau, a manganese nodule field comprising nodules up to ~7 cm in diameter were located within a fine-grained matrix (Figure B3). At 5274 m in the WZFZ, a poorly sorted substrate was encountered comprising irregularly shaped gravel and cobble sized material within a fine-grained matrix (Figure B3). Some of this material could be comprised of manganese nodules. Similarly, at 6084 m, the substrate comprised of fine-grained sediments with lesser amounts of gravels and cobbles up to ~6 cm in diameter of mixed composition (Figure B3). At the Afanasy Nikitin Seamount, the bottom temperature was 1.42°C at 4724 m and the seafloor was composed of predominantly fine-grained sediment with a small number of gravel-sized fragments of unknown composition (Figure B3).

3.2 Amphipod community composition

A total of 3864 amphipods were sampled from the Zenith Plateau and WZFZ, and 203 amphipods were samples from the Afanasy Nikitin Seamount comprising of 13 species from eight families: Alicellidae (4), Uristidae (3), Cylocaridae (1), Eurytheneidae (1), Eusiridae (1), Hirondelleidae (1), Scopelocheiridae (1), and Valettiopsidae (1) (Figure 39; Table B1). Two species have been formally described from material collected by this sampling effort, *Stephonyx sigmacrus* Weston, Peart, & Jamieson, 2020 (Lysianassoidea: Uristidae) and *Civifractura serendipia* Weston, Peart, & Jamieson, 2020 (Allicelloidea: Alicellidae; Weston et al., 2020). Further, four additional species have not been previously described. The 25 16S and 21 COI sequences used to inform species identification were deposited into GenBank (16S: MN251311–MN251335 & COI: MN26162–MN262182; Table B2).

Five species were present at both the WZFZ and Afanasy Nikitin Seamount, specifically *Eurythenes maldoror* d'Udekem d'Acoz & Havermans, 2015, *Alicella gigantea*

Chevreux, 1899, *Paralicella caperesca* Shulenberger & Barnard, 1976, *Paralicella tenuipes* Chevreux, 1908, and *Cyclocaris* sp. While *Abyssorchomene gerulicorbis* (Shulenberger & Barnard, 1976), *Civifractura serendipia*, *B. schellenbergi*, *Valettietta* sp. nov., *S. sigmacrus*, and *Cleonardo* sp. indent. were only present at the Zenith Plateau and WZFZ, and *Hirondellea* sp. nov. and *Abyssorchomene distinctus* (Birstein & Vinogradov, 1960) were only recovered from the Afanasy Nikitin Seamount. At abyssal depths, *P. tenuipes* and *P. caperesca* were numerically dominant, with *P. tenuipes* present at every depth. The relative abundance of *P. tenuipes* decreased from 96.5% at 6162 m to 61.7% at 6537 m, which coincided with the presence of *B. schellenbergi*. *Bathycallisoma schellenbergi* was only present at 6537 and 6546 m and accounted for 32.6% and 55% of the catch, respectively. Cluster analysis between the Zenith Plateau, WZFZ, and Afanasy Nikitin Seamount did not identify any significant groupings (average similarity 57.23%; Table B4).

Six distinct communities were identified in comparing the eight East Indian Ocean sites with 32 Pacific Ocean sites at species-level identification (Figure 40A; Fujji et al., 2013; Lacey et al., 2016). The East Indian Ocean sites were delimited within Cluster 4. The comparative sites were comprised of Clusters 1, 2, 3, 5, and 6. The comparative site clustering was nearly equivalent to those identified by Lacey et al. (2016), with a slight exception to Clusters 3, 5, and 6 due to more accurate identification of *Eurythenes* spp. from the Peru Chile Trench (Eustace et al., 2016). Cluster 1 is comprised of two deep hadal sites from Peru Chile Trench. Cluster 2 contained the three hadal sites from New Hebrides Trench, and the eight sites deeper than 6097 m from Kermadec Trench. Cluster 3 comprised of two abyssal sites and one shallow hadal site (6173 m) from Peru Chile Trench. Cluster 5 included the four bathyal sites, one abyssal site (4192 m), and one shallow hadal (6097 m) from Kermadec Trench. Cluster 6 comprised of the four bathyal and five abyssal stations from New Hebrides Trench, all stations from South Fiji Basin (4100 m), and one abyssal site (5242 m) from Kermadec Trench. The average dissimilarity between Cluster 4 and the comparative clusters was 81.51%, where the lowest dissimilarity was to Cluster 6 (New Hebrides Trench bathyal and abyssal; 71.88 %) and highest dissimilarity was to Cluster 1 (Peru-Chile Trench hadal; 97.52%; Table B4). The dissimilarity was attributed to at least five different species, where *P. tenuipes*

consistently contributed the greatest to the difference in community assemblage (Table B4).

Two distinct communities were resolved when identification was to the genus level (Figure 40B). Cluster A comprised of all the East Indian Ocean sites, the bathyal and abyssal comparison sites, and two hadal sites from the Kermadec and New Hebrides trenches. Cluster B contained 13 of the 14 hadal subduction trench sites. Similarity within Cluster A (60.01%) was attributed to *Paralicella* and *Abyssorchomene* (Table B5). While Cluster B had a lower similarity (55.63%) and was defined by *Hirondellea* and *Bathycallisoma*. Between the two clusters, the dissimilarity level was 80.42% (Table B5). The near-exclusive presence of *Hirondellea* in Cluster B and *Paralicella* and *Abyssorchomene* in Cluster A accounted for 18.92%, 17.92%, and 15.69% of the dissimilarity, respectively (Table B5). *Bathycallisoma* (14.97%) and *Eurythenes* (10.96%) also contributed to the dissimilarity between clusters, as presence and abundance varied at some depths (Table B5).

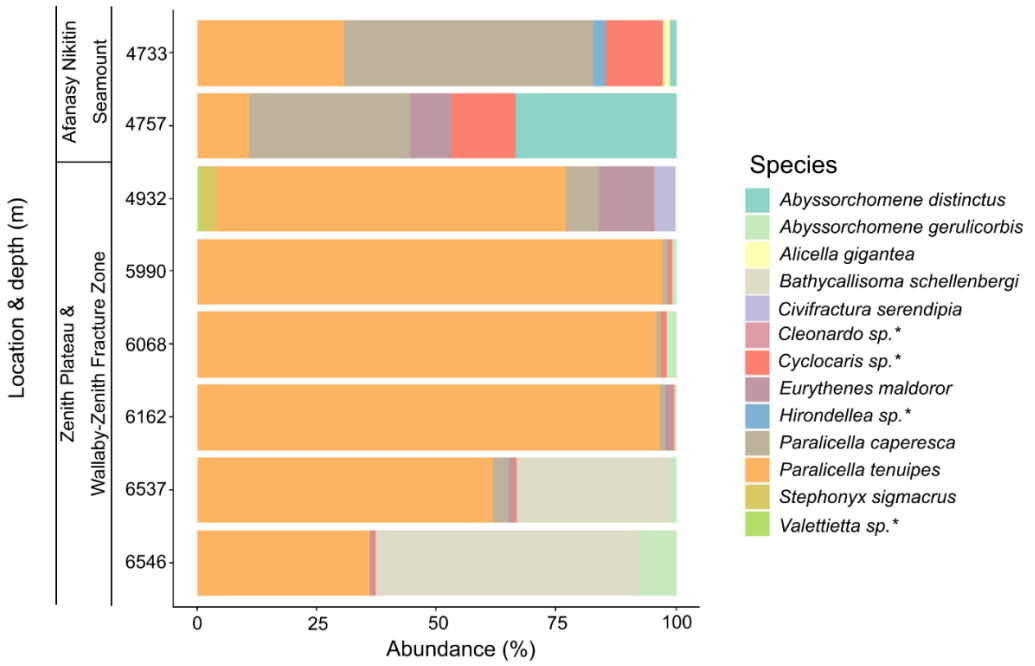

Figure 39. Relative abundance of amphipod species identified by depth from the Zenith Plateau & Wallaby-Zenith Fracture Zone, and the Afanasy Nikitin Seamount. The asterisks indicate potentially undescribed species.

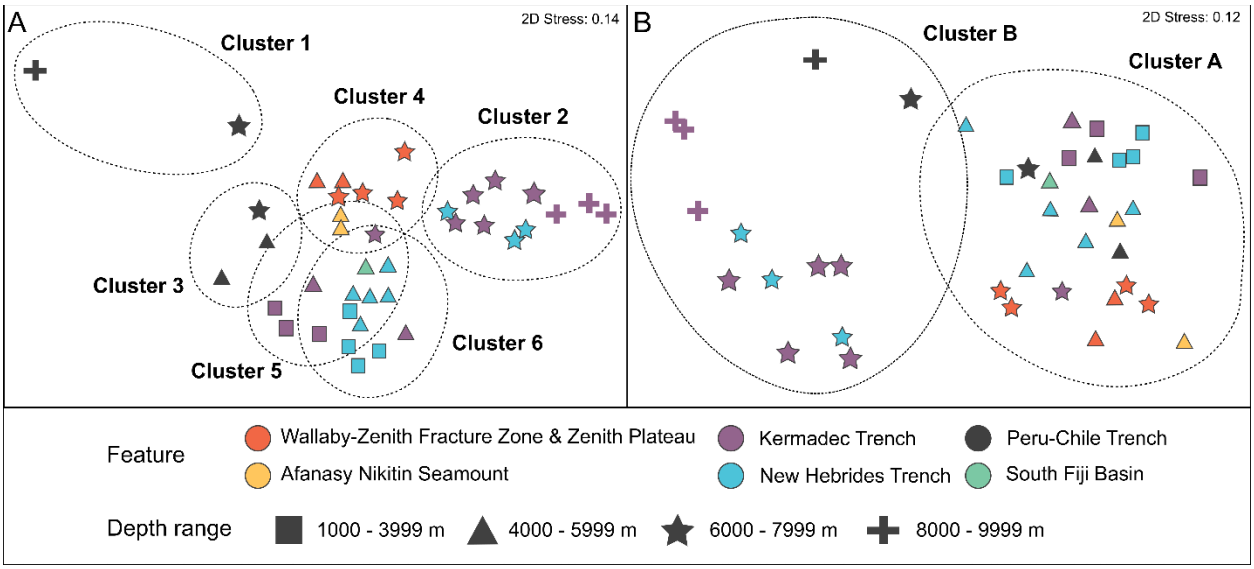

Figure 40. Community structure and amphipod abundance in abyssal and hadal environments using non-metric multidimensional scaling ordination: (A) Species-level identifications, and (B) Genus-level identifications. Colour denotes location, and shapes denote the depth range of sampling sites. Encircling lines denote community grouping identified by SIMPROF.

3.3 Bathycallisoma schellenbergi demographics and phylography

A total of 146 females, 138 males, 367 juveniles, and a single intersex individual were identified (Table B6). None of the females were ovigerous. Females were proportionally more abundant at 6537 m at 33.3% versus 19.7% at 6546 m. A higher percentage of males were at the slightly deeper depth (22.4% at 6546 m as compared to 16.3% at 6537 m). Juveniles consisted of 49.6% of the population at 6537 m and 57.9% at 6546 m. The male: female ratio was biased towards females at 6537 m ($p < 0.01$). At 6456 m, there were significantly more juveniles than mature amphipods ($p < 0.001$). At each depth, there was one juvenile cohort peak, two male cohort peaks, and three female cohort peaks (Figure B4).

Species-delimitation analysis based on a concatenated topology resolved one species of *B. schellenbergi* across the five populations (acceptance rate: 0.1683, merge: 49976, split: 50024, mean number of species: 3.67; Figure 41). Geographic structuring of samples was apparent, with the WZFZ population and the four Pacific Ocean trench populations forming reciprocally monophyletic clades (posterior probability 0.85). Within the Pacific Ocean trench clade, two sub-groups were present: 1) the New Hebrides and Massau trenches (posterior probability 0.96), and 2) the Tonga and Kermadec trenches (posterior probability 1).

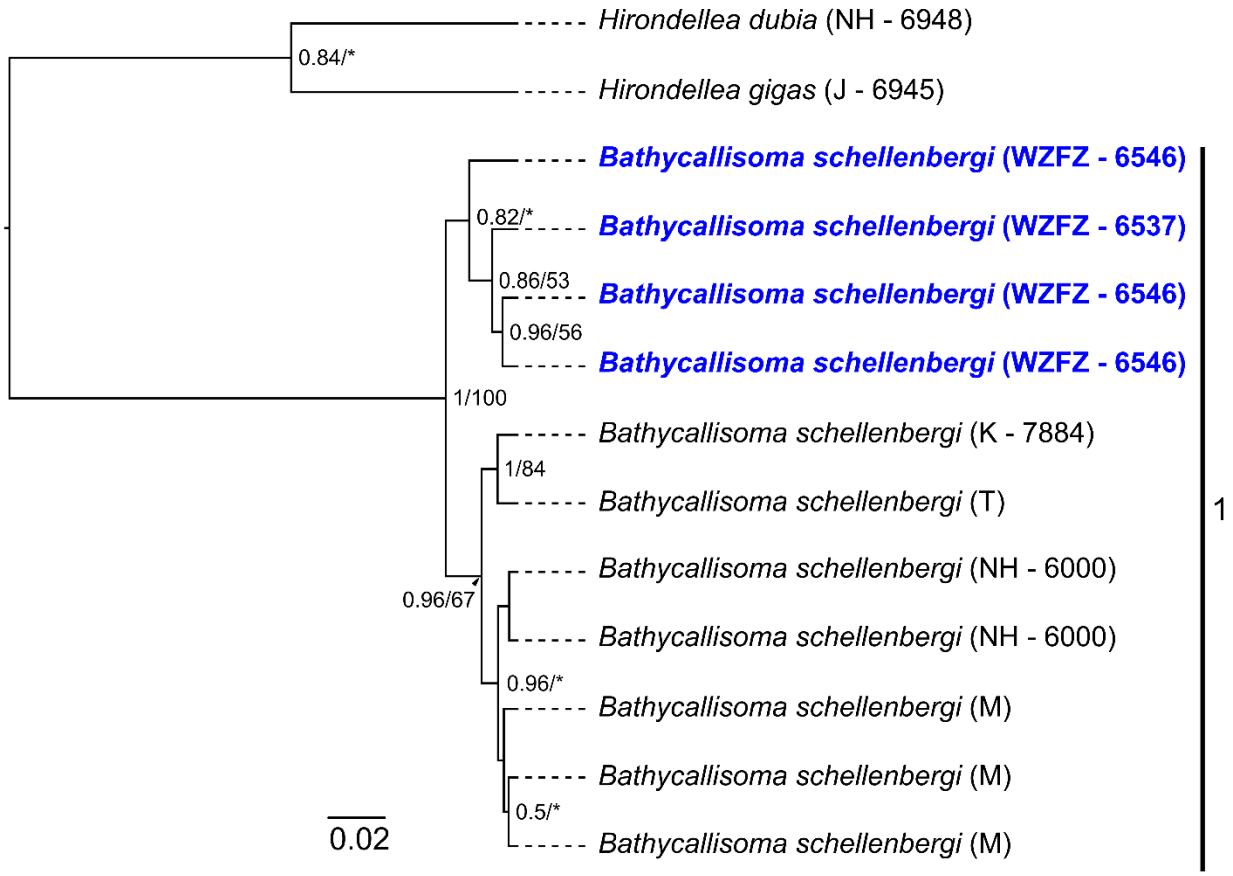

Figure 41. Bayesian tree showing the relationship of *Bathycallisoma schellenbergi* from the Wallaby-Zenith Fracture Zone (bold blue) with four other populations using a combined dataset of 16S rDNA and COI sequences (Table B3). Bayesian posterior probabilities and maximum-likelihood bootstrap supports are shown on branch nodes. Values less than 0.50 or values not supported by the alternative method are not stated or depicted by an asterisk. For the locations, J is Japan Trench, K is Kermadec Trench, M is Massau Trench, NH is New Hebrides Trench, T is Tonga Trench, and WZFZ is Wallaby-Zenith Fracture Zone. The depth (m) of the specimen is included if known.

4. Discussion

The WZFZ was the first non-subduction hadal feature to be studied allowing us to further elucidate the effect of total area, topography, and total depth on scavenging amphipod community structure. This initial description of a hadal fracture zone highlights that while non-subduction features only account for a minor fraction of the global hadal area, sampling them is important to gain a more comprehensive understanding of drivers of community ecology and distribution of species at hadal depths.

4.1 Non-subduction hadal habitat

While the geological and environmental survey of WZFZ showed similarities in temperature and seabed substrate to subduction trenches, there were also distinct habitat differences with respect to total area and depth, and topography. The Zenith Plateau and WZFZ‘s temperature ranges and the seabed substrate, comprised of fine-grained sediment and cobble-sized material, were comparable to subduction trenches (Lacey et al., 2016; Stewart and Jamieson 2018). However, the geomorphology of the WZFZ differed from subduction trenches concerning the total area, topography, and total depth (Jamieson et al., 2009a). When compared with hadal trenches, the WZFZ is small, with only 2.3% and 43.4% of the total area of the Kermadec Trench and New Hebrides Trench, respectively (Stewart & Jamieson, 2018). Multibeam bathymetry mapping confirmed that the WZFZ was a flat-bottomed feature, lacking the characteristic V-shape cross-section of a subduction trench (Figure B1). Mapping further showed the WZFZ to be 1158 m shallower than reported elsewhere (e.g., Smith & Marks, 2014), albeit still hadal. The variation between satellite altimetry and multibeam measurements is not unique to the WZFZ, instead, it is another instance highlighting the lack of fine-resolution topography data for the deep sea (Weatherall et al., 2015; Mayer et al., 2018; Stewart and Jamieson, 2019).

4.2 Scavenging amphipod community

This study at the WZFZ and Afanasy Nikitin Seamount adds to the limited sampling of abyssal and hadal depth amphipods in the Indian Ocean (Birstein & Vinogradov, 1964; Treude et al., 2002; Cousins et al., 2013), expands the known occurrence of some species and uncovers ultra-deep-sea diversity. The two locations showed strong comparability in community assemblages, possibly reflecting the same abyssal

biogeographical province and comparability in abiotic conditions (Walting et al., 2013). The amphipods were from the Alicelloidea and Lysianassoidea superfamilies, which are both well-represented scavengers at these depths (Lacey et al., 2016). The only non-scavenger species identified was a single *Cleonardo* sp. indent. (Eusiroidea: Eusiridae) specimen from 6162 m in the WZFZ. This adds to the limited distribution data for this genus, with *Cleonardo biscayensis* Chevreux, 1908, *Cleonardo maxima* Birstein & M. Vinogradov, 1964, and *Cleonardo longipes* Birstein & M. Vinogradov, 1964 documented at abyssal depths in the northern Indian Ocean (Birstein and Vinogradov, 1964; Hendrycks and Conlan, 2003). From these two superfamilies, cosmopolitan species in the genera *Paralicella*, *Abyssochromene*, *Eurythenes*, and *Cyclocaris* were abundantly present (Duffy et al., 2016, Lacey et al., 2016). This study expanded the distribution of *A. distinctus*, *A. gerliocoribis*, *P. tenupies*, and *P. caperesa* from the Pacific and Atlantic Oceans and into the East Indian Ocean (Duffy et al., 2016; Lacey et al., 2016). Two species were found with their first known occurrence in the Indian Ocean: *E. maldoror* from the Weddell Sea, Argentinian Basin, and North Pacific Ocean (d'Udekem & Havermans, 2015) and *A. gigantea* from the Pacific Ocean (Jamieson et al., 2013). The presence of *E. maldoror* and *A. gigantea* support the hypothesis that dispersal of these large amphipods across wide geographic distances could partially be attributed to deep-water circulation patterns, like the Antarctic Bottom Water, and their strong swimming ability (Havermans, 2016). *Bathycallisoma schellenbergi* was abundantly present at the two deepest WZFZ sampling sites. In addition to common and cosmopolitan species, rare and possibly endemic species, such as *S. sigmacrus* and *C. serendipia* from 4932 m at the WZFZ (Weston et al., 2020) and the two specimens of *Hirondellea* sp. nov. from 4733 m at the Afanasy Nikitin Seamount, were also present. *Valettietta* sp. nov. was found in low numbers at both abyssal and hadal depths in the WZFZ. While outside the scope of this study, *Valettietta* sp. nov. is likely to be a vicarious species with *Valettietta gracilis* Lincoln & Thurston, 1983 and *Valettietta anacantha* (Birstein & Vinogradov, 1963), which are considered to have disjunct distributions in the Atlantic and Pacific Oceans, respectively (Lincoln & Thurston, 1983).

When compared to the South Fiji Basin and the Peru-Chile, Kermadec, and New Hebrides trenches, the amphipod community of the WZFZ and Afanasy Nikitin Seamount

was found to be distinct at species-level identification (Cluster 4, Figure 40A) and part of a bathyal and abyssal community assemblage with genus-level identifications (Group B, Figure 40B). This highlights that community composition analysis can vary based on level identification as different genera have species with either broad or restricted geographic and or bathymetric distributions. Furthermore, the cluster analysis indicated the amphipod community at hadal depths of the WZFZ was an extension of the abyssal community, even with a large population of *B. schellenbergi*. This seemingly abyssal community was driven by the consistent abundance of *P. tenuipes* and the presence of *Cyclocaris* sp. nov. and *P. caperesca*, which are considered abyssal species with the physiological capability to live at shallow hadal depths (Lacey et al., 2016).

We interpret these results to indicate that the WZFZ exhibited a transitional amphipod community composition, with the abyssal community extending to hadal depths and with select hadal species, *B. schellenbergi*, present below 6500 m. This gradual shift across the abyssal-hadal transition zone contrasts the ecotone community shifts observed in the Peru-Chile, Kermadec, and New Hebrides trenches between 6000–7000 m (Jamieson et al., 2011; Lacey et al., 2016). Jamieson et al. (2011) hypothesised that this biological shift between the two zones is not strictly driven by hydrostatic pressure but primarily by the change in seafloor topography from flat abyssal plains to the steep-sloped trench. The differences in topography and seismic activity between the abyssal plain and trenches result in distinct depositional environments and habitats (Ichino et al., 2015). Here in the WZFZ, the gradual change in the community assemblage across the abyssal-hadal transition zone is likely attributed to the similarities in the topography and depositional environments between the Zenith Plateau and the shallow, hadal basin. Further exploration is required to assess whether other similar hadal geomorphic features are also characterised by abyssal fauna with select hadal species.

While the rate of community change across the abyssal-hadal transition zone contrasts between the WZFZ and hadal trenches, competitive exclusion appears to also occur in non-subduction systems. *Bathycallisoma schellenbergi* and *E. maldoror* show evidence for competitive exclusion, which prevents both large amphipod species with similar feeding ecologies to cohabitate at the WZFZ's maximum depths (Ingram & Hessler, 1983; Blankenship & Levin, 2007; Lacey et al., 2016). With *E. maldoror* being

recovered across the entire sampling depth of WZFZ this suggests that *E. maldoror* is physiologically able to withstand the higher hydrostatic pressures (Downing et al., 2018). However, with the low number of *E. maldoror* individuals at the deepest depth (6546 m), *B. schellenbergi* potentially outcompetes it for food. Alternatively, the pressure-adapted enzymes of *B. schellenbergi* (Downing et al., 2018) may be more efficient at increased pressure and/or *E. maldoror* may tolerate hadal pressure but pay a greater physiological cost.

4.3 Bathycallisoma schellenbergi demographics and phylogeography

Bathycallisoma schellenbergi were found at the 6537 m and 6546 m stations and comprised of multiple stages of juveniles and adults, except for ovigerous females as consistent with other studies (Perrone et al., 2002, Blankenship et al., 2006, Eustace et al., 2013, 2016, Lacey et al., 2018). While there were some significant differences between the sex ratios between the two depths, such a small difference in depth (9 m) is unlikely to drive the observed differences. This precludes drawing comparisons to ontogenetic vertical stratification patterns displayed by populations inhabiting hadal subduction trenches (Lacey et al., 2018). Differences in makeup could be explained by a combination of small-scale and non-depth related factors, such as topography, slope, and sediment type.

The WZFZ *B. schellenbergi* population does pose as an initial contrast with the lack of depth distribution of subduction trench populations (Blankenship et al., 2006; Lacey et al., 2018). Curiously, the WZFZ population's bathymetric range appeared to be compressed to less than 200 m from the floor of the fracture zone. It is unclear why *B. schellenbergi* were not present along the slope from the Zenith Plateau, as they have been known to have a shallower bathymetric range (~5600m, Lacey et al., 2016). A possible explanation is that the slope does not provide suitable habitat as individuals were not recovered at intermediate depths. Future studies should consider increasing the number of sampling points on a transect or decreasing the vertical distance between sites to resolve the restricted bathymetric distributions in shallow hadal habitats.

While *B. schellenbergi* has been recovered from several trenches (Kilgallen & Lowry, 2015; Lacey et al., 2018), finding it in the relatively remote and small WZFZ was unexpected, and questions whether it is the same species. Indeed, *B. schellenbergi* has

a complex systematic history, with a recent synonymization of *Bathycallisoma pacific* and *Scopelocheirus schellenbergi* (Kilgallen and Lowry, 2015). However, in this case, individuals did not show morphological differences from the Dahl (1959) description and Kilgallen & Lowry (2015) re-description. DNA sequencing and phylogenetic analysis indicated that the species within the WZFZ is indeed *B. schellenbergi* (Figure 41).

While the mtDNA phylogeny resolved a single species, a degree of phylogeographic structure was observed between the five *B. schellenbergi* populations. There is a clear discontinuity between the WZFZ and the Pacific Ocean populations. A level of genetic differentiation is expected for the same species residing in two ocean basins, irrespective of whether they are demographically isolated or interconnected by unsampled intermediate populations (Ritchie et al., 2017). The low level of divergence between these clades is perhaps more suggestive of some connectivity given the amount of geological separation and hence the time required to accumulate more genetic differences, if not speciate entirely (Hendry et al., 2009). Additionally, there was a suggestion of phylogeographic structuring by distance between the Pacific Ocean trenches, but this is less pronounced than might be expected given the reduced levels of geographic separation to facilitate even occasional gene flow (Ritchie et al., 2017). While these phylogeographic patterns are preliminary and based on a relatively low number of individuals and genes, this finding does merit further investigation. A future genomics study should be aimed at assessing the extent to which hadal features represent demographically and evolutionary independent units, by leveraging high-throughput sequencing methods, such RAD-seq or microsatellites (Ritchie et al., 2017; Taylor et al., 2017). *Bathycallisoma schellenbergi*, *H. dubia*, or *H. gigas* could be model species for this study, as they are found in several disjunct hadal features (Ritchie et al., 2015).

As *B. schellenbergi* are known from the Java Trench (Kilgallen & Lowry, 2015), an obvious question is how they are present in the WZFZ, ~2100 km south of Java Trench. Given this dataset indicates intra-specific levels of divergence among five populations, there are two plausible hypotheses for the presence of a population in the WZFZ. Firstly, the WZFZ may represent a spillover population from the larger Java Trench. This is plausible given that *B. schellenbergi* are strong swimmers and can tolerate shallower depths (~5600 m; Lacey et al., 2016). There are ~1.4 million km2 of discrete features

deeper than 5600 m between the Java Trench and Diamantina Fracture Zone that could provide a complex corridor network for gene flow in the East Indian Ocean (Figure 38A). A second possibility is that *B. schellenbergi* ancestrally had an abyssal-centric cosmopolitan distribution, analogous to *A. gigantea* or *Paralicella* spp., but subsequently became restricted to hadal depths (Jamieson et al., 2013; Corrigan et al., 2014). This is now reflected by allopatric populations in subduction trenches and non-subduction features, including the WZFZ. While determining the mechanism the present-day distribution *of B. schellenbergi* is outside the scope this study, *B. schellenbergi* does present as a model taxon for future work to understand how the geological age and historical position of features, deep-water current patterns, and species' life history shape hadal fauna distributions and connectivity between features.

4.4 Significance for hadal ecology

Finding *B. schellenbergi* at hadal depths in the WZFZ indicates that characteristically hadal fauna, or fauna that are exclusively hadal elsewhere, has the potential to be found in non-subduction features. We now would expect to find *B. schellenbergi* populations at the Diamantina Fracture Zone and within the 5748 km^2 of seafloor deeper than 6500 m in the Wharton Basin (Figure 38A). Moreover, this finding in the East Indian Ocean could suggest there are other large swathes of seafloor hosting quintessentially hadal fauna, such as the North West Pacific Basin (~6500 m), which is located between the Northern Mariana and Izu-Bonin trenches. Likewise, the Philippine Basin, between the Ryukyu and Philippine trenches, reaches hadal depths and may help explain why *H. gigas* are present in each of these trenches (France, 1993). Non-subduction features could also explain the present distribution of other hadal fauna, such as the holothurian *Prototrochus bruuni* (Hansen, 1956) and the sea star *Eremicaster vicinus* Ludwig, 1907, found in many Pacific Ocean trenches (Jamieson, 2015).

By concentrating sampling efforts on subduction trenches, the definition of hadal has been unintentionally restricted. The WZFZ indicates that from a biological perspective the hadal zone is more than the 27 subduction trenches and does encompass any location exceeding 6000 m regardless of geomorphic setting or total area. The community and population dynamics in these habitats are shaped not only by topography and total depth but also by resource limitations and physiological constraints. Thus, to unravel the

ecological patterns of the ocean's deepest zone, sampling efforts and research programmes need to extend past the deepest point of large and often geographically isolated subduction trenches. Future efforts should focus on, or include, adjoining features such as fracture zones, troughs, and basins, as well as more detailed genetics studies to further disentangle the complexities of connectivity and species distribution in the hadal zone.

5. Acknowledgements

We would like to thank Nick Cuomo for assistance with lander deployments, Prof Darren Evans and Dr James Kitson (Newcastle University, UK) for bench space in the Molecular Diagnosis Facility, Ed Hendrycks (Canadian Museum of Nature, Canada) for guidance on the Cleonardo sp. identification, and Dr Shannon Flynn (Newcastle University, UK) for constructive comments on manuscript drafts. We extend thanks to the Captain and crew on the 2017 *RV Sonne* Expedition SO258 Leg 1, especially joint Chief Scientists Dr Reinhard Werner (GEOMAR, Germany) and Prof Hans-Joachim Wagner (University of Tübingen, Germany) and Oleg Lechenko and Julia Marinova (P.P. Shirshov Institute of Oceanology of the Russian Academy of Sciences, Russia) for the acquisition and processing of the bathymetric data. We are appreciative of the Reviewers for their constructive comments and suggestions that improved the manuscript.

Supplementary Materials

Appendix B, pages 227-235

Chapter 6: Global geographic differentiation and cryptic speciation within the hadal dwelling amphipod, *Bathycallisoma schellenbergi*

Bathycallisoma schellenbergi (Birstein & Vinogradov, 1958) shortly after recovery.

1. Introduction

As the last marine frontier, the hadal zone is comprised of 47 subduction trenches, troughs, and transform faults that create pockets of habitats in the Pacific, Indian, Atlantic, and Southern oceans (Stewart & Jamieson, 2018). These features differ from the gradual continuum of the bathyal and abyssal zones, as hadal features are geographically isolated, largely formed, and situated at tectonic convergence boundaries (Stern, 2002; Jamieson, 2015). As such, the geologic age of the feature and history of tectonic plate movement influence the degree of isolation from other hadal features (Belyaev, 1989). Most hadal features are situated thousands of kilometers from the nearest hadal feature (Stewart & Jamieson, 2018). Each feature is distinct in its environmental conditions and geomorphic attributions, shaped by a unique suite of extrinsic factors (Jamieson et al., 2010). Feature location and proximity to land can influence sediment, nutrient, and primary productivity fluxes (Wenzhöfer et al., 2016; Glud et al., 2021). The biogeographic province and overlying surface primary productivity (oligotrophic to eutrophic) shapes the amount of POM reaching the hadal zone (Ichino et al., 2015). Further, the global and local hydrography patterns control the oxygen supply, temperature, and salinity of the feature (Kawabe & Fujio, 2010). Thus, the traditional view is that hadal features represent evolutionarily and demographically independent units (Wolff, 1960; Belyaev, 1989), resulting from long-term geographical isolation and evolutionary selection pressures.

This conventional view that hadal features are hotspots of endemism with taxa restricted to a single or geographically connected set of features has been derived from several key taxa, such as the Holothuroidea, Annelida, Isopoda, and Amphipoda (Belyaev, 1989). Within Amphipoda, nearly 68% of the known species have only been documented to be present at one hadal feature (Appendix C). A further 28% of the species have been sampled from two-four hadal features (Appendix C). Thus, the assumption that hadal species have restricted distributions is largely supported by historical sampling efforts.

However, this perception that hadal features are endemic hotspots is being increasingly tested. The known geographic range of *Alicella gigantea* Chevreux, 1899 is as expansive as its body size — ranging from the abyssal plains in the North Atlantic Ocean (De Broyer & Thurston, 1987) to hadal depths of the Wallaby-Zenith Fracture Zone

in the East Indian Ocean (Weston et al., 2021), and then extending into the Kermadec and New Hebrides trenches in the western South Pacific Ocean (Jamieson et al., 2013; Lacey et al., 2016). Two other examples are the characteristically hadal species *Hirondellea gigas* (Birstein & Vinogradov, 1955) and *Hirondellea dubia* Dahl, 1959. *Hirondellea gigas* inhabits the western Pacific Trenches, including the Philippines, Mariana, Japan, Izu-Bonin, and Kuril-Kamchatka trenches (France, 1993; Ritchie et al., 2015; Lacey et al., 2016; Ritchie et al., 2017; Jazdzewska & Mamos, 2019). Whereas *H. dubia* is found in the western South Pacific trenches, specifically Kermadec, Tonga, and New Hebrides trenches (Lacey et al., 2016; Wilson et al., 2018). Although, *H. dubia* has been recovered from abyssal depths of the Mariana Trench (Ritchie et al., 2015), suggesting its geographic and bathymetric distribution range is likely more expansive than currently understood. This knowledge gap for *H. dubia* and other hadal species may be largely attributed to lack of sampling and/or inherent sampling gear biases, such as benthic trawling and baited traps.

Beyond trench-specific endemism, species limited to trench clusters within regional proximity, and species capable of excursions to adjoining abyssal depths, there are few examples of multiple regional and pan oceanic species that are quintessentially hadal. One amphipod that challenges the concept of trench and regional hadal endemism is *Bathycallisoma schellenbergi* (Birstein & Vinogradov, 1958). This cosmopolitan scavenger is distributed across a lower abyssal to hadal depth range (5600–9104 m) in hadal subduction and non-subduction features in four oceans (Kilgallen & Lowry, 2015). This vast hadal distribution includes the Java Trench and Wallaby-Zenith Zone in the Indian Ocean, Puerto Rico Trench in the Atlantic Ocean, Orkney Trench in the Southern Ocean, and Tonga, Kermadec, Massau, New Hebrides, Japan, and Kuril-Kamchatka trenches in the Pacific Ocean (Figure 42; Birstein & Vinogradov, 1958; Dahl 1959; Birstein & Vinogradov, 1964; Blankenship & Levin, 2007; Kilgallen & Lowry, 2015; Ritchie et al., 2015; Lacey et al., 2016; Jazdzewska & Mamos, 2019; Weston et al., 2021). Curiously, *B. schellenbergi* has been considered absent from the Peru-Chile (Atacama) Trench (Fujii et al., 2013). Many of these presence observations were made during the foundational *Vityaz* and *Galathea* expeditions, thus limited historical samples are available for current studies. However, DNA barcoding and phylogenetic study are uncovering cryptic

speciation in the ultra-deep ocean, especially prevalent within Amphipoda (Havermans et al., 2013; Ritchie et al., 2015; Weston et al., 2020). *Bathycallisoma schellenbergi* does have a complicated systematic history with a recent revision that synonymized two other species, *Bathycallisoma pacifica* Dahl, 1959 and *Scopelocheirus schellenbergi* Birstein & Vinogradov, 1958 (Kilgallen &, Lowry 2015). Preliminary mtDNA analysis did suggest that the Wallaby-Zenith Fracture Zone, Tonga, Kermadec, and New Hebrides trench populations are indeed the same species (Weston et al., 2021). Phylogeographic structuring was evident, with a split between ocean basins and Pacific Ocean populations separated by geographical distance. While this study was limited and based on a relatively low number of individuals, the findings did indicate *B. schellenbergi* to be a model species for assessing the extent to which hadal features represent demographically and evolutionary independent units.

Investigating the global distribution of a hadal species requires an equally extensive specimen collection. Hadal science has been limited by the number of sampling campaigns, especially to Pacific Ocean features outside the Pacific Ocean. These challenges were overcome with the Five Deeps Expedition in 2018-2019 (Jamieson, 2020). During the circumglobal expedition, baited landers were deployed to the Puerto Rico, South Sandwich, Java, Mariana, Tonga, Santa Cruz, and San Cristobal trenches and the Diamantina Fracture Zone. Remarkably, *B. schellenbergi* was recovered from each hadal feature sampled. These newly collected specimens combined with those recovered during five previous sampling campaigns since 2011 amounts to an unparalleled dataset to test hadal speciation and investigate how geochronology of the hadal feature formation has shaped speciation.

The study leverages this specimen collection to assess for cryptic speciation and explore phylogeographic patterns. This study hypothesises that (1) there is a single species of *B. schellenbergi*, and (2) each hadal feature sampled hosts a genetically differentiated population separated by isolation-by-distance and oceanic basins. To test this, sequence variation at partial regions of the mitochondrial 16S ribosomal DNA (16S) and cytochrome oxidase I (COI) is assessed between specimens from 12 hadal features across the Pacific, Atlantic, Indian, and Southern oceans.

2. Methods and Materials

2.1 Specimen collection and morphological identification

Bathycallisoma schellenbergi specimens were collected throughout 13 sampling campaigns to 12 hadal features between 2011–2019 (Figure 42; Table 7): Atacama Trench (2018; SO261), Java Trench (2019; FDE-JAV), Diamantina Fracture Zone (2019; FDE-DIA); Kermadec Trench (2011 & 2012; Cruise KAH1109 & KAH1202), Mariana Trench (2019; FDE-MAR), New Hebrides Trench (2013; KAH1310) Puerto Rico Trench (2018; FDE-PRT); San Cristobal and Santa Cruz trenches (2019; FDE-SOL), South Sandwich Trench (2019; FDE-SST), Tonga Trench (2019; FDE-TON); Wallaby-Zenith Fracture Zone (2017; SO258). Specimens were recovered using baited free-fall landers (Jamieson et al., 2009). The lander vehicle design specifications did vary between sampling campaigns. Each lander vehicle was consistently equipped with a bespoke invertebrate funnel trap that was baited with whole mackerel (Scombridae; Jamieson et al., 2011). Landers remained on the seafloor for 7–12 hours.

Upon recovery of lander vehicles, specimens were preserved using 70% ethanol upon initial sorting on deck. In the laboratory, specimens were morphologically identified following Kilgallen & Lowry (2015) using a stereomicroscope (Wild Heerbrugg M8). Dissected appendages, particularly gnathopod 1 & 2, were dissected, temporarily mounted with glycerol, and imaged with a Leica DMi8 inverted microscope and DFC295 camera.

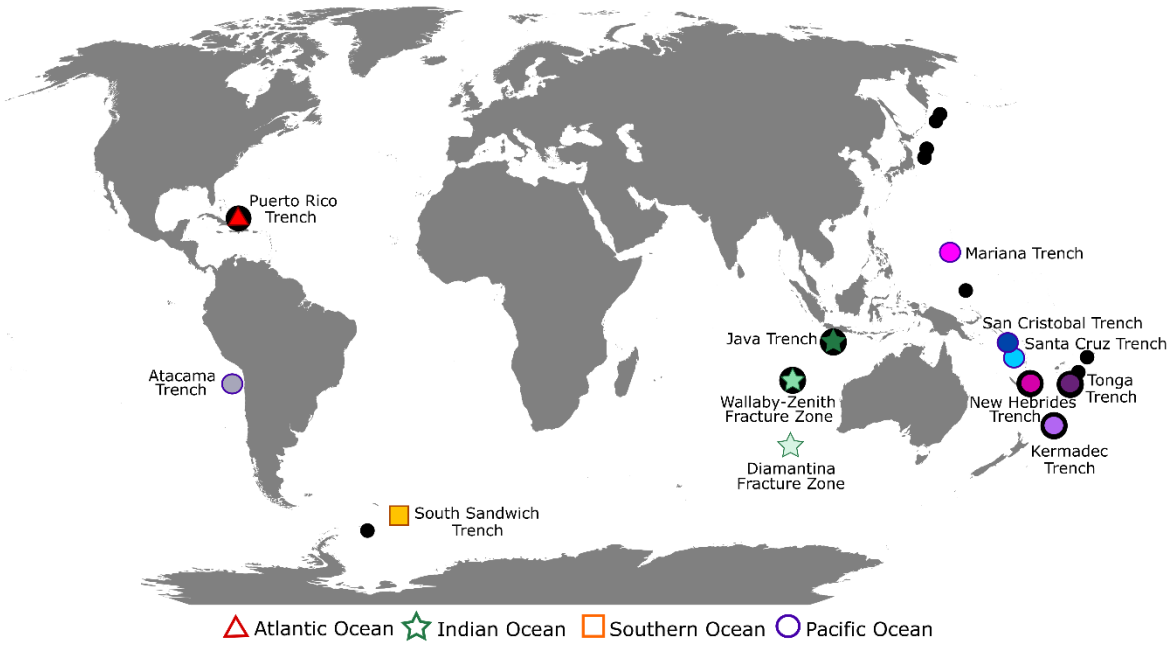

Figure 42. Distribution of *Bathycallisoma schellenbergi* and sampling locations. Black circles represent published records (adapted from Kilgallen & Lowry, 2015; Weston et al., 2021). Coloured shapes represent the 12 study locations, where the colour represents the hadal feature (labeled) and the shape denotes the ocean basin.

Table 7. Collection information for *Bathycallisoma schellenbergi* collected from 13 sampling campaigns to 12 hadal features between 2011-2019.

Location	Depth (m)	Latitude	Longitude	Date	Year	Expedition
Atacama Trench	5920	-20.3435	-71.1213	27-Mar	2018	SO261
	6025	-20.3435	-71.1304	27-Mar	2018	SO261
	6714	-21.7416	-71.2578	24-Mar	2018	SO261
Diamantina Fracture Zone	7009	-33.6311	101.3555	14-Mar	2019	FDE-DIA
Java Trench	6957	-11.1200	114.9283	7-Apr	2019	FDE-JAV
	7176	-11.1283	114.9418	5-Apr	2019	FDE-JAV
Kermadec Trench	6709	-32.3783	-177.0937	22-Feb	2012	KAH1202
	6878	-32.3778	-177.1923	23-Feb	2012	KAH1202
	7291	-32.5871	-177.2957	1-Dec	2011	KAH1109
Mariana Trench	7094	11.0783	142.0300	29-Apr	2019	FDE-MAR
	7507	11.0266	141.9566	29-Apr	2019	FDE-MAR
New Hebrides Trench	6000	-20.8218	168.5832	19-Nov	2013	KAH1310
	6228	-20.6485	168.6138	21-Nov	2013	KAH1310
	6948	-20.7945	168.5462	24-Nov	2013	KAH1310
Puerto Rico Trench	6954	19.3907	-67.8102	18-Dec	2018	FDE-PRT
	7505	19.4933	-67.8267	18-Dec	2018	FDE-PRT
	8370	19.7167	-67.3083	19-Dec	2018	FDE-PRT
San Cristobal Trench	7220	-11.2478	162.9858	19-May	2019	FDE-SOL
	8407	-11.3167	163.0048	19-May	2019	FDE-SOL
Santa Cruz Trench	6844	-10.9267	164.7113	20-May	2019	FDE-SOL
	7431	-11.3167	163.0048	19-May	2019	FDE-SOL
	8428	-11.7032	165.6187	22-May	2019	FDE-SOL
South Sandwich Trench	6640	-60.5050	-25.5333	3-Feb	2019	FDE-SST
	7400	-60.4783	-25.5383	3-Feb	2019	FDE-SST
	8100	-57.5350	-23.9717	5-Feb	2019	FDE-SST
	8266	-55.2298	-26.1731	10-Feb	2019	FDE-SST
Tonga Trench	6793	-23.1810	-174.3415	6-Jun	2019	FDE-TON
	7273	-23.0183	-174.3433	30-May	2019	FDE-TON
	7928	-23.1202	-174.4235	6-Jun	2019	FDE-TON
Wallaby-Zenith Fracture Zone	6537	-22.2655	102.4413	10-Jun	2017	SO258
	6546	-22.2481	102.4236	11-Jun	2017	SO258

2.2 mtDNA Barcoding (Extraction, PCR Amplification, and Sequencing)

A total of the 210 specimens from each of the 12 features were selected for the mtDNA barcoding (Table 8). Each feature population was sub-sampled to cover the minimum and maximum bathymetric range recovered by the baited landers. For features with fewer than 10 *B. schellenbergi* specimens recovered (i.e., Mariana Trench), fewer specimens were selected for mtDNA barcoding as to maintain the availability of physical material for future use.

Total genomic DNA was extracted following a magnetic bead-based protocol developed for mammalian tissue using GITC lysis (Protocol 6.3; Oberacker et al., 2019). A solution of TNES buffer, Proteinase K (Fisher Scientific), and RNAse A (New England Biolabs, NEB) were added to 1.2 ml reaction tubes. The head of each amphipod was dissected and a piece of tissue no greater than 2 mm^3 was added to each tube. The tubes were centrifuged to 1000 rpm to ensure tissue was submerged and incubated overnight at 50^oC. Total liquid contents were transferred into 1.2 ml 96-well deep-well plates and pipette mixed with 1.5x GITC lysis buffer. Isopropanol was added to each well and the plate was shaken on a microplate mixer at 1200 rpm (STARLAB). Sera-Mag™ SpeedBeads Carboxylate Modified Magnetic Particles (SpeedBeads) were diluted to 1:50 with low TE and then added to the cell lysate. The plate was placed on 3D-printed magnetic rack (Protocol A1; Oberacker et al., 2019), and the supernatant was discarded after the beads settled. Genomic DNA was beads cleaned by one round of isopropanol and two rounds of freshly made 80% ethanol. After the final discard of the supernatant, the SpeedBeads were air-dried for approximately 10 minutes. The SpeedBeads were eluted with 45 µl of low TE (pH 7) and the supernatant was transferred into individual tubes.

Extracted DNA quantity and integrity were measured with a 4200 TapeStation (Agilent). Of the extracted 210 specimens, only 128 specimens met the DNA quantity and integrity conditions (Table 8). Samples with concentrations <35 ng/µl and/or DIN <4.0 were excluded from downstream laboratory analysis, except for Diamantina Fracture Zone. While all specimens from Diamantina Fracture Zone failed to meet the DNA quality and integrity mark, amplification and sequencing of both regions were attempted.

The 128 specimens that met the DNA quantity and integrity conditions and those from Diamantina Fracture Zone were assessed at two partial mtDNA barcoding regions, 16S (260 bp) and COI (624 bp). The primer sets used for amplification were AMPH1 (France & Kocher, 1996) and ‘Drosophila-type’ 16SBr (Palumbi et al., 2002) for 16S and LCO1490 and HCO12198 (Folmer et al., 1994) for COI. PCR protocols were followed as described in Ritchie et al. (2015). Sequences were cleaned enzymatically using Exonuclease 1 and Antarctic Phosphatase (New England Biolabs), and they were sequenced with an ABI 3730XL sequencer (Eurofins Genomics, Germany).

Electropherograms were viewed and trimmed by eye in MEGA 7 (Kumar et al., 2016). Nucleotide sequence quality and absence of contamination were verified on NCBI BLASTn. Each COI sequence was translated into their amino acid sequence to assess for stop codon presence.

Table 8. The number of *Bathycallisoma schellenbergi* that were extracted for total genomic DNA, sequenced at the partial 16S and COI regions, and used to generate a concatenated 16S + COI dataset.

Location	Depth (m)	Extracted	16S	COI	16S+COI
Atacama Trench	5920	4	2	2	2
	6025	12	5	4	4
	6738	7	5	3	3
Diamantina Fracture Zone	7009	16	7	0	0
Java Trench	6957	2	2	2	2
	7176	14	14	13	13
Kermadec Trench	6709	9	4	4	4
	6878	5	2	2	2
	7291	4	4	3	3
Mariana Trench	7094	3	3	3	3
	7507	2	2	2	2
New Hebrides Trench	6000	5	3	3	3
	6228	8	3	4	3
	6948	10	2	2	2
Puerto Rico Trench	6954	12	2	1	1
	7505	4	3	3	3
	8370	6	4	3	2
San Cristobal Trench	7200	8	7	3	3
	8407	8	8	4	4
Santa Cruz Trench	6844	4	3	2	2
	7231	9	9	5	5
	8428	2	1	1	1
South Sandwich Trench	6640	4	2	2	2
	7400	11	7	6	6
	8100	2	2	2	2
	8266	3	1	1	1
Tonga Trench	6793	5	5	2	2
	7273	7	7	2	2
	7928	5	5	3	3
Wallaby-Zenith Fracture Zone	6537	9	4	4	4
	6546	10	5	5	5
TOTAL		210	133	96	94

2.3 mtDNA Phylogenetic Analyses

The phylogenetic relationship between the hadal feature *B. schellenbergi* populations was investigated using a concatenated 16S (124 bp) + COI (425 bp) dataset. Three species were selected as outgroups, with sequences retrieved from GenBank. *Hirondellea dubia* (16S: KP456071, COI: KP713902) and *H. gigas* (16S: KP456078, COI: KP713912) were selected as hadal fauna placed in a separate family (Hirondellidae), and *Paracallisoma* sp. (16: KX034319, COI: KX365241) was selected as the only available comparative sequences from a genus is in the same family, Scopelocheiridae (Ritchie et al., 2015; Ritchie et al., 2017). Nucleotide sequences were aligned with MAFFT v7 (Katoh et al., 2017). The optimal evolutional model for each 16S and COI alignment was identified in MEGA v7 (Kumar et al., 2016) as the Hasegawa, Kishino, and Yano model (HKY) with gamma distribution for 16S and COI (Hasegawa et al., 1985). Phylogeographic relationships were constructed using the Bayesian Evolutionary Analysis by Sampling Trees (BEAST) software package v1.10.4 (Suchard et al., 2018). Two independent runs were performed for 40,000,000 generations sampling every 10,000 generations using an uncorrelated relaxed clock. Outputs were assessed with Tracer v1.7 to ensure convergence (effective sample size > 200; Rambaut et al., 2018) and combined in LogCombiner v1.8.4. The first 4,000,000 states were discarded, and the maximum clade credibility tree was generated in TreeAnnotator v1.8.4 (Drummond et al., 2012). The final tree was viewed in FigTree v1.4.3 and annotated using Inkscape v0.92.2.

Two approaches were used to assess for patterns of cryptic speciation and delimit putative species. The Bayesian Poisson Tree Process (bPTP) model was used to infer species boundaries through the PTP webserver (Zhang et al., 2013; http://species.h-its.org/ptp/). The BEAST-derived concatenated topology was used as the input tree. The bPTP analysis was conducted for 200,000 generations of MCMC sampling, with a thinning value of 100 and burn-in of 25%. Genetic divergences were compared within and between hadal feature populations by quantifying the sequence divergence using the Kimura 2-parameter (K2P) distance model (Kimura, 1980) for both the 16S sequence data (206 bp and included Diamantina Fracture Zone) and the COI sequences data (425 bp). The pairwise K2P inter-feature and intra-feature distance were calculated in MEGA v7 (Kumar et al., 2016). The K2P distance model has been used to detect cryptic

speciation between other lysianassoid genera, including *Orchomene* (Havermans et al., 2011)*, Eurythenes* (Havermans et al., 2013), and *Eurythenes plasticus* (Weston et al., 2020).

A 16S + COI concatenated alignment (700 bp) was used to construct a haplotype network to assess and visualize genetic variability between the hadal feature populations. The haplotype network was inferred using the statistical parsimony method (TCS method; Templeton et al., 1992) in PopART v1.7 (Leigh & Bryant, 2015).

3 Results

3.1 Phylogeny and species delimitation

From the 210 specimens selected for DNA barcoding, 133 individuals were successfully sequenced for 16S (210 bp) and 96 were sequenced for COI (559 bp; Table 8). All 12 sampled hadal features are represented by 16S. While for COI, only 11 of the hadal features are represented, as none of the 16 individuals from the Diamantina Fracture Zone were successfully amplified for COI. The initial NCBI BLASTn identification did match each sequence to publicly available *B. schellenbergi* data. For 16S, the percent identity ranged from 99.2–100% to *B. schellenbergi*, and the percent identity with COI sequences ranged from 95.6-100%.

A phylogeny across 11 of the 12 sampled hadal features was constructed based on 97 individuals (e.g., excluded Diamantina Fracture Zone; Figure 43). The final alignment consisted of 124 sites for 16S and 425 sites for COI, with, respectively, 34 and 107 sites being parsimony-informative sites. The three outgroups did partition the topology, with *H. gigas* and *H. dubia* being sister taxa. *Paracallisoma* sp. was more closely placed with the two *Hirondellea* spp., which is less expected as *Paracallisoma* sp. and *B. schellenbergi* are part of the Scopelocheiridae family. Between the sampled specimens, the topology showed six well-supported clades. Clade 1 was the most basal with specimens from the Atacama Trench (BPP: 1). Clade 2 was comprised of specimens from the South Sandwich Trench (BPP: 0.73). Within Clade 2, there are two supported sub-groups (BPP: 0.95) of amphipods recovered from 6000-7400 m and those from >8000 m. Clades 3–6 shared a well-supported node (BPP: 0.86) were separated into 2 clusters (e.g., Clades 3 & 4 and Clades 5 & 6). Clade 3 were amphipods from Puerto Rico Trench (BPP: 0.99). Clade 4 included individuals from both Java Trench and the Wallaby-Zenith Fracture Zone. While there was some separation within Clade 4 between the two features, two individuals from the Wallaby-Zenith Fracture Zone were place in between those from Java Trench. Clade 5 consisted of specimens from the Kermadec and Tonga trenches, one amphipod from the New Hebrides Trench, and another amphipod from the Santa Cruz Trench (BPP: 0.95). Clade 6 included amphipods from the Mariana and San Cristobal trenches and the 14 other individuals from the Santa Cruz and New Hebrides

trenches. There was a lack of an apparent pattern of sub-clustering by feature within Clade 6.

To evaluate for the indication of cryptic species, two analytical approaches were applied to infer species delineation. The first was the bPTP based on the 16S + COI topology. The bPTP modeled estimated the number of species to be between 6 and 17, with a mean of 8.35 (acceptance rate: 0.381, merge: 99947, split: 100053; Figure 43). The outgroups were each delimitated as a distinct species. Within the study amphipods, Clade 1 and Clade 2 were estimated to be distinct lineages, with 0.55 and 0.67 support. Clades 3–6 were found to be a separate lineage together, albeit with low support of 0.40.

The second delineation approach was the K2P distance analysis, which was conducted for the 16S and COI datasets individually, to allow for the Diamantina Fracture Zone amphipods to be included in the 16S dataset (Figure 44). The level of 16S intra-feature divergence was consistent and low within each feature population (ranged from 0-1.5%), except for the Atacama Trench that ranged from 0-4.2%. The level of the 16S sequence divergence was low between the eleven hadal feature populations, with inter-feature distance ranged between 0–4% and lacked a barcoding gap (Figure 44A). A slightly different pattern was present within the COI dataset (Figure 44B). The level of intra-feature COI sequence divergences ranged from 0-2.4%, with the Wallaby-Zenith Fracture Zone having the highest intra-feature divergence. A high level of sequence divergence was present between the Atacama Trench population (Clade 1) and other feature populations and Clades, where the inter-feature distances ranged from 3.6-6.9%. Furthermore, there was a clear barcoding gap between the highest intra-feature (0.5%) and lowest inter-feature (3.6%) divergences. This divergence exceeded the ‘4x’ criterion (Birky et al., 2005), which assumes that a cluster represents independent species-level lineages when all the pairwise inter-clade divergences exceed four times the maximum intra-clade divergence (Havermans et al., 2013). The Atacama Trench at COI was the only instance the ‘4x’ criterion was exceeded. The sequence divergence between the other 10 populations was lower, ranging from 0–5.9%.

3.2 Haplotype network

Without outgroup species, the haplotype network was constructed using a longer dataset than for the tree, with 206 sites for 16S and 559 sites for COI. Overall, the

haplotype network showed a similar pattern of grouping to the phylogeny (Figure 45). The Atacama Trench population was the most distant from the network, with 20 mutational steps between South Sandwich Trench population. The South Sandwich Trench was the second most divergent with eight mutational steps from the Java Trench population. The two Indian Ocean populations were closely linked within the network, even sharing a featured haplotype. The Puerto Rico Trench population was situated as a close intermediary between the Indian Ocean populations and the west Pacific Ocean populations, separated by only three and four mutational steps, respectively. The placement of the west Pacific Ocean feature populations was less distinct by feature. The Mariana Trench population was more closely situated to the San Cristobal Trench population. The New Hebrides Trench population was placed surrounding the San Cristobal and Santa Cruz trench populations, with one individual highly distinct from the rest of the individuals. The Tonga and Kermadec trench populations linked together and five mutational steps from the Santa Cruz Trench population.

The haplotype diversity was high within most of the features, where each feature contained a least three haplotypes that were separated by at least one mutational step. There was no dominant haplotype by feature, and few haplotypes were shared between individuals. The highest level of haplotype sharing was among eight individuals, with seven from the Java Trench and one from the Wallaby-Zenith Fracture Zone. The Puerto Rico Trench had comparatively the lowest diversity with three haplotypes between six individuals. The San Cristobal and Santa Cruz trench populations had the highest number of shared haplotypes between features, with three different haplotypes shared among individuals. The Tonga and Kermadec trench populations also shared one haplotype.

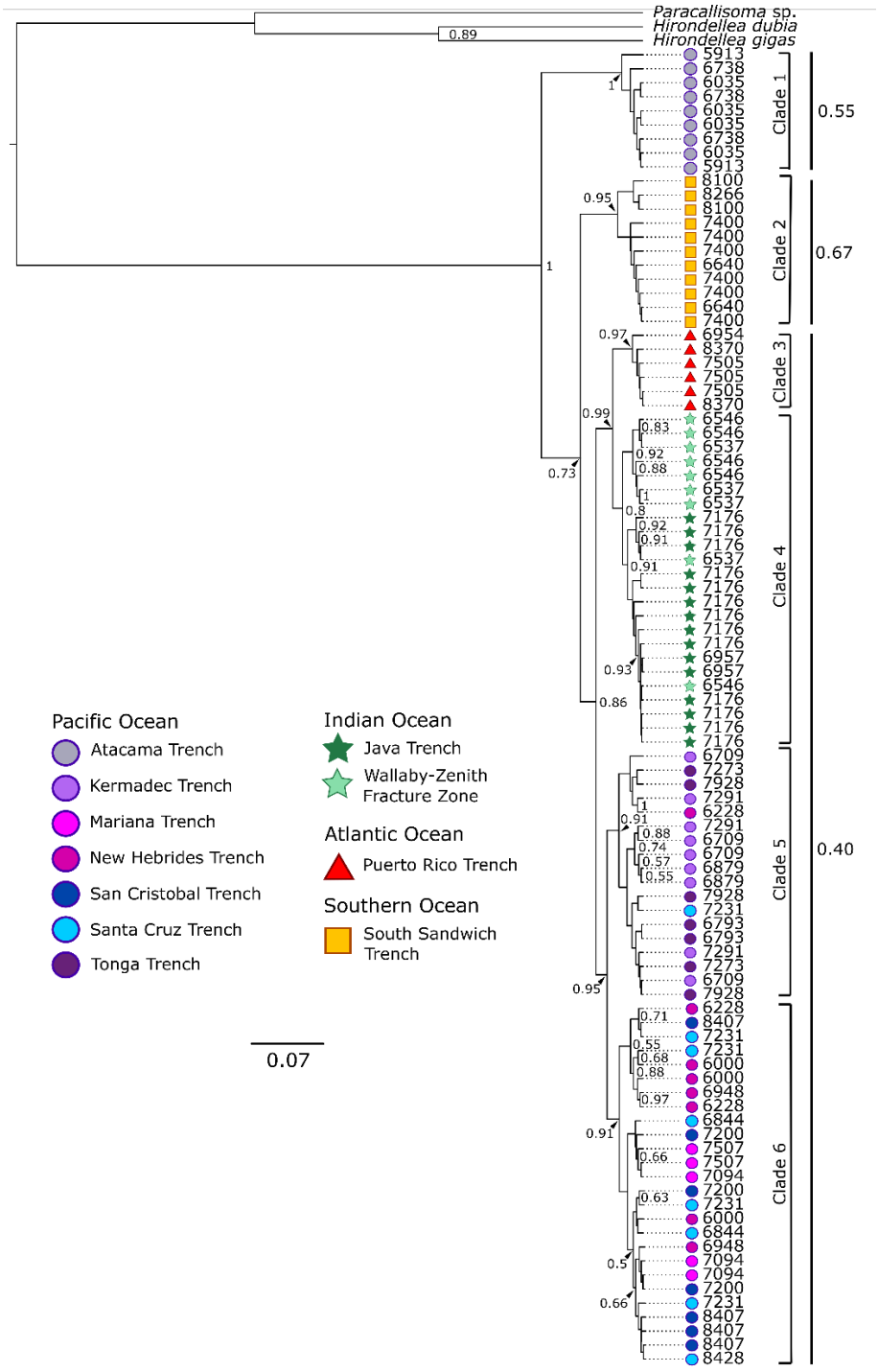

Figure 43. Bayesian phylogeny showing the relationship of *Bathycallisoma schellenbergi* recovered from 11 hadal features based on a concatenated 16S rRNA (124 bp) and COI (425 bp) dataset. Branch nodes show Bayesian posterior probabilities greater than 0.50. The six distinct clades are indicated. Species delimitation inference by the bPTP model analysis is shown on the right side of the phylogeny.

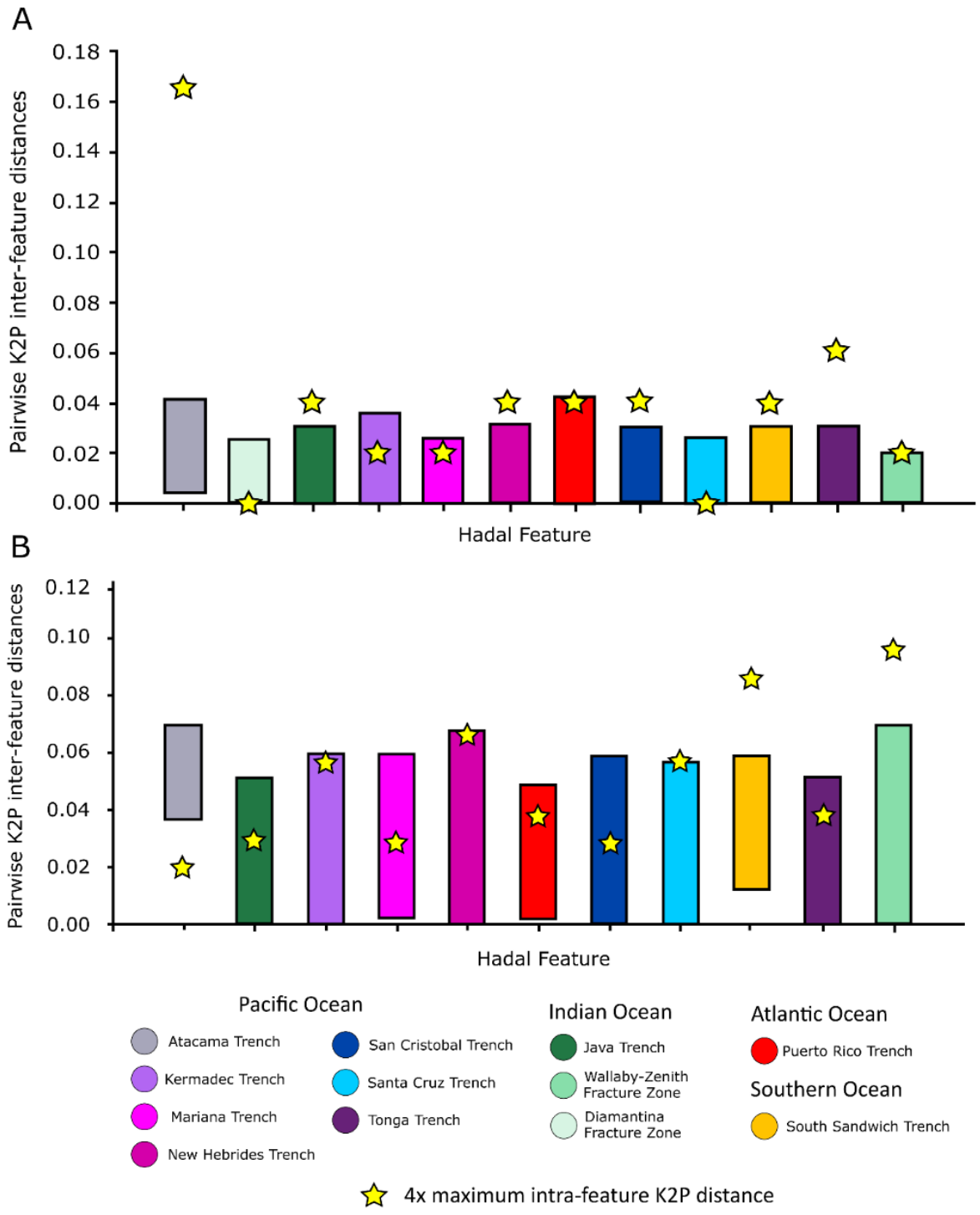

Figure 44. Pairwise K2P inter-feature distances for (A) 16S rRNA and (B) COI by hadal feature. The star represents 4x the maximum pairwise K2P intra-feature distance.

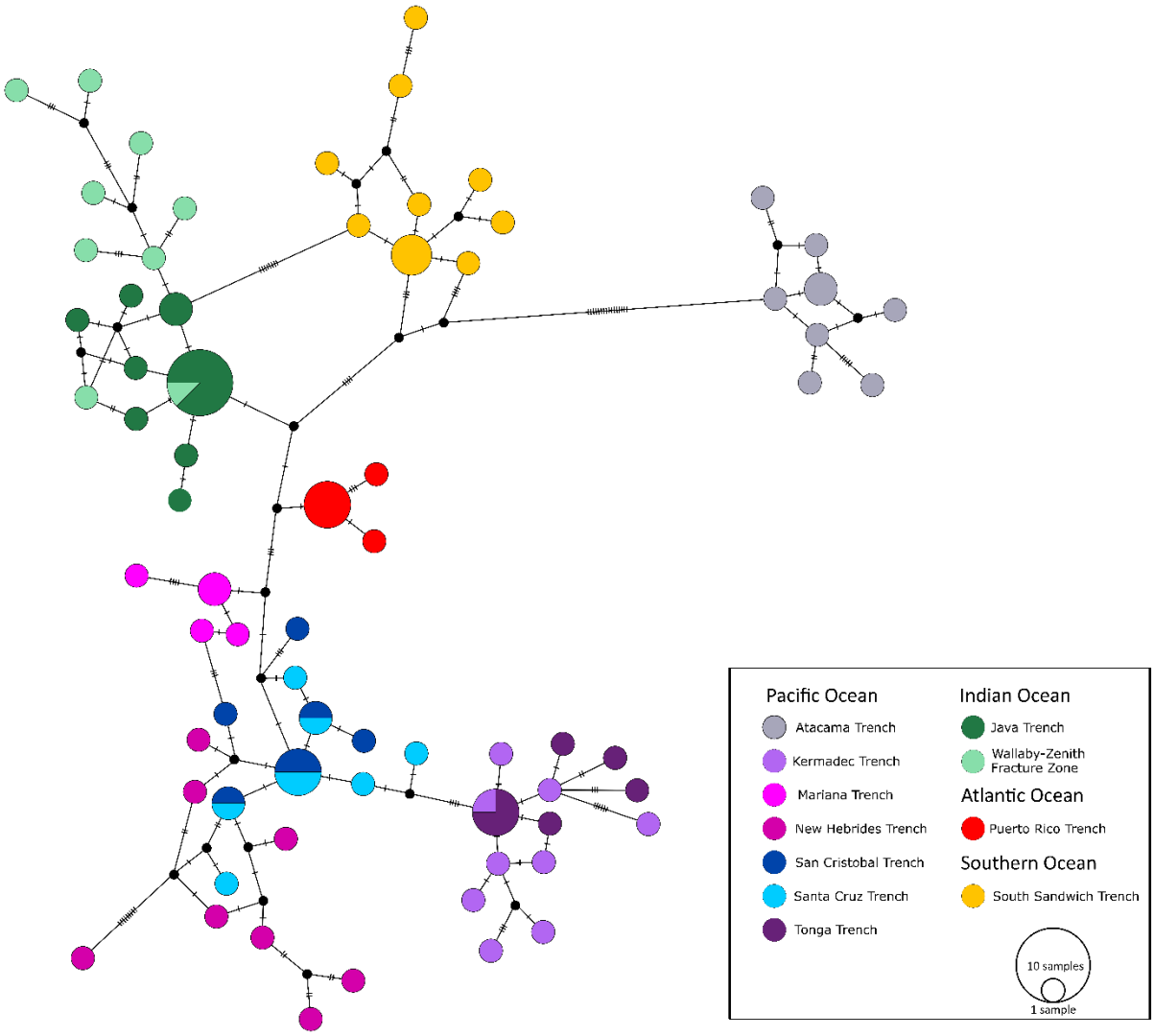

Figure 45. Statistical parsimony (TCS) haplotype network of *Bathycallisoma schellenbergi* based on a concatenated dataset (16S rRNA + COI; 700 bp). Colours represent each hadal feature samples, with colour shade groups by the ocean. The circle size proportional to the number of individuals with a given haplotype. The lines between haplotypes denote the number of base pair differences between haplotypes. The small black dots represent predicted but not directly sampled haplotypes.

4 Discussion

Contemporary hadal ecological research has often been limited to a single hadal feature or several features across the Pacific Ocean and typically based on relatively few physical specimens. In recent years, these limitations are being eroded as a greater number of sites and specimens are being studied, culminating with the global specimen collection from the Five Deeps Expedition. The study begins to show the benefit and research breadth of this specimen collection by successfully sequencing 94 *Bathycallisoma* individuals at two mtDNA regions, specifically 16S and COI, from 11 hadal features in four oceans. The salient finding of this study is that *Bathycallisoma schellenbergi* is not one distinct lineage but comprised of geographically differentiated clades.

4.1 Cryptic speciation within Bathycallisoma?

The initial question of this study was whether the morphologically identified *B. schellenbergi* specimens from 12 hadal features are the same species. The mtDNA delineation evidence indicated cryptic speciation, with at least two putative species (Figure 43). Specifically, the Atacama and South Sandwich Trench populations may each be genetically divergent enough to represent distinct, cryptic species. For the Atacama Trench population, both delimitation approaches provided congruent evidence of a distinct species-level lineage (Figure 44). The K2P divergence method showed a barcoding gap for COI, where the level of inter-trench and intra-trench divergences were comparable with previously reported divergences for lysianassoid amphipods (~5%; Havermans et al., 2011; Havermans et al., 2013). The South Sandwich Trench population, however, was only inferred a distinct species-level lineage by the bPTP analysis. The applied species delimitation methods inferred the Atlantic, Indian, and West Pacific Ocean populations to be the same species.

Cryptic speciation with *Bathycallisoma* does seem plausible. This question has surrounded the species since the initial descriptions and genera were raised. Dahl (1959) initially raised the genus *Bathycallisoma* for a new species, *B. pacifica* from the Kermadec Trench. While that description was in press, Birstein & Vinogradov (1958) published the description of *Scopelocheirus schellenbergi* from the Kuril-Kamchatka Trench. Both papers included in synonymy the account of aff. *Paracallisoma* spec. Schellenberg 1955

from the Puerto Rico Trench. In response to this possible double description, Dahl specified that the Kermadec specimen was distinct from the Kuril-Kamchatka Trench specimen based on the shape of the first gnathopod and other minor characteristics. These morphological character differences were not observable by Kilgallen & Lowry (2015) when *Scopelocheirus* was collapsed into *Bathycallisoma*. However, Ritchie et al. (2015) sampled both *Bathycallisoma* and *Bathycallisoma* (*Scopelocheirus*) from the Kermadec Trench and found sufficient evolutionary distance between them to be considered different species. More distinctively, *Bathycallisoma* (*Scopelocheirus*) was placed ancestral to the Lysianassoidea (Ritchie et al., 2015). This level of divergence between *Bathycallisoma* and *Bathycallisoma* (*Scopelocheirus*) was not detected here, with this more specimen comprehensive study. The evolutionary distance separating the Atacama Trench, South Sandwich Trench, and the other four clades are comparatively low, as compared to the *H. gigas* and *H. dubia* outgroups (Figure 43). While the taxonomic assessment as part of this study did not indicate observable differences between populations, closer taxonomic work should be conducted and guided by the mtDNA delimitation results to identify diagnostic differences.

While there is comparability in the delimitation results with other lysianassoid amphipods, the *Bathycallisoma* sequence data was different in resolution. First, the 16S data alone was unable to resolve any distinction of geographic clades or species lineages, whereas COI provided differentiation and resolution between populations. In contrast, the same partial 16S region for *Eurythenes* does allow for a species-delimitation (Weston et al., 2020). In the case of the Diamantina Fracture Zone specimens, the 16S pairwise comparison and BLASTn results did strongly indicate that they are *Bathycallisoma*. Thus, future DNA barcoding of *Bathycallisoma* specimens should prioritize sequencing COI or sequence both regions for comparability.

4.2 Phylogeographic patterns–evidence for refugia and allopatric separation?

The second component of this study was to investigate phylogeographic patterns between the populations and whether any genetic variation could be explained by geographic isolation. Both the phylogeny and haplotype network did show a strong degree of phylogeographic structuring between features. Six clades were identified within the phylogeny, with a clear discontinuity between the four oceans and between the east

and west Pacific Ocean (Figure 43). The ocean basin partitioning does align with the initial differentiation previously seen between the Wallaby Zenith Fracture Zone and four west Pacific Ocean trenches (Weston et al., 2021). In addition to ocean basin structuring, there was a lower but distinguishable level of structuring by distance within the Indian Ocean populations (Clade 4) and the central west and southwest Pacific Ocean populations (Clades 5–6). This structuring was more apparent within the haplotype network between the geographically close features (Figure 45), namely the Java Trench and the Wallaby-Zenith Fracture Zone (~ 2100 km), the Santa Cruz and San Cristobal trenches (~340 km; Stewart & Jamieson, 2018), and the Kermadec and Tonga trenches (~1000 km; Stewart & Jamieson, 2018). However, the high genetic diversity illustrated by the haplotype network and relatively few shared haplotypes may be more indicative of incomplete lineage sorting between these populations.

One phylogeographic pattern was particularly surprising–the relatively genetic similarity between the Java and Puerto Rico trench populations. These features are geographically separated ~19,000 km (Stewart & Jamieson, 2018), which includes the Mid-Atlantic Ridge and no continuous hadal depth corridor. Mid-ocean ridges and landmasses have been shown to prevent dispersal on the shallower abyssal plains (McClain & Hardy, 2010). While it is not possible to evaluate the level of genetic connectivity between these populations with this data, the lack of shared haplotype leads to the hypothesis of no present-day connectivity.

These results indicate complex interaction of geological, biological, and historical factors have shaped the diversity and distributional patterns of *Bathycallisoma* across the hadal zone. The mtDNA data suggest three main patterns: 1) the feature populations have experienced long-term isolation and harbour more endemic diversity, 2) a level of cryptic speciation is present, especially among the Atacama and South Sandwich trench populations, and 3) the divergence time is relatively recent. The starting question remains–how did *Bathycallisoma* come to have a cosmopolitan distribution when it is restricted to the hadal zone?

While there are limits with the dataset, there is an opportunity to present a working hypothesis that *Bathycallisoma* represents an example for refugia and allopatric speciation in the hadal zone. *Bathycallisoma schellenbergi* is considered to have a depth

range spanning 5600-9104 m (Kilgallen & Lowry, 2015) but has only be recovered in a feature that extends to hadal depths and appears absent along the abyssal plains (Lacey et al., 2015; Weston et al., 2021). In particular, *B. schellenbergi* was only found at the bottom 200 m of the Wallaby-Zenith Fracture Zone, even though shallower depths were sampled (Weston et al., 2021). While this could be interpreted as a sampling bias or sampling absence, it is growing increasingly more plausible that *Bathycallisoma* only resides in these features. Unless there is a corridor of hadal connectivity between features, a population is geographically isolated to a feature, which may be inferred in the haplotype network (Figure 45). Thus, the ancestral population must have had a wider bathymetric range to facilitate the cosmopolitan distribution. Weston et al. (2021) hypothesised that the ancestral *Bathycallisoma* had an abyssal-centric range, analogous to *A. gigantea* or *Paralicella* spp., that facilitated a cosmopolitan distribution and has subsequently became restricted to hadal depths.

Extending this rationale question is then–why did the ancestral *Bathycallisoma* have an abyssal-centric range and what led to a restriction to hadal depths? Corrigan et al. (2014) postulated that deep-sea Amphipoda underwent adaptive speciation during the Eocene-Oligocene transition (~75-50 Ma), as the climate cooled and primary productivity increased. They further estimated that abyssal scavengers, namely *Paralicella*, *Eurythenes*, and *Abyssochomene*, arose during the Miocene Epoch (~15-5 Ma); however, *Bathycallisoma* or other hadal amphipods (e.g., *H. gigas* or *H. dubia*) were not included. During the Miocene and Pliocene Epoch, the deep-ocean temperatures are estimated to be 3-6^{o}C warmer than present-day conditions (McClain & Hardy, 2010; Herold et al., 2012; Hansen et al., 2013). For deep-sea organisms, a warmer temperature could allow for wider eurybathic and deeper distribution, as the temperature is less of a physiological limitation (McClain & Hardy, 2010). If the ancestral *Bathycallisoma* arose about the same time as *Paralicella* and *Eurythenes*, then it is plausible it could have had a more abyssal-centric range.

Following the Mid-Miocene Climatic Optimum (~11.6 to 5.3 Ma), the climate and ocean began a long-term period of cooling to current conditions (Herold et al., 2013; Hansen et al., 2013). As cooling began, deep-sea organisms' ranges begin to narrow (McClain & Hardy, 2010). While counterintuitive, the ancestral *Bathycallisoma* may have

possessed the pressure-adaptions necessary and the competitive advantage to survive in the hadal features during a period of the glacial cycle. Now, the present-day *Bathycallisoma* populations reflect a signature of refugial bathymetric range truncation (Stewart et al., 2010; Lau et al., 2020), where feature populations are allopatrically separated - entirely isolated from each other or have limited genetic exchange between neighboring feature populations.

The Atacama and South Sandwich trench populations are of particular interest. The Atacama Trench is unique among trenches with a 25% lower O_2 (Glud et al., 2021) and the South Sandwich Trench is below 0^{o}C (Jamieson, 2015). Further, the age of both trenches is comparatively younger than West Pacific Ocean trenches (Stern, 2002), with Atacama Trench estimated to begin convergence ~23 Ma (Gagnon et al., 2005) and South Sandwich Trenches formed between 15-10 Ma (Larter et al., 2003) In response to these environmental conditions, these populations may have been under stronger adaptive selection pressures to survive in these trenches and thus undergone allopatric speciation.

4.3 Future investigations

This study used two mtDNA genetic markers to investigate the first-order question of species identity and provide an initial survey of the broad phylogeographic patterns of *Bathycallisoma* across the hadal zone. While 16S and COI were the selected genetic markers due to low intraspecific but relatively high interspecific variation (Avies et al., 1987), mtDNA analyses can only investigate the evolution of the non-recombining, maternally inherited mitochondrial genome. Thus, mtDNA analyses are limited in their application to population genetic investigations (Lau et al., 2020). Despite these established limitations, there is still utility in single-locus mtDNA studies to provide a compelling first assessment of phylogeographic patterns (Bowen et al., 2014; Lau et al., 2020). Bowen et al. (2014) encourage that comparative phylogeography work should begin with simple genetic markers, like mtDNA sequences, to provide a foundational reference of the underlying population structure and demographic history before proceeding with detailed genomic studies of selection and adaptation. Further, this work provides an essential step to understanding how the geochronology of hadal feature

formation has shaped the historical and present connectivity and driven speciation across the hadal zone.

Two key questions stem from these results and warrant further investigation. Firstly, what is the level of the gene flow and connectivity, if any, between the clades and features? Secondly, has allopatric separation driven cryptic speciation? To begin to address these questions, a future population genomics study should use *Bathycallisoma* and leverage a high-throughput sequencing method.

One approach is to use neutral and unlinked loci within single-nucleotide polymorphisms (SNPs), which are sequenced randomly across the whole genome. A powerful method is restriction-site associated DNA sequencing (RAD-seq), which allows reliable data to be obtained for the study of population genetic processes even when only limited numbers of specimens are sequenced (Baird et al., 2008; Ali et al., 2016). RAD-seq has been particularly useful for genotyping and investigating population structure in species lacking a reference genome (Catchen et al., 2011; Andrews et al., 2016; Rochette et al., 2019). However, the study design of a RAD-seq project is critical as RAD-seq possesses three unique sources of error that can hinder the success of a RAD-seq project, namely allelic dropout, PCR duplication, and low coverage of loci (Andrews et al., 2016; Rochette et al., 2019). These are particularly important sources of error to consider when working deep-sea amphipods as the quality of DNA can be low (Ritchie et al., 2017). Additionally, deep-sea amphipods have large genomes (~6–34 Gb) with a large section of transposable elements and/or repeated arrays (Ritchie et al., 2017). Together, this can pose a suite of substantial bioinformatic hurdles that can impact interpretations (Deagle et al., 2015). There are several methods to minimize these challenges, including estimation of the number of cut sites (Herrera et al., 2015; Rivera-Colón et al., 2020), selection of protocol that minimizes PCR duplications (BestRAD; Ali et al., 2016), and an initial assessment of phylogeographic patterns between populations (Schwentner & Lörz, 2020). Thus, this dataset lays the foundation for future investigations to assess the extent to which hadal features represent demographically and evolutionary independent units.

5 Acknowledgments

The KAH1109, KAH1202, and KAH1310 Expeditions were part of HADEEP II-IV, which were funded by TOTAL Foundation (France) through the projects ‘Multi-disciplinary investigations of the deepest scavengers on Earth’ (2010–2012) and ‘Trench Connection’ (2013–2015). The SO261 was funded by HADES–ERC Advanced Grant ‘Benthic diagenesis and microbiology of hadal trenches’ (Grant # 669947). The Five Deeps Expeditions were funded by Victor Vescovo of Caladan Oceanic LLC (USA). Molecular work and sequencing were funded by the ‘Hadal Zones of our Overseas Territories’ by the Darwin Initiative funded by the UK Government (DPLUS093).

Chapter 7: Summary: Addressing the “Who”, “Where”, “How”, & “Why” in the hadal zone

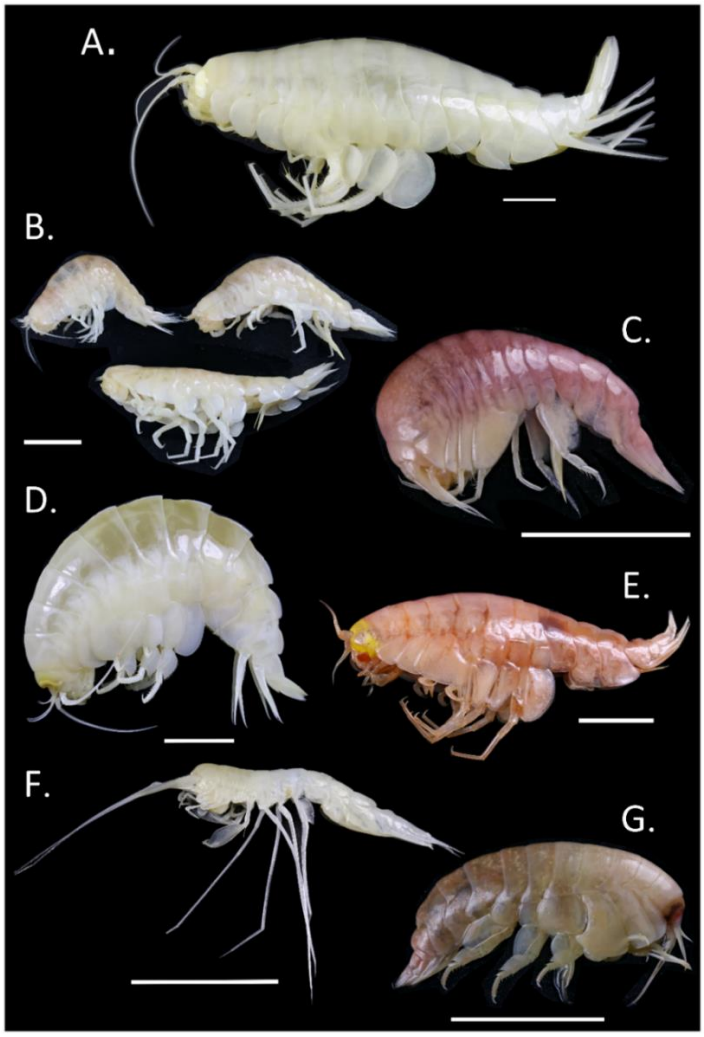

Collection of beautiful hadal Amphipoda. (A) *Alicella gigantea* Chevreux, 1899 from 7094 m in the Mariana Trench. (B) *Bathycallisoma schellenbergi* (Birstein & Vinogradov, 1958) from 8370 m in the Puerto Rico Trench. (C) Stegocephalidae gen. sp. from 8380 m in the Puerto Rico Trench. (D) *Eurythenes magellanicus* (H. Milne Edwards, 1848) from 8094 m in the Mariana Trench. (E) *Hirondellea gigas* (Birstein & Vinogradov, 1955) from 10,936 m in Mariana Trench. (F) *Hyperiopsis laticarpa* Birstein & M. Vinogradov, 1955 from 10,936 m in the Mariana Trench. (G) *Stephonyx* sp. nov. from 8380 m in the Puerto Rico Trench. Scale bar 1 cm.

"*I begin to feel rather dissatisfied with a mere local collection; little is to be learnt by it. I should like to take some one family to study thoroughly, principally with a view to the theory of the origin of species. By that means I am strongly of opinion that some definite results might be arrived at...*"

- Alfred Russel Wallace, writing to his friend Henry Walter Bates in an 1847 letter

1. Introduction

Since 1948, our biological understanding of the hadal zone has shifted from one devoid of life to one of rich biodiversity. With the first successful hadal trawl by the *Albatross* at the Puerto Rico Trench, the number of biological questions exponentially increased (Jamieson, 2015). The foundational questions of the field have been what is the diversity of life in the hadal zone, what are their geographic and bathymetric distributions, and what adaptions are necessary to thrive in the extreme environment? The Soviet RV *Vitjaz* and Danish RV *Galathea* expeditions, beginning in the 1950s, were the first major hadal-focused sampling campaigns (Jamieson, 2015). Together, these expeditions provide the first systematic sampling of many trenches and laid the taxonomic foundation for the hadal fauna. The most diverse and commonly sampled groups were polychaetes (Annelidea, ~164 species), bivalves (Mollusca, ~101 species), gastropods (Mollusca, ~85 species), amphipods (Amphipoda, ~80 species), and holothurians (Echinodermata, ~59 species) (Belyaev, 1989; Jamieson, 2015). Over the past 60 years, with each research expedition, more species are being discovered and drivers of hadal ecology and evolution are being tested and understood.

As highlighted through topic modeling in **Chapter 1**, hadal ecology is both moving towards a direction of an experimental era but still closely connected to the explorational and observational eras. Scavenging amphipods represent a model taxon to expand our understanding of how the hadal environment drives diversity, shapes the structure of populations and communities, and influences connectivity of populations between the geographically disjunct hadal features.

Thus, this thesis aimed to move the state of hadal ecology forward by first laying a firm foundation in amphipod taxonomy to answer the question of "who", and then building upwards to begin to unravel the questions of "where", "why", and even "why not". Further, this thesis was approached from a biogeographic perspective and took a multidisciplinary approach, drawing on theory and techniques from evolutionary and

population biology, genetics, systematics, physiology, earth sciences, history, and environmental management. The temporal scope of this thesis spanned across the Cenozoic Era, moving from deep-sea adaptive radiation in the Eocene Epoch to documenting microplastic pollution impacts of the Anthropocene. Three main research themes were woven through this thesis to advance the understanding of local, regional, and global biogeographic patterns across the hadal zone.

Theme 1. Expand the known and described diversity of deep-sea scavenging amphipods through an integrative taxonomic approach.

Theme 2. Assess the patterns of amphipod community structure and population dynamics in a non-subduction hadal feature.

Theme 3. Test the traditional hypothesis that hadal ecosystems are evolutionarily and demographically independent units by investigating the level of genetic connectivity between hadal populations.

2. Theme 1 – The Species

The species is one of the fundamental units of measure in biology and ecology. The species allows for investigating diversity at a location, making comparisons across space and time, understanding the eco-evolutionary drivers of diversity, and, critically for the future, establishing effective conservation and management strategies. Thus, species identification is a first-order step in the understanding of the eco-evolutionary dynamics in the hadal zone.

Our ability to identify and delimit species depends on the availability of diagnostic characters that provide a clear separation of intraspecific variability and interspecific variation (Schwentner & Lörz, 2020). Within deep-sea Peracarids, this is not a trivial exercise–identification is often challenged by phenotypic plasticity, a limited number of specimens, material that is damaged, and/or characters that are tough to objectively discern (Birky et al., 2005; Havermans et al., 2013; Weston et al., 2020). Because of these challenges, diversity can be underestimated and the misinterpretation of species distribution, life history, and population dynamics. In the deep-sea, there are a growing number of instances of genetics uncovering cryptic diversity (Havermans et al., 2013).

One of the most notable examples is within the amphipod genus *Eurythenes* and a prevalent member of the deep-sea, benthopelagic community, *Eurythenes gryllus*

(Stoddart & Lowry, 2004; Havermans et al., 2013). *Eurythenes gryllus* has been the focus of a suite of ecological and physiological studies (Hargrave, 1985; Ingram & Hessler, 1987; Christiansen et al., 1990; Thurston et al., 2002; Blankenship et al., 2006; Blankenship & Levin, 2007; Premke & Graeve, 2009), given its cosmopolitan distribution and extensive eurybathic range (Barnard, 1961; Ainley et al., 1986; Thurston et al., 2002; Fujii et al., 2013). Questions to the identification of *E. gryllus* were first raised by France & Kocher (1996). Cryptic speciation with the *gryllus*-complex has since been confirmed by integrative taxonomic studies (Havermans et al., 2013; 2016; Eustace et al., 2016). Since 2015, *Eurythenes* has grown from three to 10 described species (d'Udekem d'Acoz & Havermans, 2015; Narahara-Nakano et al., 2018; Weston et al., 2020a). Furthermore, at least five distinct genetic lineages are awaiting formal description and likely more to be discovered (Havermans et al., 2013; Horton et al., 2020). Importantly, this elevated diversity with *Eurythenes* has led to a revised conception of demographic trends, distributional patterns, biogeography, and drivers of speciation.

While species is one of the most fundamental ecological concepts, it is also one of the most problematic and debated concepts (Baum & Shaw, 1995). The concept of species was derived to provide order, consistency, and allow for comparisons, and further a species is not a static entity but a snapshot along an evolutionary gradient. As such, there are multiple existing ways to defining a species, like the morphological species and phylogenetic species concepts (de Queiroz, 2005; Elredge & Cracraft, 1980). Now with multiple tools for discovery, such as DNA barcoding, there are continued qualitative challenges to reach an agreement on defining and delimiting a species with multiple lines of evidence (Padial et al., 2010). This qualitative challenge has led to incongruence between traditional systematics and molecular systematics (Ritchie et al., 2015). This incongruence becomes practically problematic when morphological and molecular lines of evidence are conducted by different groups, and further worsened by minimal collaboration. The discovery, description, and ecological findings are more robust when these multiple lines of evidence are brought together using an integrative taxonomic approach. Among scavenging amphipods, d'Udekem d'Acoz & Havermans (2015) provides a strong case example for applying integrative taxonomy to *Eurythenes*.

Implemented throughout this thesis was an integrative approach to specimen identification–this relied heavily on marrying together morphological assessments with DNA barcoding of the partial mitochondrial regions of 16S rRNA (16S) and cytochrome c oxidase I (COI). **Chapters 2** and **3** were focused on the cryptic genus *Eurythenes*, which led to the ninth and tenth species in the genus. Namely, *Eurythenes plasticus* from hadal depths of the Mariana Trench, and *Eurythenes atacamensis,* a particularly unique lineage that is the dominant amphipod species at hadal depths in the Peru-Chile Trench. **Chapter 4** focused on two species from the abyssal depths of the Wallaby-Zenith Fracture Zone. The first species, *Stephonyx sigmacrus*, provided a practical example that collecting multiple lines of evidence is not always possible. While several genomic extraction methods were used, there was never success of PCR amplification. However, the morphology of the basis of the 5th and 6th pereopods was distinguishing enough from all other species in the genus, indicating that it likely a distinct and undescribed species. The second species in **Chapter 4** was *Civifractura serendipia*. While *S. sigmacrus* presented the practical challenges to an integrative approach, *C. serendipia* is an exemplar example of the power of the integrative approach against the limitations of few specimens, phenotypic plasticity, and cryptic speciation. Specifically, the preliminary DNA barcoding results indicated this species would be better placed in the *Tectovalopsis* genus if based solely on morphology. **Chapter 5** used the integrative approach to support the identification of 13 species from the Wallaby-Zenith Fracture Zone and the Afanasy Nikitin Seamount in the underrepresented Indian Ocean. Here, it was particularly important to correctly identify *Eurythenes maldoror* and differentiate between *Abyssorchomene gerulicorbis* at the Wallaby-Zenith Fracture Zone and *Abyssochomene distinctus* at the Afanasy Nikitin Seamount. While only two species were further described as new species (i.e., *S. sigmacrus* and *C. serendipia*), four other species are candidates for undescribed species (i.e., *Cleonardo* sp. indent, *Cyclocaris* sp., *Hirondellea* sp., and *Valettietta* sp. nov.). **Chapter 6** provided a foundational investigation into the species identity, revealed a level of cryptic speciation, and provided a survey of the broad phylogeographic patterns of *Bathycallisoma* across the hadal zone. While there are interpretational limits to DNA barcoding, this work provided a starting context and survey of the underlying population

structure and demographic history before proceeding with detailed genomic studies of selection and adaption.

While each thesis chapter had a strong emphasis on the "who" question, **Chapters 2, 3,** and **4** were taxonomically focused but not limited to taxonomy. These studies used the species as an opportunity to glean additional information to expand hadal ecology, whether it be investigating vertical ontogenetic stratification, systematics, and anthropogenic impacts. **Chapter 2** drew attention to the ubiquity and pervasiveness of marine plastic pollution in the ocean. This was particularly striking that the remoteness does not buffer the hadal zone from impacts on land. **Chapter 3** investigated bathymetric trends of juveniles and females to provide an interpretation of the ecological strategy of vertical ontogenetic stratification across the oligotrophic Atacama Trench. **Chapter 4** demonstrated that the bathymetric range of *Stephonyx* extends into the abyssal zone, elevated diversity with the Alicellidae family, and further that morphological and genetically the Alicellidae family is not monophyletic.

Additionally, in parallel with the thesis, time was spent curating, identifying, and selectively barcoding amphipods collected from the 2014 RV *Falkor* (FK14409) to the Mariana Trench, the 2018 RV *Sonne* (SO261) to the Atacama Trench, and the circumglobal 2018-2019 Five Deeps Expedition. These efforts did provide support to thesis chapters, like the discovery of *E. plasticus*. Importantly, these efforts have led to the expansion of the global hadal amphipod records by 20% (Appendix C). This is improving our knowledge of bathymetric and distributional ranges of species. Further, at least 10 of the species are likely new to science and awaiting description.

3. Theme 2 – The Location

This thesis asked "where" hadal fauna live. The most straightforward answer lies in the definition of the hadal, any place that is deeper than 6000 m. However, the definition of hadal is not so simple. While the maximum depth of the hadal zone is clearly defined (the maximum ocean depth), there has been a debate within the literature on the minimum depth. The minimum depth of the hadal zone has been promoted by the biology and the high degree of endemism in the trenches identified by the *Vitjaz* and *Galathea* expeditions (Wolff, 1960, 1970; Belyaev, 1989). Wolff (1960) originally suggested 6000 m as the minimum hadal depth, as it represents 58% of measured endemism, but also postulated

that the limit could be between 6800–7000 m. Although endemism >6000 m can vary between trenches due to feature-specific environmental and geologic attributes (Belyaev, 1989), it is generally accepted that 6000–7000 m represents the 'abyssal-hadal transition zone' (Jamieson et al., 2011). To account for this transition zone, the minimum depth has more recently also been considered 6500 m (Briones et al., 2009). However, it is most used within the literature for the minimum hadal depth to be 6000 m.

To add complexity, the definition of hadal has been based on subduction trench features, potentially unintentionally restricted. Subduction trenches account for ~93.7% of the total hadal area. The remaining ~6.3% area consists of troughs, fractures, trench faults, and other features that are not necessarily associated with plate convergence zones (Jamieson, 2015). Until 2017, only subduction trench features had been explored and sampled. Further, most studies are largely based on one or a few trenches in the Pacific Ocean and largely limited to the deepest depths (Jamieson, 2018; **Chapter 1**). The baited lander deployments to the Wallaby-Zenith Fracture Zone, Indian Ocean on the RV *Sonne* SO258 were the first opportunity to address the "where" question. Explicitly, does 'hadal' mean any depths exceeding 6000 m, or is 'hadal' limited to subduction trenches >6000 m?

Chapters 4 and **5** focused on the Wallaby-Zenith Fracture Zone, with **Chapter 5** focused more directly on the "where" question. The scope of the question was focused on amphipods, as they allow for comparisons between studied subduction trench features. The hadal trench scavenging community is distinct from the shallower abyssal community. Further, the shift in communities has been found to abruptly occurs across the abyssal-hadal transition zone (Jamieson et al., 2011; Fujii et al., 2013; Lacey et al., 2016). The community composition findings at the Wallaby-Zenith Fracture Zone indicated a contrasting pattern, a gradual shift from abyssal to hadal depths. While the community at the bottom of the Wallaby-Zenith Fracture Zone (6537–6546 m) was largely abyssal species, there was an abundant population of *Bathycallisoma schellenbergi* (Birstein & Vinogradov, 1958). The presence of this quintessential hadal fauna was surprising and ecological noteworthy–both at the time of recovery and now. The presence of *B. schellenbergi* in a small (4150 km^2) and remote fracture zone that is just deep

enough to fit the definition of hadal (6625 m) opens the possibility of *B. schellenbergi* and other hadal trench fauna to inhabit other non-subduction hadal features.

More directly, from a biological perspective, the hadal zone is more than the 27 subduction trenches and does encompass any location exceeding 6000 m, regardless of geomorphic setting or total area. Thus, to move hadal ecology forward, sampling more than the largest and geographically isolated subduction test is imperative to disentangle the complexities of connectivity and species distribution in the hadal zone. Future expeditions should target features like the Diamantina Fracture Zone in the Indian Ocean, Agulhas Fracture Zone in the South Atlantic Ocean, and the Philippine Basin in the West Pacific Ocean (Jamieson & Stewart, 2021). **Chapter 6** began to answer the call to sample underrepresented hadal features, particularly focusing on *B. schellenbergi*, that were largely recovered during the Five Deeps Expedition. This includes some of the first biological observations made at the South Sandwich Trench, Diamantina Fracture Zone, and the Santa Cruz and San Cristobal trenches.

The habitat and environmental conditions necessary for amphipods are likely different than for other hadal taxa. Thus, the “where” question should be expanded out to other taxa, such a snailfish, cusk eels, and decapods (Linley et al., 2016; Swan et al., 2021) to holistically answer what it means to be hadal. Further, there is much more work need to understand how factors, like temperature, dissolved oxygen, surface primary productivity, currents, geologic age, and seismicity, shape the distribution of hadal biodiversity.

4. Theme 3 – The How & Why

The hadal zone is comprised of 47 subduction trenches, troughs, and transform faults that create pockets of habitats in the Pacific, Indian, Atlantic, and Southern oceans. The traditional view is that hadal features hotspots for endemism (Wolff, 1960; Belyaev, 1989). Further, they represent evolutionarily and demographically independent units resulting from extreme environmental conditions, long-term geographical isolation, and evolutionary selection pressures. However, this perception that hadal features are local or regional endemic hotspots is being increasingly tested. For example, *Alicella gigantea* Chevreux, 1899 has been found in the North Atlantic, Indian Ocean, and the South Pacific

Ocean. Further, Ritchie et al. (2017) found evidence for occasional gene flow between five disparate, abyssal populations of *Paralicella* spp. across the Pacific Ocean.

Moreover, one of the main lingering questions from **Chapter 5** (Weston et al., 2021) was why and how are *B. schellenbergi* at the Wallaby-Zenith Fracture Zone. Two hypotheses were put forward — 1) the Wallaby-Zenith Fracture Zone population represents a spillover population from the larger Java Trench, thus indicate a level of genetic connectivity between hadal; and 2) an ancestral *B. schellenbergi* had an abyssal-centric cosmopolitan distribution and became restricted to hadal depths, thus now reflected by allopatric populations. These questions about *B. schellenbergi* fall under the broader biogeographic umbrella to *describe* the spatial distribution of past, present, and potential future hadal species and *explain* the underlying causes of those distributions. Thus, *B. schellenbergi* presents a model species for hadal biogeographic research.

Chapter 6 took the next step in answering the “how” and “why” questions. Doing this required *B. schellenbergi* specimens to be collected from multiple hadal features spanning their global distribution and preserved to allow for future genetics-based analysis. Amassing the specimen collection needed can only be done through a highly ambitious and novel sampling campaign, like the circumglobal 2018-2019 Five Deeps Expedition (Jamieson, 2020). During the Five Deeps Expedition, baited landers were first deployed to the Puerto Rico Trench, then subsequently to the South Sandwich Trench, the Agulhas and Diamantina fracture zones, then the Java, Mariana, Santa Cruz, San Cristobal, and Tonga trenches, and finally the Molloy Deep in the Arctic Ocean. The presence of *B. schellenbergi* in the baited trap was a constant throughout the whole Five Deeps Expedition, apart from the Agulhas Fracture Zone and Molloy Deep, which are both shallower than 6000 m.

Chapter 6 leveraged an unprecedented *B. schellenbergi* specimen collection, spanning 12 hadal features in the Pacific, Atlantic, Southern, and Indian oceans. This study directly picked up where **Chapter 5** left off by first asking whether it was the same species (*B. schellenbergi*) at each feature, and then what was the phylogeographic signal separating the populations? This study used DNA barcoding as the tool to first explore for phylogeographic “gold mines” (Bowen et al., 2014). The work provided an initial snapshot of the underlying population structure and demographic history of the

populations. The results of this work suggest two key findings. First, *Bathycallisoma* represents a species-complex, with Atacama Trench hosting the most divergent population. Second, while there is phylogeographic structuring by ocean basins and regional proximity, the populations in each feature have experienced long-term isolation and harbour more endemic genetic diversity. This initial snapshot suggests that connectivity between the feature populations is minimal, at best. One hypothesis to explain the cosmopolitan distribution of geographically isolated populations is these are relict populations from ancestral *Bathycallisoma* with a more eurybathic distribution due to a historically warmer deep ocean.

This work hit on a hadal phylogeographic “gold mine” and lays the foundation for a more detailed genomic study to quantify the level of genetic connectivity between the population. While not included in the thesis, a subsequent RAD-seq study has been conducted with the same DNA barcoded individuals to generate thousands of polymorphic loci and SNPs. While the results from a RAD-seq study can yield insightful results for population genetics and phylogenetics of non-model species (Schwentner & Lörz, 2020), the quality of the DNA, library preparation methods, and sequencing strategy can affect the outcome (Rochette et al., 2019). Deep-sea amphipods pose two large challenges from the beginning — large genomes (Ritchie et al., 2017) and poor DNA quality because of depressurisation during recovery. Deagle et al. (2015) found the 47 GB genome of the Antarctic krill led to SNPs present in multicopy genomic regions instead of single-copy nuclear loci. One information gap for this work is the genome size of *Bathycallisoma*, but we conservatively estimated it to be 20 Gb based on the similar body size to *Hirondellea gigas* and *E. maldoror* (Ritchie et al., 2017). To further control for inherent challenges, the BestRad protocol (Ali et al., 2016) was selected for the library preparation to minimize PCR duplicates and the 128 multiplexed samples were pair-end sequenced on two lanes of an Illumina HighSeq 4000. With 68 Gb of sequencing data, bioinformatics has been a substantial endeavor. At the time of the thesis submission, a substantial amount of computing resources and human resources have been allocated to this task. While bioinformatics challenges are being tackled in processing the data, the DNA barcoding work has provided the biological foundation for the RADseq project.

Importantly, **Chapter 6** represents the scientific power to utilize a global hadal specimen collection and the opportunity to investigate these broad phylogeographic patterns. Future investigations should be focused on other hadal amphipod genera, specifically among *Hirondellea*, *Eurythenes,* and *A. gigantea*. This allows for comparative phylogeography and the testing of different drivers of speciation across the abyssal and hadal zone for scavenging amphipods. The next step will be expanding these questions to other taxa, as specimens become available. This work will help shed light on vertebrate biogeography across the hadal zone, such as snailfish, and with epibenthic fauna, especially those with larval stages.

5. Looking Forward

5.1. Advancing hadal biogeography

The global phylogeography of *Bathycallisoma* (**Chapter 6**) demonstrates that the biogeography data is now available, at least for scavenging amphipods. The main outstanding question from **Chapter 6** was how and why is the distribution of *Bathycallisoma* cosmopolitan across the hadal zone? A working hypothesis is that these features host relic populations from an ancestral lineage whose bathymetric range shifted with a cooling deep sea. Now, the range of *Bathycallisoma* has been truncated to hadal features, which are inherently geographically separated.

Given the challenges of sampling the deep-sea, the biogeography of hadal fauna has historically been characterised more by conjecture than data (McClain & Hardy, 2010). Now, modern sampling techniques, higher resolution sampling efforts, molecular and genetic methods, and expansion of specimen collection allow for the testing of existing hypotheses. The crux of **Chapter 6** question and hypothesis are embedded with one of the first and long-standing questions within hadal ecology — the origin of the hadal fauna.

Since the first hadal organisms were recovered, there has been a discussion surrounding the age of the hadal community. This discussion has been framed in context historical positioning of the hadal trenches and historical oceanography (McClain & Hardy, 2010). The trenches are estimated to have formed between 155 Ma with the Mariana Trench to 10.5 Ma with South Sandwich Trench (Stern, 2002; Larter et al., 2003). The physical environment of the deep-sea used to be much warmer than the modern

deep-sea, specifically at the Eocene/Paleocene boundary (55 Ma) the temperature was ~14ºC warmer (Waelbroeck et al., 2001). Additionally, there have been two alternating types of ocean circulation–a high-latitude deep-water thermocline and a salinity-induced stratification halotherm (McClain & Hardy, 2010). Transitions between these two types have been associated with deep-water anoxia (McClain & Hardy, 2010). Considering the historical geologic and oceanographic setting, hadal fauna has been hypothesised to have two different origins — 'ancient' and 'secondary' fauna. Wolff (1960) posited that hadal taxa are either relics from the pre-Eocene ocean or represent a new invasion of the eurybathic species following the cooling period following the Eocene. This work was built solely on morphology and systematics. The most recent ancestral molecular dating analysis within Amphipoda has indicated a shallow-water ancestor colonised the deep-sea at ~70 Ma at the Cretaceous-Paleogene boundary, and three scavenger lineages data to the Eocene–Oligocene boundary (Corrigan et al., 2014). While, more supportive a secondary fauna hypothesis, this study was limited to abyssal fauna in the North Atlantic Ocean and relatively few molecular markers.

A major knowledge gap remains on the origin of the hadal fauna. Yet, hadal biogeography is now in a uniquely timely position to attempt to address this gap, by leveraging extensive specimen collections, advanced genomic approaches, computational abilities, and plate reconstruction methodologies (McClain & Hardy 2010). Future work should use amphipods as a model system for reconstructing and deriving time-calibrated phylogenies. Given the challenges with amphipod genome size and quality, such work could utilize the whole mitogenome, due to their stability, size, and heritability patterns. The generated phylogeny should also provide a geographical context. The phylogenomic and molecular clock analysis can be calibrated and paired with tectonic plate reconstructions. Together, this work would help unlock how the geochronology of hadal feature formation has shaped diversification and distribution throughout the hadal zone.

5.2. Strengthening interdisciplinary links across hadal science

Hadal science has been experiencing strong exponential growth since 2010 (**Chapter 1**; Jamieson, 2018). The growth of hadal science can be largely attributed to advances in the diversity and capability of technology and equipment to take physical

samples (e.g., sediment, water, and biological), make *in-situ* measurements (Glud et al., 2021), full-ocean bathymetric mapping capabilities, application of advanced genomic techniques (Ritchie et al., 2017), and collect still images and videos (Jamieson, 2020). This growth is exemplified by the DSV *Limiting Factor*, which removes the technological barrier to repeatedly access the hadal zone. The topic modeling has highlighted several research strengths within hadal science, represented by the high similarity between topics and articles (Figure 46). One of the tightest links is by making geographic comparisons at the taxonomic level in microbiology and amphipods and then across the community and ecosystem levels. As more hadal features are being explored and sampled, these topics will continue to grow over the next decade.

Topic modeling did draw attention to the dissimilarity between some topics (Figure 46). These weaker connections can indicate research gaps and future research goals may benefit from cultivating those links. One area with much potential growth is linking together the geochemistry and geophysical with biology and ecology. This will explicitly support understanding of a range of topics, such as seasonal dynamics of population and communities, the role of environmental conditions to shape diversity and adaption to feature-specific conditions, and the influence of seismicity on turnover, local extinctions, and carbon availability.

While the range of topics uncovered by topic modeling broad, there was a noticeable lack of topics or words on conservation and management, deep-sea mining, climate change, and most strikingly other anthropogenic impacts. The hadal depth has been shown to not be a barrier to anthropogenic impacts, notably with the accumulation of plastic in sediments (Peng et al., 2018), ingestion of plastic by amphipods (Jamieson et al., 2019; Weston et al., 2020), and bioaccumulation of PCBs (Jamieson et al., 2017). Multiple direct and indirect anthropogenic pressures are being placed on the hadal zone and the shallower deep-sea. Among the deep-sea research community, there is growing attention to developing effective ecosystem-based management strategies and monitoring to protect biodiversity and habitats and maintain ecosystem services and functions (Danovaro et al., 2020). Recent deep-sea expert elicitation of monitoring focus concluded that benthic biodiversity research should prioritize macro- and megafauna, with

bacteria being a non-priority. Further, conservation efforts should focus on vulnerable deep-sea habitats and connectivity between populations (Danovaro et al., 2020).

Hadal science will continue to progress towards the observation era. Overall, this thesis supported the progression of the hadal ecology forward by growing the known and described the diversity of deep-sea scavenging amphipods, investigating the amphipod community structure at underrepresented hadal features, and providing the first global phylogeographic study. Together, this thesis expands our knowledge of hadal communities to features beyond subduction trenches and contributes to the disentanglement of the environmental, tectonic, and drivers of contemporary diversity across the hadal zone.

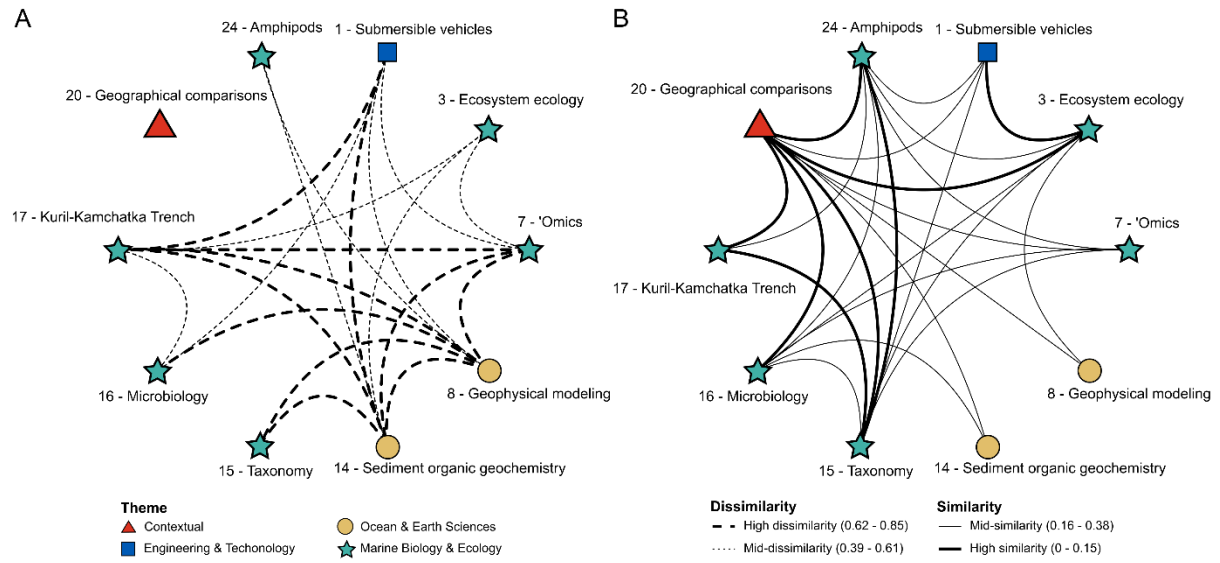

Figure 46. Topic modeling gap analysis between the ten topics with the highest number of articles between 2015-2020. A) Dissimilarity between topics, suggestive of research gaps. B) Similarity between topics, indicating research strengths.

References

Ainley, D.G., Fraser, W.R., Sullivan, C.W., Torres, J.J., Hopkins, T.L. and Smith, W.O., 1986. Antarctic mesopelagic micronekton: evidence from seabirds that pack ice affects community structure. *Science*, *232*(4752), pp.847-849. doi:10.1126/science.232.4752.847

Andrews, K.R., Good, J.M., Miller, M.R., Luikart, G. and Hohenlohe, P.A., 2016. Harnessing the power of RADseq for ecological and evolutionary genomics. *Nature Reviews Genetics*, *17*(2), p.81.

Ali, O.A., O'Rourke, S.M., Amish, S.J., Meek, M.H., Luikart, G., Jeffres, C. and Miller, M.R., 2016. RAD capture (Rapture): flexible and efficient sequence-based genotyping. *Genetics*, *202*(2), pp.389-400. doi:10.1534/genetics.115.183665

Alomar, C. and Deudero, S., 2017. Evidence of microplastic ingestion in the shark *Galeus melastomus* Rafinesque, 1810 in the continental shelf off the western Mediterranean Sea. *Environmental Pollution*, *223*, pp.223-229. doi:10.1016/j.envpol.2017.01.015

Aria, M. and Cuccurullo, C., 2017. *bibliometrix*: An R-tool for comprehensive science mapping analysis. *Journal of Informetrics*, *11*(4), pp.959-975.

Avise, J.C., Arnold, J., Ball, R.M., Bermingham, E., Lamb, T., Neigel, J.E., Reeb, C.A. and Saunders, N.C., 1987. Intraspecific phylogeography: the mitochondrial DNA bridge between population genetics and systematics. *Annual Review of Ecology and Systematics*, *18*(1), pp.489-522.

Baird, N.A., Etter, P.D., Atwood, T.S., Currey, M.C., Shiver, A.L., Lewis, Z.A., Selker, E.U., Cresko, W.A. and Johnson, E.A., 2008. Rapid SNP discovery and genetic mapping using sequenced RAD markers. *PloS One*, *3*(10), p.e3376. doi:10.1371/journal.pone.0003376

Barnard, J.L., 1961. Gammaridean Amphipoda. *Galathea Report*, *5*, pp.23-128.

Barnard, J.L., 1962. South Atlantic abyssal amphipods collected by RV *Vema*. Columbia University Press.

Barnard, J.L., 1967. Bathyal and abyssal gammaridean Amphipoda of Cedros Trench, Baja California. *Bulletin of the United States National Museum*.

Barnard, J.L. and Ingram, C.L., 1986. The supergiant amphipod *Alicella gigantea* Chevreux from the North Pacific gyre. *Journal of Crustacean Biology*, *6*(4), pp.825-839. doi:10.2307/1548395

Barnard, J.L. and Ingram, C.L., 1990. Lysianassoid Amphipoda (Crustacea) from deep-sea thermal vents. *Smithsonian Contributions to Zoology*.

Barnard, J.L., 1991. The families and genera of marine gammaridean Amphipoda (except marine gammaroids) Part 2. *Records of the Australian Museum Supplement*, *13*, pp.419-866.

Baum, D.A. and Shaw, K.L., 1995. Genealogical perspectives on the species problem. *Experimental and Molecular Approaches to Plant Biosystematics*, *53*(289-303), pp.123-124.

Beermann, J., Westbury, M.V., Hofreiter, M., Hilgers, L., Deister, F., Neumann, H. and Raupach, M.J., 2018. Cryptic species in a well-known habitat: applying taxonomics to the amphipod genus *Epimeria* (Crustacea, Peracarida). *Scientific Reports*, *8*(1), pp.1-26. doi:10.1038/s41598-018-25225-x

Bellan-Santini, D., 1983. Amphipodes profonds de Mediterranee.(Campagnes biomede I, polymede I et II). *Bollettino del Museo Civico di Storia Naturale di Verona*, *10*, pp.263-313.

Bellan-Santini, D., 1997. Amphipods of the cold seep community on the South Barbados accretionary prism. *Crustaceana*, *70*(1), pp.1-30.

Bellas, J., Martínez-Armental, J., Martínez-Cámara, A., Besada, V. and Martínez-Gómez, C., 2016. Ingestion of microplastics by demersal fish from the Spanish Atlantic and Mediterranean coasts. *Marine Pollution Bulletin*, *109*(1), pp.55-60. doi:10.1016/j.marpolbul.2016.06.026

Belyaev, G.M., 1989. Deep-sea ocean trenches and their fauna. Moscow: Nauka.

Besseling, E., Foekema, E.M., Van Franeker, J.A., Leopold, M.F., Kühn, S., Rebolledo, E.B., Heße, E., Mielke, L.J.I.J., IJzer, J., Kamminga, P. and Koelmans, A.A., 2015. Microplastic in a macro filter feeder: Humpback whale *Megaptera novaeangliae*. *Marine Pollution Bulletin*, *95*(1), pp.248-252. doi:10.1016/j.marpolbul.2015.04.007

Birky, C.W., Wolf, C., Maughan, H., Herbertson, L. and Henry, E., 2005. Speciation and selection without sex. *Hydrobiologia*, *546*(1), pp.29-45. doi:10.1007/s10750-005-4097-2

Birstein, J.A. and Vinogradov, M.E., 1955. Pelagicheskie gammaridy (Amphipoda, Gammaridea) Kurilo-Kamchatskoi Vpadiny. *Akademiya Nauk SSSR, Trudy Instituta Okeanologii*, *12*, pp.219-257.

Birstein, J.A. and Vinogradov, M.E., 1958. Pelagicheskie gammaridy (Amphipoda–Gammaridea) severozapadnoi chasti Tixogo Okeana. *Trudy Instituta Okeanologii*, *27*, pp.219-257.

Birstein, J.A. and Vinogradov, M.E., 1960. Pelagicheskie gammaridy tropicheskoi chasti Tixogo Okeana. *Akademiya Nauk SSSR, Trudy Instituta Okeanologii*, *34*, pp.165-241.

Birstein, Y.A. and Vinogradov, M.E., 1963. Deep-sea pelagic amphipods of the Philippine Trench. *Trudy Instituta okeanologii. Akademiya nauk SSSR*, *71*, pp.81-94.

Birstein, J.A. and Vinogradov, M.E., 1964. Pelagic gammarid amphipods of the northern part of the Indian Ocean. *Akademiya Nauk SSSR, Trudy Instituta Okeanologii*, *65*, pp.152-195.

Blankenship, L.E. and Levin, L.A., 2007. Extreme food webs: Foraging strategies and diets of scavenging amphipods from the ocean's deepest 5 kilometers. *Limnology and Oceanography*, *52*(4), pp.1685-1697.

Blankenship, L.E., Yayanos, A.A., Cadien, D.B. and Levin, L.A., 2006. Vertical zonation patterns of scavenging amphipods from the hadal zone of the Tonga and Kermadec Trenches. *Deep Sea Research Part I: Oceanographic Research Papers*, *53*(1), pp.48-61.

Borowsky, B., 1984. The use of the males' gnathopods during precopulation in some gammaridean amphipods. *Crustaceana*, *47*(3), pp.245-250.

Bouckaert, R., Vaughan, T.G., Barido-Sottani, J., Duchêne, S., Fourment, M., Gavryushkina, A., Heled, J., Jones, G., Kühnert, D., De Maio, N. and Matschiner, M., 2019. BEAST 2.5: An advanced software platform for Bayesian evolutionary analysis. *PLoS computational biology*, *15*(4), p.e1006650. doi:10.1371/journal.pcbi.1006650

Bowen, A.D., Yoerger, D.R., Taylor, C., Mccabe, R., Howland, J., Gomez-Ibanez, D., Kinsey, J.C., Heintz, M., McDonald, G., Peters, D. and Young, C., 2009. The Nereus hybrid underwater robotic vehicle. *Underwater Technology*, *28*(3), pp.79-89.

Bowen, B.W., Shanker, K., Yasuda, N., Celia, M., Malay, M.C.M.D., von der Heyden, S., Paulay, G., Rocha, L.A., Selkoe, K.A., Barber, P.H. and Williams, S.T., 2014. Phylogeography unplugged: comparative surveys in the genomic era. *Bulletin of Marine Science*, *90*(1), pp.13-46.

Brasier, M.J., Wiklund, H., Neal, L., Jeffreys, R., Linse, K., Ruhl, H. and Glover, A.G., 2016. DNA barcoding uncovers cryptic diversity in 50% of deep-sea Antarctic polychaetes. *Royal Society Open Science*, *3*(11), p.160432. doi:10.1098/rsos.160432

Brandt, A., Błażewicz-Paszkowycz, M., Bamber, R.N., Mühlenhardt-Siegel, U., Malyutina, M.V., Kaiser, S., De Broyer, C. and Havermans, C., 2012. Are there widespread peracarid species in the deep sea (Crustacea: Malacostraca)?. *Polish Polar Research*, pp.139-162. doi:10.2478/v10183−012−0012−5

Brandt, A., Elsner, N., Brenke, N., Golovan, O., Malyutina, M.V., Riehl, T., Schwabe, E. and Würzberg, L., 2013. Epifauna of the Sea of Japan collected via a new epibenthic sledge equipped with camera and environmental sensor systems. *Deep Sea Research Part II: Topical Studies in Oceanography*, *86*, pp.43-55. doi:10.1016/j.dsr2.2012.07.039

Brandt, A. and Malyutina, M.V., 2015. The German-Russian deep-sea expedition KuramBio (Kurile Kamchatka biodiversity studies) on board of the RV *Sonne* in 2012 following the footsteps of the legendary expeditions with RV *Vityaz*. *Deep Sea Research Part II: Topical Studies in Oceanography*, *111*, pp.1-9. doi:10.1016/j.dsr2.2014.11.001

Brandt, A., Gutt, J., Hildebrandt, M., Pawlowski, J., Schwendner, J., Soltwedel, T. and Thomsen, L., 2016. Cutting the umbilical: new technological perspectives in benthic deep-sea research. *Journal of Marine Science and Engineering*, *4*(2), p.36. doi:10.3390/jmse4020036

Bregazzi, P.K., 1972. Life cycles and seasonal movements of *Cheirimedon femoratus* (Pfeffer) and *Tryphosella kergueleni* (Miers)(Crustacea: Amphipoda). *British Antarctic Survey Bulletin*, *30*, pp.1-34.

Briones, E.E., Rice, J. and Ardron, J., 2009. Global open oceans and deep seabed (GOODS) biogeographic classification. *UNESCO, IOC*, *54*.

Brito-Morales, I., Schoeman, D.S., Molinos, J.G., Burrows, M.T., Klein, C.J., Arafeh-Dalmau, N., Kaschner, K., Garilao, C., Kesner-Reyes, K. and Richardson, A.J., 2020. Climate velocity reveals increasing exposure of deep-ocean biodiversity to future warming. *Nature Climate Change*, *10*(6), pp.576-581. doi:10.1038/s41558-020-0773-5

Bühring, S.I. and Christiansen, B., 2001. Lipids in selected abyssal benthopelagic animals: links to the epipelagic zone?. *Progress in Oceanography*, *50*(1-4), pp.369-382. doi:10.1016/S0079-6611(01)00061-1

Bruun, A.F., 1956. Animal life of the deep-sea bottom. *The Galathea Deep Sea Expedition*, *1952*, pp.149-195.

Charette, M.A. and Smith, W.H., 2010. The volume of Earth's ocean. *Oceanography*, *23*(2), pp.112-114. doi:10.5670/oceanog.2010.51

Chevreux, E., 1889. Amphipodes nouveaux provenant des campagnes de l'Hirondelle 1887-1888. *Au Siège de la Société,* 14, pp.284-289.

Chevreux, E., 1899. Sur deux espèces géantes d'amphipodes provenant des campagnes du yacht Princesse Alice. *Bulletin de la Societe Zoologique de France*, 24, pp.152-158

Chevreux, E., 1905. Description d'un amphipode (*Katius obesus*, nov. gen. et sp.), suivie d'une liste des amphipodes de la tribu des Gammarina ramenés par le filet à grande ouverture pendant la dernière campagne de la Princesse-Alice en 1904. *Bulletin du Musée océanographique de Monaco*, 35, pp.1–7.

Chevreux, E., 1905. Diagnoses d'amphipodes nouveaux provenant des campagnes de la Princesse-Alice dans l'Atlantique nord. *Bulletin de l'Institut Océanographique*, 117, pp.1-13.

Chevreux, E., 1909. Diagnoses d'amphipodes nouveaux provenant des campagnes de la Princesse-Alice dans l'Atlantique Nord. *Bulletin de l'Institut Océanographique, Monaco*, 150, pp.1-7.

Chevreux, E., 1910. Diagnoses d'amphipodes nouveux provenant des campagnes de la Princesse-Alice dans l'Atlantique nord. *Bulletin de l'Institut Océanographique*, 156, pp.1-4.

Chevreux, E., 1919–1920. Note préliminaire sur les amphipodes recueillis par les expéditions du Travailleur et du Talisman (1880–1883). *Bulletin du Muséum National D'Histoire Naturelle*, *Paris*, 1919, pp.574-580.

Chiba, S., Saito, H., Fletcher, R., Yogi, T., Kayo, M., Miyagi, S., Ogido, M. and Fujikura, K., 2018. Human footprint in the abyss: 30-year records of deep-sea plastic debris. *Marine Policy*, *96*, pp.204-212. doi:10.1016/j.marpol.2018.03.022

Chakrabarty, P., Warren, M., Page, L.M. and Baldwin, C.C., 2013. GenSeq: An updated nomenclature and ranking for genetic sequences from type and non-type sources. *ZooKeys*, (346), p.29.

Christiansen, B., Pfannkuche, O. and Thiel, H., 1990. Vertical distribution and population structure of the necrophagous amphipod *Eurythenes gryllus* in the West European Basin. *Marine Ecology Progress Series*, pp.35-45.

Clarke, K.R., Somerfield, P.J. and Gorley, R.N., 2008. Testing of null hypotheses in exploratory community analyses: similarity profiles and biota-environment linkage. *Journal of Experimental Marine Biology and Ecology*, *366*(1-2), pp.56-69. https://doi10.1016/j.jembe.2008.07.009

Clarke, K.R. and Gorley, R.N., 2015. Getting started with PRIMER v7. *PRIMER-E: Plymouth, Plymouth Marine Laboratory*, *20*.

Coleman, C.O., 2003. "Digital inking": How to make perfect line drawings on computers. *Organisms Diversity and Evolution*, *3*(4), p.303.

Coleman, C.O., 2009. Drawing setae the digital way. *Zoosystematics and Evolution*, *85*(2), pp.305-310. doi:10.1002/zoos.200900008

Cornils, A. and Held, C., 2014. Evidence of cryptic and pseudocryptic speciation in the *Paracalanus parvus* species complex (Crustacea, Copepoda, Calanoida). *Frontiers in Zoology*, *11*(1), pp.1-17. doi:10.1186/1742-9994-11-19

Corrigan, L.J., Horton, T., Fotherby, H., White, T.A. and Hoelzel, A.R., 2014. Adaptive evolution of deep-sea amphipods from the superfamily Lysiassanoidea in the North Atlantic. *Evolutionary Biology*, *41*(1), pp.154-165. doi:10.1007/s11692-013-9255-2

Costa, C., Fanelli, E., Marini, S., Danovaro, R. and Aguzzi, J., 2020. Global deep-sea biodiversity research trends highlighted by science mapping approach. *Frontiers in Marine Science*, *7*, p.384. doi:10.3389/fmars.2020.00384

Cousins, N.J., Horton, T., Wigham, B.D. and Bagley, P.M., 2013. Abyssal scavenging demersal fauna at two areas of contrasting productivity on the Subantarctic Crozet Plateau, southern Indian Ocean. *African Journal of Marine Science*, *35*(2), pp.299-306. https://doi10.2989/1814232X.2013.802747

Cressey, D., 2014. Submersible loss hits research. *Nature News*, *509*(7501), p.408.

d'Udekem d'Acoz, C. and Havermans, C., 2015. Contribution to the systematics of the genus *Eurythenes* SI Smith in Scudder, 1882 (Crustacea: Amphipoda: Lysianassoidea: Eurytheneidae). *Zootaxa*, (1). doi:10.11646/zootaxa.3971.1.1

Dahl, E., 1959. Amphipoda from depths exceeding 6000 meters. In *Galathea Report*.

Dahl, E., 1979. Deep-sea carrion feeding amphipods: Evolutionary patterns in niche adaptation. *Oikos*, pp.167-175. doi:10.2307/3543994

Dallwitz, M.J., Paine, T.A. and Zurcher, E.J., 1999. User's guide to the DELTA Editor. (accessed 23 October 2018)

Daniell, J., Jorgensen, D.C., Anderson, T., Borissova, I., Burq, S., Heap, A., Hughes, M., Mantle, D., Nelson, G., Nichol, S. and Nicholson, C., 2010. Frontier basins of the west Australian continental margin: Post-survey report of marine reconnaissance and geological sampling survey GA2476.

Danovaro, R., Snelgrove, P.V. and Tyler, P., 2014. Challenging the paradigms of deep-sea ecology. *Trends in Ecology & Evolution*, *29*(8), pp.465-475. doi:10.1016/j.tree.2014.06.002

Danovaro, R., Fanelli, E., Aguzzi, J., Billett, D., Carugati, L., Corinaldesi, C., Dell'Anno, A., Gjerde, K., Jamieson, A.J., Kark, S. and McClain, C., 2020. Ecological variables for developing a global deep-ocean monitoring and conservation strategy. *Nature Ecology & Evolution*, *4*(2), pp.181-192. doi:10.1038/s41559-019-1091-z

de Queiroz, K., 2005. Ernst Mayr and the modern concept of species. *Proceedings of the National Academy of Sciences*, *102*(suppl 1), pp.6600-6607. doi:10.1073/pnas.0502030102

Deichmann, J.L., Mulcahy, D.G., Vanthomme, H., Tobi, E., Wynn, A.H., Zimkus, B.M. and McDiarmid, R.W., 2017. How many species and under what names? Using DNA barcoding and GenBank data for west Central African amphibian conservation. *PloS One*, *12*(11), p.e0187283. doi:10.13971/journal.prone.0187283

Diffenthal, M. and Horton, T., 2007. *Stephonyx arabiensis* (Crustacea: Amphipoda: Lysianassoidea: Uristidae), a new deep-water scavenger species from the Indian Ocean, with a key to the genus *Stephonyx*. *Zootaxa*, *1665*(31-4), p.1.

Dixon, D.R., Pruski, A.M. and Dixon, L.R., 2004. The effects of hydrostatic pressure change on DNA integrity in the hydrothermal-vent mussel *Bathymodiolus azoricus*: implications for future deep-sea mutagenicity studies. *Mutation Research/Fundamental and Molecular Mechanisms of Mutagenesis*, *552*(1-2), pp.235-246. doi:10.1016/j.mrfmmm.2004.06.026

Downing, A.B., Wallace, G.T. and Yancey, P.H., 2018. Organic osmolytes of amphipods from littoral to hadal zones: Increases with depth in trimethylamine N-oxide, scyllo-inositol and other potential pressure counteractants. *Deep Sea Research Part I: Oceanographic Research Papers*, *138*, pp.1-10. doi:10.1016/j.dsr.2018.05.008

Drummond, A.J., Ho, S.Y., Phillips, M.J. and Rambaut, A., 2006. Relaxed phylogenetics and dating with confidence. *PLoS Biology*, *4*(5), p.e88. doi:10.1371/journal.pbio.0040088

Drummond, A.J., Suchard, M.A., Xie, D. and Rambaut, A., 2012. Bayesian phylogenetics with BEAUti and the BEAST 1.7. *Molecular Biology and Evolution*, *29*(8), pp.1969-1973. doi:10.1093/molbev/mss075

Duffy, G.A., Gutteridge, Z.R., Thurston, M.H. and Horton, T., 2016. A comparative analysis of canyon and non-canyon populations of the deep-sea scavenging amphipod *Paralicella caperesca*. *Journal of the Marine Biological Association of the United Kingdom*, *96*(8), pp.1687-1699. doi:10.1017/S0025315415002064

Ebbe, B., Billett, D.S., Brandt, A., Ellingsen, K., Glover, A., Keller, S., Malyutina, M., Martínez Arbizu, P., Molodtsova, T., Rex, M. and Smith, C., 2010. Diversity of abyssal marine life. *Life in the World's Oceans: Diversity, Distribution, and Abundance, edited by: McIntyre, A*, pp.139-160.

Eldredge, N. and Cracraft, J.O.E.L., 1980. Phylogenetic patterns and the evolutionary process. New York: Columbia University Press.

Englisch, U., Coleman, C.O. and Wägele, J.W., 2003. First observations on the phylogeny of the families Gammaridae, Crangonyctidae, Melitidae, Niphargidae, Megaluropidae and Oedicerotidae (Amphipoda, Crustacea), using small subunit rDNA gene sequences. *Journal of Natural History*, *37*(20), pp.2461-2486. doi:10.1080/00222930210144352

Escobar-Briones, E., Nájera-Hillman, E. and Álvarez, F., 2010. Unique 16S rRNA sequences of *Eurythenes gryllus* (Crustacea: Amphipoda: Lysianassidae) from the Gulf of Mexico abyssal plain. *Revista Mexicana de Biodiversidad*, *81*, pp.177-185.

Eustace, R.M., Kilgallen, N.M., Lacey, N.C. and Jamieson, A.J., 2013. Population structure of the hadal amphipod *Hirondellea gigas* (Amphipoda: Lysianassoidea) from the Izu-Bonin Trench. *Journal of Crustacean Biology*, *33*(6), pp.793-801. doi:10.1163/1937240X-00002193

Eustace, R.M., Ritchie, H., Kilgallen, N.M., Piertney, S.B. and Jamieson, A.J., 2016. Morphological and ontogenetic stratification of abyssal and hadal *Eurythenes gryllus* sensu lato (Amphipoda: Lysianassoidea) from the Peru–Chile Trench. *Deep Sea Research Part I: Oceanographic Research Papers*, *109*, pp.91-98. doi:10.1016/j.dsr.2015.11.005

Ezard, T., Fujisawa, T. and Barraclough, T., 2015. R package *splits*: SPecies' LImits by Threshold Statistics, version 1.0-19/r52. https://R-Forge.R-project.org/projects/splits/

Feinerer, I., Hornik, K., and Meyer, D. 2008. Text mining infrastructure in R. *Journal of Statistical Software*, *25*(5), pp.1-54.

Foekema, E.M., De Gruijter, C., Mergia, M.T., van Franeker, J.A., Murk, A.J. and Koelmans, A.A., 2013. Plastic in north sea fish. *Environmental Science & Technology*, *47*(15), pp.8818-8824. doi:10.1021/es400931b.

Folmer, O., Black, M., Hoeh, W., Lutz, R. and Vrijenhoek, R., 1994. DNA primers for amplification of mitochondrial cytochrome c oxidase subunit I from diverse metazoan invertebrates. *Molecular Marine Biological Biotechonology*, 3, 294–299.

Forrest, A., Giacovazzi, L., Dunlop, S., Reisser, J., Tickler, D., Jamieson, A. and Meeuwig, J.J., 2019. Eliminating plastic pollution: How a voluntary contribution from industry will drive the circular plastics economy. *Frontiers in Marine Science*, *6*, p.627. doi:3389/fmars.2019.00627

France, S.C. and Kocher, T.D., 1996. Geographic and bathymetric patterns of mitochondrial 16S rRNA sequence divergence among deep-sea amphipods, *Eurythenes gryllus*. *Marine Biology*, *126*(4), pp.633-643.

Fujii, T., Kilgallen, N.M., Rowden, A.A. and Jamieson, A.J., 2013. Deep-sea amphipod community structure across abyssal to hadal depths in the Peru-Chile and Kermadec trenches. *Marine Ecology Progress Series*, *492*, pp.125-138.

Gagnon, K., Chadwell, C.D. and Norabuena, E., 2005. Measuring the onset of locking in the Peru–Chile Trench with GPS and acoustic measurements. *Nature*, *434*(7030), pp.205-208. doi:10.1038/nature03412

Garlitska, L., Neretina, T., Schepetov, D., Mugue, N., De Troch, M., Baguley, J.G. and Azovsky, A., 2012. Cryptic diversity of the 'cosmopolitan' harpacticoid copepod *Nannopus palustris*: Genetic and morphological evidence. *Molecular Ecology*, *21*(21), pp.5336-5347. doi:10.1111/mec.12016

GEBCO, 2015. GEBCO_2014 Grid [WWWDocument]. Gen.Bathymetr.ChartOcean. (URL) ⟨http://www.gebco.net/data_and_products/gridded_bathymetry_data/gebco_30_second_grid/⟩ (accessed 05.11.19).

Geersen, J., Voelker, D. and Behrmann, J.H., 2018. Oceanic trenches. In *Submarine Geomorphology* (pp. 409-424). Springer, Cham.

Geersen, J., 2019. Sediment-starved trenches and rough subducting plates are conducive to tsunami earthquakes. *Tectonophysics*, *762*, pp.28-44. doi:10.1016/j.tecto.2019.04.024

Geyer, R., Jambeck, J.R. and Law, K.L., 2017. Production, use, and fate of all plastics ever made. *Science Advances*, *3*(7), p.e1700782. doi:10.1126/sciadv.1700782

Glover, A.G., Wiklund, H., Chen, C. and Dahlgren, T.G., 2018. Point of View: Managing a sustainable deep-sea 'blue economy' requires knowledge of what actually lives there. *Elife*, *7*, p.e41319.

Glud, R.N., Wenzhöfer, F., Middelboe, M., Oguri, K., Turnewitsch, R., Canfield, D.E. and Kitazato, H., 2013. High rates of microbial carbon turnover in sediments in the deepest oceanic trench on Earth. *Nature Geoscience*, *6*(4), pp.284-288. doi:10.1038/ngeo1773

Glud, R.N., Berg, P., Thamdrup, B., Larsen, M., Stewart, H.A., Jamieson, A.J., Glud, A., Oguri, K., Sanei, H., Rowden, A.A. and Wenzhöfer, F., 2021. Hadal trenches are dynamic hotspots for early diagenesis in the deep sea. *Communications Earth & Environment*, *2*(1), pp.1-8. doi:10.1038/s43247-020-00087-2

Grassle, J.F. and Maciolek, N.J., 1992. Deep-sea species richness: Regional and local diversity estimates from quantitative bottom samples. *The American Naturalist*, *139*(2), pp.313-341.

Greenville, A.C., Dickman, C.R. and Wardle, G.M., 2017. 75 years of dryland science: Trends and gaps in arid ecology literature. *PloS One*, *12*(4), p.e0175014. doi:10.1371/journal.pone.0175014

Griffiths, C.L., 1977. Deep-sea amphipods from west of Cape Point, South Africa. *Annals of the South African Museum*, 73, pp.93-104.

Hornik, K. and Grün, B., 2011. *topicmodels*: An R package for fitting topic models. *Journal of Statistical Software*, *40*(13), pp.1-30. doi:10.18637/jss.v040.i13

Guggolz, T., Meißner, K., Schwentner, M., Dahlgren, T.G., Wiklund, H., Bonifácio, P. and Brandt, A., 2020. High diversity and pan-oceanic distribution of deep-sea polychaetes: *Prionospio* and *Aurospio* (Annelida: Spionidae) in the Atlantic and Pacific Ocean. *Organisms Diversity & Evolution*, pp.1-17. doi:10.1007/s13127-020-00430-7

Guindon, S., Dufayard, J.F., Lefort, V., Anisimova, M., Hordijk, W. and Gascuel, O., 2010. New algorithms and methods to estimate maximum-likelihood phylogenies: assessing the performance of PhyML 3.0. *Systematic Biology*, *59*(3), pp.307-321. doi:10.1093/sysbio/syq010

Hampel, A., Kukowski, N., Bialas, J., Huebscher, C. and Heinbockel, R., 2004. Ridge subduction at an erosive margin: The collision zone of the Nazca Ridge in southern Peru. *Journal of Geophysical Research: Solid Earth*, *109*(B2). doi:10.1029/2003JB002593

Hansen, J., Sato, M., Russell, G. and Kharecha, P., 2013. Climate sensitivity, sea level and atmospheric carbon dioxide. *Philosophical Transactions of the Royal Society A: Mathematical, Physical and Engineering Sciences*, *371*(2001), p.20120294. doi:10.1098/rsta.2012.0294

Hargrave, B.T., 1985. Feeding rates of abyssal scavenging amphipods (*Eurythenes gryllus*) determined in situ by time-lapse photography. *Deep Sea Research Part A. Oceanographic Research Papers*, *32*(4), pp.443-450. doi:10.1016/0198-0149(85)90090-1

Hasegawa, M., Kishino, H. and Yano, T.A., 1985. Dating of the human-ape splitting by a molecular clock of mitochondrial DNA. *Journal of Molecular Evolution*, *22*(2), pp.160-174.

Havermans, C., Nagy, Z.T., Sonet, G., De Broyer, C. and Martin, P., 2010. Incongruence between molecular phylogeny and morphological classification in amphipod crustaceans: A case study of Antarctic lysianassoids. *Molecular Phylogenetics and Evolution*, *55*(1), pp.202-209. doi:10.1016/j.ympev.2009.10.025

Havermans, C., Sonet, G., d'Acoz, C.D.U., Nagy, Z.T., Martin, P., Brix, S., Riehl, T., Agrawal, S. and Held, C., 2013. Genetic and morphological divergences in the cosmopolitan deep-sea amphipod *Eurythenes gryllus* reveal a diverse abyss and a bipolar species. *PLoS One*, *8*(9), p.e74218. doi:10.1371/journal.pone.0074218

Havermans, C., 2016. Have we so far only seen the tip of the iceberg? Exploring species diversity and distribution of the giant amphipod *Eurythenes*. *Biodiversity*, *17*(1-2), pp.12-25. doi:10.1080/14888386.2016.1172257

Havermans, C. and Smetacek, V., 2018. Bottom-up and top-down triggers of diversification: A new look at the evolutionary ecology of scavenging amphipods in the deep sea. *Progress in Oceanography*, *164*, pp.37-51. doi:10.1016/j.pocean.2018.04.008

Hendry, A.P., Bolnick, D.I., Berner, D. and Peichel, C.L., 2009. Along the speciation continuum in sticklebacks. *Journal of Fish Biology*, *75*(8), pp.2000-2036. https://doi10.1111/j.1095-8649.2009.02419.x

Hendrycks, E.A. and Conlan, K.E., 2003. New and unusual abyssal gammaridean Amphipoda from the north-east Pacific. *Journal of Natural History*, *37*(19), pp.2303-2368. https://doi10.1080/00222930210138926

Hendrycks, E.A., 2007. A new species of *Valettiopsis* Holmes, 1908 (Crustacea: Gammaridea: Lysianassoidea) from abyssal waters off California. *Zootaxa*, *1501*(1), pp.45-56.

Herold, N., Huber, M., Müller, R.D. and Seton, M., 2012. Modeling the Miocene Climatic Optimum: Ocean circulation. *Paleoceanography*, *27*(1). doi:10.1029/2010PA002041

Herrera, S., Reyes-Herrera, P.H. and Shank, T.M., 2015. Predicting RAD-seq marker numbers across the eukaryotic tree of life. *Genome Biology and Evolution*, *7*(12), pp.3207-3225. doi:10.1093/gbe/evv210

Hessler, R.R., Ingram, C.L., Yayanos, A.A. and Burnett, B.R., 1978. Scavenging amphipods from the floor of the Philippine Trench. *Deep Sea Research*, *25*(11), pp.1029-1047.

Hiraoka, S., Hirai, M., Matsui, Y., Makabe, A., Minegishi, H., Tsuda, M., Rastelli, E., Danovaro, R., Corinaldesi, C., Kitahashi, T. and Tasumi, E., 2020. Microbial community and geochemical analyses of trans-trench sediments for understanding the roles of hadal environments. *The ISME Journal*, *14*(3), pp.740-756. https://doi10.1038/s41396-019-0564-z

Hofreiter, M., Serre, D., Poinar, H.N., Kuch, M. and Pääbo, S., 2001. Ancient DNA. *Nature Reviews Genetics*, *2*(5), pp.353-359.

Holmes, S.J., 1908. The Amphipoda collected by the US Bureau of Fisheries steamer Albatross off the west coast of North America, in 1903 and 1904, with descriptions of a new family and several new genera and species. *Proceedings of the United States National Museum*, 35, pp.489-543.

Holmquist, J.G., 1985. The grooming behavior of the terrestrial amphipod *Talitroides alluaudi*. *Journal of Crustacean Biology*, *5*(2), pp.334-340. doi:10.2307/1547882

Horn, D.A., Granek, E.F. and Steele, C.L., 2020. Effects of environmentally relevant concentrations of microplastic fibers on Pacific mole crab (*Emerita analoga*) mortality and reproduction. *Limnology and Oceanography Letters*, *5*(1), pp.74-83. doi:10.1002/lol2.10137

Horton, T., 2004. Revision of the amphipod genus *Valettiopsis* Holmes, (Crustacea: Lysianassoidea), with the addition of three new species. *Journal of Natural History*, *38*(14), pp.1735-1755.

Horton, T. and Thurston, M.H., 2014. A revision of the bathyal and abyssal necrophage genus *Cyclocaris* Stebbing, 1888 (Crustacea: Amphipoda: Cyclocaridae) with the addition of two new species from the Atlantic Ocean. *Zootaxa*, *3796*(3), pp.507-527. http://dx.doi.org/10.11646/zootaxa.3796.3.6

Horton, T., Cooper, H., Vlierboom, R., Thurston, M., Hauton, C. and Young, C.R., 2020. Molecular phylogenetics of deep-sea amphipods (*Eurythenes*) reveal a new undescribed species at the Porcupine Abyssal Plain, North East Atlantic Ocean. *Progress in Oceanography*, *183*, p.102292. doi:10.1016/j.pocean.2020.102292

Hurley, D.E., 1963. Amphipoda of the Family Lysianassidae from the West Coast of North and Central America. University of Southern California Press.

Ichino, M.C., Clark, M.R., Drazen, J.C., Jamieson, A., Jones, D.O., Martin, A.P., Rowden, A.A., Shank, T.M., Yancey, P.H. and Ruhl, H.A., 2015. The distribution of benthic biomass in hadal trenches: A modelling approach to investigate the effect of vertical and lateral organic matter transport to the seafloor. *Deep Sea Research Part I: Oceanographic Research Papers*, *100*, pp.21-33. doi:10.1016/j.dsr.2015.01.010

Ingram, C.L. and Hessler, R.R., 1983. Distribution and behavior of scavenging amphipods from the central North Pacific. *Deep Sea Research Part A. Oceanographic Research Papers*, *30*(7), pp.683-706. http://dx.doi.org/10.1016/0198-0149(83)90017-1

Ingram, C.L. and Hessler, R.R., 1987. Population biology of the deep-sea amphipod *Eurythenes gryllus*: Inferences from instar analyses. *Deep Sea Research Part A. Oceanographic Research Papers*, *34*(12), pp.1889-1910.

Intergovernmental Oceanographic Commission, 2001. Standardization of undersea feature names–Guidelines, proposal form terminology. *International Hydrographic Bureau, Monaco*.

Jamieson, A.J., Fujii, T., Solan, M. and Priede, I.G., 2009. HADEEP: Free-falling landers to the deepest places on Earth. *Marine Technology Society Journal*, *43*(5), pp.151-160.

Jamieson, A.J., Fujii, T., Mayor, D.J., Solan, M. and Priede, I.G., 2010. Hadal trenches: The ecology of the deepest places on Earth. *Trends in Ecology & Evolution*, *25*(3), pp.190-197. doi:10.1016/j.tree.2009.09.009

Jamieson, A.J., 2011. Ecology of deep oceans: Hadal trenches. In: Encyclopedia of Life Sciences (ELS). John Wiley & Sons, Ltd, Chichester. doi:10.1002/9780470015902.a0023606

Jamieson, A.J., Kilgallen, N.M., Rowden, A.A., Fujii, T., Horton, T., Lörz, A.N., Kitazawa, K. and Priede, I.G., 2011. Bait-attending fauna of the Kermadec Trench, SW Pacific Ocean:Eevidence for an ecotone across the abyssal–hadal transition zone. *Deep Sea Research Part I: Oceanographic Research Papers*, *58*(1), pp.49-62. doi:10.1016/j.dsr.2010.11.003

Jamieson, A.J., Lacey, N.C., Lörz, A.N., Rowden, A.A. and Piertney, S.B., 2013. The supergiant amphipod *Alicella gigantea* (Crustacea: Alicellidae) from hadal depths in the Kermadec Trench, SW Pacific Ocean. *Deep Sea Research Part II: Topical Studies in Oceanography*, *92*, pp.107-113. doi:10.1016/j.dsr2.2012.12.002

Jamieson, A., 2015. The hadal zone: life in the deepest oceans. Cambridge University Press.

Jamieson, A.J., 2016. Landers: Baited cameras and traps., In: *Biological Sampling in* the Deep Sea (Eds. M. Clarke, M. Consalvey, A.A. Rowden), Wiley-Blackwell, Oxford, pp.228-259.

Jamieson, A.J., Malkocs, T., Piertney, S.B., Fujii, T. and Zhang, Z. 2017. Bioaccumulation of persistent organic pollutants in the endemic keystone fauna in the deepest ocean habitat. *Nature Ecology & Evolution*, 1, pp.51. doi:10.1038/s41559-016-0051

Jamieson, A.J., 2018. A contemporary perspective on hadal science. *Deep Sea Research Part II: Topical Studies in Oceanography*, *155*, pp.4-10. https://doi10.1016/j.dsr2.2018.01.005

Jamieson, A.J., Brooks, L.S.R., Reid, W.D., Piertney, S.B., Narayanaswamy, B.E. and Linley, T.D., 2019. Microplastics and synthetic particles ingested by deep-sea amphipods in six of the deepest marine ecosystems on Earth. *Royal Society Open Science*, *6*(2), p.180667. http://dx.doi.org/10.1098/rsos.180667

Jamieson, A.J., Ramsey, J. and Lahey, P., 2019. Hadal manned submersible. *Sea Technology*, 60(9), pp.22-24.

Jamieson, A.J., Stewart, H.A. and Nargeolet, P.H., 2020. Exploration of the Puerto Rico Trench in the mid-twentieth century: Today's significance and relevance. *Endeavour*, *44*(1-2), p.100719. doi:10.1016/j.endeavour.2020.100719

Jamieson, A.J. and Vecchione, M., 2020. First in situ observation of Cephalopoda at hadal depths (Octopoda: Opisthoteuthidae: Grimpoteuthis sp.). *Marine Biology*, *167*(6), pp.1-5. doi:10.1007/s00227-020-03701-1

Jamieson, A.J. and Stewart, H.A., 2021. Hadal zones of the Northwest Pacific Ocean. *Progress in Oceanography*, *190*, p.102477. doi:10.1016/j.pocean.2020.102477

Johnson, W.S., Stevens, M. and Watling, L., 2001. Reproduction and development of marine peracaridans. *Advances in Marine Biology*, 39, pp.105–260. http://dx.doi.org/10.1016/S0065-2881(01)39009-0

Jażdżewska, A.M. and Mamos, T., 2019. High species richness of Northwest Pacific deep-sea amphipods revealed through DNA barcoding. *Progress in Oceanography*, *178*, p.102184. doi:10.1016/j.pocean.2019.102184

Katoh, K., Rozewicki, J. and Yamada, K.D., 2019. MAFFT online service: multiple sequence alignment, interactive sequence choice and visualization. *Briefings in Bioinformatics*, *20*(4), pp.1160-1166. doi:10.1093/bib/bbx108

Kaufmann, R.S., 1994. Structure and function of chemoreceptors in scavenging lysianassoid amphipods. *Journal of Crustacean Biology*, *14*(1), pp.54-71.

Kawabe, M. and Fujio, S., 2010. Pacific Ocean circulation based on observation. *Journal of Oceanography*, *66*(3), pp.389-403.

Kilgallen, N.M., 2015. Three new species of *Hirondellea* (Crustacea, Amphipoda, Hirondelleidae) from hadal depths of the Peru-Chile Trench. *Marine Biology Research*, *11*(1), pp.34-48. http://dx.doi.org/10.1080/17451000.2014.889309

Kilgallen, N.M. and Lowry, J.K., 2015. A review of the scopelocheirid amphipods (Crustacea, Amphipoda, Lysianassoidea), with the description of new taxa from Australian waters. *Zoosystematics and Evolution*, *91*, p.1. https://doi10.3897/zse.91.8440

Kimura, M., 1980. A simple method for estimating evolutionary rates of base substitutions through comparative studies of nucleotide sequences. *Journal of Molecular Evolution*, *16*(2), pp.111-120.

King, N.J. and Priede, I.G., 2008. *Coryphaenoides armatus*, the Abyssal Grenadier: global distribution, abundance, and ecology as determined by baited landers. In *American Fisheries Society Symposium* (Vol. 63, pp. 139-161). American Fisheries Society.

Kitson, J.J., Hahn, C., Sands, R.J., Straw, N.A., Evans, D.M. and Lunt, D.H., 2019. Detecting host-parasitoid interactions in an invasive Lepidopteran using nested tagging DNA metabarcoding. *Molecular Ecology*, *28*(2), pp.471-483. doi:10.1111/mec.14518

Klages, M. and Gutt, J., 1990. Comparative studies on the feeding behaviour of high Antarctic amphipods (Crustacea) in laboratory. *Polar Biology*, *11*(1), pp.73-79. doi:10.1007/BF00236524

Kobayashi, H., Hatada, Y., Tsubouchi, T., Nagahama, T. and Takami, H., 2012. The hadal amphipod *Hirondellea gigas* possessing a unique cellulase for digesting wooden debris buried in the deepest seafloor. *PLoS One*, *7*(8), p.e42727.

Krishna, K.S., Bull, J.M., Ishizuka, O., Scrutton, R.A., Jaishankar, S. and Banakar, V.K., 2014. Growth of the Afanasy Nikitin seamount and its relationship with the 85 E Ridge, northeastern Indian Ocean. *Journal of Earth System Science*, *123*(1), pp.33-47.

Kumar, S., Stecher, G. and Tamura, K., 2016. MEGA7: molecular evolutionary genetics analysis version 7.0 for bigger datasets. *Molecular Biology and Evolution*, *33*(7), pp.1870-1874. doi:10.1093/molbev/msw054

Kyo, M., Hiyazaki, E., Tsukioka, S., Ochi, H., Amitani, Y., Tsuchiya, T., Aoki, T. and Takagawa, S., 1995, October. The sea trial of" KAIKO", the full ocean depth research ROV. In *'Challenges of Our Changing Global Environment'. Conference Proceedings. OCEANS'95 MTS/IEEE* (Vol. 3, pp. 1991-1996). IEEE.

Lacey, N.C., Rowden, A.A., Clark, M.R., Kilgallen, N.M., Linley, T., Mayor, D.J. and Jamieson, A.J., 2016. Community structure and diversity of scavenging amphipods from bathyal to hadal depths in three South Pacific Trenches. *Deep Sea Research Part I: Oceanographic Research Papers*, *111*, pp.121-137. doi:10.1016/j.dsr.2016.02.014

Lacey, N.C., Mayor, D.J., Linley, T.D. and Jamieson, A.J., 2018. Population structure of the hadal amphipod *Bathycallisoma* (*Scopelocheirus*) *schellenbergi* in the Kermadec Trench and New Hebrides Trench, SW Pacific. *Deep Sea Research Part II: Topical Studies in Oceanography*, *155*, pp.50-60. doi:10.1016/j.dsr2.2017.05.001

Larter, R.D., Vanneste, L.E., Morris, P. and Smythe, D.K., 2003. Structure and tectonic evolution of the South Sandwich arc. *Geological Society, London, Special Publications*, *219*(1), pp.255-284. doi:10.1144/GSL.SP.2003.219.01.13

Lau, S.C., Wilson, N.G., Silva, C.N. and Strugnell, J.M., 2020. Detecting glacial refugia in the Southern Ocean. *Ecography*, *43*(11), pp.1639-1656. doi:10.1111/ecog.04951

Leduc, D., Rowden, A.A., Glud, R.N., Wenzhöfer, F., Kitazato, H. and Clark, M.R., 2016. Comparison between infaunal communities of the deep floor and edge of the Tonga Trench: Possible effects of differences in organic matter supply. *Deep Sea Research Part I: Oceanographic Research Papers*, *116*, pp.264-275. doi:10.1016/j.dsr.2015.11.003

Leray, M., Yang, J.Y., Meyer, C.P., Mills, S.C., Agudelo, N., Ranwez, V., Boehm, J.T. and Machida, R.J., 2013. A new versatile primer set targeting a short fragment of the mitochondrial COI region for metabarcoding metazoan diversity: application for characterizing coral reef fish gut contents. *Frontiers in Zoology*, *10*(1), pp.1-14. doi:10.1186/1742-9994-10-34

Lichtenstein, H. 1822. Crustacea. In: Mandt MG (Ed), Observationes in historiam naturalem et anatomiam comparatam in itinere Groenlandico factae. Dissertatio in auguralis quam consensu et auctoritate gratiosi medicorumordinis in universitate literaria berolinensi ut summi in medicina et chirurgia honores rite sibi concedantur die XXII. M. Iulii A. MDCCCXXII H.L.Q.S., publice defendet auctor Martinus Gulielmus Mandt Beyenburgensis. Opponentibus: J.Th. v. Brandt Med. Cd., J. Ollenroth Med. Cd., E. Gabler Med. Cd.; Formis Brueschckianis, Berlin, pp.31–37.

Lincoln, R.J. and MH, T., 1983. *Valettietta*, a new genus of deep-sea amphipod (Gammaridea: Lysianassidae) with descriptions of two new species from the North Atlantic Ocean.

Linley, T.D., Gerringer, M.E., Yancey, P.H., Drazen, J.C., Weinstock, C.L. and Jamieson, A.J., 2016. Fishes of the hadal zone including new species, in situ observations and depth records of Liparidae. *Deep Sea Research Part I: Oceanographic Research Papers*, *114*, pp.99-110. doi:10.1016/j.dsr.2016.05.003

Linley, T.D., Stewart, A.L., McMillan, P.J., Clark, M.R., Gerringer, M.E., Drazen, J.C., Fujii, T. and Jamieson, A.J., 2017. Bait attending fishes of the abyssal zone and hadal boundary: Community structure, functional groups and species distribution in the Kermadec, New Hebrides and Mariana trenches. *Deep Sea Research Part I: Oceanographic Research Papers*, *121*, pp.38-53. doi:10.1016/j.dsr.2016.12.009

Longhurst, A., Sathyendranath, S., Platt, T. and Caverhill, C., 1995. An estimate of global primary production in the ocean from satellite radiometer data. *Journal of Plankton Research*, *17*(6), pp.1245-1271.

Lowry, J.K. and De Broyer, C., 2008. Alicellidae and Valettiopsidae, two new callynophorate families (Crustacea: Amphipoda). *Zootaxa*, *1843*(1), pp.57-66.

Lowry, J.K. and Kilgallen, N.M., 2014. A generic review of the lysianassoid family Uristidae and descriptions of new taxa from Australian waters (Crustacea, Amphipoda, Uristidae). *Zootaxa*, *3867*(1), pp.1-92.

Lowry, J.K. and Stoddart, H.E., 1989. *Stephonyx*, a new, widespread genus of lysianassoid Amphipoda. *Zoologica Scripta*, *18*(4), pp.519-525. doi:10.11646/zootaxa.3867.1.1

Lowry, J.K. and Stoddart, H.E., 1996. New lysianassoid amphipod species from Namibia and Madagascar (Lysianassidae Dana, 1849 and Podoprionidae fam. nov.). *Bollettino del Museo Civico di Storia Naturale di Verona*, *20*, pp.225-247.

Lowry, J.K. and Stoddart, H.E., 2011. The new deep-sea families Cebocaridae fam. nov., Cyclocaridae fam. nov. and Thoriellidae fam. nov. (Crustacea: Amphipoda: Lysianassoidea). *Zootaxa*, *2747*(1), pp.53-68.

Lusher, A.L., O'Donnell, C., Officer, R. and O'Connor, I., 2016. Microplastic interactions with North Atlantic mesopelagic fish. *ICES Journal of Marine Science*, *73*(4), pp.1214-1225. doi:10.1093/icesjms/fsv241

Macdonald, P.D.M., 2018. *mixdist*: Finite Mixture Distribution Models. R package version 0.5-4. https://cran.r-project.org/web/packages/mixdist/index.html. Accessed 17 March 2018

Madsen, F.J., 1961. On the zoogeography and origin of the abyssal fauna. *Galathea Rep*, *4*, pp.177-218.

Mair, L., Mill, A.C., Robertson, P.A., Rushton, S.P., Shirley, M.D., Rodriguez, J.P. and McGowan, P.J., 2018. The contribution of scientific research to conservation planning. *Biological Conservation*, *223*, pp.82-96. doi:10.1016/j.biocon.2018.04.037

Markmann, M. and Tautz, D., 2005. Reverse taxonomy: an approach towards determining the diversity of meiobenthic organisms based on ribosomal RNA signature sequences. *Philosophical Transactions of the Royal Society B: Biological Sciences*, *360*(1462), pp.1917-1924. doi:10.1098/rstb.2005.1723

Marghany, M., Mansor, S. and Shariff, A.R.B.M., 2016, June. Genetic algorithm for investigating flight MH370 in Indian Ocean using remotely sensed data. In *IOP Conference Series: Earth and Environmental Science* (Vol. 37, No. 1, p. 012001). IOP Publishing. https://doi10.1088/1755-1315/37/1/012001

Mayer, L., Jakobsson, M., Allen, G., Dorschel, B., Falconer, R., Ferrini, V., Lamarche, G., Snaith, H. and Weatherall, P., 2018. The Nippon Foundation—GEBCO Seabed 2030 project: The quest to see the world's oceans completely mapped by 2030. *Geosciences*, *8*(2), p.63. https://doi 10.3390/geosciences8020063

McClain, C.R. and Hardy, S.M., 2010. The dynamics of biogeographic ranges in the deep sea. *Proceedings of the Royal Society B: Biological Sciences*, *277*(1700), pp.3533-3546. http://dx.doi.org/10.1098/rspb.2010.1057

Millard, J.W., Freeman, R. and Newbold, T., 2020. Text-analysis reveals taxonomic and geographic disparities in animal pollination literature. *Ecography*, *43*(1), pp.44-59. doi:10.1111/ecog.04532

Mills, S., Leduc, D., Drazen, J.C., Yancey, P., Jamieson, A.J., Clark, M.R., Rowden, A.A., Mayor, D.J., Piertney, S., Heyl, T. and Bartlett, D., 2016. 10,000 m under the sea: An overview of the HADES expedition to Kermadec Trench. In *Kermadec Discoveries and Connections* (pp. 36-38).

Milne Edwards, H., 1848. Sur un crustacé amphipode, remarquable par sa grande taille. In *Annales des Sciences Naturelles* (Vol. 3, No. 9, p. 398).

Momma, H., Watanabe, M., Hashimoto, K. and Tashiro, S., 2004, January. Loss of the full ocean depth ROV kaiko-Part 1: ROV Kaiko — A review. In *The Fourteenth International Offshore and Polar Engineering Conference*. International Society of Offshore and Polar Engineers, pp.191-193.

Montecino, V. and Lange, C.B., 2009. The Humboldt Current System: Ecosystem components and processes, fisheries, and sediment studies. *Progress in Oceanography*, *83*(1-4), pp.65-79. doi:10.1016/j.pocean.2009.07.041

Murakami, A., Thompson, P., Hunston, S. and Vajn, D., 2017. 'What is this corpus about?': Using topic modelling to explore a specialised corpus. *Corpora*, *12*(2), pp.243-277. doi:10.3366/cor.2017.0118

Murphy, F., Ewins, C., Carbonnier, F. and Quinn, B., 2016. Wastewater treatment works (WwTW) as a source of microplastics in the aquatic environment. *Environmental Science & Technology*, *50*(11), pp.5800-5808. doi:10.1021/acs.est.5b05416

Narahara, Y., Tomikawa, K. and Torigoe, K., 2012. Four species of the genus *Stephonyx* (Crustacea: Amphipoda: Uristidae) from Japan, with description of a new species. *Journal of Natural History*, *46*(23-24), pp.1477-1507. doi:10.1080/00222933.2012.675598

Narahara-Nakano, Y., Nakano, T. and Tomikawa, K., 2018. Deep-sea amphipod genus Eurythenes from Japan, with a description of a new *Eurythenes* species from off Hokkaido (Crustacea: Amphipoda: Lysianassoidea). *Marine Biodiversity*, *48*(1), pp.603-620. doi:10.1007/s12526-017-0758-4

Nikita, M., 2019. *ldatuning*: Tuning of the Latent Dirichlet Allocation Models Parameters. R package version 1.0.0. https://CRAN.R-project.org/package=ldatuning

Oberacker, P., Stepper, P., Bond, D.M., Höhn, S., Focken, J., Meyer, V., Schelle, L., Sugrue, V.J., Jeunen, G.J., Moser, T. and Hore, S.R., 2019. Bio-On-Magnetic-Beads (BOMB): Open platform for high-throughput nucleic acid extraction and manipulation. *PLoS Biology*, *17*(1), p.e3000107. doi:10.1371/journal.pbio.3000107

Oguri, K., Kawamura, K., Sakaguchi, A., Toyofuku, T., Kasaya, T., Murayama, M., Fujikura, K., Glud, R.N. and Kitazato, H., 2013. Hadal disturbance in the Japan Trench induced by the 2011 Tohoku–Oki Earthquake. *Scientific Reports*, *3*(1), pp.1-6. doi:10.1038/srep01915

Olierook, H.K., Merle, R.E., Jourdan, F., Sircombe, K., Fraser, G., Timms, N.E., Nelson, G., Dadd, K.A., Kellerson, L. and Borissova, I., 2015. Age and geochemistry of magmatism on the oceanic Wallaby Plateau and implications for the opening of the Indian Ocean. *Geology*, *43*(11), pp.971-974. https://doi10.1130/G37044.1

Padial, J.M., Miralles, A., De la Riva, I. and Vences, M., 2010. The integrative future of taxonomy. *Frontiers in Zoology*, *7*(1), pp.1-14. doi:10.1186/1742-9994-7-16

Palumbi, S.R., 1994. Genetic divergence, reproductive isolation, and marine speciation. *Annual Review of Ecology and Systematics*, *25*(1), pp.547-572. doi:10.1146/annurev.es.25.110194.002555

Palumbi, S., Martin, A. and Romano, S., 2002. The simple fool's guide to PCR, version 2.0. University of Hawaii, Honolulu, 45.

Peng, G., Bellerby, R., Zhang, F., Sun, X. and Li, D., 2020. The ocean's ultimate trashcan: Hadal trenches as major depositories for plastic pollution. *Water Research*, *168*, p.115121. doi:10.1016/j.watres.2019.115121

Peng, X., Chen, M., Chen, S., Dasgupta, S., Xu, H., Ta, K., Du, M., Li, J., Guo, Z. and Bai, S., 2018. Microplastics contaminate the deepest part of the world's ocean. *Geochemical Perspectives Letters*, *9*(1), pp.1-5. doi:10.7185/geochemlet.1829

Peoples, L.M., Norenberg, M., Price, D., McGoldrick, M., Novotny, M., Bochdansky, A. and Bartlett, D.H., 2019. A full-ocean-depth rated modular lander and pressure-retaining sampler capable of collecting hadal-endemic microbes under *in situ* conditions. *Deep Sea Research Part I: Oceanographic Research Papers*, *143*, pp.50-57. doi:10.1016/j.dsr.2018.11.010

Perrone, F.M., Dell'Anno, A., Danovaro, R., Croce, N.D. and Thurston, M.H., 2002. Population biology of *Hirondellea* sp. nov.(Amphipoda: Gammaridea: Lysianassoidea) from the Atacama Trench (south-east Pacific Ocean). *Journal of the Marine Biological Association of the UK*, *82*(3), pp.419-425.

Pinheiro, J., Bates, D., DebRoy, S., Sarkar, D. and R Core Team, 2020. *nlme*: Linear and Nonlinear Mixed Effects Models. R package version 3.1-148, https://CRAN.R-project.org/package=nlme

Premke, K., Klages, M. and Arntz, W.E., 2006. Aggregations of Arctic deep-sea scavengers at large food falls: temporal distribution, consumption rates and population structure. *Marine Ecology Progress Series*, *325*, pp.121-135. https://doi.org/10.3354/meps325121

Premke, K. and Graeve, M., 2009. Metabolism and physiological traits of the deep-sea amphipod *Eurythenes gryllus*. *Vie et Milieu-Life and Environment*, *59*(3/4), pp.251-260.

Team, R.C., 2017. R: A language and environment for statistical computing. R Foundation for Statistical Computing, Vienna, Austria. URL https://www.R-project.org/. Accessed 15 November 2017

Rambaut, A., Drummond, A.J., Xie, D., Baele, G. and Suchard, M.A., 2018. Posterior summarization in Bayesian phylogenetics using Tracer 1.7. *Systematic Biology*, *67*(5), p.901. doi:10.1093/sysbio/syy032

Ratnasingham, S. and Hebert, P.D., 2007. BOLD: The Barcode of Life Data System (http://www.barcodinglife.org). *Molecular Ecology Notes*, *7*(3), pp.355-364. doi:10.1111/j.1471-8286.2007.01678.x

Reid, W.D., Cuomo, N.J. and Jamieson, A.J., 2018. Geographic and bathymetric comparisons of trace metal concentrations (Cd, Cu, Fe, Mn, and Zn) in deep-sea lysianassoid amphipods from abyssal and hadal depths across the Pacific Ocean. *Deep Sea Research Part I: Oceanographic Research Papers*, *138*, pp.11-21. doi:10.1016/j.dsr.2018.07.013

Ritchie, H., Jamieson, A.J. and Piertney, S.B., 2015. Phylogenetic relationships among hadal amphipods of the Superfamily Lysianassoidea: Implications for taxonomy and biogeography. *Deep Sea Research Part I: Oceanographic Research Papers*, *105*, pp.119-131. doi:10.1016/j.dsr.2015.08.014

Ritchie, H., Jamieson, A.J. and Piertney, S.B., 2017. Genome size variation in deep-sea amphipods. *Royal Society Open Science*, *4*(9), p.170862. doi:10.1098/rsos.170862

Ritchie, H., Jamieson, A.J. and Piertney, S.B., 2017. Population genetic structure of two congeneric deep-sea amphipod species from geographically isolated hadal trenches in the Pacific Ocean. *Deep Sea Research Part I: Oceanographic Research Papers*, *119*, pp.50-57. doi:10.1016/j.dsr.2016.11.006

Ritchie, H., Jamieson, A.J. and Piertney, S.B., 2018. Heat-shock protein adaptation in abyssal and hadal amphipods. *Deep Sea Research Part II: Topical Studies in Oceanography*, *155*, pp.61-69. doi:10.1016/j.dsr2.2018.05.003.

Rivera-Colón, A.G., Rochette, N.C. and Catchen, J.M., 2021. Simulation with RADinitio improves RADseq experimental design and sheds light on sources of missing data. *Molecular Ecology Resources*, *21*(2), pp.363-378. doi:10.1111/1755-0998.13163

Rochette, N.C., Rivera-Colón, A.G. and Catchen, J.M., 2019. Stacks 2: Analytical methods for paired-end sequencing improve RADseq-based population genomics. *Molecular Ecology*, *28*(21), pp.4737-4754. doi:10.1111/mec.15253

Ryan, W.B., Carbotte, S.M., Coplan, J.O., O'Hara, S., Melkonian, A., Arko, R., Weissel, R.A., Ferrini, V., Goodwillie, A., Nitsche, F. and Bonczkowski, J., 2009. Global multi-resolution topography synthesis. *Geochemistry, Geophysics, Geosystems*, *10*(3).

Sainte-Marie, B., 1991. A review of the reproductive bionomics of aquatic gammaridean amphipods: Variation of life history traits with latitude, depth, salinity and superfamily. In *VIIth International Colloquium on Amphipoda* (pp. 189-227). Springer, Dordrecht.

Sands, C.J., McInnes, S.J., Marley, N.J., Goodall-Copestake, W.P., Convey, P. and Linse, K., 2008. Phylum Tardigrada: an “individual” approach. *Cladistics*, *24*(6), pp.861-871. doi:10.1111/j.1096-0031.2008.00219.x

Saunders, P.M., 1981. Practical conversion of pressure to depth. *Journal of Physical Oceanography*, *11*(4), pp.573-574.

Sborshchikov, I.M., Murdmaa, I.O., Matveenkov, V.V., Kashintsev, G.L., Golmshtock, A.I. and Al'Mukhamedov, A.I., 1995. Afanasy Nikitin Seamount within the intraplate deformation zone, Indian Ocean. *Marine Geology*, *128*(1-2), pp.115-126. doi:10.1016/0025-3227(95)01995-G

Schliep, K.P., 2011. *phangorn*: phylogenetic analysis in R. *Bioinformatics*, *27*(4), pp.592-593. https://doi10.1093/bioinformatics/btq706

Schliep, K., Potts, A.J., Morrison, D.A. and Grimm, G.W., 2017. Intertwining phylogenetic trees and networks. *Methods in Ecology and Evolution*, 8, pp.1212–1220. doi:10.1111/2041-210X.12760

Schlining, K., Von Thun, S., Kuhnz, L., Schlining, B., Lundsten, L., Stout, N.J., Chaney, L. and Connor, J., 2013. Debris in the deep: Using a 22-year video annotation database to survey marine litter in Monterey Canyon, central California, USA. *Deep Sea Research Part I: Oceanographic Research Papers*, *79*, pp.96-105. http://dx.doi.org/10.1016/j.dsr.2013.05.006

Schwentner, M. and Lörz, A.N., 2020. Population genetics of cold-water coral associated Pleustidae (Crustacea, Amphipoda) reveals cryptic diversity and recent expansion off Iceland. *Marine Ecology*, p.e12625. doi:10.1111/maec.12625

Sclater, J.G. and Fisher, R.L., 1974. Evolution of the east: Central Indian Ocean, with emphasis on the tectonic setting of the Ninety-East Ridge. *Geological Society of America Bulletin*, *85*(5), pp.683-702. doi:10.1130/0016-7606(1974)85<683:EOTECI>2.0.CO;2

Senna, A.R. and Serejo, C.S., 2007. A new deep-sea species of *Stephonyx* (Lysianassoidea: Uristidae) from off the central coast of Brazil. *Nauplius*, *15*(1), pp.7-14.

Serejo, C.S. and Wakabara, Y., 2003. The genus *Valettiopsis* (Crustacea, Gammaridea, Lysianassoidea) from the southwestern Atlantic, collected by the RV *Marion Dufresne*. *Zoosystema*, *25*(2), pp.187-196.

Sheard, K., 1938. The amphipod genera *Euonyx*, *Syndexamine* and *Paradexamine*. *Records of the South Australian Museum*, *6*(2), pp.169-186.

Shulenberger, E. and Barnard, J.L., 1976. Amphipods from an abyssal trap set in the North Pacific Gyre. *Crustaceana*, pp.241-258.

Silge, J. and Robinson, D., 2017. Text mining with R: A tidy approach. "O'Reilly Media, Inc.".

Smith, S.I., 1882. *Eurythenes* Lillgeborg. In: Scudder, S.H. (Ed.), Zoologicus, N., 1882. An alphabetical list of all generic names that have been employed by naturalists for recent and fossil animals from the earliest times to the close of the year 1879. 1. Supplemental list of Genera in Zoology. US Government Printing Office, 21(1), pp.376.

Smith, C.R., De Leo, F.C., Bernardino, A.F., Sweetman, A.K. and Arbizu, P.M., 2008. Abyssal food limitation, ecosystem structure and climate change. *Trends in Ecology & Evolution*, *23*(9), pp.518-528. doi:10.1016/j.tree.2008.05.002

Smith, W.H. and Marks, K.M., 2014. Seafloor in the Malaysia Airlines flight MH370 search area. *Eos, Transactions American Geophysical Union*, *95*(21), pp.173-174.

Sorrentino, R., Souza-Filho, J.F. and Senna, A.R., 2018. A new species of *Stephonyx* (Amphipoda, Amphilochida, Lysianassoidea) from Brazil. *Zootaxa*, *4388*(4), pp.537-546. doi:10.11646/zootaxa.4388.4.5.

Stebbing, T.R.R., 1888. Report on the Amphipoda collected by HMS Challenger during the years 1873-1876*, Zoology*, *29*, pp.1-1737.

Stern, R.J., 2002. Subduction zones. *Reviews of Geophysics*, *40*(4), pp.3-1.

Stewart, H.A. and Jamieson, A.J., 2018. Habitat heterogeneity of hadal trenches: considerations and implications for future studies. *Progress in Oceanography*, *161*, pp.47-65. doi:10.1016/j.pocean.2018.01.007

Stewart, H.A. and Jamieson, A.J., 2019. The five deeps: The location and depth of the deepest place in each of the world's oceans. *Earth-Science Reviews*, *197*, p.102896. doi:10.1016/j.earscirev.2019.102896.

Stewart, J.R., Lister, A.M., Barnes, I. and Dalén, L., 2010. Refugia revisited: individualistic responses of species in space and time. *Proceedings of the Royal Society B: Biological Sciences*, *277*(1682), pp.661-671.

Stock, J.H. and ILIFFE, T.M., 1990. Amphipod crustaceans from anchihaline cave waters of the Galapagos Islands. *Zoological Journal of the Linnean Society*, *98*(2), pp.141-160. doi:10.1111/j.1096-3642.1990.tb01213.x

Stoddart, H.E. and Lowry, J.K., 2004. The deep-sea lysianassoid genus *Eurythenes* (Crustacea, Amphipoda, Eurytheneidae n. fam.). *Zoosystema*, *26*(3), pp.425-468.

Suchard, M.A., Lemey, P., Baele, G., Ayres, D.L., Drummond, A.J. and Rambaut, A., 2018. Bayesian phylogenetic and phylodynamic data integration using BEAST 1.10. *Virus Evolution*, *4*(1), p.vey016. doi:10.1093/ve/vey016

Sumida, P.Y., Alfaro-Lucas, J.M., Shimabukuro, M., Kitazato, H., Perez, J.A., Soares-Gomes, A., Toyofuku, T., Lima, A.O., Ara, K. and Fujiwara, Y., 2016. Deep-sea whale fall fauna from the Atlantic resembles that of the Pacific Ocean. *Scientific Reports*, *6*(1), pp.1-9. doi:10.1038/srep22139

Swan, J.A., Jamieson, A.J., Linley, T.D. and Yancey, P.H., 2021. Worldwide distribution and depth limits of decapod crustaceans (Penaeoidea, Oplophoroidea) across the abyssal-hadal transition zone of eleven subduction trenches and five additional deep-sea features. *Journal of Crustacean Biology*. doi:10.1093/jcbiol/ruaa102

Swofford, D.L., 2003. PAUP*. Phylogenetic Analysis Using Parsimony (*and other methods). Version 4. Sunderland, Massachusetts: Sinauer Associates.

Syed, S., Borit, M. and Spruit, M., 2018. Narrow lenses for capturing the complexity of fisheries: A topic analysis of fisheries science from 1990 to 2016. *Fish and Fisheries*, *19*(4), pp.643-661. doi:10.1111/faf.12280

Tamburri, M.N. and Barry, J.P., 1999. Adaptations for scavenging by three diverse bathyal species, *Eptatretus stouti*, *Neptunea amianta* and *Orchomene obtusus*. *Deep Sea Research Part I: Oceanographic Research Papers*, *46*(12), pp.2079-2093.

Taylor, M.L., Gwinnett, C., Robinson, L.F. and Woodall, L.C., 2016. Plastic microfibre ingestion by deep-sea organisms. *Scientific Reports*, *6*(1), pp.1-9. doi:10.1038/srep33997

Taylor, M.L. and Roterman, C.N., 2017. Invertebrate population genetics across Earth's largest habitat: The deep-sea floor. *Molecular Ecology*, *26*(19), pp.4872-4896. doi:10.1111/mec.14237

Thiel, H., 2003. Anthropogenic impacts on the deep sea. *Ecosystems of the World*, pp.427-472.

Thomson, C.W. and Murray, J., 1895 Report on the Results of the Voyage of H.M.S. Challenger during the Years 1873–76, Narrative, Vol. A(1). London: HM Stationery Office.

Thurston, M.H., 1979. Scavenging abyssal amphipods from the north-east Atlantic Ocean. *Marine Biology*, *51*(1), pp.55-68.

Thurston, M.H. and Bett, B.J., 1995. Hatchling size and aspects of biology in the deep-sea amphipod genus *Eurythenes* (Crustacea: Amphipoda). *Internationale Revue der gesamten Hydrobiologie und Hydrographie*, *80*(2), pp.201-216. http://dx.doi.org/10.1002/iroh.19950800209.

Thurston, M.H., Petrillo, M. and Della Croce, N., 2002. Population structure of the necrophagous amphipod *Eurythenes gryllus* (Amphipoda: Gammaridea) from the Atacama Trench (south-east Pacific Ocean). *Marine Biological Association of the United Kingdom. Journal of the Marine Biological Association of the United Kingdom*, 82(2), p.205-211.

Treude, T., Janßen, F., Queisser, W. and Witte, U., 2002. Metabolism and decompression tolerance of scavenging lysianassoid deep-sea amphipods. *Deep Sea Research Part I: Oceanographic Research Papers*, *49*(7), pp.1281-1289. https://doi10.1016/S0967-0637(02)00023-7

Tulloch, A.I., Sutcliffe, P., Naujokaitis-Lewis, I., Tingley, R., Brotons, L., Ferraz, K.M.P., Possingham, H., Guisan, A. and Rhodes, J.R., 2016. Conservation planners tend to ignore improved accuracy of modelled species distributions to focus on multiple threats and ecological processes. *Biological Conservation*, *199*, pp.157-171. doi:10.1016/j.biocon.2016.04.023

Tyler, P.A., 2003. Epilogue: exploration, observation, and experimentation. *Ecosystems of the World*, pp.473-476.

Xu, Y., Ge, H. and Fang, J., 2018. Biogeochemistry of hadal trenches: Recent developments and future perspectives. *Deep Sea Research Part II: Topical Studies in Oceanography*, *155*, pp.19-26. doi:10.1016/j.dsr2.2018.10.006

Varpe, Ø. and Ejsmond, M.J., 2018. Semelparity and iteroparity. *Natural History of Crustacea*, *5*, pp.97-124.

Veevers, J.J. and Cotterill, D., 1978. Western margin of Australia: Evolution of a rifted arch system. *Geological Society of America Bulletin*, *89*(3), pp.337-355.

Watling, L., Guinotte, J., Clark, M.R. and Smith, C.R., 2013. A proposed biogeography of the deep ocean floor. *Progress in Oceanography*, *111*, pp.91-112. https://doi10.1016/j.pocean.2012.11.003

Weatherall, P., Marks, K.M., Jakobsson, M., Schmitt, T., Tani, S., Arndt, J.E., Rovere, M., Chayes, D., Ferrini, V. and Wigley, R., 2015. A new digital bathymetric model of the world's oceans. *Earth and Space Science*, *2*(8), pp.331-345. doi:10.1002/2015EA000107

Wei, T. and Simko, V., 2017. R package 'corrplot': Visualization of a Correlation Matrix (Version 0.84). Available from https://github.com/taiyun/corrplot

Wenzhöfer, F., 2019. The Expedition SO261 of the Research Vessel *Sonne* to the Atacama Trench in the Pacific Ocean in 2018. *Reports on Polar and Marine Research*, *729*. https://epic.awi.de/id/eprint/49388/1/BzPM_0729_2019.pdf

Wenzhöfer, F., Oguri, K., Middelboe, M., Turnewitsch, R., Toyofuku, T., Kitazato, H. and Glud, R.N., 2016. Benthic carbon mineralization in hadal trenches: Assessment by in situ O_2 microprofile measurements. *Deep Sea Research Part I: Oceanographic Research Papers*, *116*, pp.276-286.

Werner, R., Wagner, H.J. and Hauff, F., 2017. RV *Sonne* Fahrtbericht/Cruise Report SO258/1: INGON: The Indian-Antarctic Break-up Engima, Fremantle (Australia)-Colombo (Sri Lanka) 07.06.-09.07. 2017. https://doi10.3289/GEOMAR_REP_NS_38_2017. Accessed 1 August 2020.

Wesch, C., Elert, A.M., Wörner, M., Braun, U., Klein, R. and Paulus, M., 2017. Assuring quality in microplastic monitoring: About the value of clean-air devices as essentials for verified data. *Scientific Reports*, *7*(1), pp.1-8. doi:10.1038/s41598-017-05838-4

Westgate, M.J., Barton, P.S., Pierson, J.C. and Lindenmayer, D.B., 2015. Text analysis tools for identification of emerging topics and research gaps in conservation science. *Conservation Biology*, *29*(6), pp.1606-1614. doi:10.1111/cobi.12605

Weston, J.N., Carrillo-Barragan, P., Linley, T.D., Reid, W.D. and Jamieson, A.J., 2020. New species of *Eurythenes* from hadal depths of the Mariana Trench, Pacific Ocean (Crustacea: Amphipoda). *Zootaxa*, *4748*(1), pp.163-181. doi:10.11646/zootaxa.4748.1.9

Weston, J.N., Peart, R.A. and Jamieson, A.J., 2020. Amphipods from the Wallaby-Zenith Fracture Zone, Indian Ocean: New genus and two new species identified by integrative taxonomy. *Systematics and Biodiversity*, *18*(1), pp.57-78. doi:10.1007/s00227-020-03798-4

Weston, J.N., Peart, R.A., Stewart, H.A., Ritchie, H., Piertney, S.B., Linley, T.D. and Jamieson, A.J., 2021. Scavenging amphipods from the Wallaby-Zenith Fracture Zone: Extending the hadal paradigm beyond subduction trenches. Marine Biology, 168(1), pp.1-14. doi:10.1007/s00227-020-03798-4

White, L.T., Gibson, G.M. and Lister, G.S., 2013. A reassessment of paleogeographic reconstructions of eastern Gondwana: Bringing geology back into the equation. *Gondwana Research*, *24*(3-4), pp.984-998. https://doi10.1016/j.gr.2013.06.009

Wickham, H., 2016. *ggplot2*: Elegant Graphics for Data Analysis. Springer-Verlag New York.

Wilson, G.D. and Ahyong, S.T., 2015. Lifestyles of the species-rich and fabulous: the deep-sea crustaceans. *The Natural History of the Crustacea*, *2*, pp.279-98.

Wilson, J.P., Schnabel, K.E., Rowden, A.A., Peart, R.A., Kitazato, H. and Ryan, K.G., 2018. Bait-attending amphipods of the Tonga Trench and depth-stratified population structure in the scavenging amphipod *Hirondellea dubia* Dahl, 1959. *PeerJ*, *6*, p.e5994. doi:10.7717/peerj.5994

Winfield, I., Hendrickx, M.E. and Ortiz, M., 2017. *Stephonyx californiensis* sp. nov. (Amphipoda: Lysianassoidea: Uristidae), a new bathyal scavenger species from the Central Gulf of California, Mexico, and comments on the bathymetric and geographic distribution of the *Stephonyx* species group. *Journal of Natural History*, *51*(47-48), pp.2793-2807. doi:10.1080/00222933.2017.1384076

Wolff, T., 1960. The hadal community, an introduction. *Deep Sea Research (1953)*, *6*, pp.95-124.

Wolff, T., 1970, December. The concept of the hadal or ultra-abyssal fauna. In *Deep Sea Research and Oceanographic Abstracts* (Vol. 17, No. 6, pp. 983-1003). Elsevier.

Yamaguchi, A., Ikeda, T., Watanabe, Y. and Ishizaka, J., 2004. Vertical distribution patterns of pelagic copepods as viewed from the predation pressure hypothesis. *Zoological Studies*, *43*(2), pp.475-485.

Yang, Z., 1994. Maximum likelihood phylogenetic estimation from DNA sequences with variable rates over sites: approximate methods. *Journal of Molecular Evolution*, *39*(3), pp.306-314.

Zhang, J., Kapli, P., Pavlidis, P. and Stamatakis, A., 2013. A general species delimitation method with applications to phylogenetic placements. *Bioinformatics*, *29*(22), pp.2869-2876. doi:10.1093/bioinformatics/btt499

1

Appendix A

Supplemental Information for Chapter 4: Amphipods from the Wallaby-Zenith Fracture Zone, Indian Ocean: New genus and two new species identified by integrative taxonomy

Table A1. 79 characters scored for morphological phylogenetic analysis.

#1. Eyes
1. Present
2. absent

#2. Rostrum
1. present
2. absent

#3. Antenna 1 length to Antenna 2
1. longer than
2. subequal to
3. shorter than

#4. Antenna 1 peduncle article 1
1. shorter than article 2
2. subequal to article 2
3. longer than article 2

#5. Antenna 1 peduncle article 2
1. shorter than article 3
2. subequal to article 3
3. longer than article 3

#6. Antenna 1 accessory flagellum
1. present
2. absent

#7. Antenna 2 peduncle article 4
1. shorter than article 5
2. subequal to article 5
3. longer than article 5

#8. Head lateral cephalic lobe
1. reduced
2. well developed

#9. head lateral cephalic lobe shape
1. absent/reduced
2. rounded
3. truncated
4. triangular

#10. Mandibular incisors
1. asymmetrical
2. symmetrical

#11. Incisor teeth
1. smooth
2. both smooth and toothed
3. toothed

#12. Mandible left lacinia mobilis
1. well developed
2. reduced
3. absent

#13. Left lacinia mobilis shape
1. longer than broad
2. as long as broad
3. broader than long

#14. Mandible right lacinia mobilis
1. well developed
2. reduced
3. absent

#15. Right lacinia mobilis shape
1. longer than broad
2. as long as broad
3. broader than long
4. absent

#16. Molar
1. strongly triturating
2. small triturating surface
3. no triturating surface

#17. Mandibular molar triturating surface
1. absent
2. tiny
3. small - medium
4. large

#18. mandibular palp
1. inserted proximal to molar
2. inserted adjacent to molar
3. inserted distal to molar

#19. Maxilla 1 inner plate
1. numerous setae on medial margin over 10
2. moderate setae on medial margin between 5 and 10
3. less than 5 setae on medial margin

#20. Maxilla 1 palp
1. 2 articles
2. 1 article

#21. Maxilla 1 palp size
1. reduced
2. large

#22. Maxilla 1 palp distal
1. robust setae and smooth margin
2. robust setae and scalloped 3 toothed margin
3. robust setae, scalloped more or less than 3 teeth
4. slender setae and smooth margins

#23. Maxilla 2 inner plate
1. strongly shorter than outer plate
2. slightly shorter than or subequal to outer plate

#24. Maxilla 2 inner plate width
1. subequal in width to outer plate
2. narrower than outer plate
#25. Maxilliped inner plate
1. apically angled
2. apically transverse or weakly angled
#26. Maxilliped inner plate distal excavation
1. present
2. absent
#27. Maxilliped inner plate distal robust setae
1. on corner only
2. along distal margin
3. absent
#28. Maxilliped palp length
1. strongly exceeding outer plate
2. just reaching past outer plate
#29. Maxilliped palp dactyl
1. well developed
2. reduced
#30. Maxilliped palp dactylus inner apical tooth
1. present
2. absent
#31. Coxa 1 length
1. shorter than coxa 2
2. slightly shorter than coxa 2
3. subequal or longer in length to coxa 2 and 3
4. same length as coxa 2, but both shorter than coxa 3
#32. Coxa 1 expansion
1. narrowing ventrally
2. same width ventrally as anterior
3. expanding ventrally
#33. Gnathopod 1 ischium length
1. shorter than merus
2. subequal to merus
3. slightly longer than merus (1.1-1.5x)
4. much longer than merus (>1.5 x)
#34. Gnathopod 1 carpus
1. shorter than propodus
2. subequal to propodus
3. longer than propodus
#35. Gnathopod 1 propodus
1. simple
2. subchelate
#36. Gnathopod 1 palm angle
1. absent (simple)
2. transverse
3. weakly angled
4. strongly angled
5. obtuse
#37. Gnathopod 1 dactylus length
1. short less than half propodus
2. medium around half propodus
3. long over half propodus
#38. Gnathopod 2 coxa shape
1. parallel sided
2. tapering
3. ventrally expanded
#39. Gnathopod 2 ischium
1. shorter than merus
2. subequal to merus
3. longer than merus
#40. Gnathopod 2 distal article size
1. rectolinear
2. expanded
#41. Gnathopod 2 carpus length
1. shorter than propodus
2. subequal to propodus
3. longer than propodus
#42. Gnathopod 2 propodus chelation
1. simple
2. subchelate
#43. Gnathopod 2 palm angle
1. transverse
2. angled
#44. Gnathopod 2 palm shape
1. convex
2. straight
3. concave
#45. Gnathopod 2 dactylus
1. shorter than palm
2. reaching to the end of palm
3. overreaching palm
#46. Pereopod 3 merus
1. much longer than carpus
2. longer than carpus
3. subequal to carpus
4. shorter than carpus
#47. Pereopod 3 carpus
1. shorter than propodus
2. subequal to propodus
3. longer than propodus
#48. Pereopod 3 dactylus
1. short - less 0.4 x propodus
2. medium - 0.4 - 0.6 x propodus
3. long - greater than 0.6 x propodus
#49. Pereopod 4 coxa posterior lobe
1. present, well developed
2. absent
3. present, slightly developed
#50. Pereopod 4 distal articles
1. same as pereopod 3
2. differing from pereopod 3
#51. Pereopods 5 basis
1. narrow
2. expanded

#52. Pereopod 5 basis posterior margin
1. bevelled
2. rounded
3. straight
#53. Pereopod 5 basis ventral lobe
1. rounded
2. truncated
3. angled
4. absent
#54. Pereopod 6 basis
1. narrow
2. expanded
#55. Pereopods 6 basis posterior margin
1. bevelled
2. smooth rounded
#56. Pereopods 6 basis ventral lobe
1. rounded
2. truncated
3. angular
4. absent
#57. Pereopod 7 basis
1. narrow
2. expanded
#58. Pereopod 7 basis posterior margin
1. rounded
2. bevelled
3. straight
#59. Pereopod 7 basis posteroventral lobe
1. rounded
2. truncated
3. angular
4. absent
#60. Pereopods 5-7 merus
1. narrow
2. expanded
#61. Pereopods 5 -7 dactylus
1. short
2. long

#62. Epimeron 3 posteroventral corner
1. rounded/subquadrate
2. with small tooth
3. acute, no distinct tooth
4. large acute tooth
#63. Uropods length in situ
1. all subequal
2. uropod 3 long than uropods 1 and 2
#64. Uropod 1 outer ramus
1. shorter than inner ramus
2. subequal to inner ramus
3. longer than inner ramus
#65. Uropod 1 peduncular distal lobe
1. present
2. absent
#66. Uropod 2 outer ramus
1. shorter than inner ramus
2. subequal to inner ramus
3. longer than inner ramus
#67. Uropod 2 inner ramus notch
1. present
2. absent
#68. Uropod 3 outer ramus article 2
1. short less than 0.2 article 1
2. long/medium greater than 0.2 x article 1

#69. Uropod 3 outer ramus length
1. shorter than inner ramus
2. subequal to inner ramus
3. longer than inner ramus

#70. Uropod 3 rami width
1. narrow
2. wide
#71. Telson length
1. longer than wide
2. as long as wide
3. wide than long
#72. Telson lobes apical width
1. narrow
2. broad
#73. Telson cleft
1. entire
2. shallow
3. medium
4. deep
#74. Body Pereon
1. smooth
2. sculptured
#75. Body pleon
1. smooth
2. carinated
#76. Urosome 1 carination
1. present
2. absent
#77. Urosomite 1 dorsal setae
1. present
2. absent
#78. Urosomite 2 dorsal tooth
1. present
2. absent
#79. Urosomite 3 dorsal setae
1. present
2. absent

1

Table A2. Matrix of 79 scored morphological characters versus species for morphological phylogenetic analysis. Bold represents specimens assessed by both the morphological and molecular analyses. Asterisks represent outgroups.

	1	2	3	4	5	6	7	7
	1234567890123456789012345678901234567890123456789012345678901234567890123456789							23456789
Alicella gigantea Chevreux, 1899	2233312221213233131121221222213333111131321121111122222221211221112122114112222							
***Alicella gigantea* (WZFZ4932)**	2233312221213233131121221222213333111131321121111122222221211221112122114112222							
Apotectonia heterostegos Barnard & Ingram, 1990	2233313222113243131121221211212331111313222221111223232131121221222214111222							
***Civifractura serendipia* gen. et sp. nov.**	2223311221213232331121111221112233241331323122111221221211113222121311 14121222							
Cyclocaris franki Horton & Thurston, 2014	1133211222121343132122111211124133111131322222111122122121122222212222114112222							
Cyclocaris guilelmi Chevreux, 1899	1133211111221343132112111211124232111131322222121122122121122221212221114112222							
Cyclocaris lowryi Horton & Thurston, 2014	1133211221121343122122111221124233111131321222121122122121111221212222114111222							
Cyclocaris tahitensis Stebbing, 1888	1233211111121343122122111211124133111131323221111221221211121222122321 14112222							
Diatectonia typhodes Barnard & Ingram, 1990	2233313232213232231121212221121133231331322211311122122121111221121221 14111222							
c.f. *Diatectonia* (NH3400a)	2223313221213232231121112221111233231131322212111122122121112222221111 14111211							
Paralicella caperesca Schulenberger & Barnard, 1976	2233213222113213121121221111233312321313222111211222221211121212122221 14111222							
Paralicella fusiformis (Birstein & M. Vinogradov, 1955)	2233313222113223131121121121231312321311212221111221221211121212121211 14112222							
Paralicella similis Birstein & Vinogradov, 1960	1233213222113223131121111211213212323313222221211221211211222121223321 24112222							
Paralicella tenuipes Chevreux, 1908	1233313222113223141122211111231212323312223211212212212211212121222112 24112222							
Paralicella vaporalis Barnard & Ingram, 1990	2233312231213122241124111121112132231131222212121122122121112122112122124112121							
Tectovalopsis diabolus Barnard & Ingram, 1990	2223313231213232231121111211112233231331322222111221221211112122121211 14111222							
Tectovalopsis fusilus Barnard & Ingram, 1990	2223312231113232331121111221112213241131322212111221221211112222121321 14111212							
Tectovalopsis nebulosus Barnard & Ingram, 1990	2223313231213232331121111221112233231331222312111122122121112222121211 14111212							
Tectovalopsis regalatus Barnard & Ingram, 1990	2233311221213132331121212221122133242131322312111122122121112222121221 14121222							
Tectovalopsis ruffoi (Serejo & Wakabara, 2003)	2223313221213132331121212221122243241331322212111221221211112221121211 14111222							
Tectovalopsis wegeneri Barnard & Ingram, 1990	2223313221213232231121112221111233231131322212111221221211112222121111 14111212							
***Tectovalopsis wegeneri* (NH2500)**	2223313221213232231121112221111233231131322212111221221211113222221111 14111211							
***Tectovalopsis wegeneri* (NH3400)**	2223313221213232231121112221111233231131322212111221221211112222221111 14111211							
***Tectovalopsis* sp. (PC4602)**	2233313221223232231121212221111233241331322212111221221211112221121211 14111212							
***Tectovalopsis* sp. (M5641)**	2233312231221132232121212221121233231131322222111221221211113222121311 14111222							
Transectonia torrentis Barnard & Ingram, 1990	2213313221211223122121211211123232241131322222211221221211111122121321 23111222							
Valettietta anacantha (Birstein & Vinogradov, 1963)	2233212222311211421121211221122231231131222222121122122121111222112222214111212							
Valettietta gracilis Lincoln & Thurston, 1983	2213312232311111421121212221123231231131312312121122122321311321212231114111222							
Valettietta lobata Lincoln & Thurston, 1983	2223312132312121421121212221123231232132222112121122122321311322112232114111121							
Valettietta punctata Bellan-Santini, 1985	2223312122312121421121212221123131222131321122111122122321311312212221114111221							
Valettiopsis concava Hendrycks, 2007	2133311242312121421121212221121133221131321122112113412422311212212231114221222							
Valettiopsis dentata Holmes, 1908	2133312242311121421121212221121132221131321123121122122121111212112221124111222							
Valettiopsis lincolni Horton, 2004	2233311242311111421121212221121113222113212212211312242242241231211223112411222							
Valettiopsis longidactyla Horton, 2004	2133313242311111431121211211221312311313222221111221221213123222122211 24111222							
Valettiopsis macrodactyla Chevreux, 1909	2133312232311111421121212211121132222132122323123122122322312312212221124111222							
Valettiopsis minuta Horton, 2004	2133312222312121421121212211122131232332222222123122122422412312222221124111222							
**Hirondellea brevicaudata* Chevreux, 1910	1233313221211343123121111213112122123313232122211112212212111212222222123112222							
**Podoprion ruffoi* Lowry & Stoddart, 1996	1233313231311343122114212211122231252332221224233122122121112112232121113112222							
***Diatectonia* sp. (NH3400b) *Not included**	22 331 2212132322311211122211112332311313222121111221221211112222221111 14111211							

Table A3. Taxa used for molecular phylogenetic analysis including collection location, depth (m), GenBank accession numbers with previously published sequences, sequences added by this study in bold, and references for visual identification and sequences. 'No amp' means no usable PCR product.

Family	Genus	Species	Location	Depth (m)	16S	COI	His3	28S	Identification Ref.	Sequence Ref.
Alicellidae	*Alicella*	*gigantea* Chevreux, 1899	New Hebrides Trench	4694	KP456084	KP713894	-	-	Ritchie et al., 2015	Ritchie et al., 2015
Alicellidae	*Alicella*	*gigantea* Chevreux, 1899	Afanasy Nikitin Seamount	4733	**MK503195**	**MK503205**	**MK503223**	**MK503215**	This study	This study
Alicellidae	*Alicella*	*gigantea* Chevreux, 1899	Wallaby-Zenith Fracture Zone	4932	**MK503196**	**MK503206**	No amp	No amp	This study	This study
Alicellidae	*Alicella*	*gigantea* Chevreux, 1899	New Hebrides Trench	5180	KP456085	KP713895	-	-	Ritchie et al., 2015	Ritchie et al., 2015
Alicellidae	*Alicella*	*gigantea* Chevreux, 1899	Kermadec Trench	7000	JX436323	JX436324	-	-	Jamieson et al., 2013	Jamieson et al., 2013
Alicellidae	*Alicella*	*gigantea* Chevreux, 1899	Kermadec Trench	7000	KP456083	KP713893	-	-	Ritchie et al., 2015	Ritchie et al., 2015
Alicellidae	c.f. *Diatectonia*	sp.**	New Hebrides Trench	3400	**MK503199**	**MK503209**	**MK503225**	**MK503217**	Lacey et al., 2016	This study
Alicellidae	*Civifractura*	*serendipia* gen. et sp. nov.	Wallaby-Zenith Fracture Zone	4932	**MK503197**	**MK503207**	**MK503224**	**MK503216**	This study	This study
Alicellidae	*Civifractura*	*serendipia* gen. et sp. nov.	Wallaby-Zenith Fracture Zone	4932	**MK503198**	**MK503208**	No amp	No amp	This study	This study
Alicellidae	*Diatectonia*	sp.**	New Hebrides Trench	3400	**MK503200**	**MK503210**	**MK503226**	**MK503218**	Lacey et al., 2016	This study
Alicellidae	*Paralicella*	*caperesca* Schulenberger & Barnard, 1976	New Hebrides Trench	2500	KP456105	KP713921	-	-	Ritchie et al., 2015	Ritchie et al., 2015
Alicellidae	*Paralicella*	*caperesca* Schulenberger & Barnard, 1976	New Hebrides Trench	2500	KP456097	KP713920	-	-	Ritchie et al., 2015	Ritchie et al., 2015
Alicellidae	*Paralicella*	*caperesca* Schulenberger & Barnard, 1976	Crozet Island	4192	KF430270	KF430243	KF430300	KF484699	Corrigan et al., 2014	Corrigan et al., 2014
Alicellidae	*Paralicella*	*caperesca* Schulenberger & Barnard, 1976	Peru-Chile Trench	5329	KP456108	KP713922	-	-	Ritchie et al., 2015	Ritchie et al., 2015
Alicellidae	*Paralicella*	*caperesca* Schulenberger & Barnard, 1976	Kermadec Trench	6007	KP456101	KP713924	-	-	Ritchie et al., 2015	Ritchie et al., 2015
Alicellidae	*Paralicella*	*caperesca* Schulenberger & Barnard, 1976	Kermadec Trench	6007	KP456099	KP713925	-	-	Ritchie et al., 2015	Ritchie et al., 2015
Alicellidae	*Paralicella*	*caperesca* Schulenberger & Barnard, 1976	Peru-Chile Trench	6173	KP456107	KP713923	-	-	Ritchie et al., 2015	Ritchie et al., 2015
Alicellidae	*Paralicella*	*tenuipes* Chevreux, 1908	South Fiji Basin	4100	KP456106	KP713927	-	-	Ritchie et al., 2015	Ritchie et al., 2015
Alicellidae	*Paralicella*	*tenuipes* Chevreux, 1908	South Fiji Basin	4100	KP456098	KP713926	-	-	Ritchie et al., 2015	Ritchie et al., 2015
Alicellidae	*Paralicella*	*tenuipes* Chevreux, 1908	Mariana Trench	5469	KP456111	KP713929	-	-	Ritchie et al., 2015	Ritchie et al., 2015
Alicellidae	*Paralicella*	*tenuipes* Chevreux, 1908	Mariana Trench	5469	KP456110	KP713928	-	-	Ritchie et al., 2015	Ritchie et al., 2015
Alicellidae	*Paralicella*	*tenuipes* Chevreux, 1908	Kermadec Trench	6007	KP456104	KP713932	-	-	Ritchie et al., 2015	Ritchie et al., 2015
Alicellidae	*Paralicella*	*tenuipes* Chevreux, 1908	Kermadec Trench	6007	KP456103	KP713933	-	-	Ritchie et al., 2015	Ritchie et al., 2015
Alicellidae	*Paralicella*	*tenuipes* Chevreux, 1908	Peru-Chile Trench	6173	KP347450	KP713934	-	-	Ritchie et al., 2015	Ritchie et al., 2015
Alicellidae	*Paralicella*	*tenuipes* Chevreux, 1908	Japan Trench	6945	KP456113	KP713931	-	-	Ritchie et al., 2015	Ritchie et al., 2015
Alicellidae	*Tectovalopsis*	sp.	Peru-Chile Trench	4602	**MK503201**	**MK503211**	**MK503227**	**MK503219**	Fujii et al., 2013	This study
Alicellidae	*Tectovalopsis*	sp.	Mariana Trench	5641	**MK503202**	**MK503212**	**MK503228**	**MK503220**	This study	This study
Alicellidae	*Tectovalopsis*	*wegeneri* Barnard & Ingram 1990	New Hebrides Trench	2500	KP456087	KP713945	-	-	Ritchie et al., 2015	Ritchie et al., 2015
Alicellidae	*Tectovalopsis*	*wegeneri* Barnard & Ingram 1990	New Hebrides Trench	2500	KP456086	KP713946	-	-	Ritchie et al., 2015	Ritchie et al., 2015
Alicellidae	*Tectovalopsis*	*wegeneri* Barnard & Ingram 1990	New Hebrides Trench	3400	**MK503203**	**MK503213**	**MK503229**	**MK503221**	Lacey et al., 2016	This study
Alicellidae	*Tectovalopsis*	*wegeneri* Barnard & Ingram 1990	New Hebrides Trench	4694	**MK503204**	**MK503214**	**MK503230**	**MK503222**	Lacey et al., 2016	This study
Cyclocaridae	*Cyclocaris*	sp.	New Hebrides Trench	4100	KP456091	KP713898	-	-	Ritchie et al., 2015	Ritchie et al., 2015
Cyclocaridae	*Cyclocaris*	*franki* Horton & Thurston, 2014	Angola	1975	KF430272	KF430245	KF484701	KF430302	Corrigan et al., 2014	Corrigan et al., 2014
Eurytheneidae	*Eurythenes*	*gryllus* (Lichtenstein, 1822)	Mid-Atlantic Ridge	2453	KF430273	KF430246	KF484702	KF430303	Corrigan et al., 2014	Corrigan et al., 2014
Lanceolidae	*Lanceola*	sp.	Peru-Chile Trench	1037	KP456062	KP713953	-	-	Ritchie et al., 2015	Ritchie et al., 2015
Valettiopsidae	*Valettietta*	*anacantha* (Birstein & Vinogradov, 1963)	Mariana Trench	5467	KP456096	KP713949	-	-	Ritchie et al., 2015	Ritchie et al., 2015
Valettiopsidae	*Valettietta*	*anacantha* (Birstein & Vinogradov, 1963)	Kermadec Trench	6007	KP456094	KP713950	-	-	Ritchie et al., 2015	Ritchie et al., 2015
Valettiopsidae	*Valettietta*	*gracilis* Lincoln & Thurston, 1983	New Hebrides Trench	4694	KP456130	KP713951	-	-	Ritchie et al., 2015	Ritchie et al., 2015

**These specimens are in GenBank as *Tectovalopsis wegeneri* per results from this study.

Table A4. Nucleotide frequencies and length for the 36 sequences (10 for 16S, 10 for COI, 8 for H3, and 8 for 28S) in this study.

Sequence	Species	Location-depth (m)	T%	C%	A%	G%	Length (bp)
16S	*Alicella gigantea*	ANS-4733	36.7	11.2	27.0	25.1	259
	Alicella gigantea	WZFZ-4932	35.3	11.9	27.9	24.9	269
	Civifractura serendipia gen. et sp. nov.	WZFZ-4932	32.4	12.2	31.5	23.9	238
	Civifractura serendipia gen. et sp. nov.	WZFZ-4932	32.1	12.3	31.7	23.8	252
	c.f. *Diatectonia*	NH-3400	36.1	10.8	27.5	25.7	269
	Diatectonia sp.	NH-3400	36.0	11.0	27.6	25.4	272
	Tectovalopsis sp.	PC-4602	34.1	14.0	28.0	23.9	264
	Tectovalopsis sp.	M-5641	33.6	12.3	29.1	25.0	268
	Tectovalopsis wegeneri	NH-3400	36.1	10.6	27.0	26.2	263
	Tectovalopsis wegeneri	NH-4694	38.0	9.2	27.7	25.1	271
COI	*Alicella gigantea*	ANS-4733	35.3	21.2	26.5	17.0	258
	Alicella gigantea	WZFZ-4932	35.1	21.4	26.7	16.8	547
	Civifractura serendipia gen. et sp. nov.	WZFZ-4932	34.0	21.9	27.4	16.6	547
	Civifractura serendipia gen. et sp. nov.	WZFZ-4932	34.2	21.8	27.5	16.5	550
	c.f. *Diatectonia*	NH-3400	32.7	22.9	26.9	17.6	621
	Diatectonia sp.	NH-3400	33.1	22.8	26.8	17.3	623
	Tectovalopsis sp.	PC-4602	31.8	23.3	26.4	18.5	503
	Tectovalopsis sp.	M-5641	31.4	24.9	23.2	20.5	547
	Tectovalopsis wegeneri	NH-3400	33.5	22.0	26.1	18.4	624
	Tectovalopsis wegeneri	NH-4694	32.8	22.7	26.5	18.0	622
His3	*Alicella gigantea*	ANS-4733	20.0	35.4	18.4	26.2	305
	Civifractura serendipia gen. et sp. nov.	WZFZ-4932	21.9	33.1	19.2	25.8	260
	c.f. *Diatectonia*	NH-3400	21.5	34.4	18.5	25.6	270
	Diatectonia sp.	NH-3400	20.5	35.1	18.5	26.0	308
	Tectovalopsis sp.	PC-4602	20.4	35.3	18.8	25.6	309
	Tectovalopsis sp.	M-5641	20.4	35.3	19.1	25.2	309
	Tectovalopsis wegeneri	NH-3400	20.7	35.0	18.4	25.9	294
	Tectovalopsis wegeneri	NH-4694	20.9	34.8	18.2	26.0	296
28S	*Alicella gigantea*	ANS-4733	21.7	22.4	28.3	27.6	254
	Civifractura serendipia gen. et sp. nov.	WZFZ-4932	21.1	22.3	29.1	27.5	251
	c.f. *Diatectonia*	NH-3400	21.3	22.5	28.3	27.9	258
	Diatectonia sp.	NH-3400	21.3	22.5	27.9	28.3	258
	Tectovalopsis sp.	PC-4602	21.9	21.9	28.1	28.1	242
	Tectovalopsis sp.	M-5641	21.2	22.3	28.5	28.1	260
	Tectovalopsis wegeneri	NH-3400	21.3	22.5	28.5	27.7	253
	Tectovalopsis wegeneri	NH-4694	21.4	22.6	29.0	27.0	252

Table A5. Output of bPTP species delimitation analysis.

Phylogenetic Tree	No. seq.	bPTP parameters	Delimitation probabilities (heuristic search)
16S + COI (Figure 3)	36	Acceptance rate = 0.21566, merge = 50266, split = 49769, estimated no. of species between 13 & 24, mean = 16.51	1 = 1.000, 2 = 1.000, 3 = 0.961, 4 = 0.991 5 = 0.997, 6 = 0.668, 7 = 1.000, 8 = 1.000, 9 = 1.000, 10 = 0.602, 11 = 0.963, 12 = 0.945, 13 = 0.627, 14 = 0.728, 15 = 0.728, 16 = 0.513
16S + COI + His3 + 28S (Figure 4)	11	Acceptance rate = 0.04466, merge = 50228, split = 49769, estimated no. of species between 5 & 10, mean = 8.04	1 = 1.000, 2 = 1.000, 3 = 0.999, 4 =0.987, 5 = 0.987, 6 = 0.915, 7 = 0.982, 8 = 0.982

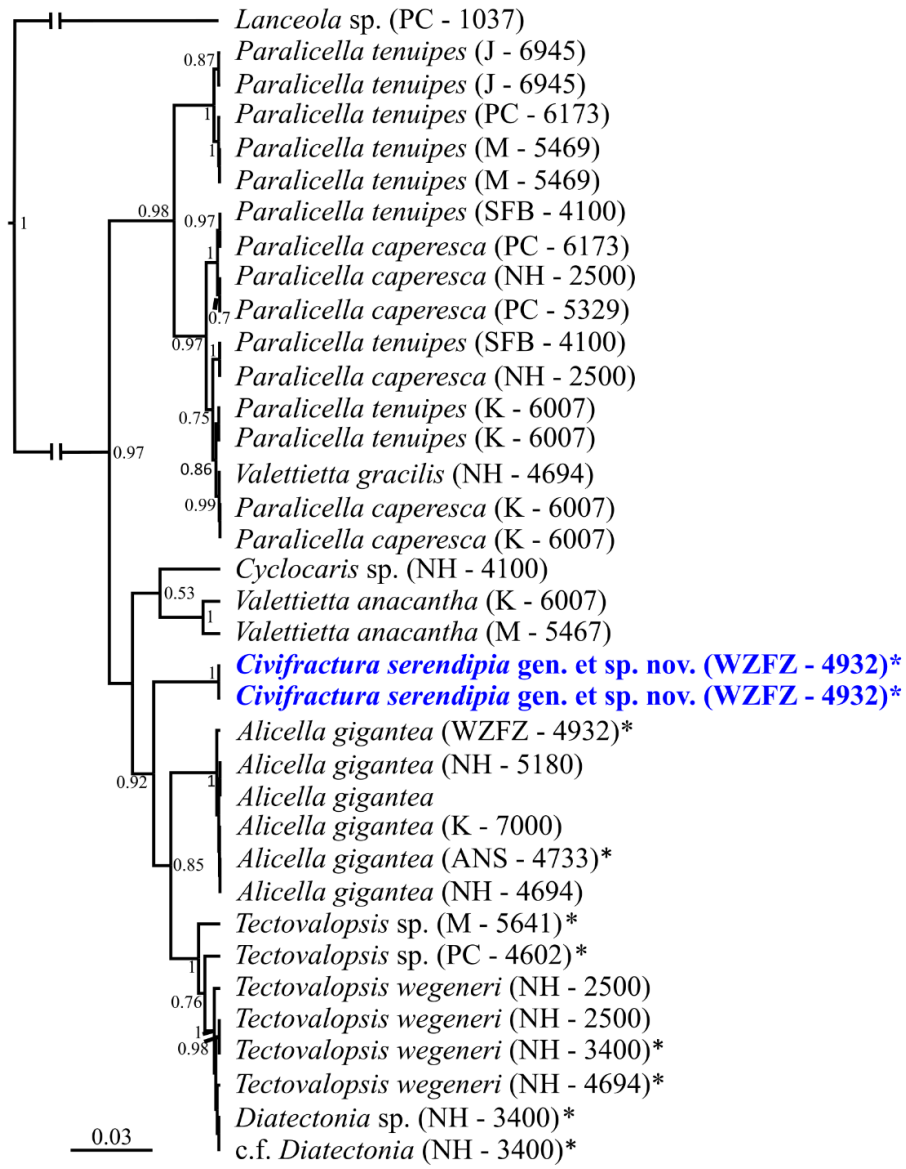

Figure A1. Bayesian tree showing the relationships between amphipod species based on 16S sequence data. Bayesian posterior probabilities greater than 50% are shown on branch nodes. Asterisks denote the sequences added by this study. Branches are labelled by species name and collection location and depth (m). Family is denoted on right. For the locations, PC is Peru-Chile Trench, M is Mariana Trench, NH is New Hebrides Trench, WZFZ is Wallaby-Zenith Fracture Zone, ANS is Afanasij Nikitin Seamount, J is Japan Trench, K is Kermadec Trench, and SFB is South Fiji Basin. For complete reference of sequences see Table A3.

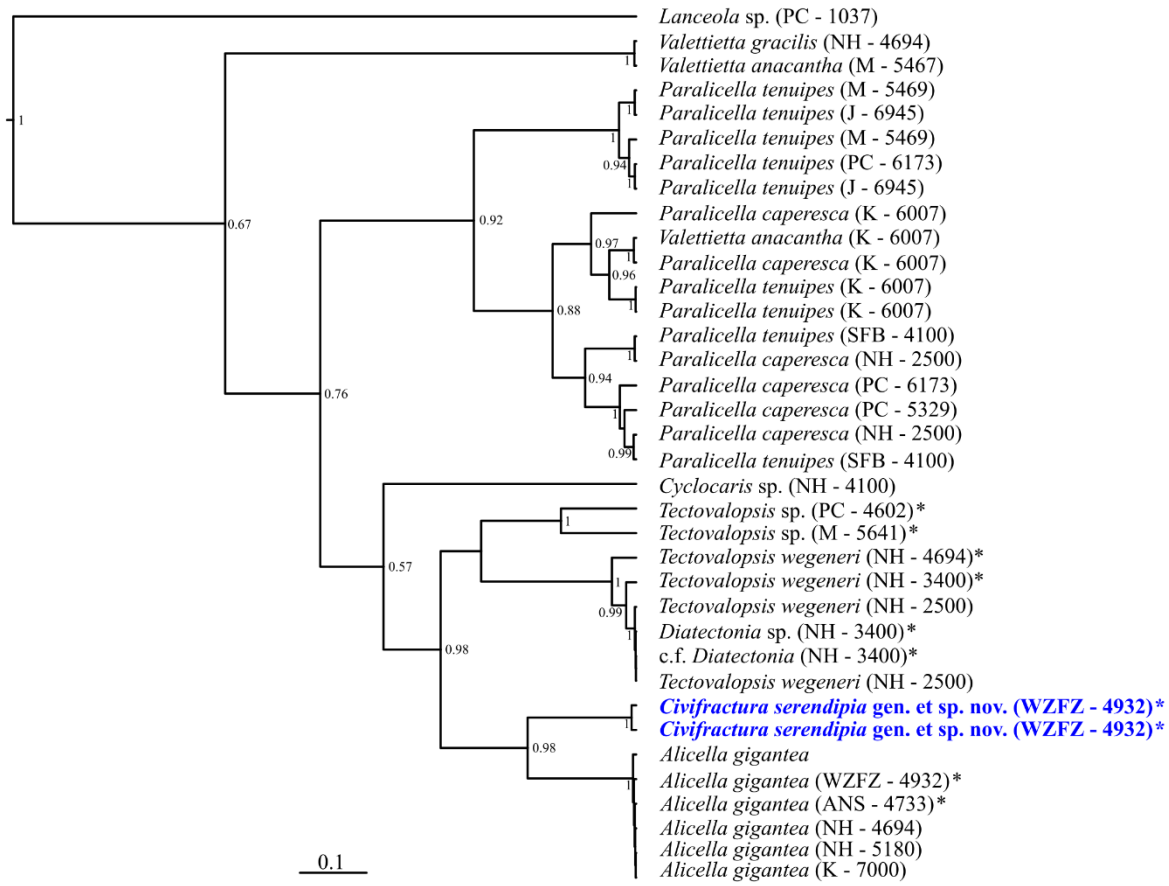

Figure A2. Bayesian tree showing the relationships between amphipod species based on COI sequence data. Bayesian posterior probabilities greater than 50% are shown on branch nodes. Asterisks denote the sequences added by this study. Branches are labelled by species name and collection location and depth (m). Family is denoted on right. For the locations, PC is Peru-Chile Trench, M is Mariana Trench, NH is New Hebrides Trench, WZFZ is Wallaby-Zenith Fracture Zone, ANS is Afanasij Nikitin Seamount, J is Japan Trench, K is Kermadec Trench, and SFB is South Fiji Basin. For complete reference of sequences see Table A3.

Appendix B

Supplemental Information for Chapter 5: Scavenging amphipods from the Wallaby-Zenith Fracture Zone: Extending the hadal paradigm beyond subduction trenches

Table B1. Number of amphipods recovered by species and depth from the Zenith Plateau and Wallaby-Zenith Fracture Zone, and the Afanasy Nikitin Seamount. The asterisks indicate potentially undescribed species.

		Zenith Plateau & Wallaby-Zenith Fracture Zone						Afanasy Nikitin Seamount	
	Depth (m)	4932	5990	6068	6162	6537	6546	4733	4757
Family	**Species**	**Counts**							
Alicellidae	*Alicella gigantea* Chevreux, 1899	1	-	-	-	-	-	1	-
	Civifractura serendipia Weston, Peart, & Jamieson 2020	31	-	-	-	-	-	-	-
	Paralicella caperesca Shulenberger & Barnard, 1976	48	11	1	6	13	-	39	43
	Paralicella tenuipes Chevreux, 1908	517	1167	92	492	246	341	23	14
Cyclocaridae	*Cyclocaris* sp.*	2	11	1	2	2	4	9	17
Eurytheneidae	*Eurythenes maldoror* d'Udekem d'Acoz & Havermans, 2015	80	1	-	7	4	7	-	11
Eusiridae	*Cleonardo* sp.*	-	-	-	1	-	-	-	-
Hirondelleidae	*Hirondellea* sp.*	-	-	-	-	-	-	2	-
Scopelocheiridae	*Bathycallisoma schellenbergi* Birstein & Vinogradov, 1958	-	-	-	-	130	523	-	-
Valettiopsidae	*Valettietta* sp.*	5	1	-	-	-	1	-	-
Uristidae	*Abyssorchomene distinctus* (Birstein & Vinogradov, 1960)	-	-	-	-	-	-	1	43
	Abyssorchomene gerulicorbis (Shulenberger & Barnard, 1976)	-	9	2	2	4	74	-	-
	Stephonyx sigmacrus Weston, Peart, & Jamieson 2020	23	-	-	-	-	-	-	-
	No. Individuals	707	1200	96	510	399	950	75	128
	No. Species	8	6	4	6	6	6	6	5
	Shannon Diversity Index	1.97	1.56	1.25	1.61	1.68	1.63	1.73	1.60

Table B2. Species, location and depth (m), and 16S and COI sequence accession numbers for amphipods from the Wallaby-Zenith Fracture Zone (WZFZ) and Afanasy Nikitin Seamount (ANS) added to GenBank by this study and Weston et al. 2020.

Species	Location	Depth (m)	16S	COI
Abyssorchomene distinctus	ANS	4757	MN251311	MN262162
Abyssorchromene gerulicorbis	WZFZ	5990	MN251312	MN262163
Abyssorchromene gerulicorbis	WZFZ	6546	MN251313	MN262164
Alicella gigantea	ANS	4733	MK503195	MK503205
Alicella gigantea	WZFZ	4932	MK503196	MK503206
Bathycallisoma schellenbergi	WZFZ	6537	MN251314	MN262165
Bathycallisoma schellenbergi	WZFZ	6537	MN251315	MN262166
Bathycallisoma schellenbergi	WZFZ	6546	MN251316	MN262167
Bathycallisoma schellenbergi	WZFZ	6546	MN251317	MN262168
Bathycallisoma schellenbergi	WZFZ	6546	MN251318	MN262169
Civifractura serendipia	WZFZ	4932	MK503197	MK503208
Civifractura serendipia	WZFZ	4932	MK503198	MK503209
Cleonardo sp.	WZFZ	6162	MN251319	MN262170
Cyclocaris sp.	WZFZ	5990	MN251320	No amp
Eurythenes maldoror	ANS	4757	MN251321	MN262171
Eurythenes maldoror	WZFZ	4932	MN251322	MN262172
Eurythenes maldoror	WZFZ	4932	MN251323	MN262173
Eurythenes maldoror	WZFZ	4932	MN251324	MN262174
Eurythenes maldoror	WZFZ	6162	MN251325	MN262175
Eurythenes maldoror	WZFZ	6537	MN251326	No amp
Eurythenes maldoror	WZFZ	6546	MN251327	MN262176
Hirondellea sp.	ANS	4733	MN251328	No amp.
Paralicella caperesca	ANS	4757	MN251329	MN262177
Paralicella caperesca	ANS	4757	MN251330	No amp
Paralicella caperesca	WZFZ	4932	MN251331	MN262178
Paralicella tenuipes	WZFZ	5990	MN251332	MN262179
Paralicella tenuipes	WZFZ	4932	MN251333	MN262180
Paralicella tenuipes	WZFZ	6537	MN251334	MN262181
Valettietta sp.	WZFZ	4932	MN251335	MN262182

Table B3. Species, sequence accession numbers and references for all samples included in the analysis of the *Bathycallisoma schellenbergi* dataset. WZFZ abbreviation for the Wallaby-Zenith Fracture Zone.

Species	16S	COI	Location	Reference
B. schellenbergi	KP308148	KP713939	Kermadec Trench	Ritchie et al., 2015
B. schellenbergi	KP456060	KP713938	New Hebrides Trench	Ritchie et al., 2015
B. schellenbergi	KP456061	KP713937	New Hebrides Trench	Ritchie et al., 2015
B. schellenbergi	MN251314	MN262165	WZFZ	This study
B. schellenbergi	MN251318	MN262169	WZFZ	This study
B. schellenbergi	MN251316	MN262167	WZFZ	This study
B. schellenbergi	MN251317	MN262168	WZFZ	This study
B. schellenbergi	MF598980	MF598998	Massau Trench	Chan et al., unpublished
B. schellenbergi	MF598979	MF598997	Massau Trench	Chan et al., unpublished
B. schellenbergi	MF598978	MF598994	Massau Trench	Chan et al., unpublished
B. schellenbergi	AY256969	AY256968	Tonga Trench	Blankenship et al., unpublished
Hirondellea dubia	KP456071	KP713902	New Hebrides Trench	Ritchie et al., 2015
Hirondellea gigas	KP456077	KP713911	Japan Trench	Ritchie et al., 2015

Table B4. SIMPER analysis of amphipod abundance with species-level identifications in the Zenith Plateau and Wallaby-Zenith Fracture Zone (WZFZ), Afanasy Nikitin Seamount (ANS), Kermadec Trench (KT), New Hebrides Trench (NHT), South Fiji Basin (SFB), and Peru-Chile Trench (PCT). The (dis)similarities between Cluster 4 (WZFZ & ANS) and the five other cluster groups identified by SIMPROF are presented by increasing dissimilarity with percentage contribution of each species that counts for >90% of that value.

	Cluster 4 – WZFZ & ANS	
	(Similarity 57.23)	
Cluster 4 – WZFZ & ANS	Species	%
	Paralicella tenuipes	45.55
	Paralicella caperesca	17.5
	Cyclocaris sp.	17.32
	(Dissimilarity 71.88)	
	Species	%
	Paralicella tenuipes	17.70
	Abyssorchomene abyssorum	10.91
Cluster 6 - NHT Bathyal & Abyssal	*Eurythenes gryllus*	9.53
	Abyssorchomene gerulicorbis	7.38
	Eurythenes maldoror	6.39
	Cyclocaris sp.	6.26
	Paracallisoma sp.	6.05
	Bathycallisoma schellenbergi	6.02
	(Dissimilarity 73.62)	
	Species	%
	Paralicella tenuipes	23.07
	Cyclocaris sp.	9.16
Cluster 5 - KT Bathyal & Abyssal	*Eurythenes maldoror*	7.58
	Abyssorchomene distinctus	7.39
	Bathycallisoma schellenbergi	6.88
	Abyssorchomene musculosus	6.60
	Paralicella caperesca	6.36
	Abyssorchomene gerulicorbis	5.61
	(Dissimilarity 78.32)	
	Species	%
	Paralicella tenuipes	15.44
	Abyssorchomene chevreuxi	13.24
	Eurythenes sp. abyssal	7.94
Cluster 3 - PCT Abyssal	*Cyclocaris* sp.	7.67
	Eurythenes maldoror	6.40
	Paralicella caperesca	5.72
	Abyssorchomene gerulicorbis	5.50
	Bathycallisoma schellenbergi	4.82
	Abyssorchomene distinctus	4.77
	(Dissimilarity 86.23)	
	Species	%
Cluster 2 – KT & NHT Hadal	*Paralicella tenuipes*	21.53
	Hirondellea dubia	16.96
	Bathycallisoma schellenbergi	13.95
	Paralicella caperesca	9.55
	Cyclocaris sp.	8.95
	(Dissimilarity 97.52)	
	Species	%
	Paralicella tenuipes	17.66
	Eurythenes sp. hadal	14.64
Cluster 1 - PCT Hadal	*Hirondellea thursoni*	11.65
	Paralicella caperesca	9.64
	Cyclocaris sp.	7.98
	Eurythenes maldoror	6.56
	Abyssorchomene gerulicorbis	5.75

Table B5. SIMPER analysis of amphipod abundance with genus-level identifications showing the (dis)similarities within and between the two cluster groups identified by SIMPROF.

	Cluster A		Cluster B	
	(Similarity 60.01)		(Dissimilarity 80.42)	
Cluster A - Bathyal to Abyssal and Hadal Trough	Genus	%	Genus	%
	Paralicella	44.63	*Hirondellea*	18.92
	Abyssochromene	27.49	*Paralicella*	17.92
			Abyssochromene	15.69
			Bathycallisoma	14.97
			Eurythenes	10.96
Cluster B – Hadal Trench			(Similarity 55.63)	
			Genus	%
			Hirondellea	60.70
			Bathycallisoma	30.69

Table B6. Total counts of juveniles, intersex, females, and males for *Bathycallisoma schellenbergi* from the Wallaby-Zenith Fracture Zone and results of a one-tailed binomial test to determine significant bias in ratios.

Depth (m)	Juvenile	Intersex	Female	Male	Male: Female Ratio	Mature: Juvenile Ratio
6537	64	1	43	21	0.49*	1.02^{ns}
6546	303	0	103	117	1.14^{ns}	0.72**

ns: non-significant, *$p < 0.01$, **$p < 0.001$

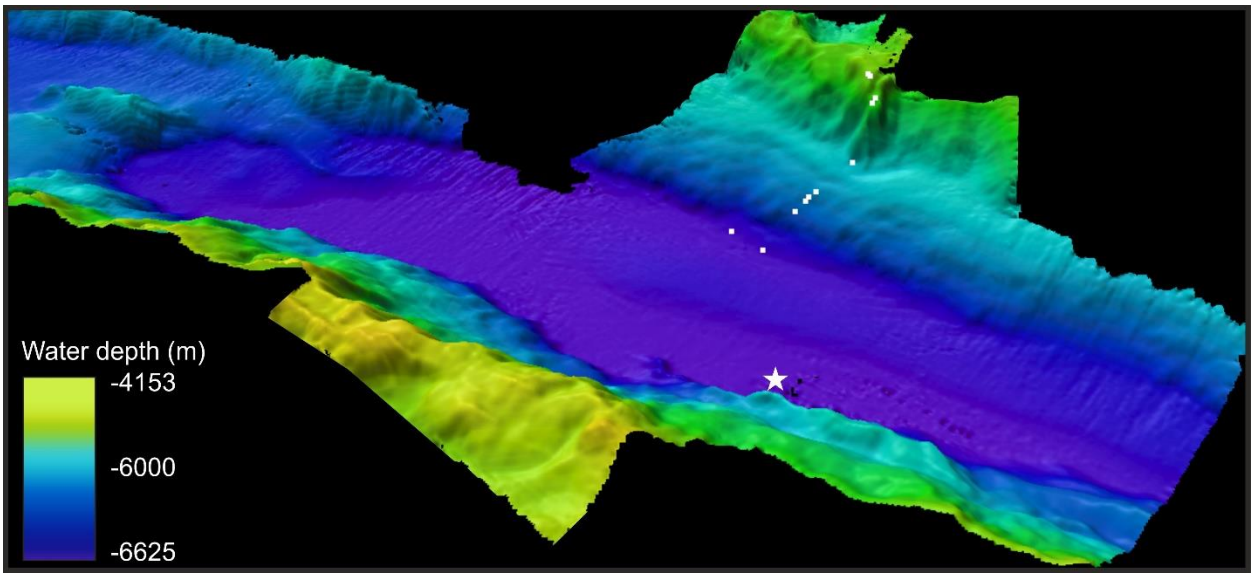

Figure B1. Perspective view of the Wallaby Zenith Fracture Zone looking north with x4 vertical exaggeration. White squares indicate lander deployment sites, white star indicates deepest point. Multibeam bathymetric data acquired during *RV Sonne* Expedition SO258 (Werner et al. 2017).

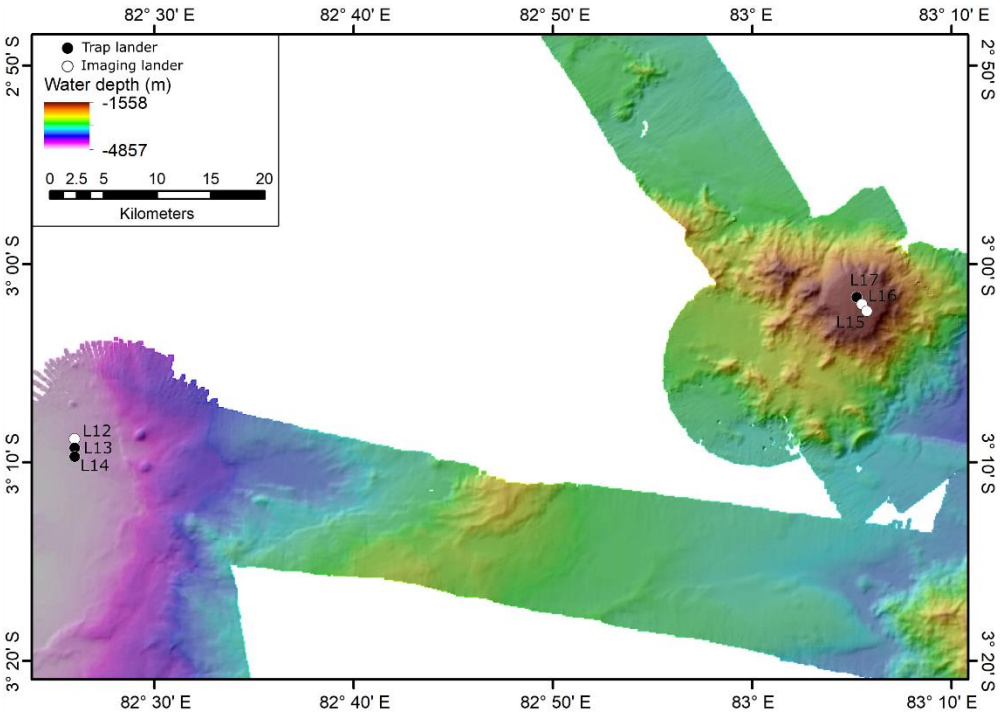

Figure B2. Map of Afanasy Nikitin Seamount with multibeam bathymetric data acquired during *RV Sonne* Expedition SO258 (Werner et al. 2017). Trap lander deployments indicated by black circles. Imaging lander deployments indicated by white circles. Only sites L12-14 were included in this study.

Figure B3. Representative images from the imaging landers showing seafloor characteristics and associated fauna from (A) Afanasy Nikitin Seamount (ANS) including *Barathrites iris* Zugmayer, 1911, hermit crab, and small decapods, (B) Zenith Plateau (ZP) with prominent manganese nodules, *Bassozetus* sp., brittle star, and c.f. *Cerataspis monstrosus* Gray, 1828, and Wallaby-Zenith Fracture Zone (WZFZ) (C) with *Eurythenes maldoror* d'Udekem d'Acoz & Havermans, 2015 and (D) *Bassozetus* spp.

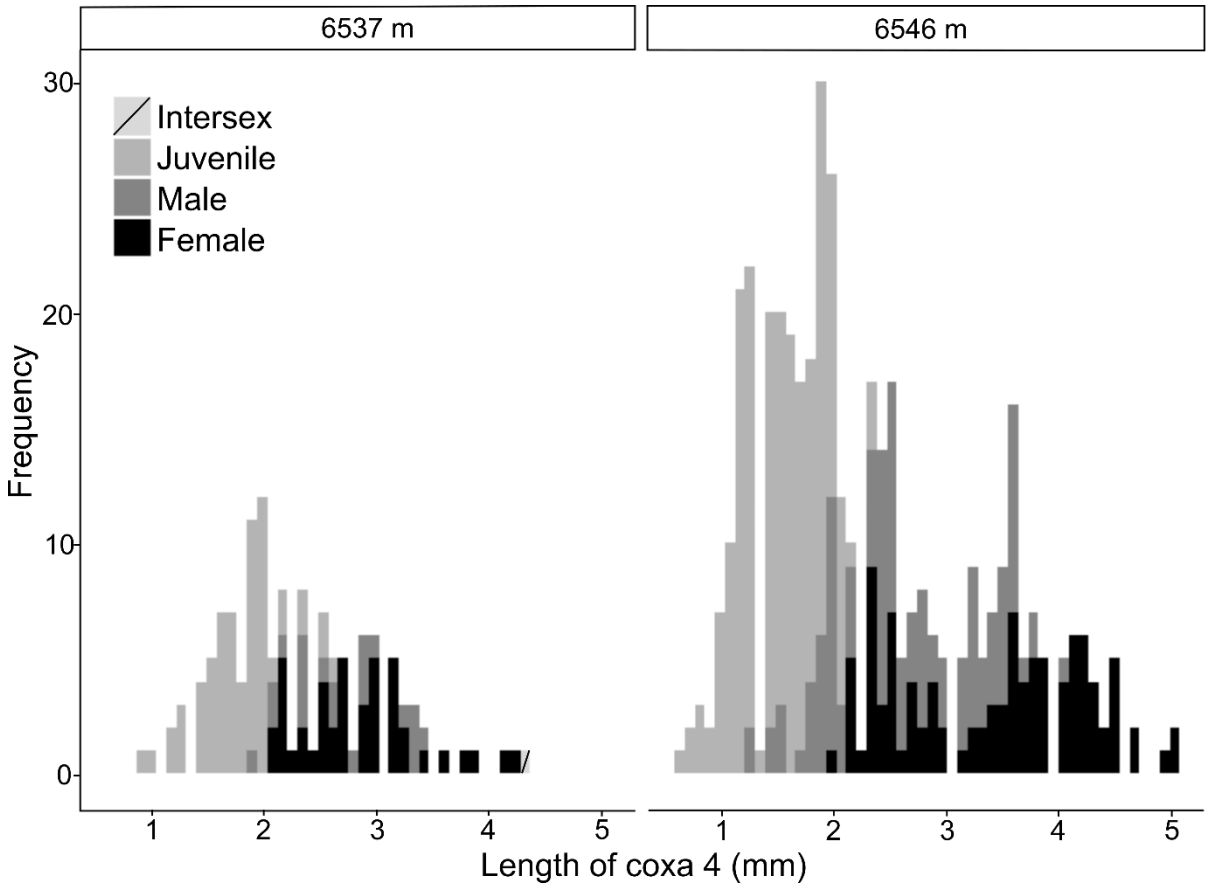

Figure B4. Frequency of coxa 4 length of intersex, juvenile, male, and female *Bathycallisoma schellenbergi* from 6537 and 6546 m at the Wallaby-Zenith Fracture Zone.

Appendix C

Summary of all records of hadal Amphipoda–includes published records and those in review and in prepation.

Table C1. Compilation of all published and known records of Amphipoda recovered from hadal depths (>6000 m). Feature abbreviations: AT - Aleutian Trench, BT–Banda Trench (Weber Basin), BVT–Bougainville Trench, DFZ–Diamantina Fracture Zone, IBT–Izu-Bonin Trench (Izu-Ogasawara Trench), JT–Japan Trench, JVT–Java Trench (Sunda Trench), KT–Kermadec Trench, KKT–Kuril-Kamchatka Trench, MST - Massau Trench, MT- Mariana Trench, NBT–New Britain Trench, NHT–New Hebrides Trench, NPAC–Pacific Ocean, PCT–Peru Chile Trench, PHT–Philippine Trench, PLT–Palau Trench, PRT –Puerto Rico Trench, SCBT - San Cristobal Trench, SCZT –Santa Cruz Trench, SST - South Sandwich Trench, TT–Tonga Trench, VT(MT)- Volcano Trench (now in Mariana Trench), WZFZ–Wallaby Zenith Fracture Zone, and YT–Yap Trench. Pelagic species denoted by *. Cryptic species-complex denoted by **.

	Feature	Depth (m)	Species Authority	Record Reference
SUPERFAMILY: Alicelloidea, Lowry & De Broyer 2008				
FAMILY: Alicellidae, Lowry & De Broyer, 2008				
Paralicella microps	JT	6580	(Birstein & Vinogradova, 1958)	Belyaev, 1989
	KKT	8000	-	Belyaev, 1989
	IBT	8480	-	Belyaev, 1989
*Paralicella tenuipes***	KT	4786-7000	Chevreux, 1908	Belyaev, 1989
	KT	5242-7291	-	Lacey et al., 2016
	MT	5156-7507	-	Jamieson et al., *In Prep Mariana Paper*
	NHT	3400-6228	-	Lacey et al., 2016
	PCT	6173-7050	-	Fujii et al., 2013
	TT	7300	-	Belyaev, 1989
	TT	6256	-	Wilson et al., 2018
	WZFZ	4932-6546	-	Weston et al., 2021
Paralicella c.f. tenuipes	DFZ	7009	-	Five Deeps Expedition
	SCBT	6515	-	Five Deeps Expedition
Paralicella caperesca	KT	4329-6007	Shulenberger & Barnard, 1976	Jamieson et al., 2011
	MT	5156-6142	-	Jamieson et al., *In Prep Mariana Paper*
	NHT	2000-6228	-	Lacey et al., 2016
	PCT	4602-6173	-	Fujii et al., 2013
	TT	6256	-	Wilson et al., 2018
	WZFZ	4932-6537	-	Weston et al., *2021*
Paralicella cf. *fusiformis*	TT	6253-6256	(Birstein & Vinogradov, 1955)	Wilson et al., 2018
Alicella gigantea	KT	6265-7000	Chevreux, 1899	Jamieson et al., 2013

	MT	6846-7507	-	Jamieson et al., *In Prep Mariana Paper*
	NBT	8225-8903	-	Shi et al., 2018
	NPAC	6000	-	Barnard & Ingram, 1986
	SCBT	6515	-	Five Deeps Expedition
	SCZT	7431	-	Five Deeps Expedition
	TT	6253-6256	-	Wilson et al., 2018
Alicellidae sp. 1	MT	7949-9059	Lowry & De Broyer, 2008	Jamieson et al., *In Prep Mariana Paper*
Alicellidae sp. 2	MT	7888	Lowry & De Broyer, 2008	Jamieson et al., *In Prep Mariana Paper*
FAMILY: Valettiopsidae, Lowry & De Broyer, 2008				
Valettietta anacantha	KT	6007	(Birstein & Vinogradova, 1963)	Jamieson et al., 2011
	KT	2197-7000	-	Lacey et al., 2016
	MT	6010-6865	-	Jamieson et al., *In Prep Mariana Paper*
	NHT	5300-6228	-	Lacey et al., 2016
Valettietta sp. nov.	WZFZ	4932-6546	Lincoln & Thurston, 1983	Weston et al., *2021*
SUPERFAMILY: Dexaminoidea, Leach, 1814				
FAMILY: Pardaliscidae, Boeck, 1871				
*Halice aculeata**	BVT	6500	Chevreux, 1912	Belyaev, 1989
	IBT	4000-6500	-	Belyaev, 1989
	KKT	4200-8050	-	Belyaev, 1989
	TT	7100-10500	-	Belyaev, 1989
Halice quarta	IBT	8480-9000	Birstein & Vinogradova, 1955	Belyaev, 1989
	KKT	6000-8500	-	Belyaev, 1989
	KKT	8183-9574	-	Jażdżewska & Mamos, 2019
	MT	10,000	-	Belyaev, 1989
	MT	10,877-10,925	-	Jamieson et al., *In Prep Mariana Paper*
	TT	9120-9120	-	Belyaev, 1989
*Halice rotunda**	BVT	4050-8400	Birstein & Vinogradova, 1960	Belyaev, 1989
	TT	9120	-	Belyaev, 1989
Halice (Synopioides) secundus	KT	6960-7000	(Stebbing,1888)	Dahl, 1959
	PHT	10,150-10,190	-	Dahl, 1959
*Halice subquarta**	KT	9400	Birstein & Vinogradova, 1960	Belyaev, 1989
	PHT	7420-7880	-	Belyaev, 1989
	TT	10,500	-	Belyaev, 1989
	YT	7190-7250	-	Belyaev, 1989
Halice sp. 1	KKT	8183-8743	Boeck, 1871	Jażdżewska & Mamos, 2019
Pardaliscoides longicaudatus	KT	6180	Dahl, 1959	Dahl, 1959
	PHT	9820-10,000	-	Dahl, 1959
Princaxelia abysalis	AT	6965-7000	Dahl, 1959	Belyaev, 1989
	BVT	7974-8006	-	Belyaev, 1989
	JT	6380-7370	-	Belyaev, 1989
	IBT	6770-8830	-	Belyaev, 1989
	KT	6620-8300	-	Dahl, 1959
	KKT	6435-9530	-	Belyaev, 1989
	PHT	7420-7880	-	Belyaev, 1989
	YT	7190-8720	-	Belyaev, 1989

Princaxelia magna	JT	7190-7250	Kamenskaya,1977	Belyaev, 1989
	MT	8098-8942	-	Jamieson et al., *In Prep Mariana Paper*
	TT	7354-8411	-	Belyaev, 1989
Princaxelia jamiesoni	IBT	9316	Lörz, 2010	Lörz, 2010
	JT	7703	-	Lörz, 2010
Princaxelia cf. *jamiesoni*	KKT	7110-9574		Jażdżewska & Mamos, 2019
Princaxelia sp. nov.	DFZ	7009	Dahl, 1959	Five Deeps Expedition
FAMILY: Atylidae, Lilljeborg,1865				
Aberratylus (Lepechinella) aberrantis	VT(MT)	6330	(J.L. Bernard, 1962)	Belyaev, 1989
FAMILY: Lepechinellidae, Schellenberg, 1926				
Lepechinella ultraabyssalis	KKT	6475-8015	Birstein & Vinogradova, 1960	Belyaev, 1989
	JT	7370	-	Belyaev, 1989
Lepechinella cf. *ultraabyssalis*	KKT	5152-7119	-	Jażdżewska & Mamos, 2019
Lepechinella vitrea	YT	7190-7250	Kamenskaya, 1977	Belyaev, 1989
Lepechinella wolffi	KT	6660-6770	Dahl, 1959	Dahl, 1959
SUPERFAMILY: Eusiroidea, Stebbing, 1888				
FAMILY: Eusiridae, Stebbing, 1888				
Eusirella longisetosa	BVT	8500	Birstein & Vinogradova, 1960	Belyaev, 1989
Eusirus bathybius	BVT	7500	Schellenberg, 1955	Belyaev, 1989
	PHT	7625-7900	-	Belyaev, 1989
	PRT	7625-7900	-	Belyaev, 1989
*Eusirus fragilis**	TT	9120	Birstein & Vinogradova, 1960	Belyaev, 1989
Rhachotropis saskia	KKT	4903-8183	Lörz et al., 2018	Lörz et al., 2018
Rhachotropis flemmingi	KKT	6090-6135	Dahl, 1959	Belyaev, 1989
	JVT	6820-7160	-	Dahl, 1959
Rhachotropis sp. nov.	PHT	7420-7880	S.I. Smith, 1883	Belyaev, 1989
Rhachotropsis indent.	KT	6960-7000	-	Belyaev, 1989
Eusiridae sp.	NHT	6228	Stebbing, 1888	Lacey et al., 2016
Cleonardo indent.	WZFZ	6162	Stebbing, 1888	Weston et al., 2021
SUPERFAMILY: Haustorioidea, Stebbing, 1906				
FAMILY: Phoxocephalidae, G.O. Sars, 1891				
Harpiniopsis (Harpinia) spaercki	BT	6580-7270	(Dahl, 1959)	Dahl, 1959
Metaphoxus sp.	JT	7550	Bonnier, 1896	Belyaev, 1989
Pseudharpinia (Harpinia) abyssalis	PCT	6324-6328	(Pirlot, 1932)	Belyaev, 1989
SUPERFAMILY: Iphimedioidea, Boeck, 1871				
FAMILY: Stilipedidae, Holmes, 1908				
Alexandrella carinata	KKT	7210-7230	Birstein & Vinogradova, 1960	Belyaev, 1989
FAMILY: Epimeriidae, Boeck, 1893				
Epimeria sp. nov.	JT	6156-6207	Costa in Hope, 1851	Belyaev, 1989
	KKT	7210-7230	-	Belyaev, 1989
	DFZ	7009	-	Five Deeps Expedition
SUPERFAMILY: Liljeborgioidea, Stebbing, 1899				
FAMILY: Liljeborgiidae, Stebbing, 1899				
Liljeborgia caeca	JT	6156-6207	Birstein & Vinogradova, 1960	Belyaev, 1989
SUPERFAMILY: Lysianassoidea, Dana, 1849				
Lysianassidae sp. 1	MT	7507	Dana, 1849	Jamieson et al., *In Prep Mariana Paper*

Lysianassoidae	KKT	5000-6560	Dana, 1849	Jażdżewska & Mamos, 2019
FAMILY: Tryphosidae, Lowry & Stoddart, 1997				
Bruunosa (Tryphosa) bruuni	KT	6660-6770	(Dahl, 1959)	Dahl, 1959
Tryphosella sp. 2	KT	6007	Bonnier, 1893	Jamieson et al., 2011
Tryphosella sp.	PCT	7050	-	Fujii et al., 2013
Aff. Tryphosella sp.	PCT	8074	-	Fujii et al., 2013
Aff. Tryphosella sp. 1	MT	7949-9059	-	Jamieson et al., *In Prep Mariana Paper*
Tryphosidae gen. sp.	SCBT	7200-8407	Lowry & Stoddart, 1997	Five Deeps Expedition
	SCZT	6844-8428		Five Deeps Expedition
Onesimoides (cavimanus) carinatus	BT	6490-6650	Pirlot 1933	Dahl, 1959
Orchomene sp.	MT	10,500	Boeck, 1871	Belyaev, 1989
FAMILY: Eurytheneidae, Stoddart & Lowry, 2004				
Eurythenes atacamensis	PCT	4974-8081	Weston & Espinosa-Leal, 2021	Weston et al., *In Review Marine Biodiversity*
Eurythenes (PCT 'Hadal') atacamensis	PCT	6173-8074		Eustace et al., 2016
Eurythenes (gryllus) atacamensis	PCT	7800		Thurston et al., 2002
Eurythenes andhakarae	SST	6044-7099	d'Udekem d'Acoz & Havermans, 2015	Five Deeps Expedition
Eurythenes magellanicus	MT	7094-7094	(H. Milne Edwards, 1848)	Jamieson et al., *In Prep Mariana Paper*
	PRT	7000-7000		Five Deeps Expedition
Eurythenes maldoror	WZFZ	4932-6546	d'Udekem d'Acoz & Havermans, 2015	Weston et al., 2021
	PCT	4974-6547		RV *Sonne* 258
	KT	4193-6007		Fujii et al., 2013
	NHT	5180-6948		Lacey et al., 2016
Eurythenes plasticus	MT	6010-6949	Weston, 2020	Weston et al., 2020
Eurythenes sigmiferus	KT	6097-6097	d'Udekem d'Acoz & Havermans, 2015	Lacey et al., 2016
Eurythenes gryllus/sigmiferus	TT	6253-6256	-	Wilson et al., 2018
Eurythenes (PCT 'Abyssal') sp. nov.	PCT	4602-6173	-	Eustace et al., 2016
Eurythenes (gryllus) spp.**	IBT	6770-7850	Lichtenstein in Mandt, 1822	Belyaev, 1989
	TT	5155-6252	-	Blankenship et al., 2006
	NHT	2000-6948	-	Lacey et al., 2016
	SCBT	6515	-	Five Deeps Expedition
	KT	4329-6007		Jamieson et al., 2011
FAMILY: Hirondelleidae, Lowry & Stoddart, 2010				
Hirondellea dubia	KT	7640-7680	Dahl, 1959	Dahl, 1959
	KT	6709-9908	-	Lacey et al., 2016
	KT	6000-7966	-	Jamieson et al., 2011
	KT	9104-9856	-	Blankenship et al., 2006
	MT	5641-8942	-	Jamieson et al., *In Prep Mariana Paper*
	NHT	6000-6948	-	Lacey et al., 2016
	PRT	6954-8380	-	Five Deeps Expedition
	SCBT	6515-8407	-	Five Deeps Expedition
	SCZT	6844-8428	-	Five Deeps Expedition
	SST	6640-8266	-	Five Deeps Expedition
	TT	7349-10,787	-	Blankenship et al., 2006
	TT	6253-10,807	-	Wilson et al., 2018

	TT	6793-10,823	-	Five Deeps Expedition
Hirondellea gigas	IBT	6770-8900	(Birstein & Vinogradova, 1955)	Belyaev, 1989
	IBT	8172-9316	-	Eustace et al., 2013
	JT	7703	-	Jamieson et al., 2019
	KKT	7250-9345	-	Belyaev, 1989
	KKT	8183-9574	-	Jażdżewska & Mamos, 2019
	MT	7218-9144	-	France 1993
	MT	10,897	-	Kobayashi et al., 2012
	MT	10,897	-	Kobayashi et al., 2018
	MT	10,890	-	Jamieson et al., 2019
	MT	6864-10,925	-	Jamieson et al., *In Prep Mariana Pape*r
	MT	10,840	-	Shi et al., 2018
	PHT	8467-9604	-	France 1993
	PHT	10,020-10,190	-	Dahl, 1959
	PLT	7970-8035	-	Belyaev, 1989
	PLT	7997	-	France 1993
	VT(MT)	8530-8540	-	Belyaev, 1989
	YT	8560-8720	-	Belyaev, 1989
Hirondellea sonne	PCT	7050	Kilgallen, 2014	Kilgallen, 2014
Hirondellea thurstoni	PCT	6173-8072	Kilgallen, 2014	Kilgallen, 2014
Hirondellea (sp. nov) *thurstoni*	PCT	7800	-	Perrone et al., 2002
Hirondellea wagneri	PCT	6173	Kilgallen, 2014	Kilgallen, 2014
Hirondellea sp.	TT	6256	Chevreux, 1889	Wilson et al., 2018
Hirondellea sp. 2	SST	7400-7439	-	Five Deeps Expedition
FAMILY: Cyclocaridae, Lowry & Stoddart, 2011				
Cyclocaris tahitensis	KT	6007	Stebbing, 1888	Jamieson et al., 2011
Cyclocaris sp. (cf. *tahitensis*)	TT	6253-6256	-	Wilson et al., 2018
Cyclocaris sp. nov.	WZFZ	4932-6546	Stebbing, 1888	Weston et al., 2021
FAMILY: Scopelocheiridae, Lowry & Stoddart, 1997				
Scopelocheirus (pacifica) hopei *	KT	6960-7000	(Costa in Hope, 1851)	Belyaev, 1989
Bathycallisoma (Scopelocheirus) schellenbergi **	AT	6965-7200	(Birstein & Vinogradova, 1958)	Belyaev, 1989
	DFZ	7009	-	Five Deeps Expedition
	KT	9104	-	Blankenship et al., 2006
	KT	6097-8487	-	Lacey et al., 2016
	KT	6007-6890	-	Jamieson et al., 2011
	KKT	6000-7000	-	Belyaev, 1989
	JT	6380-7370	-	Belyaev, 1989
	JVT	6935-7060	-	Belyaev, 1989
	MT	6010-7507	-	Jamieson et al., *In Prep Mariana Paper*
	MST	6990	-	Shi et al., 2018
	NHT	5600-6948	-	Lacey et al., 2016
	PCT	5913-7836		RV *Sonne* 258
	PRT	7625-7900	-	Belyaev, 1989
	PRT	6954-8380	-	Five Deeps Expedition
	PRT	8000	-	Lacey et al., 2013
	SCBT	7200-8407	-	Five Deeps Expedition
	SCZT	6844-8428	-	Five Deeps Expedition
	SST	6640-8266	-	Five Deeps Expedition

	TT	6252-8723	-	Blankenship et al., 2006
	TT	6253-6256	-	Wilson et al., 2018
	TT	6793-7928	-	Five Deeps Expedition
	WZFZ	6537-6546	-	Weston et al., 2021
Bathycallisoma (pacifica) schellenbergi	KT	6960-7000	(Birstein & Vinogradova, 1958)	Dahl, 1959
FAMILY: Uristidae, Hurley, 1963				
Abyssorchomene (Orchomelella) abyssorum	KT	8210-8300	(Stebbing, 1888)	Dahl, 1959
Abyssorchomene gerulicorbis	KT	5173-6007	(Shulenberger & Barnard, 1976)	Jamieson et al., 2011
	WZFZ	5990-6546	-	Weston et al., 2021
Abyssorchomene (Orchomenella) gerulicorbis	KT	1488-6968	(Shulenberger & Barnard, 1976)	Lacey et al., 2016
Abyssorchomene chevreuxi	PCT	6173	(Stebbing, 1906)	Fujii et al., 2013
Abyssorchomene distinctus	TT	6253-6256	(Birstein & Vinogradova, 1960)	Wilson et al., 2018
Abyssorchomene sp.	DFZ	7009	De Broyer, 1984	Five Deeps Expedition
Stephonyx sp. nov.	PRT	8280-8370	Lowry & Stoddart, 1989	Five Deeps Expedition
Galathella (Schisturella) galatheae	KT	6960-7000	(Dahl, 1959)	Dahl, 1959
SUPERFAMILY: Stegocephaloidea, Dana, 1852				
FAMILY: Stegocephalidae, Dana, 1852				
Andaniexis australis	PCT	6324-6328	Barnard, 1932	Belyaev, 1989
Andaniexis sp.*	IBT	6770-6890	Stebbing, 1906	Belyaev, 1989
*Andaniexis stylifer**	BVT	6500-8500	Birstein & Vinogradova, 1960	Belyaev, 1989
Stegocephalus nipoma	PHT	6290-6330	(J.L. Barnard, 1961)	Belyaev, 1989
Stegocephalus sp. nov.	KKT	7600-7710	Krøyer, 1842	Belyaev, 1989
	KKT	7795-8015	-	Belyaev, 1989
Stegocephalus sp. nov. 1	JT	6380-6380	Krøyer, 1842	Belyaev, 1989
Steleuthera maremboca	PCT	6324-6380	J.L. Barnard, 1964	Belyaev, 1989
Stegocephalidae gen. sp.	PRT	6954-8380		Five Deeps Expedition
FAMILY: Andaniexinae, Berge & Vader, 2001				
*Andaniexis subabyssi**	KKT	6000-8500	Birstein & Vinogradova, 1955	Belyaev, 1989
SUPERFAMILY: Synopioidea, Dana, 1852				
FAMILY: Ampeliscidae, Krøyer, 1842				
Byblisoides arcillis	KKT	6272-6571	(J.L. Barnard, 1961)	Belyaev, 1989
FAMILY: Synopiidae, Dana, 1853				
Synopiidae	KKT	5300-6163	Dana, 1853	Jażdżewska & Mamos, 2019
SUBORDER: *Hyperiidea,* H. Milne Edwards, 1830				
SUPERFAMILY: Lanceoloidea, Bovallius, 1887				
FAMILY: Lanceolidae, Bovallius, 1887				
*Lanceola (clausii) gracilis**	KKT	4200-8000	Vinogradov, 1956	Belyaev, 1989
	PHT	6200-6750	-	Belyaev, 1989
*Lanceola sphaerica**	KKT	7800	Vinogradov, 1970	Belyaev, 1989
*Metalanceola chevreuxi**	BVT	6500-8500	Pirlot, 1931	Belyaev, 1989
	KT	9400	-	Belyaev, 1989
	TT	9100-10500	-	Belyaev, 1989
SUPERFAMILY: Scinoidea, Stebbing, 1888				
FAMILY: Scinidae, Stebbing, 1888				
*Scina chelata**	KKT	7750	Vinogradov, 1970	Belyaev, 1989
*Scina (wagleri) abyssalis**	KT	9400	Vinogradov, 1957	Belyaev, 1989
	KKT	6000-8500	-	Belyaev, 1989

	IBT	8500	-	Belyaev, 1989
SUBORDER: Hyperiopsidea, Bovallius, 1886				
SUPERFAMILY: Hyperiopsoidea, Bovallius, 1886				
FAMILY: Hyperiopsidae, Bovallius,1886				
*Hyperiopsis anomala**	TT	6900-6900	Birstein & Vinogradova, 1960	Belyaev, 1989
*Hyperiopsis laticarpa**	BVT	8500	Birstein & Vinogradova, 1955	Belyaev, 1989
	KKT	6000-8500	-	Belyaev, 1989
	IBT	8480	-	Belyaev, 1989
	MT	10,925	-	Jamieson et al., *In Prep Mariana Paper*
*Protohyperiopsis (Parargissa) affinis**	BVT	8150-8500	Birstein & Vinogradova, 1960	Belyaev, 1989
	IBT	6500	-	Belyaev, 1989
*Protohyperiopsis (Parargissa) arquata**	KKT	4200-8500	Birstein & Vinogradova, 1955	Belyaev, 1989
*Protohyperiopsis curticornis**	NHT	7000	(Birstein & Vinogradova, 1960)	Belyaev, 1989
*Protohyperiopsis longipes**	BVT	8500	(Birstein & Vinogradova, 1960)	Belyaev, 1989
FAMILY: Vitjazianidae, Birstein & Vinogradova, 1955				
*Vitjaziana gurjanovae**	IBT	4200-8480	Birstein & Vinogradova, 1955	Belyaev, 1989
SUBORDER: Senticuadata, Lowry & Myers, 2013				
SUPERFAMILY: Calliopioidea, G.O. Sars, 1895				
FAMILY: Pontogeneiidae, Stebbing, 1906				
Bathyschraderia magnifica	KT	6960-7000	Dahl, 1959	Dahl, 1959
	KT	6960-9174	Dahl, 1959	Belyaev, 1989
	TT	7354-9875	-	Belyaev, 1989
Bathyschraderia fragilis	PHT	7000-9990	Kamenskaya, 1981	Belyaev, 1989
SUPERFAMILY: Photoidea, Boeck, 1871				
FAMILY: Ischyroceridae, Stebbing, 1899				
Bonnierella linearis	PCT	6342-6328	J.L. Barnard, 1964	Belyaev, 1989
SUPERFAMILY: Hadzioidea, (Busfield, 1983)				
FAMILY: Maeridae, Krap-Schickel, 2008				
Bathyceradocus stephenseni	BT	7250-7340	Pirlot, 1934	Belyaev, 1989
	BVT	6920-7652	-	Belyaev, 1989
Metaceradocoides vitjazi	IBT	8900	Birstein & Vinogradova, 1960	Belyaev, 1989
	MT	8215-8225	-	Belyaev, 1989
	TT	6600-7370	-	Belyaev, 1989
	YT	7190-7250	-	Belyaev, 1989

Table C2. Summary of Table C1 to highlight the number of genera, species, records, and hadal features for Amphipoda recovered from hadal depths (>6000 m). Brackets represent the number of genera or species whose identification is not at the genus or species level (e.g., sp. nov., gen. sp., and indent.).

Suborder	Superfamily	Family	Number of genera	Number of species	Number of Records	Number of Features
Amphilochidea	Alicelloidea	Alicellidae	2 (+1)	2 (+8)	29	13
		Valettiopsidae	1	1 (+1)	5	4
	Dexaminoidea	Pardaliscidae	3	9 (+1)	33	12
		Atylidae	2	4	5	5
		Lepechinellidae	1	3	5	4
	Eusiroidea	Eusiridae	4 (+1)	5 (+4)	12	10
	Haustorioidea	Phoxocephalidae	3	2 (+1)	3	3
	Iphimedioidea	Stilipedidae	1	1	1	1
		Epimeriidae	1	0 (+2)	3	3
	Liljeborgioidea	Liljeborgiidae	1	1	1	1
	Lysianassoidea	Lysianassidae	0 (+1)	0 (+2)	2	2
		Tryphosidae	4 (+3)	2 (+6)	9	6
		Eurytheneidae	1	6 (+3)	19	11
		Hirondelleidae	1	5 (+2)	36	16
		Cyclocaridae	1	1 (+2)	3	3
		Scopelocheiridae	2	2	25	16
		Uristidae	3	5 (+2)	9	6
	Stegocephaloidea	Stegocephalidae	3 (+1)	4 (+3)	9	7
		Andaniexinae	1	1	1	1
	Synpoiodea	Ampeliscidae	1	1	1	1
		Synopiidae	1	1	1	1
Hyperiidea	Lanceoloidea	Lanceolidae	2	3	6	5
	Scinoidea	Scinidae	2	2	4	3
Hyperiopsidea	Hyperiopsoidea	Hyperiopsidae	2	6	10	6
		Vitjazianidae	1	1	1	1
Senticaudata	Calliopioidea	Pontogeneiidae	1	2	4	3
	Photoidea	Ischyroceridae	1	1	1	1
	Hadzioidea	Maeridae	2	2	6	6

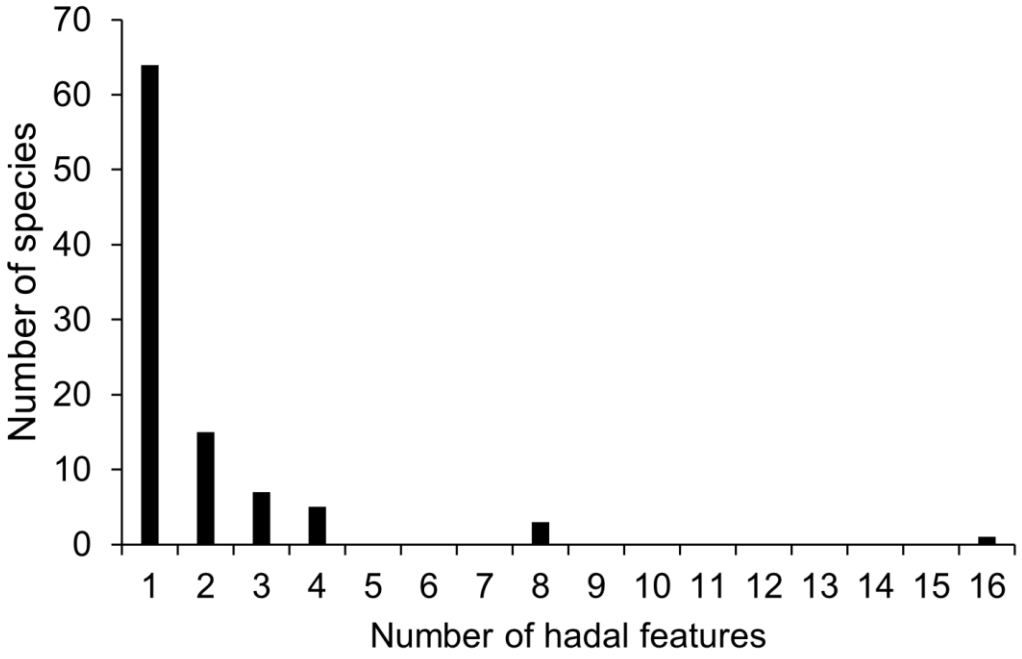

Figure C1. The number of hadal features recorded by the known species.